Chemical Biology of Microbial Anticancer Natural Products

Bladt, Tanja Thorskov

Publication date:
2013

Document Version
Publisher's PDF, also known as Version of record

Chemical Biology of Microbial Anticancer Natural Products

Tanja Thorskov Bladt
PhD Thesis
December 2013

DTU Systems Biology
Department of Systems Biology

DTU Systems Biology

Chemical Biology of Microbial Anticancer Natural Products

PhD Thesis

Tanja Thorskov Bladt

October 2013

Supervisors:

Associate Professor Thomas Ostenfeld Larsen (DTU Systems Biology)

Associate Professor Charlotte Held Gotfredsen (DTU Chemistry)

Evaluation committee:

Associate professor Olivier Taboureau, Systems Biology, DTU

Professor Olov Sterner, Lunds University, Sweden

Professor Søren Brøgger Christensen, University of Copenhagen

Chairman:

Associate Professor Kristian Fog Nielsen

Date of defence December 16th, 2013

Adress: DTU Systems Biology
Søltofts plads
Building 221
DK-2800 Kgs. Lyngby
Denmark
Phone: +45 4525 2525
Fax: +45 4588 4148
Web: www.bio.dtu.dk

Print: J&R Frydenberg A/S
København
February 2014

ISBN: 978-87-91494-77-2

Frontpage illustration: **Agar plate with *Penicillium jugorum*** (source: Tanja Thorskov Bladt)

Preface

This thesis is submitted to the Technical University of Denmark (DTU) in partial fulfillment of the requirements for the Degree of Doctor of Philosophy in Chemistry. The work has been carried out between October 2009 and October 2013, at the Department of Systems Biology (DTU Systems Biology), DTU under the main supervision of Associate Professor Thomas Ostenfeld Larsen (DTU Systems Biology) with Associate Professor Charlotte Held Gotfredsen (Department of Chemistry, DTU) as co-supervisor. The project was funded by DTU.

First of all, I would like to express great and heartfelt thanks to my two supervisors for scientific guidance and challenging discussions. **Thomas** your endless enthusiasm has always inspired and motivated me to stretch beyond my own expectations. **Lotte** thanks for always being there for me when I needed it. Special thanks to PhD student **Peter Boldsen Knudsen** for performing the initial screening in his master project, for your patience when I tried to understand the mysterious world of CLL cells and for all the times you have left Louise for one or two weeks in order to work with the assays in Heidelberg. In addition, I would like to thank Professor **Martina Seiffert** and PhD student **Claudia Dürr** at the German Cancer Research Center (DKFZ) in Heidelberg for developing and conducting the CLL assays and for opening the cell culture lab for a chemist trying to understand biology.

Special thanks to Postdoc **Maria Månsson** for always taking your time to discuss with me and for your critical proofreading of my work, you are a great source of scientific inspiring to me. Professor **Jens Christian Frisvad**, for your enthusiasm and love to fungi. Associate Professors **Kristian Fog Nielsen** for answers and discussions regarding UHPLC-MS, instruments, and data analysis. Professor **Carsten Christophersen** for scientific discussions and inspiration.

I would also like to thank a number of productive students, especially **Sara Kildgaard** for your hard work with the ophiobolins. I am also grateful to all the skilled laboratory technicians: **Hanne Jacobsen**; **Lisette Knoth-Nielsen**, **Anne Hector**, and **Ellen Kirstine Lyhne (Kir).** You help just make life easier. Credit is also due to the Carlsberg laboratories for allowing me to use their 800 MHz NMR spectrometer.

During my PhD I had the privilege to spend three months at the Tel Aviv University, Israel with Professor **Shmuel Carmeli's** group. I would like to thank Smulik for letting me come and work in your lab and enjoy 'winter' in Israel without snow. I also own the rest of his group a big thanks but especially **Anat Lodin-Friedman** and **Michal Issac** who made me feel at home and

Sivan Kalifa-Aviv for finishing my lab work. I would also like to thank the Otto Mønsted foundations for financial support whereby this exchange was made possible.

A tremendously great thanks to all my **fantastic colleagues** especially: Marie Louise, Sara, Lene, Maria, Silas, Andreas, Olivera, Ina, Pernille, Anita, Richard and Christian, for peer-to-peer training, creating a great atmosphere, and making coffee and bringing chocolate when needed. It has been a pleasure to work with all of you.

Lastly, I would like to thank my family and friends for great support especially my husband **Søren** for confidence in my ability to achieve my goals and my son **Dirch** for hugging me with excitement every time I come home from work. You have truly supported and helped me morally through difficult times.

Kgs. Lyngby, October 15, 2013,
Tanja Thorskov Bladt

Abstract

Filamentous fungi and other microorganisms have amazing abilities to synthesize structural complex, diverse and unique small organic molecules. Many are bioactive and numerous compounds such as mycotoxins, antifungal, and anticancer agents have been reported in the literature within the last more than 100 years. New natural products (NPs) are continually discovered and with the increase in selective biological assays, previously described compounds often also display novel bioactivities, justifying their presence in novel screening efforts.

Screening and discovery of compounds with activity towards chronic lymphocytic leukemia (CLL) cells is crucial since CLL is considered as an incurable disease. To discover novel agents that targets CLL cells is complicated. CLL cells rapidly undergo apoptosis *in vitro* when they are removed from their natural microenvironment, even though they are long-living cells *in vivo*. Fortunately viability of CLL cells can be maintained *in vitro* by co-cultivation with stromal cells mimicking *in vivo* conditions. This has led to the development of a co-culture assay that is ideally suited for screening of NPs.

The main goal of this study has been to discover fungal NPs with activity towards CLL cells *in vitro*. We based our screening on a combined analytical and bio-guided approach of LC-DAD-HRMS based dereplication, explorative solid-phase-extraction (E-SPE), and a co-culture platform of CLL and stromal cells.

The activity was tracked to single compounds in seven of the most active extracts in a screening setup including 289 fungal extracts. The novel ophiobolin U was isolated together with the known ophiobolin C, H, K as well as 6-epiophiobolin G, K and N from three fungal strains in the *Aspergillus* section *Usti*, and further ophiobolins were bought from commercial sources. Ophiobolin A, B, C and K induced apoptosis in CLL cells with LC_{50} values of values of 1, 2, 8, and 4 nM, respectively, with a possible narrow therapeutic window. The remaining ophiobolins were inactive. Eight other bioactive extracts were addressed and the compounds responsible for the activity towards CLL cells were identified from six of the extracts. The known compounds: penicillic acid, viridicatumtoxin, calbistrin A, brefeldin A, emestrin A, and neosolaniol monoacetate all displayed activity towards CLL cells though they all showed general cytotoxic in the assay. In the remaining two extracts the bioactive compounds were tentatively identified as cycloaspeptide E and a compound belonging to the statin family of compounds though these results are inconclusive.

A second aim of this PhD project has been to discover novel bioactive NPs using a target-guided approach based on MS and NMR. In one project a target-guided approach based on MS

lead to isolation of two new cytochalasins, sclerotionigrin A and B and the known proxiphomin from the fungal species *Aspergillus sclerotieoniger*. The compounds are moderately cytotoxic towards CLL. In a second approach three novel bioactive micropeptins produced by cyanobacteria were discovered through target-guided isolation based on NMR. The micropeptins displayed inhibitory activity towards serine proteases: chymotrypsin and elastase with IC_{50} values between 5.9 and 28.0 μM.

In conclusion, this PhD study adds to the knowledge of bioactive NPs produced by filamentous fungi, and in particular activity towards CLL cells. The results obtained here have been based on the use of a combined bio-guided and analytical dereplication approach. This PhD study also includes a review of 50 compounds or compound families with anticancer activity primarily produced by *Aspergillus*, *Penicillium* and *Talaromyces*.

Sammenfatning

Filamentøse svampe og andre mikroorganismer har en utrolig evne til at synteserne strukturelt komplekse, forskellige og unikke små organiske molekyler. Mange er bioaktive stoffer som f.eks. mykotoksiner, antifungale og anticancer aktive stoffer er blevet afrapporteret i litteraturen gennem de sidste 100 år. Der bliver stadig opdaget nye naturstoffer (NPs) og med en stigning i selektive biologiske assay udviser tidligere beskrevne stoffer ofte nye bioaktiviteter, hvilket retfærdiggør deres tilstedeværelse in nye screeningstiltag.

Screening og opdagelse af stoffer med aktivitet mod kronisk lymfatisk leukæmi (CLL) celler er vigtigt fordi CLL anses som en uhelbredelig sygdom. Opdagelse af nye kemiske stoffer der målretter CLL celler er kompliceret fordi CLL celler *in vitro* hurtigt underlægges apoptose når de fjernes fra deres naturlig mikromiljø, selvom de *in vivo* har en høj overlevelsesevne. Overlevelsesevnen for CLL celler kan heldigvis bibeholdes *in vitro* ved hjælp af kultivering sammen med stromal celler hvorved *in vivo* forhold imiteres. Dette har ført til udviklingen af et co-kultiverings assay der er velegnet til screening af NPs.

Hovedformålet af dette studie har været at opdage svampe NPs med aktivitet mod CLL celler *in vitro*. Vi baserede vores screening på en kombineret analytisk og bio-guided fremgangsmåde med LC-DAD-HRMS baseret dereplikering, 'explorative solid-phase-extraction (E-SPE)' og en co-kultiverings platform bestående af CLL og stromale celler.

Aktiviteten blev undersøgt på enkelte stoffer i syv af de mest aktive ekstrakter i et screenings setup der inkluderede 289 svampeekstrakter. Den nye ophiobolin U blev isoleret sammen med de kendte ophiobolin C, H, K og 6-epiophiobolin G, K, N fra tre stammer in *Aspergillus* sektion *Usti*. Yderligere ophioboliner blev købt kommercielt. Ophiobolin A, B, C og K inducerede apoptose in CLL celler med LC_{50} værdierne 1. 2, 8 og 4 nM med et muligt men snævert terapeutisk vindue. De resterende ophioboliner var inaktive. Otte andre bioaktive ekstrakter blev adresseret og stofferne der var ansvarlig for aktiviteten mod CLL celler blev identificeret i seks af ekstrakterne. De kendte stoffer: penicillinsyre, viridicatumtoxin, calbistrin A, brefeldin A, emestrin A, og neosolaniol monoacetate viste alle aktivitet mod CLL celler dog var de alle generelt cytotoksiske i assayet. I de to tilbageværende ekstrakter blev de bioaktive stof midlertidigt identificeret til at være cycloaspeptid E og et stof fra statin familien, dog var disse resultater ikke fyldestgørende.

Et andet mål i dette Ph.d. projekt har været at opdage nye biotaktive NPs ved hjælp af en 'target-guided' fremgangsmåde baseret på hhv. MS og NMR. I et projekt var den 'target-guided' fremgangsmåde baseret på MS hvilket ledte til isolering af to nye cytochalasiner, sclerotionigrin

A and B og den kendte proxiphomin fra svampen *Aspergillus sclerotieoniger*. Stofferne er moderat cytotoxiske mod CLL. I en anden fremgangsmåde blev tre nye bioaktive micropeptiner, produceret af cyanobakterier, opdaget gennem 'target-guided' isolering beseret på NMR. De tre micropeptiner viste inhiberende aktivitet mod serin proteaserne chymotrypsin og elastase med IC_{50} værdier mellem 5.9 og 28.0 μM.

Dette Ph.d. studie bidrager til vores viden omkring bioaktive NPs produceret af filamentøse svampe og særligt med aktivitet mod CLL celler. Resultaterne opnået her har været baseret på brugen af en kombineret bio-guided og analytisk fremgangsmåde. Dette Ph.d. studie inkluderer også et review af 50 stoffer eller stofklasser med anticancer aktivitet primært produceret af *Aspergillus*, *Penicillium* og *Talaromyces*.

Peer-reviewed papers

Paper 1 **Bladt, T.T.**; Frisvad, J.C.; Knudsen, P.B.; Larsen, T.O. Anticancer and Antifungal Compounds from *Aspergillus*, *Penicillium* and other Filamentous Fungi. *Molecules* **2013**, *18*, 11338–11376.

Paper 2 **Bladt, T.T.**; Dürr, C.; Knudsen, P.B.; Kildgaard, S.; Frisvad, J.C.; Gotfredsen, C.H.; Seiffert, M. Larsen, T.O.; Bio-Activity and Dereplication Based Discovery of Ophiobolins and Other Fungal Secondary Metabolites Targeting Chronic Lymphocytic Leukemia Cells. *Molecules*, **2013**, *18*, 14629-14650.

Paper 3 Petersen, L.M.; **Bladt, T.T.**; Dürr, D.; Seiffert, M.; Gotfredsen, C.H. Larsen, T.O. Sclerotionigrin A and B, two Novel Cytochalasans Targeting Chronic Lymphocytic Leukemia. *Manuscripts submittet to Organic Letters*, **2013**.

Paper 4 **Bladt, T.T.**; Kalifa-Aviv, S.; Larsen, T.O. Carmeli, S.; Micropeptins from *Microcystis* sp. Collected in Kabul Reservoir, Israel. *Tetrahedron*, **2013**, *70*, 936-943

Conference proceeding

Poster 1 **Bladt, T.T.**; Kildgaard, S.; Knudsen, P.B.; Gotfredsen, C.H.; Dürr, C.; Seiffert, M. Larsen, T.O. Fungal Natural Products Targeting Chronic Lymphocytic Leukaemia. *Planta Med.*, **2012**, *78*, 1158. *Poster at International Congress on Natural Products Research*, New York, USA.

Poster 2 **Bladt, T.T**; Larsen, T.O.; Gotfredsen, C.H. The Use of 2D NMR for Fungal Anticancer Natural Products. *Poster at 31th Danish NMR Meeting*, Ringkøbing, Denmark, **2010**.

Nomenclature

7-AAD	7-Amino-Actinomycin
ACN	Acetonitrile
Ahp	Amino Hydroxy Piperidone
ALK	Alkaloid Forming Agar
Amp	Amino Methoxy Piperidone
BA	Butyric Acid
BAPNA	Benzoyl-L-Arginine-*p*-Nitroanilide Hydrochloride
CLL	Chronic Lymphocytic Leukemia
COSY	Correlation Spectroscopy
CYA	Czapek Yeast Agar
DAD	Diode Array Detection
DKFZ	German Cancer Research Center
DMSO	Dimethyl Sulfoxide
DTU	Technical University of Denmark
DTU Systems Biology	Department of Systems Biology
ED_{50}	Medial Effective Dose
ESI^+	Positive Electrospray Ionization
E-SPE	Explorative Solid Phase Extraction
FA	Formic Acid
FDAA	1-Fluoro-2,4-Dinitrophenyl-5-L-Alanine Amide
Gln	Glutamine
Glu	Glutamic Acid
HA	Hexanoic Acid
HcAla	Hydroxycyclohexenyl Alanine
HMBC	Heteronuclear Multiple Bond Correlation
HMP	Hydroxy Methylproline
HRMS	High Resolution Mass Spectrometry
HSQC	Heteronuclear Single Quantum Coherence
Hty	Homotyrosine
IC_{50}	Median Inhibitory Concentration
Ile	Isoleucine
LC	Liquid Chromatography
LC_{50}	Median Lethal Concentration
Leu	Leucine
L-FDAA	(1-Fluoro-2,4-Dinitrophenyl)-5-L-Alanine Amide
LR	Long Range
MAX	Mixed mode Anion-Exchanger
MEA	Malt Extract Agar

MeOH	Methanol
MQ	Mili-Q Water
MS	Mass Spectrometry
*N*Me-Phe	*N*-Methylated-Phenylalanine
*N*Me-Tyr	*N*-Methylated-Tyrosine
nM	Nano Molar
NMR	Nuclear Magnetic Resonance
NOESY	Nuclear Overhauser Effect Spectroscopy
NPs	Natural Products
NRP	Non-Ribosomal Peptide
ORD-CD	Optical Rotatory Dispersion-Circular Dichroism
OSMAC	One Strain – Many Compounds
PBMC	Peripheral Blood Mononuclear Cells
Phe	Phenylalanine
PP	Protein Phosphatase
qTOF	Quadrupole Time Of Flight
ROESY	Rotating Frame Nuclear Overhauser Effect Spectroscopy
RP	Reverse Phase
SAR	Structure-Activity Relationship
SAX	Strong Anion-Exchanger
SCX	Strong Cation-Exchanger
SGGPNA	Suc-Gly-Gly-*p*-Nitroanilide
Thr	Threonine
TOCSY	Total Correlation Spectroscopy
Trp	Tryptophan
Tyr	Tyrosine
UHPLC	Ultra-High-Performance Liquid Chromatography
UV	Ultra Violet
Val	Valine
YES	Yeast Extract Sucrose
µM	Micro Molar

Contents

Background

Cancer is characterized by *American Cancer Society* as an "uncontrolled growth and spread of abnormal cells" [1]. Different treatments, such as surgery, radiation, hormone therapy, biological therapy, and chemotherapy are used in the struggle against cancer [1]. The use of chemotherapeutics goes back to the early 20th century, where it was discovered by 'accident' during World War I. Several hundred people were exposed to mustard gas (1,5-dichloro-3-thia-pentane) and following they showed very low white blood cell counts. This discovery was used in cancer research in the hope of finding an agent with a similar effect on certain types of blood cancers. This led to the development of the first chemotherapeutic agent, nitrogen mustard. The therapeutic effect was unfortunately only temporary [2,3]. From the first chemotherapy agents in the 1940's and up until today, more than 200 anticancer drugs has been approved for clinical use. Approx. 40 % of them are natural products (NPs) or derived from NPs [4,5].

This PhD thesis is concerned with the screening and discovery of compounds from filamentous fungi that act against a specific type of cancer, chronic lymphocytic leukemia (CLL). These cells differ from other cancer cells in that they have entered a prolonged non-dividing arrest stated in the G_0/G_1 phase of the cell cycle. This results in a defective apoptotic mechanism and allows the CLL cells to escape apoptosis [6,7]. CLL is the most common type of leukemia among adults in the Western World, accounting for 30 % of all reported cases [8]. CLL is generally considered a heterogeneous disease with a large diversity in clinical behavior between patients. When diagnosed, many patients remain asymptomatic for decades when other develops the disease rapid and progressive whereupon they die within two to three years after diagnosed [9]. The CLL cells tend to accumulate at various locations in the body of patients including the blood, lymph nodes, bone marrow, spleen, and liver, thereby they overshadow other blood cells [6]. The accumulation of CLL cells is mainly due to suppression of apoptotic cell death, rather than increased cell proliferation [10]. *In vivo*, CLL cells are associated with a survival-inducing microenvironment of stromal cells, non-malignant leukocytes, so-called nurse-like cells, as well as growth and differentiation factors [11,12]. Removed from their natural microenvironment, the CLL cells rapidly undergo apoptosis *in vitro* even though they *in vivo* are long-lived cells [13]. This dependence of the surrounding microenvironment prolongs the survival of CLL cells significantly and has led to the development of a co-culture system containing CLL and human bone marrow-derived cells. In the co-culture, the CLL cells were able to survive for several months *in vitro* [14]. The protective effects caused by these bone marrow infiltrating cells in the surrounding microenvironment, results in significantly higher resistance to chemotherapeutics. As a consequence of the diverse courses of CLL and the heterogeneous clinical response, various treatment strategies are demanded [8,15]. Patients with asymptomatic and stable disease courses are currently not treated, due to lack of any survival benefits. In these cases treatment will only be introduced if symptoms arises [9,16]. Since the 1960's alkylating agents such as chlorambucil and

fludarabine have been used as standard first-line therapy for treatment of CLL. They are still used today either as monotherapy or as combination chemotherapies or chemoimmunotherapies [17,18]. Terasawa *et al.* conclude that "no single treatment showed significantly better overall survival than any other" [18]. In general, CLL is considered as an incurable condition and applied treatment strategies primarily aim at prolonging patient survival. Consequently, there is a great need for discovery and development of new chemotherapeutic agents for treatment of CLL [16,18,19].

A co-culture assay suitable for screening fungal extracts, fractions, and single compounds has been established (section 2.1). Altogether, 289 fungal raw extracts from 137 fungal strains were screened for apoptosis-inducing activity towards CLL cell *in vitro*. The extracts that exhibited the highest bioactivity were pursued to track the activity into single fractions/compounds by a combined analytical and bio-guided approach. This approach builds on ultra-high-performance liquid chromatography-diode detector array-high resolution mass spectrometry (UHPLC-DAD-HRMS)-based dereplication for fast identification of known compounds in the extracts combined with the CLL stromal cell co-cultured assay to follow the activity during each purifications step.

This PhD thesis is organized in 6 chapters, where results and discussion from publications are used, though I have clarified and elaborated on the contents. All publications and supplementary files including experimental are enclosed in appendix. The first chapter introduces the scope of this PhD project starting with known anticancer NPs (**paper 1**) followed by an overview of the applied assays, screenings approach, and analytical NPs chemistry. Chapter 2 outlines the results and discussion of nine bioactive crude extracts and covers the whole screening process from activity to single compounds by a combined analytical and bio-guided approach (**paper 2**). Chapter 3 focuses on the results and discussion in the discovery process of bioactive ophiobolins (**paper 2**). Chapter 4 describes the structures of two new cytochalasins and their activity towards CLL cells (**paper 3**). Chapter 5 address the isolation and structure elucidation of cyclic peptides produced by cyanobacteria and covers the results of my external stay with Professor Shmuel Carmeli at Tel Aviv University, Israel (**paper 4**). Finally, chapter 6 holds the overall discussion, perspectives, and concluding remarks that enclose what I have learned during this project.

Chapter 1

Introduction

1.1 Anticancer Compounds Produced by Filamentous Fungi

Fungal NPs represent an amazingly high structural variety and complexity in their chemical scaffolds, often rich in stereochemistry, concatenated rings, and reactive functional groups. Many hypotheses about the purpose of secondary metabolism in fungi have been suggested over the years. One of the more plausible theories for NPs production is the model proposed by Williams *et al*. saying that secondary metabolites serve to improve the overall fitness of the producing organism "by acting at specific receptors in competing organisms" [20]. The structural features of many NPs provide favorable chemical interactions, making them capable of binding to receptors with remarkable affinity and specificity. Many of these compounds are even privileged structures where one compound interacts with many different biological receptors and as a result show multiple bioactivities [21]. This makes NPs very attractive for drug discovery purposes. The last fifty years intensive research in bioactive fungal NPs have, in fact, provided the world with new pharmaceuticals in infection diseases, immunopharmacology, organ transplant, cardiovascular diseases, cancer etc. [5]. Owe to the complexity of many NPs, synthetic approaches can be difficult or even impossible. Thus, we often rely on Nature's own biosynthetic machinery to create these molecules. The major biosynthetic classes in filamentous fungi are polyketides, terpenoids, and non-ribosomal peptide (NRP).

One of the best known anticancer drugs of natural origin is taxol, also known as paclitaxel (Figure 1), originally isolated from the bark of yew tree *Taxus brevifolia* [22]. Clinical development of taxol was delayed due to problems with production of sufficient quantities of the compound. This problem was solved 20 years later when it was demonstrated that taxol was produced by fungi as well [23,24]. Taxol was approved as an anticancer drug against a wide range of tumors in the 1990s and is the first billion dollar drug against cancer [25,26]. Today, taxol is routinely used to treat ovarian, breast and lung tumors as well as Kaposi's sarcoma [27].

Figure 1. Taxol, the first billion dollar anti-cancer drug developed.

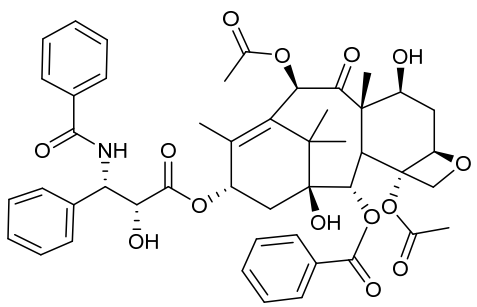

The three small antifungal polyketides terrein, brefeldin A, and griseofulvin are examples of well-known metabolites that decades after they were discovered were shown to exhibit novel anticancer activities. The small antifungal [28] polyketide terrein (Figure 2a) produced by *A. terreus* has been known since 1935 [29]. Almost 80 years later, it was found that terrein inhibits breast cancer by induction of apoptosis with a median inhibitory concentration (IC_{50}) value of 1.1 nM in MCF-7 cell line. That makes terrein 100-fold more potent than taxol against this cell line [30].

Figure 2. Small antifungal polyketides with anticancer activity: (a) Terrein, (b) Brefeldin A, and (c) Griseofulvin.

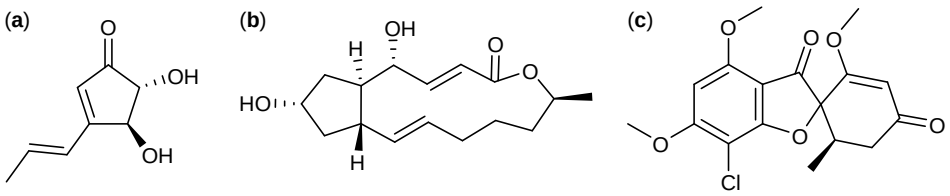

Brefeldin A (Figure 2b), another small antifungal [31,32] polyketide was identified as inducer of apoptosis in leukemia, colon, prostate, cervical, breast, and lung cancer cell lines almost 40 years after it was discovered [33–37]. The inhibiting effect of brefeldin A was demonstrated with IC_{50} values between 6.3 and 110 nM [36,37]. In this PhD project the activity of brefeldin A towards CLL cells is discussed in section 2.1 (**paper 2**).

Another known antifungal [38,39] compound, griseofulvin (Figure 2c), was discovered in 1939 [40] but first connected to cancer 30 years later [41]. In 2007, it was furthermore shown to inhibits centrosomal clustering in human squamous cancer SCC-114 cell line with an IC_{50} value of 35 μM [42,43]. 34 analogs has been synthesized for a structure-activity-relationship (SAR) study and the synthetic analog GF-15 increased the inhibitory effect of centrosomal clustering in the SCC-114 cells 39-fold with an IC_{50} value of 0.9 μM [44].

Cyclic di-peptides called diketopiperazines are some of the more potent anticancer compounds and are in general known as cell cycle inhibitors of the G2/M phase [45]. The diketopiperazine fumitremorgin C (Figure 3a) was found active against human leukemia P-388 cell line with a medial effective dose (ED_{50}) value of 10.3 μM and the analog 12,13-dihydroxyfumitremorgin C has antiproliferative effects on human leukemia U-937 and human prostate cancer PC-3 cell lines, with IC_{50} values of 1.8 and 6.6 μM, respectively [46,47].

Figure 3. Diketopiperazines with anticancer activity. (a) Fumitremorgin C, (b) Phenylahistin, and (c) Emestrin A.

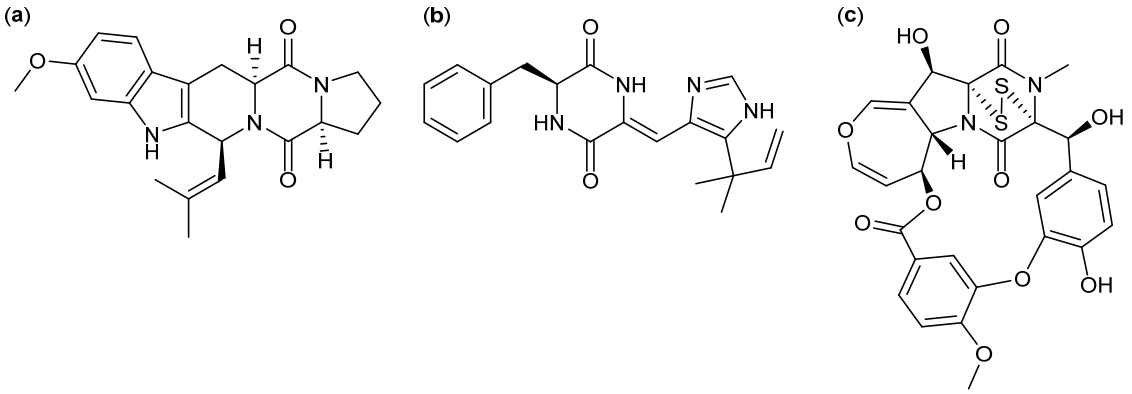

Another diketopiperazine, phenylahistin (Figure 3b), that was isolated as a mixture of enantiomers [48]. (−)-Phenylahistin was more active than (+)-phenylahistin against dermal, lung, ovary, leukemia, breast, and colon cancer cell lines with IC_{50} between 0.18 and 3.7 μM [49]. A synthetic analog, plinabulin displays very potent activity against human prostate carcinoma cell line and has now entered phase II clinical trials [50]. Recently, more than 60 synthetic analogs of plinabulin have been designed and synthesized. The more active analog with a benzoyl group coupled on the phenylalanine (Phe) unit was 10-fold more active than plinabulin with an IC_{50} value as low as 1.4 nM [50].

Another group of diketopiperazines with anticancer activity contain a poly-sulfide bridge in the diketopiperazine ring. The antifungal [51] compound emestrin A (Figure 3c) inhibits human leukemia with an IC_{50} value of 83.5 nM [52]. Eight structural analogs of emestrin A were later isolated and found to have strong antiproliferative effects on the human prostate cancer cell line with IC_{50} values down to 9.3 nM for the more potent emestrin C. Furthermore, it was proven that the activity decreased when the macro cyclic ring was opened and the polysulfide bridge in the diketopiperazine was absent [53]. The activity of emestrin A towards CLL cells are addressed in section 2.1 (**paper 2**).

The ophiobolins are a family of naturally occurring sesterterpenoids, currently constituting 35 known analogues [54–58]. They all consist of a C_{25} skeleton with a dicyclopenta[a,d]cyclooctane ring system. Some ophiobolins have an extra ring incorporated, for example ophiobolin A (Figure 4), forming a tetra-cyclic structure [59].

Figure 4. Ophiobolin A

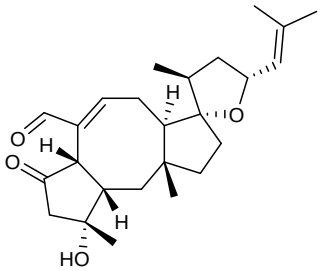

Ophiobolins exhibit a broad spectrum of inhibitory activity against cancer cell lines, including lung cancer, breast cancer, colon cancer, melanoma, leukemia and ovarian cell lines with IC_{50} values between 0.06 and 0.3 µM [60,61]. In 2012 the novel ophiobolin O was discovered and it was found to inhibit breast cancer and leukemia cell lines with IC_{50} values of 17.9 and 4.7 µM, respectively [55,56]. In 2013 the novel 3-anhydro-6-hydroxyophiobolin A was isolated and found active against lung cancer and leukemia cell lines with IC_{50} values of 6.5 and 4.1 µM, respectively [57]. This PhD study discusses in detail the activity of the ophiobolins towards CLL cells (chapter 3, **paper 2**).

A group of compounds that are biosynthesized by incorporation of amino acids into a core polyketide part is the cytochalasins and the chaetoglobosins (**paper 1**). The cytochalasins contains a Phe coupled to the polyketide chain where the chaetoglobosins have an tryptophan (Trp) moiety [62,63]. Many of the cytochalasins have shown inhibitory activities towards lung, ovarian, colon cancer as well as human leukemia with cytochalasin E (Figure 5a) as one of the most potent analogs [64,65]. The activity of three cytochalasins towards CLL cells are discussed in chapter 4 (**paper 3**).

Figure 5. (a) Cytochalasin E and (b) Chaetoglobosin B.

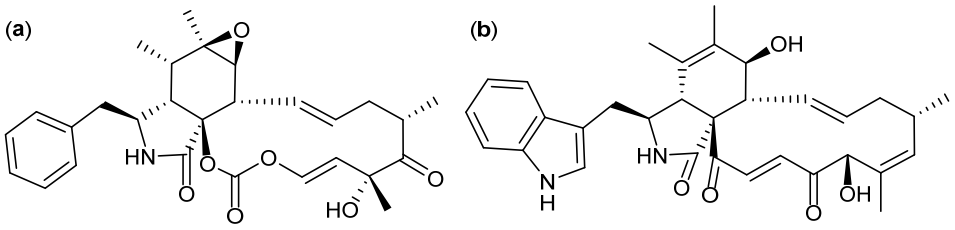

The chaetoglobosins showed activity against cancer cell lines as well. Of the more potent ones was chaetoglobosin B (Figure 5b) that inhibited human breast cancer cell line with an IC_{50} value of 3.0 µM [66] and chaetoglobosin D that inhibited breast- and adenocarcinoma cancer cell lines with IC_{50} values between 3.4 and 12.2 µM [66]. Most recently chaetoglobosin A was found to induce apoptosis in CLL cells with a median lethal concentrations (LC_{50}) value of 2.8 µM [67].

1.2 Screening Towards Chronic Lymphocytic Leukemia (CLL)

Many of the anticancer compounds used in clinical treatment today are general cytotoxic, yet they kill cancer cells more efficiently than healthy cells in the body. The activity of these compounds is often based on cells that divide very fast such as most cancer cells [68]. Side effects arise do to the fact that other cells for example hair follicles and bone marrow divide rapid as well and consequently become targets [68]. Many of these chemotherapeutics has been approved in cancer treatment despite severe side effects due to the critical and lethal consequences of cancer. Even with a high tolerance level of side effects in cancer treatment, most general cytotoxic compounds are not compatible with clinical applications and consequently most drug discovery

approaches today make a huge effort in development of selective target molecules or 'magic bullets' [21,43,68,69]. Cytotoxic response towards target cells in an assay may originate from large amounts of undesired general cytotoxic compound found in most fungal extract [70–72], which may mask the activity of compounds with selective activity present only in lower concentrations [73]. One way to address general cytotoxicity and recognize 'magic bullets' the extracts is through a orthogonal screening approach where fractions/single compounds are screened towards an array of targets cells including healthy cells. The bio-guided separation is then directed towards fractions that do not target healthy cells and with activity against single cell lines. This application is though debatable regarding crude extracts as they might contain both general cytotoxic compounds as well as compounds with selective activity.

Another way of facilitating 'magic bullets' is through phenotypic drug discovery where a mechanism unique for the cancer cells is targeted [74]. Inhibition of centrosomal clustering targeting a special mechanism unique for cancer cells is one example of phenotypic drug discovery [43].

Bioassay-guided separation of fungal extracts includes screening of various types of samples, from very complex mixtures in the crude extracts to the pure compound. This variety of samples require a very robust assay that is sensitive from the very low to the high concentrations with a minimum of both false negative and false positive samples [75]. Differences in concentrations of compounds added to the assay complicate the interpretation of the results since a higher response may be observed for a moderate active compound in high concentrations compared to a very potent compound in low concentration.

The screening towards CLL cells in this PhD project is based on two complementary bioassays, the cell viability assay, which is a rough measurement of the effect on the CLL cells and the apoptosis assay, which is a co-cultured assay measuring apoptotic cell death of the cells. CLL cells are uncultivable and whole blood samples are obtained directly from patients that matched the standard diagnostic criteria for CLL for both assays (**paper 2**).

Cell viability is evaluated using CellTiter-Glo® assay providing fast results that show the effect on CLL cells *in vitro* of fractions and single compounds. The CLL cells are only supported by conditioned media and not directly by the survival-inducing microenvironment of stromal cells. Conditioned media is enriched by soluble factors excreted from the stromal cells whereby the CLL cells survive in approximately three days, which is sufficient for this assay [14]. The CLL cells are exposed to fractions or single compounds in different concentrations and incubated for 24 hours. The results are determined by the luminescence signals generated by the luciferase reaction (Figure 6) when ATP is present and corresponds to the extent of living cells (**paper 2**).

Figure 6. The luciferase reaction where luciferin is oxidized in the presence ATP and hereby emits light catalyzed by the protein luciferase. Luminescence signals is used as a measure for cell viability after CLL cells has been exposed to fractions or single compounds.

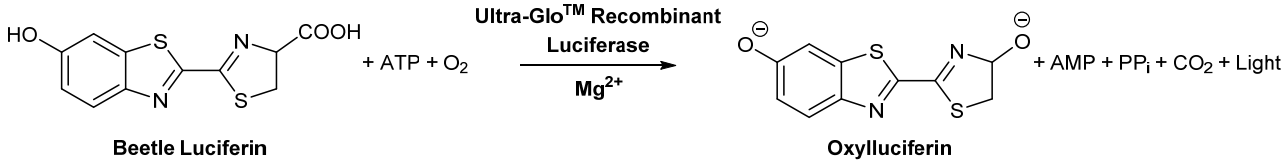

Beetle Luciferin **Oxylluciferin**

Complementary and more profound than the cell viability assay is the apoptotic assay. The CLL cells are directly supported by the survival-inducing microenvironment of stromal cells in a co-culture platform mimicking *in vivo* conditions. The co-culture platform allows the cells to survive for several months *in vitro* [14]. The CLL cells are exposed to fractions or single compounds in different concentrations and incubated for 48 hours. Apoptotic cell death is detected by staining with labeled annexin V that detects early apoptosis and 7-amino-actinomycin (7-AAD) that detect dead cells. The cell membrane of normal cell contains a strictly asymmetric lipid bilayer. The negatively charged phospholipid, called phosphatidyl serine, is located on the inside of the cell and the cell is not possible to stain (Figure 7a). The cell membrane of an apoptotic cell is flipped a phosphatidyl serine is exposed, which allows Annexin V to stain the cell (Figure 7b) [76].

Figure 7. Staining of apoptotic cell with labelled Annexin V. (a) The cell membrane of a normal cell is not possible to stain with Annexin V since phosphatidyl serine (edged, purple) is on the inside of the cell membrane. (b) When a cell become apoptotic parts of the cell membrane is flipped inside out and phosphatidyl serine is hereby translocated from the inner to the outer side of the plasma membrane. This flipping allows staining with labeled annexin V due to the exposure of phosphatidyl serine (edged, purple) in the apoptotic cell. *Figure obtained from Van Engeland et al.* [76].

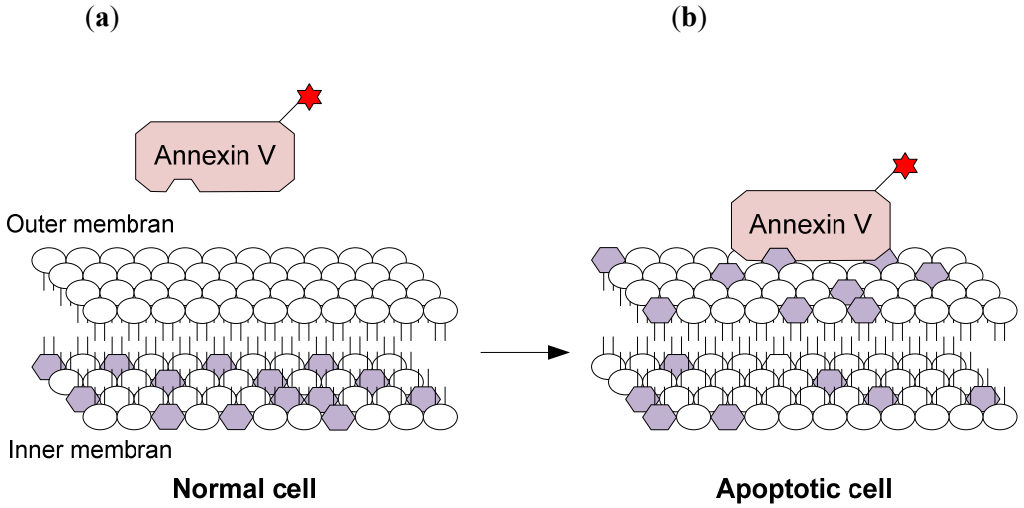

The cell membrane of a cell that die by apoptosis is opened up and DNA is exposed to the media and allow staining with 7-AAD that binds directly to DNA and indicate cell death [77]. The double-labeling enables discrimination of early apoptotic cells labeled with annexin V solely,

and dead cells which are positive for both annexin V and 7-AAD [76–78]. To study the progression of and confirm induction of apoptosis, active caspase-3 is stained using BD Cytofix/Cytoperm^{TM}. Active caspase-3 indicates the final steps of apoptosis [77,78].

1.3 Screening Approach and Profiling of Natural Products

Fungal extracts are often complex mixtures of secondary metabolites of unknown chemical compositions where the compound(s) responsible for activity is unknown. The goal for the natural product chemist is to reduce time from the bioactivity is observed to the identification of the active compound(s). Consequently, establishing a suitable strategy is essential to any screening program [79]. It is possible to distinguish between bio and targeted guided screening strategies. Bio-guided screening relies on discovery of compounds targeting a specific disease or biological mechanism. The setup requires high chemodiversity and hereby a high potential of discovering novel compounds but also include the risk of overlooking compounds with other activities. The targeted-guided screening strategy depends on few extracts tested towards many diseases or biological mechanism [73,80]. In this PhD project both bio-guided and target-guided screening approaches are applied. The target-guided approach based on MS and NMR, respectively is described in chapter 4 and 5 (**paper 3 and 4**).

The bio-guided approach was combined with dereplication based on the analysis of the spectroscopic data generated from state-of-the-art UHPLC-DAD-HRMS. The bioactivity is followed in each step from crude extract to single compound with activity (**paper 2**). In a preliminary screen, the selection of fungi is essential and needs to represent as large a biodiversity as possible, with the hope of an equally high chemodiversity (**paper 2**) [79]. The fungal collection at DTU Systems Biology covers a huge biodiversity with approx. 30,000 fungal strains capable of producing hundred thousands of compounds. One strategy to increase chemodiversity for rapid bio-testing is to select strains representing a wide variety of species with a limited number of strains from each species [79,81]. The spectrum of compounds produced by the individual strains can further be varied and increased by the 'one strain – many compounds' (OSMAC) approach, through variation of culture conditions [82]. A large number of fungi cultivated under different conditions can be extracted in micro-scale by a very fast procedure leaving enough extract for both HPLC-DAD-HRMS and bioassay. Results from the bioassay provide an initial idea of the bioactivity of each extract. Extracts with the most potent or selective bioactivities are selected for large scale incubation to pursue the observed bioactivity. Small scale prefractionation can be very helpful to lower the complexity of the crude extract and to avoid that active compounds are overlooked due to masking or concentration issues and. E-SPE applying an array of orthogonal separation techniques combined with bioassay has proven to be very powerful in prefractionation of fungal extracts [83].

Dereplication (section 1.4) is a rapid method for tentative identification of known NPs, based on detailed chemical analysis before unnecessary time is spent on rediscovery of already known compounds. New strategies and methodologies for fast dereplication have been developed within the last decade. The performance of mass spectrometers is continuously improving, including

easy access to both positive and negative ionization spectra even during fast UHPLC resulting in tentative identification of a potential active candidate. Information obtained from E-SPE (section 1.5) functions as preliminary chemical characterization and as guidance for the preparative isolation of a single compound.

Isolation is important to verify the activity of the pure compound and, if novel to elucidate the structure by nuclear magnetic resonance (NMR) spectroscopy. The absolute configuration of a compound can be messured by optical rotation or optical rotatory dispersion-circular dichroism (ORD-CD). Alternatively, if a suitable crystal can be obtained, X-ray crystallography can be applied for both structure elucidation and absolute configuration. This approach may result in new drug hits and following optimization of a drug lead e.g. through semi-synthetic analogs and bioavailability considerations etc.

1.4 MS-based Dereplication

Fungal extracts are often very complex mixtures of NPs due to mixed biosynthetic origin [79,84,85] and UHPLC-DAD-HRMS-based dereplication is an approach that ensures a high throughput and reproducibility of complex fungal extracts. This approach is based on the monoisotopic mass found in the mass spectra and hereby the elemental composition of a compound [86]. This part of the process is prone to error since the mass spectra is easily misinterpreted due to strong adduct ions such as the sodiated adduct, $[M+Na]^+$, or the ammoniated adduct, $[M+NH_4]^+$, which may lead to false identification of the pseudo molecular ion, $[M+H]^+$. Adduct patterns can be identified through mass differences between peaks in the mass spectra [86]. Mass accuracy and isotope ratio are vital for MS-based dereplication. Currently state-of-the-art HRMS has a mass accuracy of typically 1-5 ppm and accuracy of isotope ratio of 1-2 %, which drastically decreases the number of potential elementary compositions found for each peak. The formula(s) generated from the monoisotopic mass is subsequently used as a query in an appropriate database for example AntiBase2012 (40,066 compounds), which is a comprehensive database for NPs from microorganisms [87]. The high mass accuracy ensure that database searches are conducted with the fewest possible candidates [86,88]. The number of compounds with a given elementary composition can vary a lot and candidate elimination on the basis of for example ultra-violet (UV) chromophore and retention time may be necessary [86]. Small molecules in particularly polyketides and alkaloids often contains conjugated double bonds that results in more or less unique UV-chromophores. The UV data from target peaks are matched against database for tentative identification of NPs [79,89]. The use of UV spectral information is often important in the dereplication process for prioritizing between the MS-generated candidates [90,91]. The high resolution of each peak in UHPLC chromatograms has made it easier to obtain a UV spectrum of practically all compounds even in complicated mixtures such as fungal extract. This makes UV detection a readily accessible technique that is relevant in drug discovery [79]. The combined information gained from the dereplication process is used to direct the research and may function as an early stop-or-go decision to avoid spending time on rediscovering compounds.

It is very important to be incisive and balance these early stop-or-go decisions to increase the possibility of discovering novel anticancer skeletons.

1.5 Prefractionation by explorative solid phase extraction (E-SPE)

Prefractionation of complex crude fungal extracts is important to lower the complexity of the extract, increasing the relative concentration above the screening threshold, or even unmasking selectively active compounds [73,92]. Additionally, prefractionation can provide preliminary chemical characterization of interesting compounds in the fractions. E-SPE is one approach of prefractionation, which use small pre-packed columns with orthogonal stationary phases such as reverse phase (RP), normal phase, size-exclusion, and ion-exchange resins [83,93]. The goal of applying different SPE columns is to identify a column where a target molecule is selectively absorbed on the resin and unwanted compounds are eluted followed by a second step where the concentrated target molecule is eluted.

Traditionally, RP chromatography has been the favored choice for separation of NPs but co-eluting interferences of several compounds are often a huge problem due to the complexity in fungal extracts. Co-eluting interferences can be reduced or even prevented by choosing orthogonal purifications strategies [83]. The use of orthogonal stationary phases makes it possible to fully separate compounds with different functionalities even though they would co-elute on traditional RP chromatography (section 2.1, **paper 2**). New insights of the chemical functionalities of the NPs in the extract can be gained by this method and guidelines for preparative scale isolation strategies may be provided. Furthermore, the small scale E-SPE approach provides small scale fractions for bioassay [83]. The E-SPE strategy that builds on ion-exchanger columns for example strong anion-exchanger (SAX), mixed mode anion-exchanger (MAX), and strong cation-exchanger (SCX) (Figure 8) has proven to be very powerful due to the relative high percentages of ionizable functional groups in fungal NPs [83]. The mixed mode of the Oasis MAX® column possesses both RP and anion-exchange functionalities. The MAX column is able to retain both strong and weaker anions compared to the SAX column that only retrains strong anions primarily carboxylic acids [83,94].

Figure 8. Optimized collection of ion-exchangers (SAX, MAX and SCX) and normal phase (diol and amino) SPE columns in the E-SPE setup. The orthogonal stationary phases of the columns enables different selectivity of an extract. *Figure adapted from Maria Månsson*.

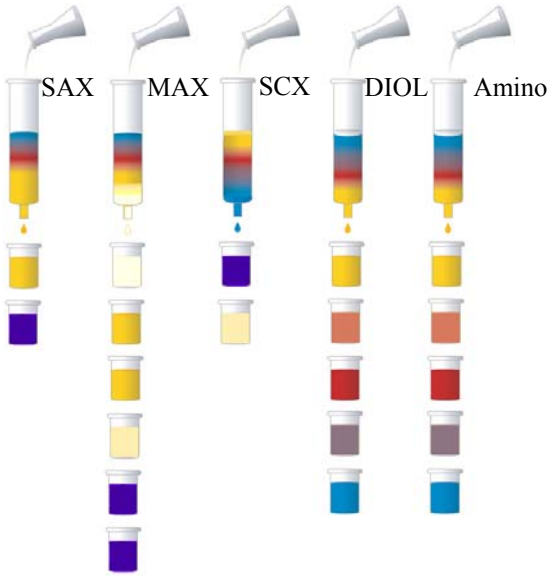

The E-SPE setup applied in this project has been developed according to the original paper by Månsson *et al.* [83]. Orthogonal to ion-exchangers are normal phase columns for example with diol- or amino-resin, which have been introduced to the protocol instead of size chromatography (LH-20) (Figure 9). The amino column has a good ability for retaining more polar compounds as well as proton donors for example alcohols and phenols. Compared to the amino, the diol stationary phase is very similar regarding separation but with a weaker retention ability compared to the amino column [95]. The reason for this adjustment is primarily based on practical arguments. LH-20 columns are not commercial available contrary to pre-packed diol and amino columns. The requirement of column packing of the LH-20 column is time-consuming and complicates the E-SPE setup especially for numerous extracts. Additionally, the pre-packed columns are more suitable for automation by for example SPE workstations. The combination of the SPE columns in the E-SPE approach offers a combined analytical and biological indication of the functionality and polarity of the active compound in a crude extract. The E-SPE approach opens the opportunity for comparative dereplication where peaks from inactive fraction are eliminated by comparison to chromatographic peaks in the active fractions. This results in a reduced number of peaks to be dereplicated compared to the crude extract and hereby time saved (**paper 2**) [83].

Chapter 2

Discovery of Fungal Secondary Metabolites Targeting CLL

The discovery of NPs with activity towards CLL was based on the great chemodiversity found at DTU Systems Biology and the CLL/stromal cell co-culture platform developed at DKFZ. In a screening campaign that covered 289 crude fungal extracts the activities in nine of the most active extracts were pursue (Figure 9) through dereplication combined with E-SPE and bioassay (**paper 2**). The 289 fungal extracts were prepared from cultivation of 137 fungal strains (Table S1 in **paper 2** supplementary file) on a selection of solid media at variable temperatures in accordance with the OSMAC approach [82]. The extracts were prepared by the micro-extraction method developed by Smedsgaard [96]. To obtain a representative sample of the fungal colonies the plugs were taken across the colony. 61 extracts showed activity towards CLL cells (Table S2 in **paper 2** supplementary file). Nine of the candidates that displayed the highest level of activity were selected for further bio-testing. Large-scale extracts were prepared from incubation on the media supporting the highest level of bioactivity, and the extracts were prefractionated before further testing.

Figure 9. Screening set-up: 289 fungal extracts (from 137 fungal strains) were tested for cytotoxic activity towards CLL cells. From the 61 extracts with activity the nine candidates that displayed the highest bioassay activity were selected for further bio testing and single compound isolation in a large scale.

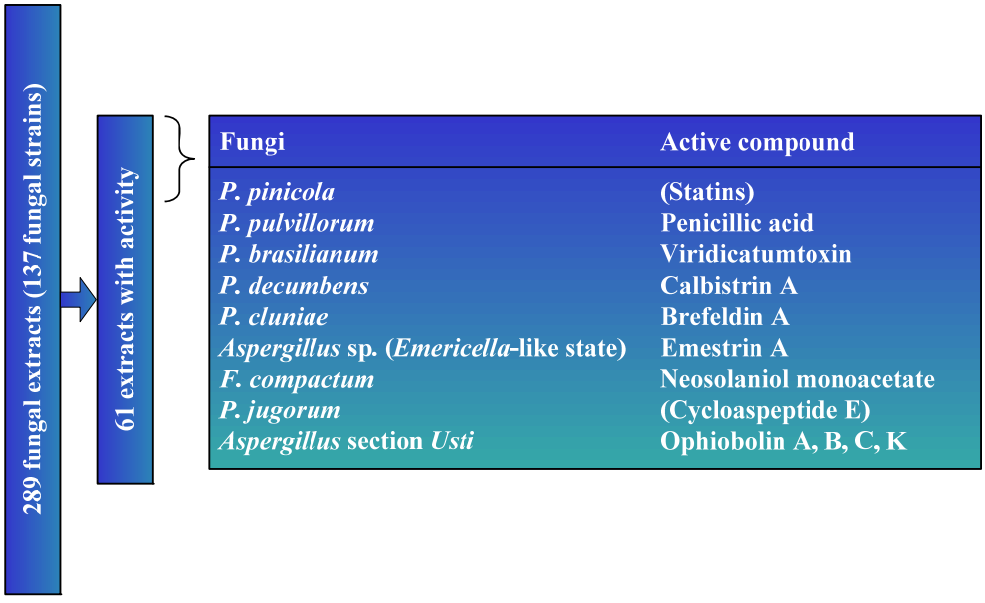

2.1 Comparative Dereplication Based on Explorative Solid Phase Extraction

The E-SPE strategy was applied to a series of highly complex extracts, i.e. *P. brasilianum* (IBT 22244), *P. decumbens* (IBT 11843), *P. cluniae* (IBT 21051), *Aspergillus* sp. (*Emericella*-like state) (IBT 22838), and *Fusarium compactum* (IBT 9034).

Penicillium brasilianum

The extract of *P. brasilianum* (IBT 22244) was very potent against CLL cells *in vitro* (≈ 5 ng/ml) with the active compound retained on both anion-exchangers (SAX and MAX) as well as the two normal-phase columns (diol and amino), while unretained on the cation-exchanger (SCX). The combined biological and chromatographic information lead to the conclusion that the bioactive compound contained a strong anion. The large scale extract was fractionated on a SAX column. Comparison of chromatographic peaks from the fraction that contained neutral/basic compounds (Figure 10a) and the fraction with acidic compounds (Figure 10b), showed that the anion-exchange was extremely selective, removing the majority of inactive compounds from the extract.

Figure 10. E-SPE strategy based on a SAX column to separate co-eluting compounds in the crude extract of *P. brasilianum*. (a) UHPLC chromatograms of the SAX fraction that contained neutral/basic compounds. The ion trace of compound I (*m/z* 462.2387) is marked with red. (b) UHPLC chromatogram of the SAX fraction that contained acidic compounds. The ion trace of compound IV (*m/z* 548.1916) is marked with blue. (c) In the crude extract compound I and IV were co-eluting on a RP C_{18} column.

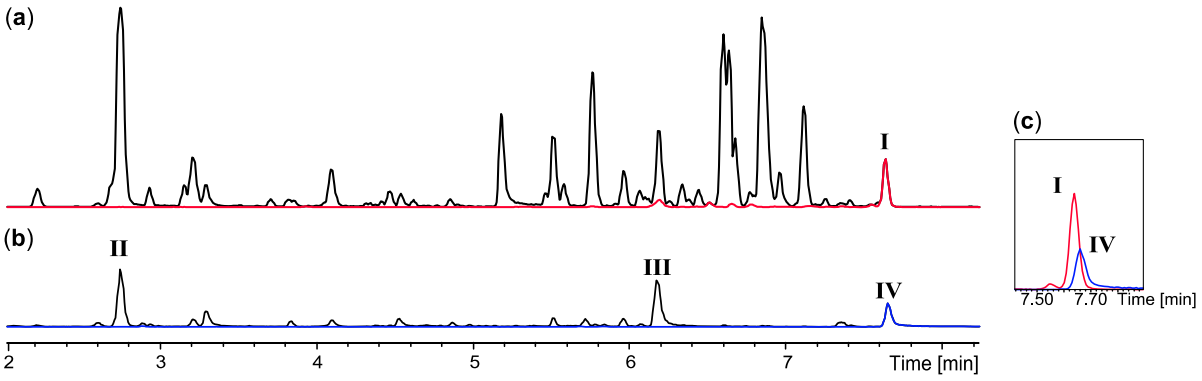

In the initial extract, the two compounds **I** and **IV** co-eluted on a C_{18} RP column (Figure 10c). These were easily and quantitatively separated on the SAX column due to the difference in charged functionalities. Only three major acidic compounds were left in the bioactive fraction (Figure 11a), which significantly simplifying the subsequent dereplication and purification process. Based on comparative HRMS analysis, compound **II** was immediately eliminated due to its presence in the inactive neutral/basic fraction. The molecular formula of compounds **III** and **IV** were established as $C_{15}H_{10}O_9$ (-0.7 ppm) and $C_{30}H_{31}NO_{10}$ (-0.2 ppm), respectively. These were used as queries in AntiBase2012 (Figure 11b) [87]. Compound **II** had no hits in AntiBase2012 that contained a strong anion, thus likely being a novel compound. Compound **IV** had two hits in

AntiBase2012. One of the candidates had no strong anion and was consequently eliminated that left viridicatumtoxin as the only candidate (Figure 11b).

Figure 11. Dereplication of the *P. brasilianum extract* (a) UHPLC chromatogram of the active SAX fraction that contained the acidic compounds as well as UV and MS spectra of the potential candidates. (b) Hits in Antibase2012.

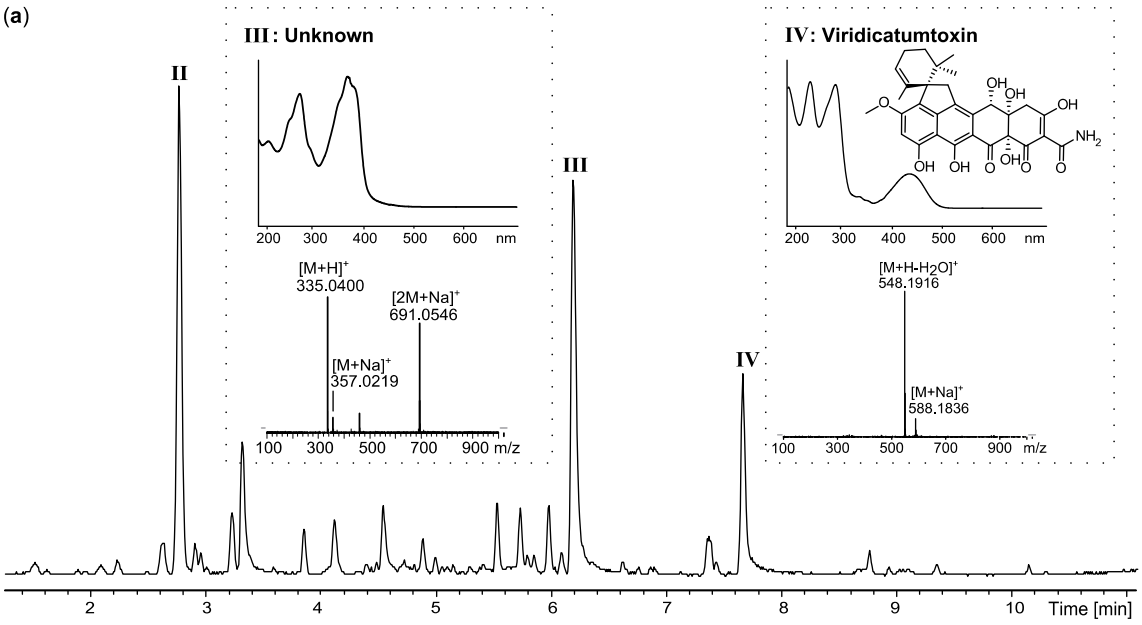

(**b**)

III: Unknown

Query	No. of candidates
$C_{15}H_{10}O_9$	1
Strong anion	0

IV: Viridicatumtoxin

Query	No. of candidates
$C_{30}H_{31}NO_{10}$	2
Strong anion	1

The identity of viridicatumtoxin as compound **IV** was confirmed 1) by comparison to the retention time and UV spectrum of an in-house standard from our database (1559 standards), 2) by the fact that it hold a strong anion, and 3) by having similar ^{1}H NMR chemical shifts as published for viridicatumtoxin [97]. Viridicatumtoxin was isolated as one of the most cytotoxic compounds tested towards CLL cells in this screening campaign with a LC_{50} value between 0.7 and 3.5 nM. Unfortunately, further testing revealed that the activity was not specific, as both CLL and stromal cells were targeted. Results from Annexin-V PE apoptosis assay displayed that the CLL cells did not die by apoptosis but more probably by necrosis though this suggestion not clearly can be distinguished by this assay.

Penicillium decumbens

One flash fraction (70 % organic) from the *P. decumbens* (IBT 11843) extract was found active towards CLL cells (≈ 200 ng/ml). Further E-SPE analysis showed that the active compound

was retained on SAX and MAX columns indicating the presence of a strong anion. By comparative dereplication tentative identifications of calbistrin A (Figure 12a) and B as well as their precursor (or decomposition product) versiol (Figure 12c) were established within the fraction.

Figure 12. Structure of (a) Calbistrin A, (b) Calbistrin C, and (c) Versiol.

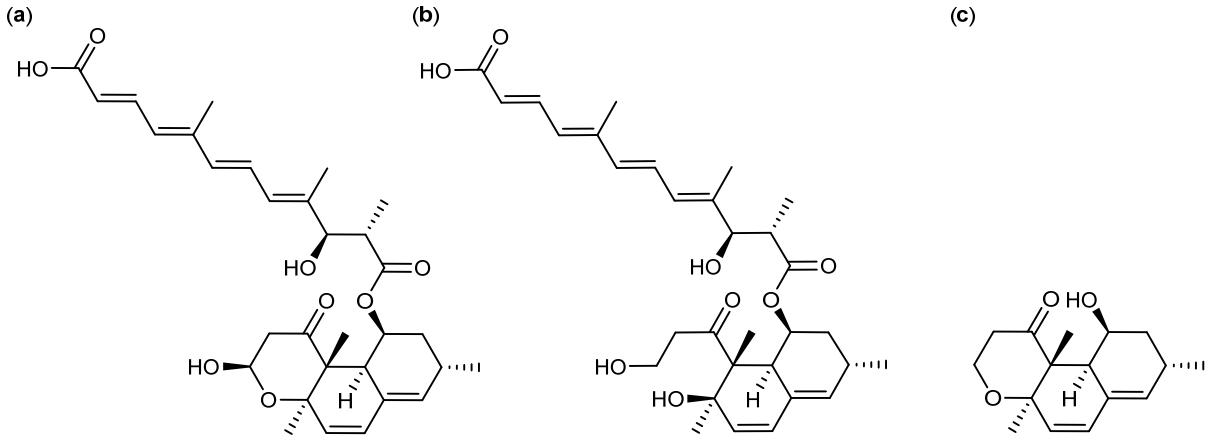

The MS based dereplication was complicated by the fact that the $[M+H]^+$ ion was absent in the mass spectra of calbistrin A and B. The presences of strong adduct- and fragmentation patterns consisting of the sodiated, $[M+Na]^+$, and the ammoniated, $[M+NH_4]^+$, adducts as well as neutral loss of one and two water molecules assisted the establishment of the monoisotopic masses and hereby the molecular formulas of calbistrin A and B. The identity of calbistrin A was confirmed by comparison of retention time and UV spectrum to an in-house standard as well as the presence of a carboxylic acid. The tentative identity of calbistrin B was confirmed by comparison of the UV spectrum to that of calbistrin A (Figure 12a). Testing of calbistrin A from our in-house metabolite collection showed general cytotoxic activity towards CLL and healthy cells. Comparative experiments with calbistrin C (Figure 12b) from the metabolite collection did not induce cell death, indicating that the pharmacophore is located in the versiol part (Figure 12c) of the molecule.

Penicillium cluniae

A bioactive flash fraction (activity approx. 100 ng/ml) from a *P. cluniae* (IBT 21051) extract was likewise subjected to E-SPE. Here, the bioactivity profiled revealed that the active compound was a medium to apolar compound with no charged functionalities. By comparative dereplication, the active compound was tentatively identified as brefeldin A (Figure 13a), which was in accordance with the profile revealed by E-SPE. The identity of brefeldin A was confirmed by its retention time and UV spectrum compared to an in-house standard. Brefeldin A is a known anticancer compound [34,98] and commercially available, thus the activity was easily confirmed

in the CLL assay. Unfortunately, the compound displayed general cytotoxic activity towards CLL cells (0.39-1.56 μM) and stromal cells in the same concentrations.

Figure 13. Examples of CLL active compounds discovered by E-SPE and comparative dereplication (a) Brefeldin produced by *P. cluniae*, (b) Emestrin A produced by *Aspergillus* sp. (*Emericella*-like state), and (c) Neosolaniol monoacetate produced by *F. compactum*.

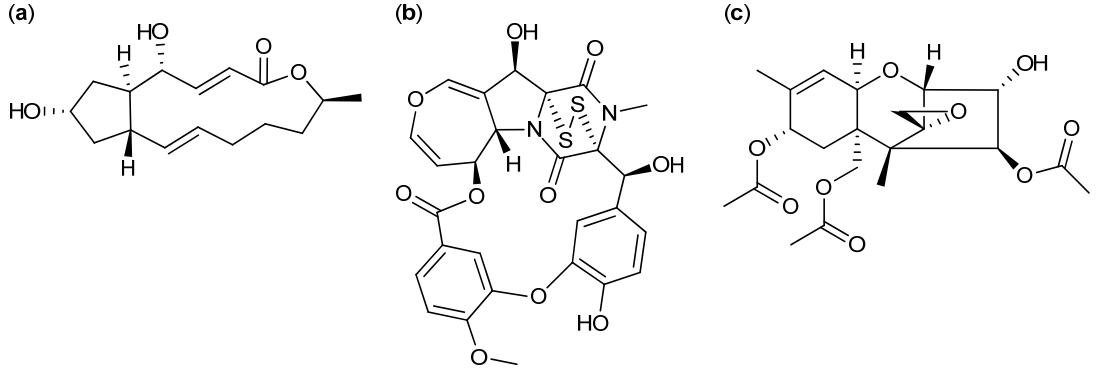

Aspergillus sp. (*Emericella*-like state)

The E-SPE strategy of the bioactive extract (≈ 40 ng/ml) from *Aspergillus* sp. (*Emericella*-like state, IBT 22838) resulted in retention of the bioactive compound on the amino normal phase SPE column. Fast comparative dereplication based on UV spectra and retention times of in-house standards as well as comparison of ^{1}H NMR chemical shifts [99] led to an identification of the known antifungal and anticancer compound, emestrin A (Figure 13b) [51,52,98]. The pure emestrin A isolated form the active fractions showed cytotoxic activity towards CLL cells and stromal cells at the same concentration levels. Accordingly, emestrin A is regarded as a generally cytotoxic compound with no therapeutic window [100]. No further work was pursued on the *Aspergillus* sp. (*Emericella*-like state) extract.

Fusarium compactum

The *F. compactum* (IBT 9034) extract displayed cytotoxic activity towards CLL cells at approximately 200 ng/ml. The bioactive compound from *F. compactum* was retained on both the diol and amino columns in the E-SPE prefractionation experiment. Comparative dereplication reviled only one candidate that might be responsible for the activity. The compound was tentatively identified as the known trichothecene, neosolaniol monoacetate (Figure 13c). The compound was isolated and the ^{1}H NMR data was compared to the literature for final identification of neosolaniol monoacetate [101]. Neosolaniol monoacetate was tested in the CLL assay and found as a generally cytotoxic, apoptosis inducing compound, why no further work was performed on the *F. compactum* extract.

Penicillium jugorum

The last example of bio-guided isolation based on E-SPE is demonstrated by the *P. jugorum* (IBT 22779) extract. The compound responsible for the activity was found in the fractions eluted by 60-70 % organic. Comparative dereplication leads to 4 potential candidates responsible for the activity. Further fractionation by the E-SPE approach eliminates compounds possessing anionic and cationic functionalities and comparative dereplication left cycloaspeptide E (Figure 14a) as the only potential candidate.

Figure 14. Structures of (a) cycloaspeptide E (tentative active), (b) Cycloaspeptide D (inconclusive data on activity), and (c) Cycloaspeptide A (tentative inactive)

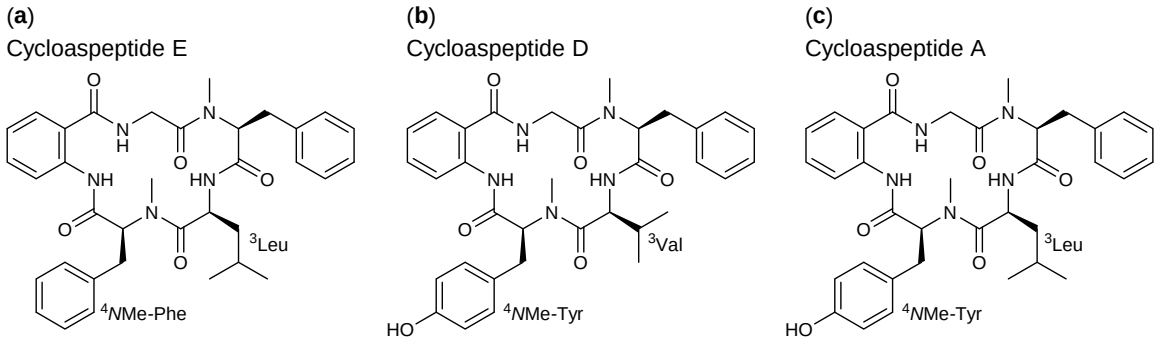

In our in-house metabolite collection we had the analog cycloaspeptide D (Figure 14b). To save time on purification of cycloaspeptide E we tested cycloaspeptide D to get an indication of the activity of the compound family. The results indicated that cycloaspeptide D induced apoptosis in CLL cells with a therapeutic window of activity around 18 µM. The results of cycloaspeptide D were considered inconclusive and cycloaspeptide D was regarded inactive due to the high concentration. Dereplication of some of the inactive fractions revealed the presence of cycloaspeptide A (Figure 14c) indicating that not all cycloaspeptide displayed activity towards CLL cells. The structural differences between cycloaspeptide E, D and A are found in the third and fourth position. In the third position have cycloaspeptide E and A leucine (Leu) where cycloaspeptide D has valine (Val). In the fourth position cycloaspeptide E has *N*-methylated-phenylalanine (*N*Me-Phe) while cycloaspeptide D and A have *N*-methylated-tyrosine (*N*Me-Tyr). If cycloaspeptide E is the compound responsible for the activity in the crude extract of *P. jugorum* the structural observations indicate that the pharmacophore is present at *N*Me-Phe moieties. Due to the time frame of the work presented herein, cycloaspeptide A in the inactive fraction was not discovered until very late in the process and no time was left to cultivate the fungus in large scale and isolate cycloaspeptide E. The E-SPE approach with the optimized collection of ion-exchangers and normal phase SPE columns has turned out to be a good combination to evaluate and follow bioactivity of fungal extracts.

2.2 MS Based Dereplication of *Penicillium pulvillorum*

The extract of *P. pulvillorum* (IBT 22393) was among the candidates that displayed the highest level of activity (≈ 1.25 µg/ml). The first five flash fractions (ranging from 15-40 % organic) were tested active against CLL cells *in vitro*. LC-DAD-HRMS revealed one major component shared between these fractions, with an elementary composition of $C_8H_{10}O_4$ (-0.7 ppm mass accuracy). AntiBase2012 [87] revealed penicillic acid as a likely candidate responsible for the observed activity (Figure 15). The tentative identification of penicillic acid was confirmed by comparison of the retention time to a standard from our in-house metabolite database as well as comparison of ^1H and ^{13}C NMR chemical shifts to the literature [102].

Figure 15. Dereplication of penicillic acid from *P. pulvillorum* mass spectrum of penicillic acid [87]. The mass spectrum shows a widespread adduct pattern that besides $[M+H]^+$ contains ions that corresponds to neutral loss of water $[M+H-H_2O]^+$ and the sodiated adduct $[M+Na]^+$, as well as the corresponding dimeric ions $[2M+H]^+$, $[2M+H-H_2O]^+$, and $[2M+Na]^+$.

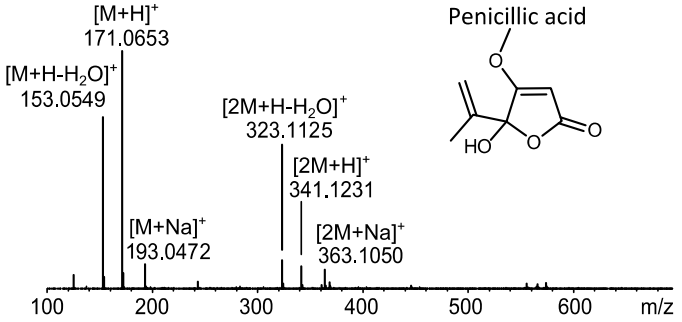

To verify the observed anti-leukemic activity in the extract, penicillic acid was purified and tested on CLL cells, resulting in induced cell death in both CLL and stromal (HS-5) cells. No further work on this extract was done as penicillic acid is regarded as generally cytotoxic compound [102].

2.3 UV Based Dereplication of *Penicillium pinicola*

The *P. pinicola* (IBT16545) extract was fractionated by RP C_{18} chromatography and fractions 9-12 (70-90 % organic) were found active against CLL cells *in vitro* at concentrations of approximately 1 mg/ml. The active fractions were analyzed by LC-DAD-MS and comparative dereplication exposed four compounds solely present in the active fractions (Figure 16, compound A-D). All other compounds in the active fractions were present in the inactive fractions as well. The first compound (A) was tentatively identified as cycloaspeptide A by the pseudomolecular ion, $[M+H]^+$, and the sodiated adduct, $[M+Na]^+$, in the mass spectrum. The identity was confirmed by compression of retention time and UV spectrum to or in-house metabolite database. Due to the fact that cycloaspeptide A was found in inactive fractions from the *P. jugorum* extract (section 2.1) this compound was eliminated as a potential candidate for the observed activity.

Figure 16. Dereplication of compounds in the active fraction from the *P. pinicola* extract. Cycloaspeptide A (A), ML-236C (B), Compactin (C), and 4a,5-dihydrocompactin (D).

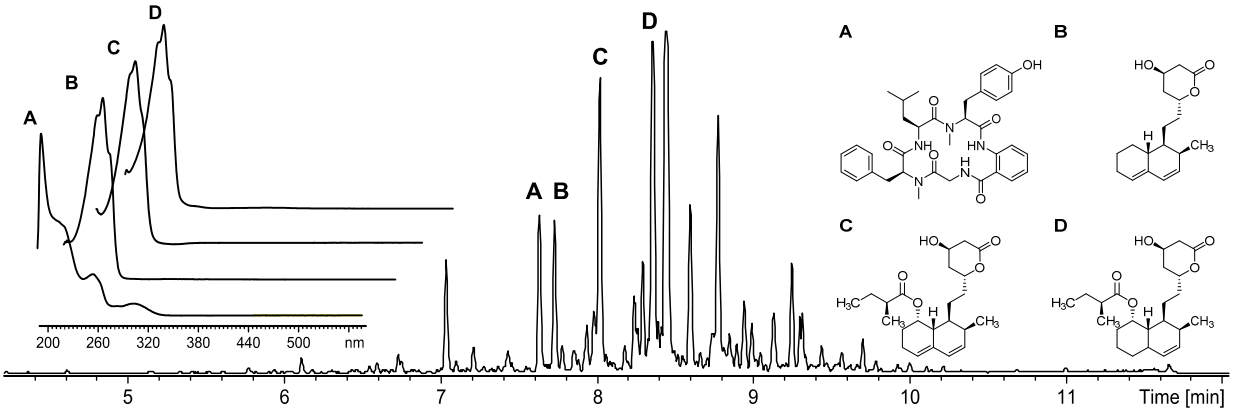

The remaining three compounds (B, C, D) displayed similar UV chromophores (Figure 16). The UV spectra were compared to our in-house metabolite database and recognized as the statins family of compounds, primarily known for their ability to inhibit synthesis of cholesterol [103,104]. By comparison of the retention times, accurate masses, and UV spectra it was possible to identify two of the statins as compactin (C) and 4a,5-dihydrocompactin (D), respectively. The remaining statin (B) was not in our in-house database and therefore only tentatively identified as the statin ML-236C.

The statins were connected to the observed activity towards CLL cells due to the high abundance in the active fractions. The statin family has previously been connected to CLL due to the suggestion that CLL cell proliferation depends on cholesterol synthesis [105]. The synthetic analog simvastatin has been included in one clinical study though patients did not significantly benefit from this drug [105]. Statins are commercially available, thus to evade time-consuming purification we bought and used compactin and simvastatin to explore the activity of the statin family towards CLL cells *in vitro*. In this study neither compactin nor simvastatin exhibited activity towards the CLL cells.

The contradictory results of the statin family being responsible for the observed activity in the crude extract are inclusive. A successive E-SPE analysis [83] of the active fraction resulted in the loss of activity. This loss of activity may be due to treatment histories of patients, lack of synergy effects or instability of the active compound(s).

Treatment histories of patients might be important for the assay results. It is not possible to grow CLL cell lines *in vitro* due to their general defect to divide and undergo mitosis. Consequently, the CLL cells applied in the bioassay are extracted from whole blood samples obtained directly from patients diagnosed with CLL. CLL is generally considered a heterogeneous disease resulting in various treatment histories for the individual patients. The CLL cells applied in the bioassay are therefore very heterogeneous and have a huge influence on the results from the bioassay. The subsequent lack of activity observed from the *P. pinicola* extract might be due to the screening of cells from different patients with different treatment histories. On a general level this variety of the cells demands a higher number of replicates of the assay to ensure the precision of the results.

Synergy effects have previously been described for compounds of the statin family where lovastatin has synergistic antifungal activity with azoles [106,107]. Similar synergistic effects might cause the observed activity towards the CLL cells and the subsequent loss of activity after further fractionation.

Instability and degradation of the active compound could be another potential explanation to the lost activity.

To follow these theories would be very interesting and perhaps lead to the identification of an effective treatment towards CLL. The time did not allow further investigation of these topics though it might be a convincing route.

2.4 Conclusion

In conclusion, our combined bio-guided, E-SPE, and dereplication based discovery approach has proven to be effective for fast dereplication and discovery of bioactive fungal natural products that target CLL cells. Comparative testing of active extracts on CLL cells as well as healthy cells allowed the exclusion of compounds with general cytotoxic activity. The optimized collection of ion-exchangers and normal phase SPE columns in the E-SPE setup has turned out to be a good combination to evaluate and follow bioactivity of fungal extracts. In the eight bioactive extracts discussed in this chapter, the compounds responsible for the activity were tentatively identified by dereplication, and the activities towards CLL cells were verified by testing the pure compounds in six of the extracts. The six active compounds, penicillic acid (*P. pulvillorum*), viridicatumtoxin (*P. brasilianum*), calbistrin A (*P. decumbens*), brefeldin A (*P. cluniae*), emestrin A (*Aspergillus* sp. (*Emericella*-like state)), and neosolaniol monoacetate (*F. compactum*), were all known and general cytotoxic. These projects were closed as soon as the activities of the compounds were confirmed. In general, cytotoxic compounds are only suitable as anti-cancer pharmaceuticals if they selectively target the cancer cells and not healthy cells, or at least have a higher impact towards the tumor cells. In the two remaining extracts cycloaspeptide E (*P. jugorum*) and the statin family of compounds (*P. pinicola*) were tentatively identified as candidates for the activity observed in the crude extract.

Chapter 3

Ophiobolins Targeting CLL Cells

Discovery of ophiobolins (Figure 17) and further activity optimization of the ophiobolins is addressed through the chemistry of closely related fungal species to obtain more analogues and discuss their pharmacophore (**paper 2**).

The bioactive extract from a new species in *Aspergillus* section *Usti* (IBT 18591) was more selective than the other active extracts from the initial screen and in consequence selected for more detailed investigations. MS- and UV-based dereplication led to the tentative identification of the ophiobolin family of compounds. Ophiobolin K and 6-epiophiobolin K (Figure 17) [108] were isolated and ophiobolin K was found very potent against CLL cells *in vitro*.

Figure 17. Structures of ophiobolin A, 3-anhydro-ophiobolin A, 3-anhydro-6-epiophiobolin A, ophiobolin B, ophiobolin C, 6-epiophiobolin G, ophiobolin H, 6-epiophiobolin K, ophiobolin K, 6-epiophiobolin N, and the new ophiobolin U.

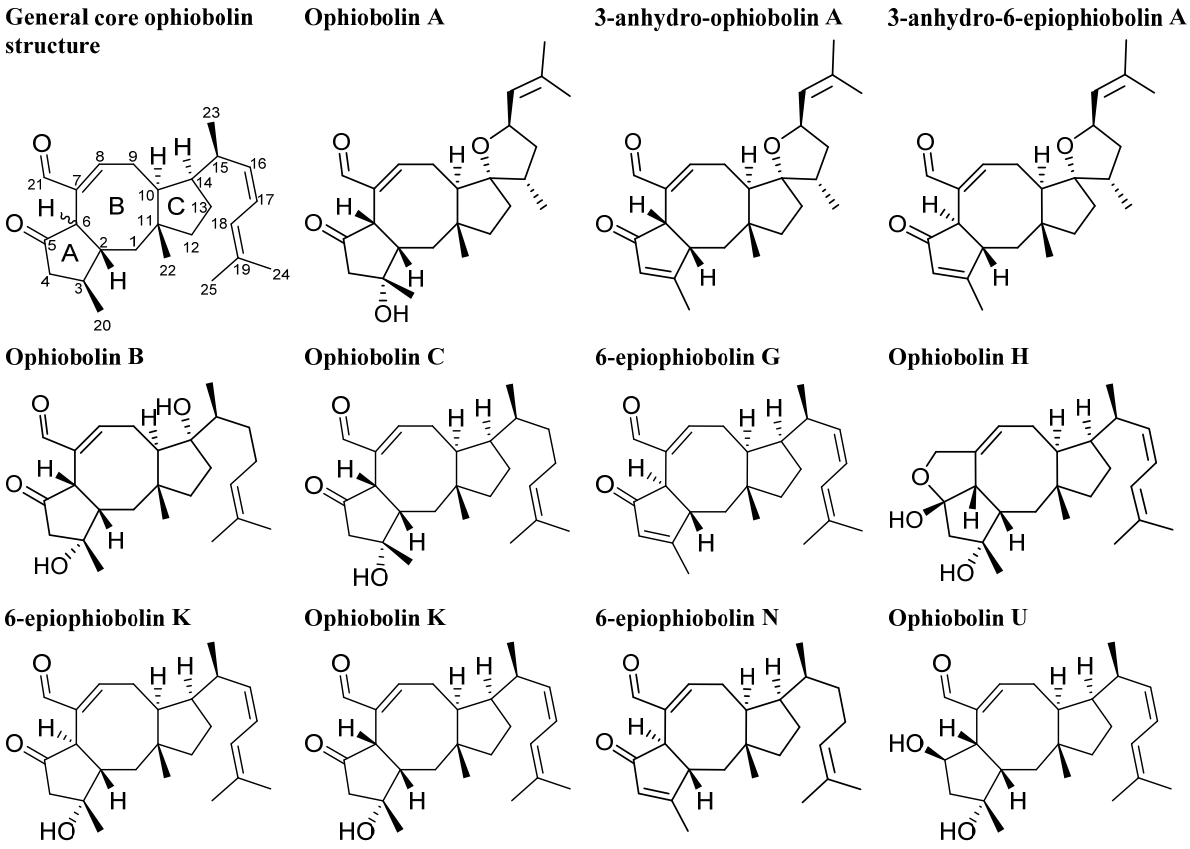

Investigation of the anti-leukemic activity and pharmacophore of the ophiobolins in the CLL/stromal cell co-culture platform were performed with the purpose of isolating a high number of naturally occurring analogs as well as identification of novel analogues. Taking advantage of the huge biodiversity available in the IBT culture collection [79], we expanded the biodiversity and hereby the expected chemodiversity with 12 closely related *Aspergilli* from the section *Usti* (Table S7 in **paper 2** supplementary file) [109]. Cultures of the 12 new strains were extracted in micro-scale [96] to explore their potential for producing ophiobolins. *A. insuetus* (IBT 28266) and *A. calidoustus* (IBT 25726) were identified as potent ophiobolin producers with one likely novel and more known ophiobolins analogs compared to the original strain (Figure 18).

Figure 18. UHPLC chromatograms of (a) the new species in *Aspergillus* section *Usti* (IBT 18591) producing ophiobolin K and 6-epiophiobolin K, (b) *A. insuetus* (IBT 28266) producing the novel ophiobolin U together with ophiobolin H, K, C as well as 6-epiophiobolin K and N and (c) *A. calidoustus* (IBT 25726) producing ophiobolin K and C as well as 6-epiophiobolin K and G.

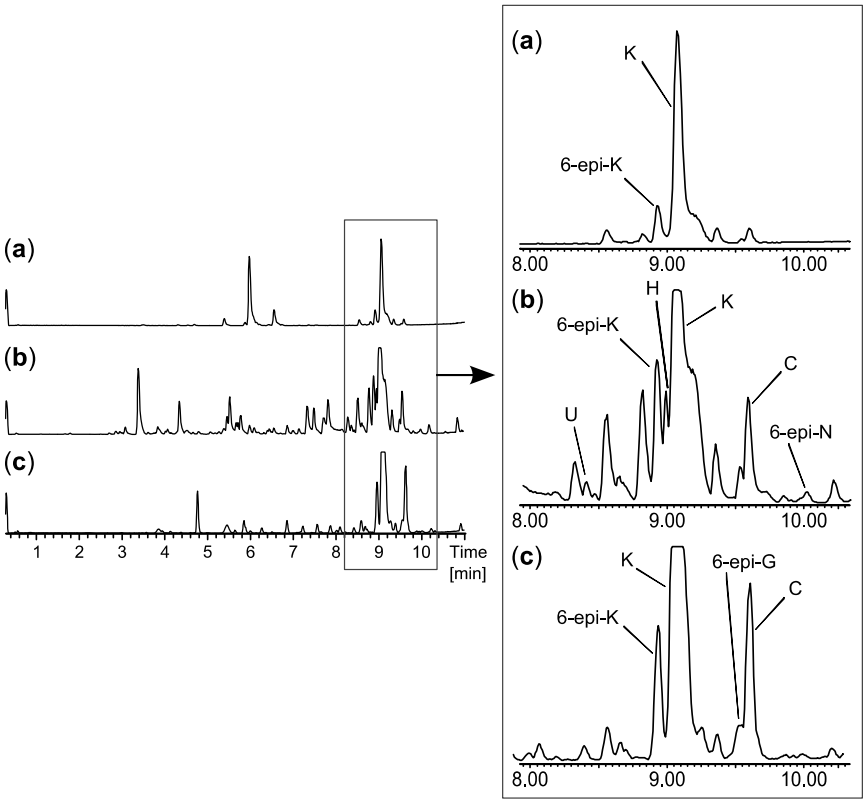

3.1 Structure elucidation of the new Ophiobolin U

The novel ophiobolin U (Figure 19) was isolated together with ophiobolin H [110] (Figure 17) and the rare 6-epiophiobolin N [111] (Figure 17) from the *A. insuetus* extract, while ophiobolin C [112] (Figure 17) and 6-epiophiobolin G [111] (Figure 17) were isolated from the *A. calidoustus* extract.

Figure 19. Structure and numbering of ophiobolin U.

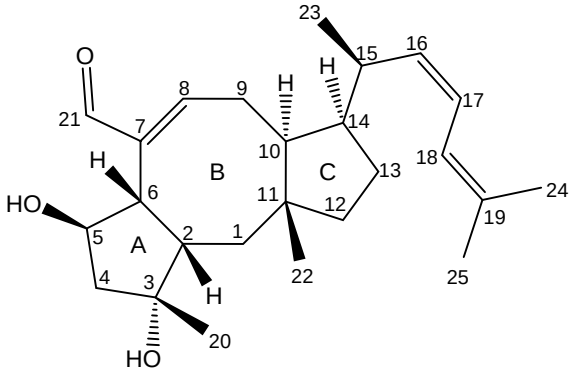

The structure of the novel ophiobolin U was elucidated by 1D and 2D NMR spectroscopy. The ^{1}H NMR spectrum of ophiobolin U was closely related to that of ophiobolin K with many practically identical chemical shifts (Table 1 and 2). The most remarkable difference between ophiobolin U and ophiobolin K was found at C5 that shifted 143.9 ppm upfield from δ_C 217.0 to 73.1 ppm in the carbon spectrum, indicating the disappearance of a ketone group. C5 had an additional heteronuclear single quantum coherence (HSQC) correlation to a proton at δ_H 4.91 ppm (H5). This significant change indicated a reduction of the ketone (C5) in ophiobolin K to a secondary alcohol in ophiobolin U. This reduction was confirmed by the correlation spectroscopy (COSY) spin system between H1-H2-H6 in ophiobolin K that in ophiobolin U was expanded with a vicinal coupling between the protons at δ_H 3.02 (H6) and 4.91 ppm (H5) and further a vicinal couplings between H5 and the diastereotopic protons at δ_H 1.87 (H4a) and 2.68 ppm(H4b), respectively (Figure 20a).

Figure 20. (a) Important DQF-COSY couplings and (b) important HMBC connectivities in the novel compound ophiobolin U.

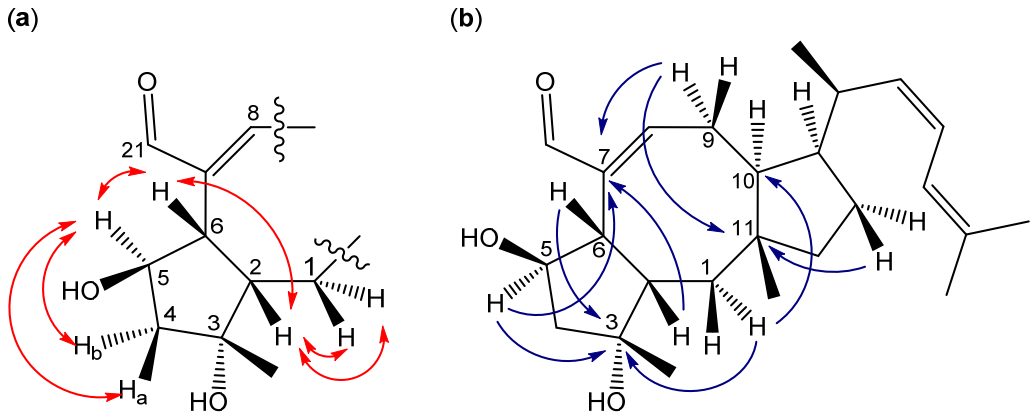

The spin systems identified in the DQF-COSY spectrum of ophiobolin U were assembled through heteronuclear multiple bond correlation (HMBC) correlations, which also enabled the identification of the quaternary carbon atoms. The most important HMBC correlations are shown in Figure 20b. The COSY spin systems were connected by HMBC connectivities further confirming the presence of the eight-membered ring. HMBC connectivities were found from H5

to the quaternary carbons at δ_C 81.9 (C3) and 142.1 ppm (C7), from the diastereotopic protons at δ_H 1.03 (H1a) and 1.58 ppm (H1b) to C3 and the carbon at δ_C 54.0 ppm (C10), and finally from H9 to C7 and the quaternary carbon at δ_C 44.1 ppm (C11). The reduction at C5 changed the chemical environment of the surrounding carbons (C2, C3, C6, C8 and C21) that were more deshielded and therefore shifted 1.8 - 6.5 ppm downfield compared to ophiobolin K (Table 1). The remaining chemical shifts in ophiobolin U matched the chemical shifts of ophiobolin K (Table 1 and 2).

Table 1. ^{13}C NMR data for ophiobolin U, ophiobolin K, 6-epiophiobolin K, ophiobolin C, ophiobolin H, 6-epiophiobolin H, and 6-epiophiobolin G. (*125 MHz in dimethyl sulfoxide (DMSO)-d_6, †125 MHz in $CDCl_3$, or ‡200 MHz in $CDCl_3$, δ_C).

ophiobolin	U‡	K*	6-epi-K*	C†	H‡	6-epi-N‡	6-epi-G†
1	35.2	34.5	41.0	36.0	35.7	45.6	45.8
2	51.0	49.2	49.6	50.8	50.9	49.3	49.2
3	81.9	76.2	74.7	76.6	80.2	179.8	178.1
4	53.4	53.9	54.7	54.6	50.8	130.0	130.2
5	73.1	217.0	216.1	217.5	116.0	209.6	208.2
6	50.5	48.3	48.2	48.4	52.8	49.9	50.0
7	142.1	140.6	141.5	141.5	138.5	140.1	139.9
8	164.1	157.6	159.9	163.8	123.6	157.3	158.1
9	25.6	24.3	30.0	24.7	25.0	31.0	30.9
10	54.0	53.0	43.1	53.4	55.0	43.1	43.8
11	44.1	43.3	44.9	43.6	43.6	45.0	45.4
12	42.0	42.2	44.4	42.6	43.0	44.5	44.3
13	26.7	25.4	27.1	22.8	26.8	27.1	27.8
14	47.4	46.2	51.4	45.2	47.2	51.1	52.1
15	35.9	34.4	31.9	32.7	35.5	31.8	32.6
16	137.7	136.9	136.0	36.8	138.0	37.1	135.7
17	122.3	121.7	123.3	26.0	121.7	25.6	124.0
18	120.2	119.9	120.1	124.3	120.4	124.4	120.0
19	135.9	134.6	135.3	131.0	135.2	131.6	136.6
20	26.3	25.7	25.2	25.4	25.4	17.4	17.3
21	198.1	193.1	194.7	195.9	71.5	193.0	193.0
22	18.6	18.2	22.8	19.0	18.7	23.1	22.9
23	20.6	19.6	21.1	16.4	20.4	18.6	21.3
24	18.3	18.0	17.9	17.6	18.2	17.7	18.2
25	26.7	25.9	26.1	25.6	26.6	25.7	26.5

Table 2. ^{1}H NMR data for ophiobolin U, ophiobolin K, 6-epiophiobolin K, ophiobolin C, ophiobolin H, 6-epiophiobolin H, and 6-epiophiobolin G. (*500 MHz in DMSO-d_6, †500 MHz in $CDCl_3$, or ‡ 800 MHz in $CDCl_3$, δ_H mult. (*J* (Hz))).

Ophiobolin	U‡	K*	6-epi-K*	C†	H‡	6-epi-N‡	6-epi-G†
1a	1.03 m	1.14 m	1.58 m	1.26 m	1.36 m	1.18 m	1.15 m
1b	1.58 m	1.58 m	1.65 m	1.81 m	1.42 m	2.04 dd (3.7; 13.2)	2.03 m
2	2.30 m	2.25 m	1.91 m	2.38 m	2.26 m	2.71 m	2.66 m
3-OH			6.51 br.s.				
4a	1.87 dd (4.1, 15.1)	2.35 m	2.21 m	2.49 m	2.10 m	6.11 s	6.04 s
4b	2.68 dd (7.9, 15.1)	2.50 m	2.77 d (16.0)	2.80 m	2.18 m		
5	4.91 dd (4.7, 7.9)						
6	3.02 d (9.6)	3.22 d (9.8)	3.04 d (10.8)	3.26 m	3.17 d (9.8)	3.54 d (3.7)	3.40 m
8	6.94 t (8.5)	7.02 t (8.5)	6.96 m	7.21 m	5.64 br.s.	6.86 dd (2.0; 6.3)	6.80 m
9a	2.24 m	2.04 m	2.27 m	2.31 m	1.70 m	2.25 m	2.20 m
9b	2.89 dd (8.5, 12.5)	2.69 m	2.65 m	2.45 m	2.50 dd (8.6; 13.8)	2.71 m	2.93 m
10	1.55 m	1.56 m	2.46 m	1.67 m	1.60 m	2.72 m	2.63 m
12a	1.38 m	1.33 m	1.38 m	1.41 m	1.40 dd (7.6; 11.7)	1.42 m	1.43 m
12b		1.35 m	1.44 m	1.44 m	1.57 m	1.51 m	1.52 m
13a	1.58 m	1.54 m	1.22 m	1.46 m	1.54 m	1.23 m	1.25 m
13b	1.78 m	1.69 m	1.57 m	1.55 m	1.76 m	1.58 m	1.67 m
14	2.09 m	2.09 m	1.87 m	2.36 m	2.05 m	1.75 m	1.89 m
15	2.72 m	2.72 m	2.61 m	1.65 m	2.68 m	1.42 m	2.55 m
16a	5.21 t (10.0)	5.23 t (9.5)	5.25 t (9.3)	1.18 m	5.20 m	0.99 m	5.11 t (1.3)
16b				1.24 m		1.45 m	
17a	6.03 m	5.99 m	6.11 m	1.95 m	5.99 m	1.94 m	6.10 m
17b				2.00 m		2.07 m	
18	6.00 m	6.04 m	6.09 m	5.09 m	5.98 m	5.12 t (7.0)	6.00 m
20	1.26 s	1.19 s	1.26 s	1.36 s	1.24 s	2.10 s	2.06 s
21a	9.26 s	9.14 s	9.12 s	9.23 s	4.48 br.s.	9.30 s	9.26 s
21b					4.59 d (12.2)		
22	0.99 s	0.91 s	0.77 s	0.90 s	0.90 s	0.86 m	0.85 s
23	0.91 d (6.7)	0.85 d (6.6)	0.92 d (6.6)	0.78 d (6.8)	0.88 d (6.7)	0.91 d (6.4)	0.97 d (6.8)
24	1.74 s	1.68 s	1.70 s	1.61 s	1.73 s	1.61 s	1.76 s
25	1.82 s	1.76 s	1.79 s	1.69 s	1.80 s	1.69 s	1.83 s

The stereochemistry of the A/B ring system in ophiobolin U (Figure 21) was assigned based on NOE correlations and chemical shifts. The A/B-*cis* ring system was established by the NOE correlations found between the protons at δ_H 2.30 (H2) and 3.02 ppm (H6), as demonstrated in Figure 21. The stereochemistry of C5 was tentatively assigned through strong NOE correlations of the diastereotopic protons at δ_H 1.87 (H4a) and 2.68 ppm (H4b). H4a had NOE correlations to the protons at δ_H 1.26 ppm (H20) and H2, while H4b had a NOE correlation to H5, which

indicated that the hydroxy group at C5 was *cis* to H6. Other important NOE correlations are shown in Figure 21.

Figure 21. Important NOE correlations in ophiobolin U.

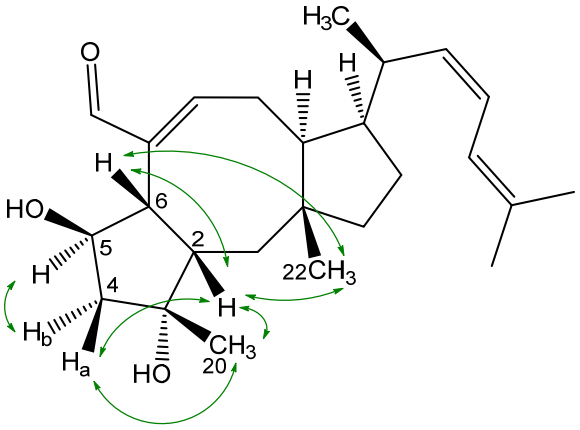

The A/B-*cis* conformation was confirmed by chemical shifts. Earlier reports showed that C1 and C22 in ophiobolins with A/B-*cis* ring structure are more upfield compared to ophiobolins with A/B-*trans* ring structure [113]. In ophiobolin U and ophiobolin K, the chemical shifts of C1 and C22 were more upfield compared to 6-epiophiobolin K, which indicate a A/B-*cis* ring structure in ophiobolin U. Other reports have showed that the A/B-*cis* ring structure in ophiobolins causes a small deshielding (0.2 - 0.3 ppm) for H2 and H8 as well as a small shielding (0.3 - 0.6 ppm) for H4 [114]. The ^{1}H chemical shifts for ophiobolin U were inconclusive regarding conformation of the A/B ring system. The residual stereocenters of ophiobolin U were biosynthesized in the same way as in the known ophiobolins due to the stereospecificity of the biosynthetic pathway of the ophiobolins [115,116].

The stereochemistry of the A/B ring system of the remaining six ophiobolins (ophiobolin K, 6-epiophiobolin K, 6-epiophiobolin N, 6-epiophiobolin G, ophiobolin H, and ophiobolin C) isolated in this study were confirmed by NOE correlations. Together with the general trend that C1 and C22 in the ophiobolins with A/B-*cis* ring structure were more upfield compared to ophiobolins with A/B-*trans* ring structure [111,113]. The shifting of chemical shifts for H2, H4, and H8 for the A/B-*cis* ring system were more ambiguous due to the small deshielding/shielding in chemical shifts and inconclusive for the seven ophiobolins. A comparison of the ^{13}C and ^{1}H chemical shifts of all the seven ophiobolins are found in table 1 and 2, respectively (full NMR data is found in table S10-S16 in **paper 2** supplementary file).

3.2 Ophiobolins Targeting CLL Cells

Besides the seven purified ophiobolins: ophiobolin A, ophiobolin B, 3-anhydroophiobolin A, and 3-anhydro-6-epiophiobolin A (Figure 17) were bought as standards with the aim of obtaining a broader understanding of the SAR of the ophiobolin family against CLL cells. Ophiobolin U was unstable and therefore not applied in any bioassay, but the remaining ten ophiobolins were tested for their cytotoxic activity towards CLL cells. Ophiobolin A, B, C, and K showed the

strongest effects with LC_{50} values between 1 and 8 nM (results compiled in Table 3 and Figure 22). Ophiobolin A and B displayed cytotoxic effects towards normal lung fibroblasts in 10 nM concentration indicating a possible narrow therapeutic window. Ophiobolin C and K displayed no effect towards normal lung fibroblasts in concentrations up to 10 nM (Figure 24). Ophiobolin-treated cells were further stained with PE-labelled Annexin-V and 7-AAD, or antibodies for activated caspase-3 prior to flow cytometric analyses. Thereby, apoptosis was identified as the mode of killing of CLL cells.

Table 3. Cell viability activity (LC_{50}) of the 10 ophiobolins towards CLL cells.

Compound	LC_{50}
Ophiobolin A	1 nM
3-anhydro-ophiobolin A	Inactive
3-anhydro-6-epiophiobolin A	Inactive
Ophiobolin B	2 nM
Ophiobolin C	8 nM
6-epiophiobolin G	Inactive
Ophiobolin H	Inactive
Ophiobolin K	4 nM
6-epiophiobolin K	Inactive
6-epiophiobolin H	Inactive

Figure 22. Effects of ophiobolin A, B, C, K and 6-epiophiobolin K on CLL cell viability. CLL cells were treated for 24 hours with increasing concentrations of the ophiobolins and cell viability was analyzed by CellTiter-Glo® assay measuring each data point as duplicate. Relative cell viability compared to DMSO control.

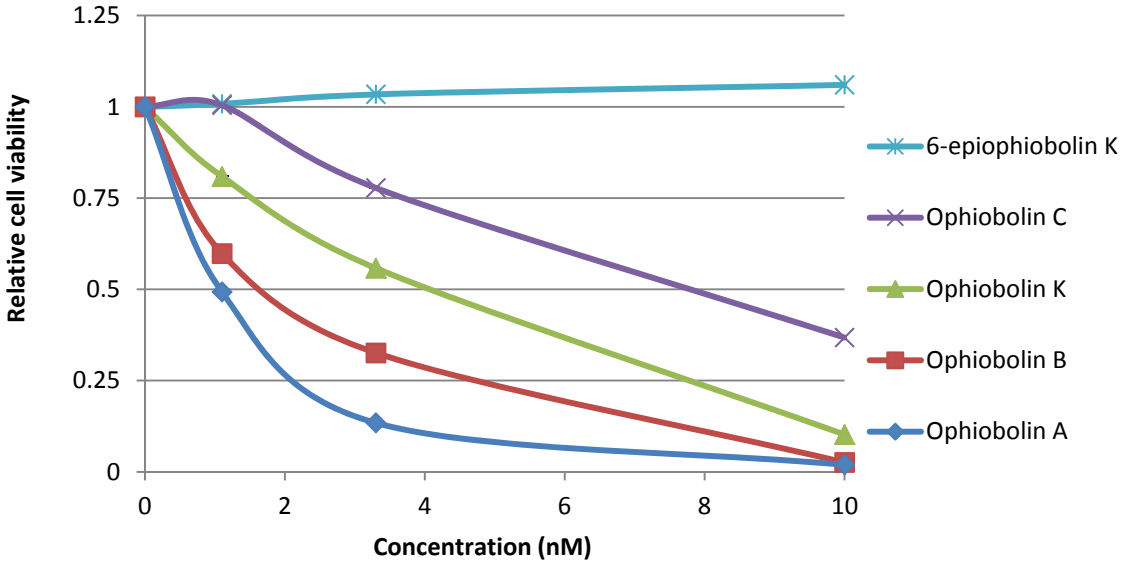

Figure 23. Effects of ophiobolin A, B, C, and K on normal lung fibroblasts cell viability. The lung fibroblasts cells were treated for 24 hours with increasing concentrations of the ophiobolins and cell viability was analyzed by CellTiter-Glo® assay measuring each data point as duplicate. Relative cell viability compared to DMSO and fludarabine control.

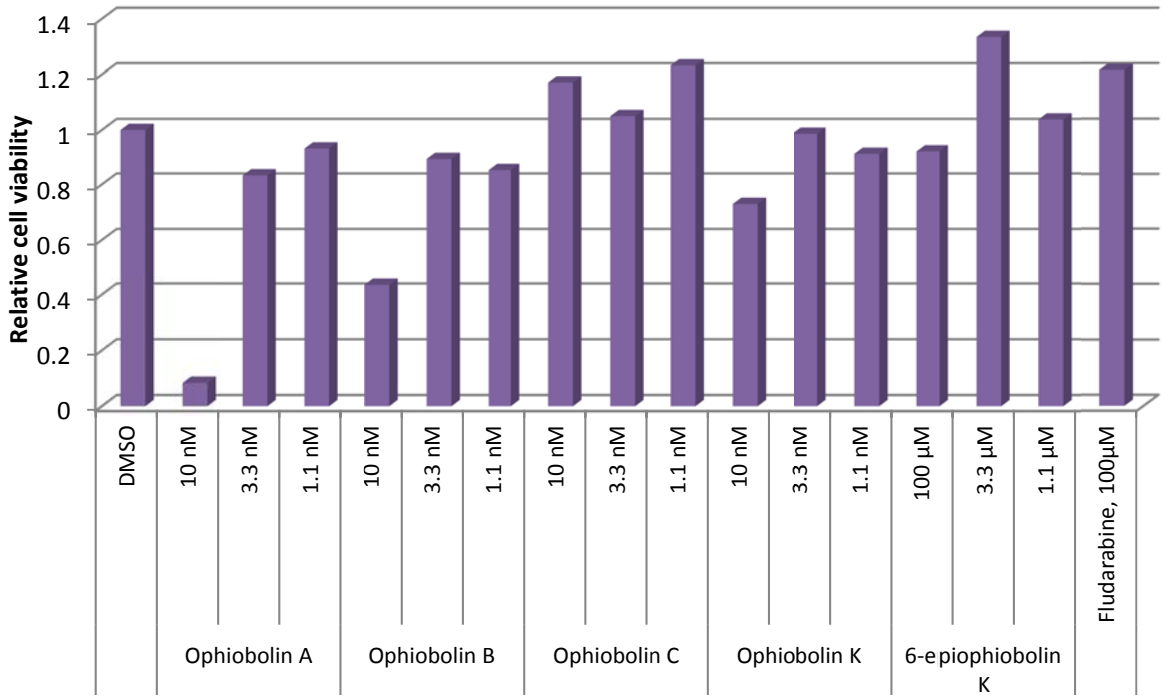

Interestingly, the remaining ophiobolins tested (3-anhydro-ophiobolin A, 3-anhydro-6-epiophiobolin A, 6-epiophiobolin G, ophiobolin H, 6-epiophiobolin K, and 6-epiophiobolin N) exhibited low or no activity towards CLL cells. In fact, 6-epiophiobolin K targeted CLL cell viability only when applied at a 100-fold higher concentration than ophiobolin B (Figure 24).

Figure 24. 6-epiophiobolin K treatment of CLL cells did not decrease cell viability in the concentration range tested in Figure 22. CLL cells were accordingly treated with up to 900 nM of 6-epiophiobolin K and cell viability was determined and compared to the active ophiobolin B.

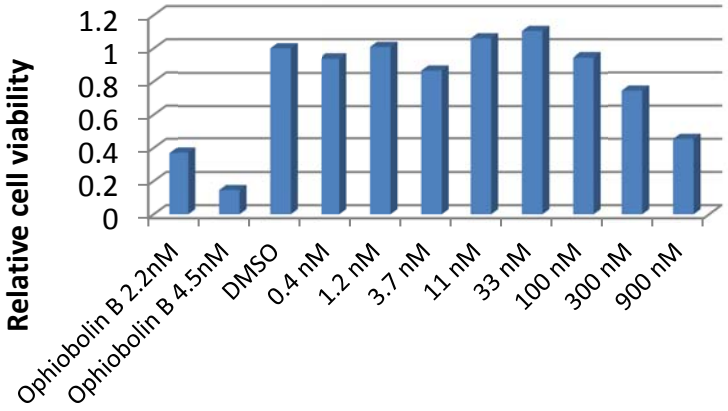

The results displayed in table 3 and figure 23-24 indicate that presence of a hydroxy group at C3 and an aldehyde at C21 is crucial for the activity of the ophiobolins. Our findings are thus in agreement with previous studies that have shown that these two groups covalently bind to calmodulin [60,117]. None of the 6-epiophiobolins tested were active against the CLL cells [117]. To earn a broader understanding of the importance of this small steric change at C6, 3D-modeling of ophiobolin K (blue) and 6-epiophiobolin K (red) were done to give a visual representation of their lowest energy conformations (Figure 25).

Figure 25. Modulated 3D structures of ophiobolin K (blue) and 6-epiophiobolin K (red) in their lowest energy conformations overlaid. H6 protons are marked in ophiobolin K (cyan) and 6-epiophiobolin K (orange). The chain extending from C14 in ring C is not displayed to get a better clarity of the structures (the cut-off point is marked with *).

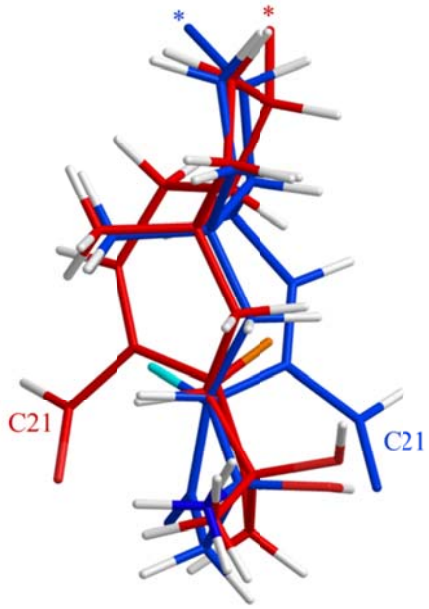

The difference in conformation between ophiobolin K and 6-epiophiobolin K involves a flipping of the eight-membered ring that result in a change of position of the C21 aldehyde from one to the other side of the plane observed in the figure. This conformational change is likely preventing the binding of calmodulin by the C21 aldehyde due to steric hindrance, resulting in the lack of activity for 6-epiophiobolin K contrasting ophiobolin K.

3.3 Conclusion

In conclusion, discovery and activity optimization of ophiobolins through closely related species from the *Aspergillus* section *Usti* has proven to be effective. One new analog, ophiobolin U, was isolated at the structure elucidated and the activities of the ophiobolins were addressed. Ophiobolins A, B, C and K displayed apoptosis inducing activity in CLL cells with LC_{50} values of 1, 2, 8, and 4 nM, respectively, with a potential narrow therapeutic window. The high activities against the CLL cells were found only in ophiobolins with a hydroxy group at C3, an aldehyde at C21, and A/B-*cis* ring structure.

Chapter 4

Sclerotionigrin A, B and Proxiphomin Targeting CLL

An important and diverse group of fungal anticancer compounds that have caught our interest are the cytochalasans due to their wide range of biological functions [62]. In particular this includes inhibitory activities towards lung, ovarian, and human colon cancer as well as human leukemia [64,65]. Recently, it was demonstrated in our group that chaetoglobosin A, produced by *Penicillium aquamarinum*, selectively induce apoptosis in CLL cells with a LC_{50} value of 2.8 µM [67]. On the basis of the expressed chemodiversity of *Aspergillus sclerotieoniger* (IBT 22905) it was selected for target-guided isolation of cytochalasins. Two new cytochalasins sclerotionigrin A and B (Figure 26) were isolated from *A. sclerotieoniger* together with the known cytochalasin proxiphomin [118].

Figure 26. Structure of sclerotionigrin A (1), B (2) (relative stereo chemistry) and proxiphomin (3) (absolute stereo chemistry).

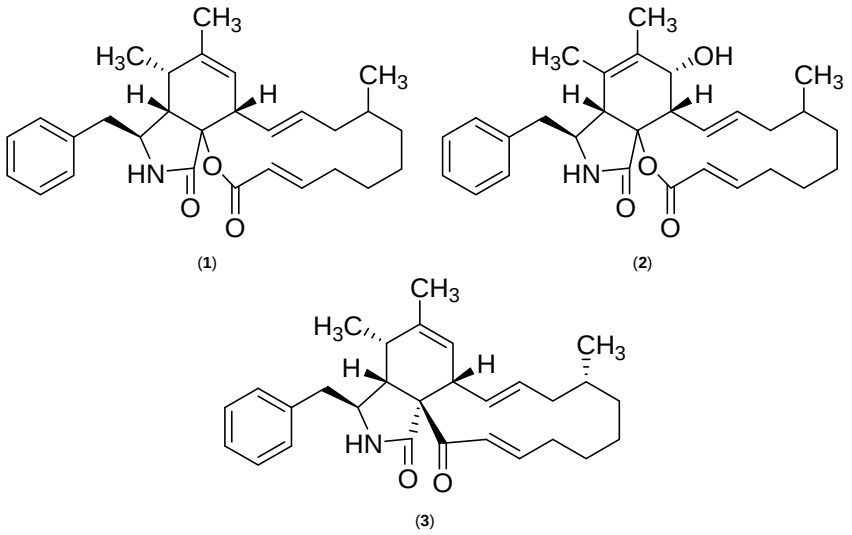

The structure of proxiphomin was tentatively identified through UHPLC-DAD-HRMS based dereplication of the crude extract. The pseudomolecular ion, $[M+H]^+$, was recognized from the mass spectrum due to the presence of the sodiated adduct, $[M+Na]^+$ and the corresponding dimeric adducts $[2M+H]^+$ and $[2M+Na]^+$. The molecular formula $C_{29}H_{37}NO_2$ was established with an accuracy of 0.8 ppm through the monoisotopic mass of $[M+H]^+$ of *m/z* 432.2901. The formula

was used as a query in Antibase2012 [87] with one resulting hit, proxiphomin. NMR data and optical rotation of proxiphomin matched published data [118].

Sclerotionigrin A was purified as a yellow powder. The UV spectrum displayed absorption maxima at 210 nm. The positive electrospray ionization (ESI^+) spectrum showed a distinct adduct pattern consisting of $[M+H]^+$, $[M+Na]^+$, $[2M+H]^+$ and $[2M+Na]^+$. The molecular formula $C_{29}H_{37}NO_3$ (12 double-bond equivalents) was gained from HRMS of $[M+H]^+$ (*m/z* 448.2843) with an accuracy of 2.3 ppm.

The ^1H NMR spectra revealed the presence of one amide proton, 15 methines (five which were vinylic and five aromatic), six methylene, and three methyls (Table 4). The DQF-COSY spectrum of sclerotionigrin A defined three spin systems. The linking between COSY spin systems and assignments of the remaining signals and quaternary carbons were accomplished through detailed analysis of HMBC experimental data (Figure 27).

Figure 27. Important HMBC correlations connecting the three COSY spin systems (marked in bold) in sclerotionigrin A. The remaining HMBC correlations are found in table 4.

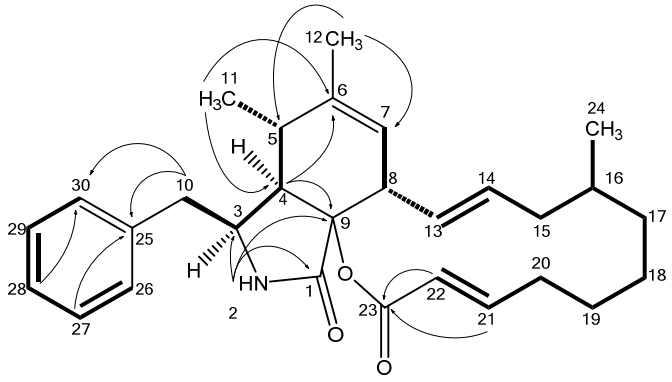

The HMBC correlations from the protons at δ_H 1.65 ppm (H10) and 7.26 (H27 and H29) to a quaternary carbon at δ_C 137.8 (C25), together with HMBC correlations from the protons at δ_H 7.14 (H26 and H30) to the carbon at δ_C 42.6 (C10) linked two of the spin systems belonging to the Phe moiety in sclerotionigrin A. The amide proton at δ_H 8.00 ppm (H2) displayed HMBC correlations to the carbons at δ_C 54.2 (C3) and 170.6 ppm (C1). Combination of these HMBC correlations established the Phe moiety of sclerotionigrin A, which was incorporated on the polyketide part of the molecule.

The polyketide part of sclerotionigrin A, was established through a large COSY spin system (from H7 to H22), equal to that seen for proxiphomin. Furthermore a COSY coupling was found between the proton at δ_H 2.57 ppm (H5) and a methyl group at 0.68 ppm (C11). This part was coupled to the PK part by a week COSY coupling between H5 and H7 identified as a w-coupling. The COSY spin system could furthermore be connected via HMBC correlations to the above mentioned Phe moiety as well as the PK part. The protons at δ_H 1.65 (H12) correlated to the carbons at δ_C 33.6 (C5) and 123.6 ppm (C7) where proton at δ_H 0.68 (H11) correlated to the carbons at δ_C 49.1 (C4) and 140.0 ppm (C6). The proton at 2.53 ppm (H4) correlated to C5, C6 and the quaternary carbon at δ_C 85.4 ppm (C9).

Table 4. NMR data for sclerotionigrin A.†

No.	δ_H (integral, mult., *J* [Hz])	δ_C	HMBC	NOESY
1	-	170.6	-	-
2	8.00 (1H, s)	-	1, 3, 4, 9	3, 10
3	3.09 (1H, td, 5.8, 3.1)	54.2	-	2, 4, 10, 11, 12, 26/30
4	2.53 (1H, dd, 4.2, 3.1)	49.1	3, 5, 6, 9	3, 10, 11, 26/30
5	2.57 (1H, m)	33.6	-	7, 8, 11
6	-	140.0	-	-
7	5.25 (1H, m)	123.6	-	5,8, 12
8	3.15 (1H, m)	45.8	-	5, 7, 13, 14
9	-	85.4	-	-
10	2.82 (2H, dd, 5.8, 2.2)	42.6	3, 4, 25, 26/30	3, 4, 26/30
11	0.68 (3H, d, 7.1)	12.8	4, 5, 6	3, 4, 5, 12, 26/30
12	1.65 (3H, s)	19.4	5, 6, 7	3, 7, 11
13	5.85 (1H, ddd, 14.8, 10.0, 1.2)	128.9	15	8, 15
14	5.22 (1H, m)	132.6	8	8, 15', 16
15	1.60 (1H, d, 13.5)	40.7	13, 14, 16	13, 15'
15'	2.07 (1H, dd, 13.5, 2.1)	40.7	-	14, 15, 16, 20', 24
16	1.36 (1H, m)	31.9	-	14, 15', 19'
17	0.61 (1H, m)	33.8	-	17', 18', 24
17'	1.66 (1H, m)	33.8	-	17
18	1.14 (1H, m)	25.9	-	18'
18'	1.53 (1H, m)	25.9	-	17, 18
19	1.29 (1H, m)	25.3	-	24
19'	1.68 (1H, m)	25.3	-	16, 21
20	2.23 (1H, m)	33.1	-	20', 21
20'	2.29 (1H, m)	33.1	-	15', 20, 22
21	6.96 (1H, ddd, 15.5, 8.6, 6.8)	151.7	23	19', 20, 22
22	5.65 (1H, d, 15.5)	120.6	20, 23	20', 21
23	-	163.5	-	-
24	0.84 (3H, d, 6.3)	20.0	15, 16, 17	15', 17, 19
25	-	137.8	-	-
26‡	7.14 (1H, d, 7.5)	129.5	10, 26/30 28	3, 4, 10, 11
27‡	7.26 (1H, t, 7.4)	128.0	25, 29	-
28	7.18 (1H, t, 7.5)	126.1	26, 30	-
29‡	7.26 (1H, t, 7.5)	128.0	25, 27	-
30‡	7.14 (1H, d, 7.5)	129.5	10, 26/30, 28	3, 4, 10, 11

† ^{1}H NMR data were obtained at 500 MHz in DMSO-d_6 and ^{13}C data were obtained at 125 MHz in DMSO-d_6. ^{13}C-NMR chemical shifts determined from HSQC and HMBC experiments. ‡It was not possible to distinguish between no. 26 and 30 as well as no. 27 and 29.

Finally the polyketide chain was closed via an ester bond assigned from HMBC correlations from the vinylic protons at δ_H 5.65 (H22) and 6.96 ppm (H21) to the carbonyl carbon at δ_C 163.5 ppm (C23) supported by the high chemical shift of the quaternary carbon at δ_C 85.4 ppm (C9) indicating that C9 is bound to oxygen, similar to what is seen in several other cytochalasins [62]. This structure accounted for all the degree of unsaturation required by the formula allowing the assignment of sclerotionigrin A.

The size of the vicinal coupling constants ($^3J_{HH}$) for H13/H14 and H21/H22 were rather large (14.8 and 15.5 Hz respectively) suggestion trans stereogeometry. NOESY experiments enabled determination of the relative stereochemistry for most of the stereogenic centers of sclerotionigrin A to be very similar to those of proxiphomin. NOE connectivities were found between the proton at δ_H 3.09 ppm (H3), δ_H 2.53 (H4) and the methyl at δ_H 0.68 ppm (H11) placing these protons at the same side of the central ring system. Other NOE connectivities were observed between the protons at δ_H 2.57 ppm (H5), 5.25 (H7) and 3.15 (H8), whereas no NOE connectivities could be seen to H3, H4 or H11, strongly indicating the positioning of H5, H7 and H8 on the opposite side of the central ring system compared to H3, H4 and H11. The stereocenters at C9 and C16 could not be assigned through NOESY correlations, however being biosynthesized by the same fungus we propose that the stereochemistry at these centers are identical to those of proxiphomin. Especially we note that the extra oxidation between C9 and C23 in other cytochalasans never leads to a change in stereochemistry at C9.[7,15] We do however note that the optical rotation of sclerotionigrin A and B are positive as opposed to that of proxiphomin and other similar cytochalasans,[15] indicating a possible difference in stereochemistry. Further experiments, e.g. X-ray crystallography or circular dichroism (CD) are needed to clarify the absolute stereochemistry of sclerotionigrin A.

Sclerotionigrin B, was isolated as a yellow powder, and displayed UV absorption maxima at 212 nm and the ESI$^+$ MS adducts $[M+H]^+$, $[M+Na]^+$, $[2M+H]^+$ and $[2M+Na]^+$. The molecular formula of sclerotionigrin B, $C_{29}H_{37}NO_4$ was deduced from the monoisotopic mass obtained from the $[M+H]^+$ ion (*m/z* 464.2797) with the accuracy of 1.2 ppm. Examination of the NMR spectra of sclerotionigrin B displayed a high similarity compared to sclerotionigrin A. Comparison of the NMR spectra of sclerotionigrin A and B (Table 4 and 5) revealed that the difference between them is located in position five, six and seven.

The Phe moiety in sclerotionigrin B was identified through a connection of the two COSY spin systems linked by HMBC correlations as demonstrated for sclerotionigrin A. The COSY spin system of the polyketide chain terminated with a proton at δ_H 3.68 ppm (H7), indicating a binding to a hydroxy group instead of the vinyllic methine group. This was also evident from the carbon chemical shift moving to δ_C 69.1 ppm (C7).

Table 5. NMR data for sclerotionigrin B.†

No.	δ_H (integral, mult., *J* [Hz])	δ_C	HMBC	NOESY
1	-	171.2	-	-
2	8.34 (1H, s)	-	3, 4, 9	3, 10’
3	3.39 (1H, m)	57.7	1, 4, 5, 9	
4	3.32 (1H, m)	47.1	1, 5, 6, 9	
5	-	123.9	-	-
6	-	134.2	-	-
7	3.68 (1H, d, 9.7)	69.1	-	8, 12, 13
8	3.05 (1H, t, 10.0)	48.3	1, 4, 7, 9, 13, 14	7, 13, 14
9	-	83.6	-	-
10	2.55 (1H, dd, 13.0, 10.1)	42.5	3, 4, 25, 26/30	3, 10’, 26/30
10’	2.92 (1H, dd, 13.0, 5.0)	42.5	3, 4, 25, 26/30	2, 3, 10, 26/30
11	1.16 (3H, s)	16.7	4, 5, 6	3, 26/30
12	1.52 (3H, s)	14.3	5, 6, 7	7
13	6.03 (1H, dd, 15.0, 11.3)	128.4	8, 15/15’	4, 7, 8, 14, 15
14	5.00 (1H, ddd, 15.0, 10.8, 3.4)	132.7	8, 15/15’	8, 13, 15, 15’
15	1.58 (1H, dd, 24.3, 11.1)	41.6	16	13, 14, 15’, 16, 17’
15’	2.00 (1H, br. d., 11.6)	41.6	-	14, 15, 16, 24
16	1.13 (1H, m)	32.5	-	15, 15’, 17’, 18, 24
17	0.52 (1H, dd, 19.4, 11.0)	34.5	-	17’
17’	1.67 (1H, m)	34.5	24	15, 16, 17, 18, 24
18	0.86 (1H, m)	26.1	-	16, 17’, 18’
18’	1.68 (1H, m)	26.1	20	18, 19, 21
19	1.30 (1H, dd, 21.5, 10.2)	25.4	-	18’, 19’
19’	1.73 (1H, m)	25.4	-	19
20	2.11 (1H, dd, 20.8, 10.9)	33.4	-	20’, 22
20’	2.41 (1H, dd, 12.7, 4.6)	33.4	-	20, 21
21	6.89 (1H, ddd, 15.7, 10.8, 5.0)	151.4	20, 23	18’, 20’, 22
22	5.79 (1H, d, 16.1)	121.3	20, 23	20, 21
23	-	163.8	-	-
24	0.83 (3H, d, 6.6)	19.9	15, 16, 17	15’, 16, 17’
25	-	137.4	-	-
26‡	7.08 (1H, d, 7.1)	128.9	10, 28, 30	3, 4, 10, 10’, 11, 27/29
27‡	7.31 (1H, t, 7.5)	128.2	25, 29	26/30, 28
28	7.23 (1H, t, 7.4)	126.3	26, 30	27/29
29‡	7.31(1H, t, 7.5)	128.2	25, 27	26/30, 28
30‡	7.08 (1H, d, 7.1)	128.9	10, 26, 28	3, 4, 10, 10’,11, 27/29

† ^{1}H NMR data were obtained at 500 MHz in DMSO-d_6 and ^{13}C data were obtained at 125 MHz in DMSO-d_6. ^{13}C-NMR chemical shifts determined from HSQC and HMBC experiments. ‡It was not possible to distinguish between no. 26 and 30 as well as no. 27 and 29.

HMBC correlations from the three protons of the methyl group at δ_H 1.52 ppm (H12) to the carbons at δ_C 123.9 (C5), 134.2 (C6) and C7, combined with correlations from the protons at δ_H 1.16 ppm (H11) to the carbons at δ_C 47.1 (C4) and 123.9 ppm (C5) and 134.2 (C6) linked the Phe moiety to the spin system in the polyketide chain (Figure 28). The remaining chemical shifts in sclerotionigrin B matched the chemical shifts of sclerotionigrin A (Table 4 and 5) and the structure of sclerotionigrin B was established.

Figure 28. Important HMBC correlations establishing the quaternary carbon C6 and C7 2. The remaining HMBC correlations are found in (Table 5. Inidividual COSY spin systems are marked in bold.

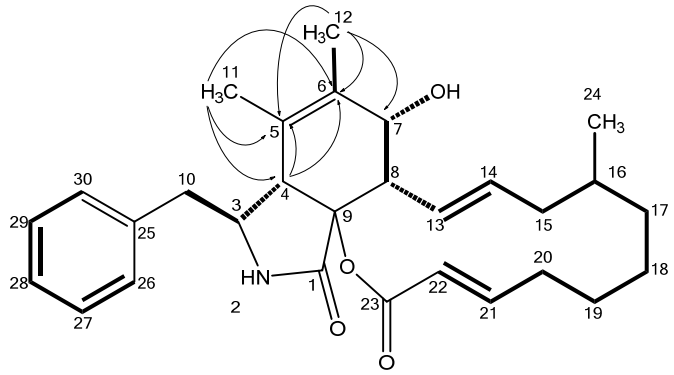

As the optical rotation of sclerotionigrin B was similar to the optical rotation of sclerotionigrin A**,** the two compounds most likely have the same relative stereochemistry, which was confirmed by NOE connectivities. The absolute stereochemistry of sclerotionigrin B has not yet been solved.

Biological testing of the cytotoxicity of compounds sclerotionigrin A, B and proxiphomin towards CLL cells *in vitro* were performed using a CellTiter-Glo® assay (**paper 2**). Proxiphomin displayed the strongest effects with estimated LC_{50} values of ca 48 µM. Where no effect was found towards healthy B-cells below 100 µM. Sclerotionigrin A and B only showed minor activities at concentrations below 100 µM (Figure S18, **paper 3**). Improvement of the anti-leukemic activity of cytochalasins can further be addressed through biocombinatorial engineering using a synthetic biology approach. The goal of such study could be to identify the gene cluster responsible for production of cytochalasins and express it in a model organism like *A. nidulans*. Subsequently incorporate a gene coding for an alternative amino acids into the cytochalasin gene cluster. This approach may enable design of cytochalasin analogs and SAR investigations of the anti-leukemic activity and could be an alternative to traditional preparation of semi-synthetic analogues.

Conclusion

In summary the two new cytochalasins, sclerotionigrin A and B have been isolated from *A. sclerotieoniger* together with the known proxiphomin casting new insights into the chemistry of this species. The latter compound displayed the strongest cytotoxic effect towards CLL.

Chapter 5

Micropeptins with Inhibitory Activity Towards Proteases

This chapter covers isolation of serine proteases inhibitors produced by cyanobacteria and are the result obtained during my external stay at Tel Aviv University. Serine proteases are often associated with the mechanisms that causes diseases such as AIDS, Alzheimer's and cancer etc. [119]. Inhibition of various proteases can slow down or even stop disease progression [120]. Cyanobacteria genera including *Microcystis* that form natural blooms are prolific producers of potent protease inhibitors [121]. The protease inhibitors are usually members of five discrete families: micropeptins [122], aerugenosins [123], microginins [124], anabaenopeptins [125] and microviridins [126]. Cyanobactrial blooms usually contain one or several of these groups covering cyclic and linear modified peptides. Modification of proteinogenic amino acids, by cyanobacteria, results in new amino acid mimics, i.e. amino hydroxy piperidone (Ahp), amino methoxy piperidone (Amp), hydroxycyclohexenyl alanine (HcAla), hydroxy methylproline (HMP), or *N*Me-Tyr to name only a few incorporated into the micropeptins. The acid residue sequence of the micropeptins is highly variable, as can be figured from the 139 members of the family [127]. Some of the positions present high tendency for acid variation while others vary only between two closely related acids. The more conservative positions in micropeptins are the first, fourth and sixth position mostly represented by isoleucine (Ile)/Val, Aph/Amp, and threonine (Thr)/HMP, respectively. The lactone ring of the micropeptins is formed by introduction of an ester bond between Thr/HMP and Ile/Val [128–130]. The side chain of the micropeptins is also highly variable in the length (0 to 3, most frequently 2 amino acids) and acid composition. The side chain is always terminated by either hydroxy acid or a short chain fatty acid (1 to 8 carbons).

It has been proposed that the Aph moiety is biosynthesized from the amino acids glutamine (Gln) or glutamic acid (Glu) by cyclisation of the δ-carbon and the nitrogen form the neighboring amino acid [131]. Another special amino acid is HcAla most probably is derived from L-arogenate, the precursor of tyrosine (Tyr) and Phe. It is presumably biosynthesized by reduction and decarboxylation of L-arogenate (Figure 29), in analogy with the biosynthesis of the proline mimicking amino acid, Choi, in the aeruginosins [132]. The biosynthetic pathway of Aph and HcAla has not yet been studied.

Figure 29. Possible biosynthetic route from L-arogenate to HcAla.

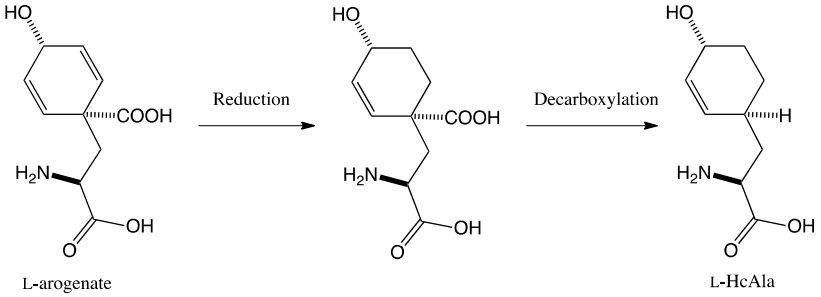

Absolute configuration of the amino acids in peptides can be achieved either by a direct approach using chiral HPLC columns or by an indirect approach using pre-column derivatization and reverse phase chromatography [133]. It is often easy to obtain a good separation and the columns are more rugged and cheaper when using the indirect method compared to the direct. The indirect pre-column derivatization with Marfey's reagent is often the favored choice for small peptides and the method applied in this project. Marfey's reagent contain a chiral center in the L-alanine part of the molecule. In the derivatization the amino acids is incorporated by nucleophilic substitution (Figure 30) [133,134].

Figure 30. Marfey's derivatization of single amino acids for determination of absolute configuration. ***Figure adapted from Hymer et al.*** [133]**.**

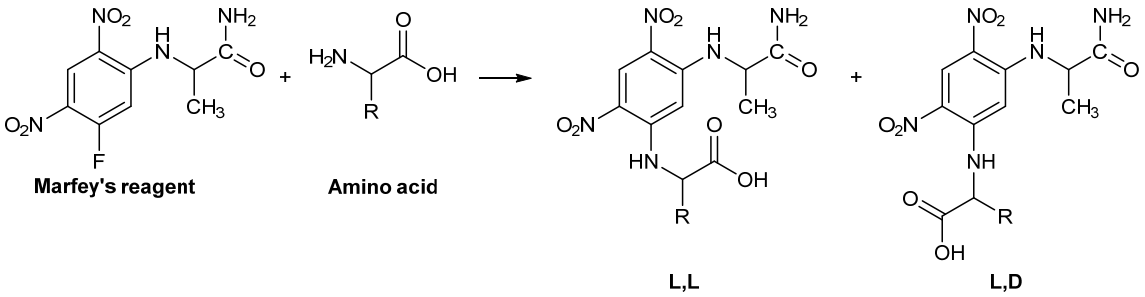

It is possible to separate L- and D-diastereomers by reverse phase chromatography. The separation is often ascribed to intramolecular hydrogen bonds between the carboxyamide and the carboxylic acid in the L,L diastereomer. In the L,D-diastereomer only weak or none hydrogen bonds are formed [133,134]. The mixture of hydrolyzed and derivatized amino acids is spiked with L and D amino acid standards for the final resolution of the stereo chemistry of the individual amino acid.

5.1 Isolation and Structural Elucidation of Micropeptins

The extracts of a *Microcystis* sp. bloom material collected in September 2009 at Kabul Reservoir, Israel was studied. Three new micropeptins KR1030, KR1002, and KR998 (Figure 32) were discovered together and the known microcyclamide GL546A (Appendix) [135]. The structure elucidation and the biological activity of the compounds are discussed below.

Figure 31. Structure of the three novel micropeptins: KR1030 (1), KR1002 (2) and KR998 (3).

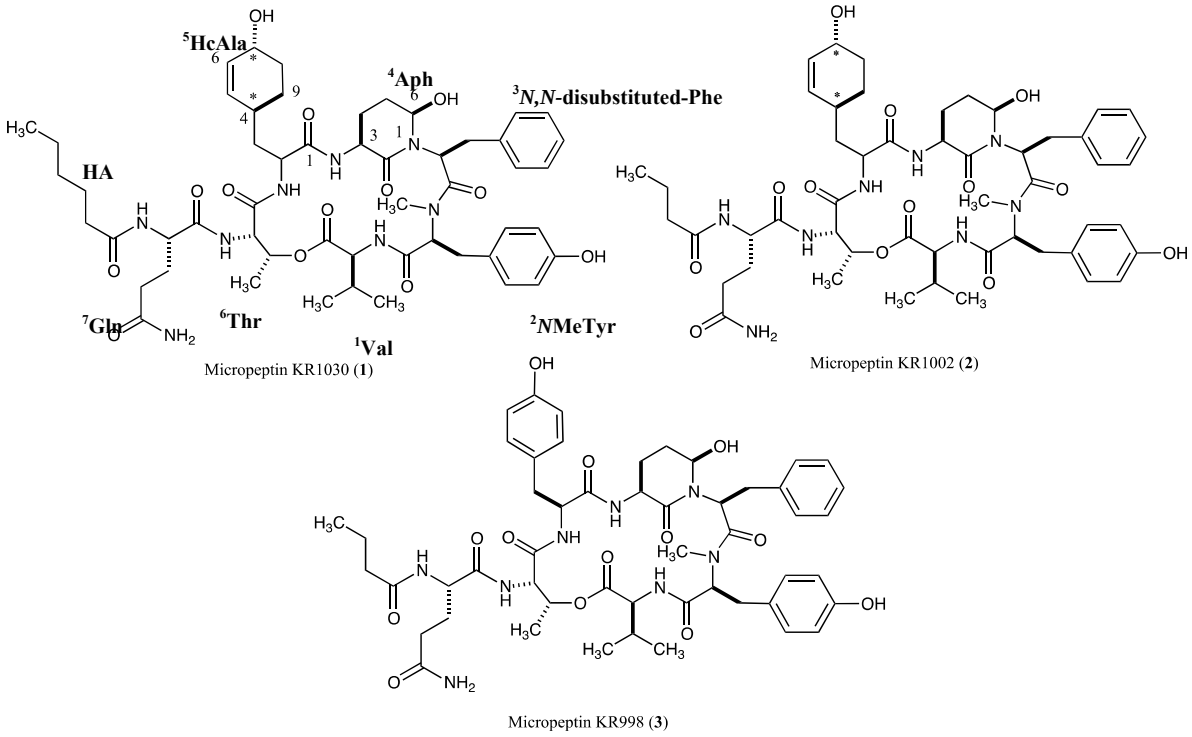

Micropeptin KR1030, presented an ESI^+ MS pseudo-molecular $[M+Na]^+$ ion at *m/z* 1053.5288, corresponding to the molecular formula $C_{53}H_{74}N_8NaO_{13}$ and 21 degrees of unsaturation. Examination of the NMR spectra of micropeptin KR1030, in DMSO-d_6, revealed its peptide nature; i.e., nine carboxyamide carbons in the ^{13}C NMR spectrum and five amide doublet protons in the ^1H NMR spectrum. Some characteristic signals suggested that it was a micropeptin type compound [136]. Taking into account the *N*Me-aromatic amino acid and the *N*,*N*-disubstituted-amino acid of the micropeptins, suggested that this micropeptin was assembled from seven amino acid moieties. In addition, a hydroxy group of secondary alcohol group, resonating at δ_H 4.61 ppm (d) and the hydroxy proton of Ahp at δ_H 5.99 ppm were evident in the ^1H NMR spectrum.

Additionally this analysis revealed two short fragments in agreement with one *N*,*N*-disubstituted aromatic amino acid (*N*,*N*-Phe), one a para substituted phenol rings (Tyr), and an extended spin system that didn't fit any proteogenic amino acid. The amide proton of this non-proteogenic amino acid (δ_H 8.40 ppm) had a COSY coupling to its α-methine proton at δ_H 4.23 ppm. Using the COSY and TOCSY correlations (**paper 4** supplementary) the α-methine proton was connected to a methylene, which in turn was connected to a methine, which was part of a 4-hydroxycyclohex-2-enyl moiety. This amino acid moiety was thus established as the rare HcAla (Figure 32) previously identified in only four cases in micropeptins [137–140].

Figure 32. Structure of the rare non-proteogenic amino acid HcAla.

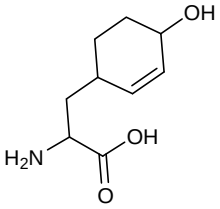

Assuming a twisted boat conformation for the cyclohexenyl moiety in HcAla, the pseudoaxial H8 ($H8_{pax}$) and H9 ($H9_{pax}$) were identified by their shift to higher field. NOE correlation of $H9_{pax}$ with H7 and of $H8_{pax}$ with H4, as well as, the rest of the NOE's of this spin system shown in Figure 33, established both as pseudoaxial, and the relative configuration of the hydroxy cyclohexenyl moiety as 4*S**,7*R**. Although the NOE pattern of H2, 3a, 3b and 4 pointed to a restricted rotation (Figure 33) it was not possible to assume the relative configuration of positions 2 and 4.

Figure 33. NOE correlations instrumental for detemining the relative configuration of the hydroxycyclohexenyl alanine moiety.

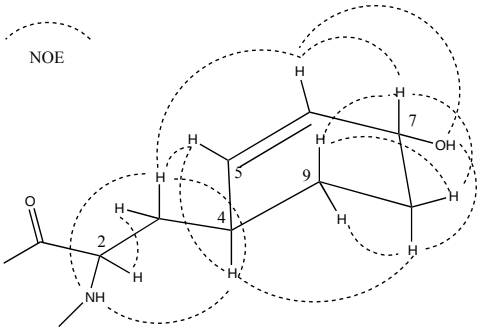

Table 6. NMR data of micropeptin KR1030 in DMSO-d_6.[a]

Position	δ_C, mult.[b]	δ_H, mult., *J* (Hz)	LR H-C correlations[c]	NOE correlations[d]
Val-1	172.2 s			
2	55.8 d	4.73 m	Val-1, *N*MeTyr-1	Val-3,4,5
3	31.0 d	2.07 m		Val-4,5,NH, Thr-3
4	19.5 q	0.84 d 6.5	Val-2,3,5	Val-2,3,NH, *N*MeTyr-*N*Me
5	17.3 q	0.71 d 6.9	Val2,3,4	Val-2,3,NH, Ahp-6-OH, *N*MeTyr-*N*Me
NH		7.36 d 9.6	*N*MeTyr-1	Val-4,5, *N*MeTyr-2,*N*Me, Ahp-6-OH
*N*MeTyr-1	169.3 s			
2	61.0 d	4.85 dd 12.0, 2.2	*N*MeTyr-1	Val-NH, *N*MeTyr-3b,5,5',*N*Me, Phe-2
3	33.0 t	2.70 dd 14.0, 12.0	*N*MeTyr-5,5'	*N*MeTyr-3b,5,5'
		3.08 dd 14.0, 2.2	*N*MeTyr-5,5'	*N*MeTyr-2,3a,5,5',,6,6'
4	127.7 s			
5,5'	130.6 dx2	6.98 dx2 8.2	*N*MeTyr-3,5,5',7	*N*MeTyr-2,3a,3b,6,6',*N*Me, Phe-2
6,6'	115.5 dx2	6.74 dx2 8.2	*N*MeTyr-4,5,5',7	*N*MeTyr-5,5',7-OH, Phe-6,6'
7	156.4 d			
7-OH		9.33 s	*N*MeTyr-6,6',7	*N*MeTyr-5,5',6,6'
*N*Me	30.5 q	2.75 s	*N*MeTyr-2, Phe-1	Val-4,5,NH, *N*MeTyr-2,5,5',6,6', Ahp-6-OH
Phe-1	170.5 s			
2	50.4 d	4.72 m	Ahp-2	*N*MeTyr-2, Phe-3a,5,5'

Table 6. *Cont.*

Position	δ_C, mult.[b]	δ_H, mult., *J* (Hz)	LR H-C correlations[c]	NOE correlations[d]
3	35.5 t	1.78 dd 14.0, 3.8	Phe-5,5’	*N*MeTyr-6,6’, Phe-2,3b,5,5’,
		2.85 dd 14.0, 12.3	Phe-2,5,5’	Phe-3a,5,5’, Ahp-6
4	136.9 s			
5,5’	129.6 dx2	6.82 dx2 7.1	Phe-5’,5,6,7	Phe-2,3a,3b,6,6’, Ahp-4a,6
6,6’	127.9 dx2	7.17 tx2 7.1	Phe-4,6’,6	*N*MeTyr-6,6’, Phe-5,5’
7	126.4 d	7.13 t 7.1	Phe-5	
Ahp-2	169.0 s			
3	48.6 d	3.61 m	Ahp-2	Phe-5,5’, Ahp-4a,NH
4	21.8 t	1.54 m		Ahp-3,4b,5
		2.39 dq 3.0, 12.3		Ahp-4a,5a,6-OH,NH
5	29.4 t	1.66 m		Ahp-4b,6,6-OH
		1.52 m		
6	73.9 d	5.05 dt 1.8,3.2		Phe-3b,5,5’, Ahp-5a,5b,6-OH
6-OH		5.99 d 3.2		Val-4’,5,NH, Ahp-5a,6, *N*MeTyr-*N*Me
NH		7.08 d 9.1	HcAla-1	Ahp-3,4b, AcAla-2,NH, Thr-3
HcAla-1	170.1 s			
2	49.6 d	4.23 brdd 10.6,8.8		Ahp-NH, HcAla-3b
3	36.4 t	1.40 brt 10.6		HcAla-3b,4,5,6,NH
		1.69 m		HcAla-2,3a
4	31.7 d	1.92 m		HcAla-3a,5,6,8pax,NH
5	132.2 d	5.37 m	HcAla-7	HcAla-3a,4,6,7
6	132.9 d	5.55 brd 10.3	HcAla-8	HcAla-3a,4,5,7,7-OH
7	65.3 d	3.95 m		HcAla-6,7,7-OH,8peq,9pax
7-OH		4.61 d 5.3	HcAla-6,7,8	HcAla-6,7,8pax
8pax	31.5 t	1.20 m		HcAla-4,7-OH,8peq,9peq
peq		1.79 m		HcAla-7,8pax,9pax
9pax	26.0 t	0.95 td 12.7,3.0		HcAla-7,8peq,9peq
peq		1.66 m	HcAla-4	HcAla-8pax,9peq
NH		8.40 d 8.8	Thr-1	Ahp-NH, HcAla-3a,4, Thr-2
Thr-1	169.5 s			
2	54.9 d	4.55 d 9.1	Thr-1	HcAla-NH, Thr-3,4
3	71.8 d	5.37 m	Val-1	HcAla-NH, Thr-2,4, Val-3
4	17.6 q	1.17 d 6.6	Thr-2,3	Thr-2,3, Gln-2
NH		7.96 d 9.1	Gln-1	Thr-4, Gln-2
Gln-1	172.8 s			
2	52.2 d	4.38 dt 6.0,8.0	Gln-1	Thr-4,NH, Gln-3a,3b,NH, HA-4
3	27.9 t	1.69 m	Gln-2,4	Gln-2,3b,NH
		1.84 m		Gln-2,3a,NH
4	31.8 t	2.07 m	Gln-5	
		2.08 m	Gln-5	
5	174.0 s			
5-NH_2 (a)		6.73 s	Gln-4	
(b)		7.21 s	Gln-5	Gln-4
NH		7.98 d 8.0	HA-1	Gln-2,3a
HA-1	172.5 s			
2	35.2 7	2.08 m	HA-1,4	HA-3
3	25.1 t	1.49 m	HA-1,4	HA-2
4	31.5 t	1.20 m	HA-1,3,5	
5	22.0 t	1.23 m	HA-3,4,6	
6	14.0 q	0.84 t 7.0	HA-5	

[a]500 MHz for ^{1}H, 125 MHz for ^{13}C. [b]Multiplicity and assignment from HSQC experiment. [c]Determined from HMBC experiment, $^nJ_{CH}$=8 Hz, recycle time 1s. [d]Selected NOE’s from a ROESY experiment.

Analysis of the COSY, total correlation spectroscopy (TOCSY), and HSQC 2D NMR experiments, (see Table 6) allowed the assignment of Val, Thr, Gln, and Ahp moieties.

The complete structure of the micropeptin was achieved by analysis of the long range (LR) correlations of the ^{1}H–^{13}C HMBC experiment (see Table 6). This procedure established the

structures of Val, *N*MeTyr, *N,N*-disubstituted-Phe, Ahp, HcAla, 3-*O*-substituted-Thr, Gln, and hexanoic acid (HA) residues.

The sequence of the amino acids of micropeptin KR1030 was assigned on the basis of HMBC and rotating frame nuclear Overhauser effect spectroscopy (ROESY) correlations as illustrated in Figure 35.

Figure 34. HMBC correlations (blue) and ROESY correlation (green) linking the amino acids and HA in micropeptin KR1030.

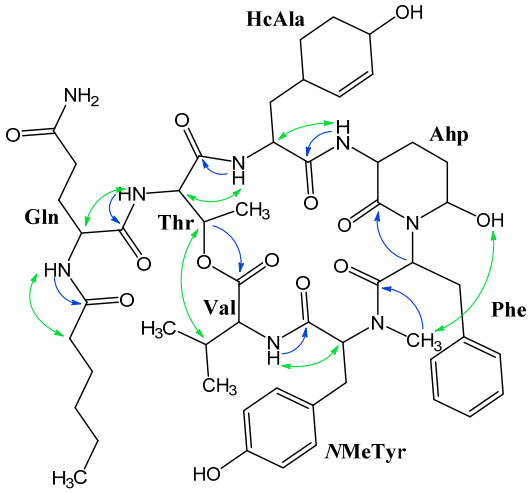

The absolute configuration of most of the amino acids in micropeptin KR1030 was established through hydrolysis to release single amino acids and derivatization with Marfey's reagent [134], followed by HPLC analysis. This demonstrated the L-configuration of Val, *N*Me-Tyr, Phe, Thr, and Glu residues. Micropeptin KR1030 contains the special amino acids Aph. The carboxyamide in Ahp was reduced to a secondary alcohol with Jones oxidation [141] prior to hydrolysis (Figure 35) and reaction with Marfey's reagent. Hereby the *3S*-configuration for the Ahp residue was determined. An attempt to determine the absolute configuration of C2 in HcAla by advances Marfey's procedure failed most probably due to its decomposition during hydrolysis.

Figure 35. Jones oxidation that liberates L-Glu from Ahp and hydrolysis to release the amino acid.

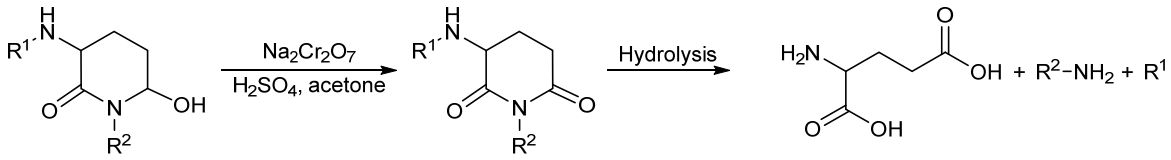

The configuration of C6 of the Ahp was determined as *R* on the basis of the *J*-values of H6, 1.8 and 3.2 Hz, with pseudo-equatorial-H5 and pseudo-axial-H5, respectively. This points to an equatorial orientation of H6. The chemical shift of the pseudo-axial-H4, δ_H 2.39 dq (3.0,12.3), which is down-field shifted by the axial 6-hydroxy-group. The trans diaxial relationship with H3 and the NOE correlation between H4pax with the 6-OH. Based on these findings the structure of micropeptin KR1030 was established.

Examination of the NMR spectra of micropeptin KR1002 revealed that the ^{1}H and ^{13}C NMR spectra are similar to those of micropeptin KR1030. The molecular formula of micropeptin KR1002, $C_{51}H_{70}N_8O_{13}$, was deduced from the high-resolution ESI^+-MS measurements of its sodiated molecular adduct ion at *m/z* 1025.4958. Comparison of the NMR data of micropeptin KR1030 and micropeptin KR1002 (Table 6 and 7) revealed that the difference between them is located in the fatty acid at the N-termini of these cyclic depsipeptides. Two methylene carbons (δ_C 31.5 and 25.1 ppm) of the aliphatic residue and four proton signals (δ_H ~1.20 ppm) were present in the spectra of micropeptin KR1030 were missing from the spectra of micropeptin KR1002. This suggests that the HA residue, in micropeptin KR1030, is replaced by a butyric acid (BA) residue, in micropeptin KR1002. Full assignment of micropeptin KR1002 was achieved by interpretation of the COSY, TOCSY, ROESY, HSQC and HMBC 2D NMR correlations (see Table 7), revealing the composition and sequence of acid residues of micropeptin KR1002 as, Val, *N*MeTyr, *N*,*N*-disubstituted-Phe, Ahp, HcAla, Thr, Gln and BA.

Table 7. NMR data of micropeptin KR1002 in DMSO-d_6.[a]

Position	δ_C, mult.[b]	δ_H, mult., *J* (Hz)	LR H-C correlations[c]	NOE correlations[d]
Val-1	172.6 s			
2	55.6 d	4.73 dd 9.8,4.2	Val-5	Val-3,4,NH, *N*MeTyr-2
3	30.9 d	2.07 m		Val-2,4,5
4	19.3 q	0.86 d 6.7	Val-2,3,5	Val-3, *N*MeTyr-*N*Me
5	17.1 q	0.71 d 6.7	Val-2,3,4	Val-3,NH, *N*MeTyr-*N*Me, Ahp-6-OH
NH		7.38 d 9.8	*N*MeTyr-1	Val-2,3, *N*MeTyr-2,*N*Me
*N*MeTyr-1	168.9 s			
2	60.9 d	4.89 dd 11.5,2.0	*N*MeTyr-1	Val-2, *N*MeTyr-3b,5,5',*N*Me
3	32.8 t	2.71 dd 13.2, 11.5	*N*MeTyr-5,5'	Val-NH, *N*MeTyr-3b,5,5',6,6'
		3.09 dd 13.2, 2.0	*N*MeTyr-4,5,5'	*N*MeTyr-2,3a,5,5'
4	127.5 s			
5,5'	130.4 dx2	6.99 dx2 8.2	*N*MeTyr-3,5',5,7	*N*MeTyr-2,3a,3b, Phe-2
6,6'	115.3 dx2	6.76 dx2 8.2	*N*MeTyr-4,6',6,7	*N*MeTyr-3a,7-OH, Phe-3a
7	156.2 s			
7-OH		9.33	*N*MeTyr-6',6,7	*N*MeTyr-6,6'
*N*Me	30.3 q	2.75 s	*N*MeTyr-2	Val-4,5,NH, *N*MeTyr-2,5,5'
Phe-1	170.3 s			
2	50.2 d	4.75 dd 11.9,3.9	Phe-1	*N*MeTyr-5,5', Phe-3a,5,5'
3	38.5 t	1.79 m	Phe-5,5'	Phe-2,3b,5,5', *N*MeTyr-6,6'
		2.85 dd 11.9,14.0	Phe-5,5'	Phe-3,5,5', Ahp-6
4	136.7 s			
5,5'	129.4 dx2	6.82 dx2 7.1	Phe-3,5',6,7	Phe-2,3a,3b, Ahp-4a
6,6'	127.7 dx2	7.17 tx2 7.1	Phe-4,5,6	HcAla-OH
7	126.2 d	7.13 t 7.1	Phe-5	Ahp-3
Ahp-2	169.3 s			
3	48.5 d	3.60 ddd 7.1,9.1,12.7		Ahp-4a,NH, Phe-7
4	21.6 t	1.55 m		Ahp-3,4b,6, Phe-6,6'
		2.39 brq 12.7		Ahp-4a,NH,6-OH
5	29.6 t	1.67 m		Ahp-6-OH, HcAla--5
		1.55 m		
6	73.7 d	5.05 brs		Phe-3b, Ahp-4,5,6-OH
6-OH		5.99 d 2.5		Ahp-4b,5,6, Val-5,NH, HcAla-NH

Table 7. *Cont.*

Position	δ_C, mult.[b]	δ_H, mult., *J* (Hz)	LR H-C correlations[c]	NOE correlations[d]
NH		7.08 d 9.1	HcAla-1	Ahp-3,4b, HcAla-2,9,NH
HcAla-1	170.0 s			
2	49.4 d	4.23 brdd 11.4,7.4		Ahp-NH, HcAla-3b,4
3	36.4 t	1.40 dt 3.7,11.4		HcAla-3b,4,5,6
		1.71 m		HcAla-2,3a
4	31.6 d	1.92 m		HcAla-2,3a,5,6,8pax,NH
5	132.0 d	5.37 brd 10.2		HcAla-3a,4,6,7
6	132.7 d	5.55 dd 10.2,1.0	HcAla-4	HcAla-3a,4,5,7,7-OH
7	65.1 d	3.94 brm		HcAla-5,6,7-OH,8peq,9pax
8 peq	31.6 t	1.79 m		HcAla-7,7-OH,8pax,9pax
pax		1.20 m		HcAla-4,8peq,9peq,7-OH
9 peq	25.8 t	1.70 m		HcAla-4,8pax,9pax
pax		0.93 brq 11.3		HcAla-7,8peq,9peq
7-OH		4.61 d 5.4	HcAla-6,7,8	HcAla-6,7,8peq,8pax
NH		8.40 d 8.4		Ahp-NH, HcAla-3a,4, Thr-2,3
Thr-1	169.1 s			
2	54.9 d	4.55 brd 9.1	Thr-1, Gln-1	HcAla-NH, Thr-4
3	71.7 d	5.39 q 6.5	Thr-4	HcAla-NH, Thr-4
4	17.6 q	1.17 d 6.5	Thr-2,3	HcAla-7-OH, Thr-2,3,NH
NH		7.91 d 9.0	Gln-1	HcAla-NH, Thr-4
Gln-1	172.2 s			
2	52.0 d	4.38 m	Gln-1	Thr-NH, Gln-3a,3b,4b
3	27.7 t	1.69 m	Gln-4	Gln-2,3b,NH, BA-3
		1.84 m		Gln-3a,NH
4	31.6 t	2.11 m	Gln-5	Gln-2,NH,5-NH_2
5	173.9 s			
5-NH_2(a)		6.72 s	Gln-4	
(b)		7.21 s		Gln-4
NH		7.99 d 7.5	BA-1	Gln-3a,4
BA-1	172.0 s			
2	37.0 t	2.09 m	BA-1,3,4	Gln-2
3	18.9 t	1.51 m	BA-1,2,4	Gln-3a
4	13.6 q	0.84 t 7.3	BA-2,3	Val-2

[a]400 MHz for ^{1}H, 100 MHz for ^{13}C. [b]Multiplicity and assignment from HSQC experiment. [c]Determined from HMBC experiment, $^nJ_{CH}$=8 Hz, recycle time 1s. [d]Selected NOE's from a ROESY experiment.

Acid hydrolysis of micropeptin KR1002 and derivatization with Marfey's reagent [134], as described above for micropeptin KR1030 followed by HPLC analysis, demonstrated the L-configurations for all of the amino acid residues except of HcAla. The absolute configuration of the Ahp residue was determined in the same way as for micropeptin KR1030. Based on these findings the structure of micropeptin KR1002 was established.

Micropeptin KR998 presented an ESI$^+$-MS pseudo-molecular $[M+Na]^+$ ion at *m/z* 1021.4666, corresponding to the molecular formula $C_{51}H_{66}N_8O_{13}$ and 23 degrees of unsaturation. Comparison of the degree of unsaturation of micropeptin KR998 with those of micropeptin KR1002, revealed two additional ones in micropeptin KR998. The ^{1}H and ^{13}C NMR spectra of micropeptin KR998 were comparable with those of micropeptin KR1002, but revealed some differences as well.

In the aromatic region of the ^{1}H NMR spectrum of micropeptin KR998, two additional doublet signals at δ_H 6.89 and 6.56 ppm (2H each) with a *J* coupling constant of 8.2 Hz. Furthermore did a singlet at δ_H 9.07 ppm occur as well as two additional benzyl protons (δ_H 3.11 and 2.50 ppm) in the aliphatic region. The signals corresponding to the HcAla in micropeptin KR1002 were missing.

In the ^{13}C NMR spectrum of micropeptin KR998 four new aromatic signals (δ_C 128.3, 129.8, 115.2 and 155.7 ppm), of a *para*-substituted phenol moiety were observed. As in the ^{1}H NMR spectrum the signals of HcAla observed in micropeptin KR1002 were missing (Table 7 and Table 8). The data summarized above and the molecular formula of micropeptin KR998 relative to that of micropeptin KR1002 suggested that in micropeptin KR998 a Tyr moiety substitute the HcAla of micropeptin KR1002. The rest of the structures of these compounds are identical. Full assignment of the tyrosine moiety and the rest of the moieties that compose micropeptin KR998 as well as their sequence were achieved using COSY, TOCSY, ROESY, HSQC and HMBC 2D NMR correlations (Table 8).

Table 8. NMR data of micropeptin KR998 in DMSO-d_6.[a]

Position	δ_C, mult.[b]	δ_H, mult., *J* (Hz)	LR H-C correlations[c]	NOE correlations[d]
Val-1	172.1 s			
2	55.9 d	4.66 dd 9.5,4.3	Val-1,3,5	Val-3,4,5,NH, Gln-NH_2
3	31.0 d	2.02 m	Val-2,4,5	Val-2,4,5,NH, Thr-2
4	19.4 q	0.85 d 5.7	Val-2,3,5	Val-2,3,NH, *N*MeTyr-*N*Me
5	17.3 q	0.70 d 6.7	Val-2,3,4	Val -2,3,NH, *N*MeTyr-*N*Me, Ahp-6-OH
NH		7.37 d 9.5	*N*MeTyr-1	Val-2,3,4,5, *N*MeTyr-2,*N*Me, Ahp-6-OH
*N*MeTyr-1	169.0 s			
2	61.0 d	4.89 brd 11.4	*N*MeTyr-1,*N*Me	Val-NH, *N*MeTyr-3b,5,5’
3	33.0 t	2.71 dd 13.4,11.4 3.08 brd 13.4	*N*MeTyr-2,5,5’ *N*MeTyr-4,5,5’	*N*MeTyr-3b,6,6’ *N*MeTyr-2,3a,5,5’
4	127.7 s			
5,5’	130.6 dx2	6.99 dx2 8.0	*N*MeTyr-3,5’,5,6,6’,7	*N*MeTyr-2,3b,*N*Me, Phe-2,3a
6,6’	11.5.5 dx2	6.77 dx2 8.0	*N*MeTyr-4,6,6’,7	*N*MeTyr-*N*Me,OH, Phe-3a
7	156.4 s			
*N*Me	30.5 q	2.75 s	*N*MeTyr-2, Phe-1	*N*MePhe-5,5’,7, Val-4,5,NH
Phe-1	170.5 s			
2	50.4 d	4.74 dd 11.3,3.6	Phe-1	*N*MeTyr-5,5’, Phe-3a,5,5’
3	35.5 t	1.78 m 2.86 dd 11.7,13.8	Phe-5,5’	*N*MeTyr-5,5’,6,6’, Phe-2,3b,5,5’ Phe-3a,5,5’, Ahp-6
4	136.9 s			
5,5’	129.6 dx2	6.83 dx2 7.1	Phe-3,5’,5,7	Phe-2,3a,3b, Ahp-3,5a,6
6,6’	127.9 dx2	7.18 tx2 7.1	Phe-4,5,5’,6’,6	Ahp-3
7	126.4 d	7.14 t 7.1	Phe-5,5’	
Ahp-2	169.0 s			
3	49.0 d	3.60 ddd 11.6,8.2,6.0	Ahp-2,4	Phe-5,5’, Ahp-4a,NH
4	21.7 t	1.62 m 2.40 brq 12.4		Ahp-3,4b Ahp-4a,5b,NH
5	29.4 t	1.68 m 1.57 m		Ahp-6,6-OH Ahp-4b

Table 8. *Cont.*

Position	δ_C, mult.[b]	δH, mult., *J* (Hz)	LR H-C correlations[c]	NOE correlations[d]
6	73.9 d	5.05 brs		Phe-3b,5,5', Ahp-5a,5b
6-OH		5.99 d 2.1		Ahp-5b,6, Val-5,NH
NH		7.07 d 10.2		Ahp-3,4b, Tyr-2,NH
Tyr-1	169.7 s			
2	53.6 d	4.35 ddd 3.8,9.0,13.0		Ahp-NH, Tyr-3a,3b,5,5',NH
3	35.1 t	2.50 dd 13.0,14.7	Tyr-2,4,5	Tyr-2,3b,5,5'
		3.11 dd 3.8,14.7		Tyr-2,3a,NH
4	128.3 s			
5,5'	129.8 dx2	6.89 dx2 8.2	Tyr-3,5,5',6,6',7	Tyr-2,3a,NH
6,6'	115.2 dx2	6.56 dx2 8.2	Tyr-4,6',6,7	Tyr-5,5',7-OH
7	155.7 s			
7-OH		9.07 s	Tyr-6,6'	Tyr-6,6'
NH		8.45 d 9.0	Thr-1	Ahp-NH, Tyr-2,3a,5,5', Thr-2,3
Thr-1	169.0 s			
2	554.4 d	4.45 brd 9.4	Thr-1,4, Gln-1	Tyr-NH, Thr-4,NH, Ahp-NH
3	72.2 d	5.37 q 6.5	Thr-4, Val-1	Ahp-NH, Tyr-NH, Thr-4
4	17.7 q	1.10 d 6.5	Thr-2,3	Thr-2,3,NH
NH		7.69 d d 9.4	Gln-1	Thr-2,3,4, Gln-2,3b
Gln-1	172.3 s			
2	52.2 d	4.30 dt 5.3,8.3	Gln-3	Thr-NH, Gln-3a,3b,4,NH
3	27.5 t	1.70 m	Gln-2,4,5	Gln-2,NH
		1.80 m	Gln-1,2,4,5	Thr-NH, Gln-2
4	31.7 t	2.05 m	Gln-2,3,5	Gln-2,NH,5-NH_2(a,b)
5	174.3 s			
5-NH_2a		6.81 s	Gln-4,5	Gln-4
b		7.24 s	Gln-5	Gln-4
NH		7.98 d 7.8	BA-1	Gln-2,a3,4
BA-1	172.4 s			
2	37.4 t	2.10 m	BA-1,3,4	
3	18.9 t	1.50 tq 7.3,7.3	BA-1,2,4	
4	13.8 q	0.85 t 7.2	BA-2,3	

[a]500 MHz for ^{1}H, 125 MHz for ^{13}C. [b]Multiplicity and assignment from HSQC experiment. [c]Determined from HMBC experiment, $^nJ_{CH}$=8 Hz, recycle time 1s. [d]Selected NOE's from a ROESY experiment.

Marfay's analysis as described above established the absolute configuration of all amino acids including C3 of Ahp as L in micropeptin KR998. The absolute configuration of C6 of the Ahp residue was determined in the same way as for micropeptin KR1030. Based on these findings the structure of micropeptin KR998 was established.

5.2 Biological Activity of Micropeptins

The crude cyanobacteria extract exhibited significant inhibition of the serine protease chymotrypsin with a concentration of 1 mg/ml. Purification of the three micropeptins from the extract revealed that they were responsible for the inhibition of chymotrypsin. The inhibitory activity of the three micropeptins was determined for serine protease: chymotrypsin, elastase and

trypsin. Chymotrypsin was inhibited with IC_{50} values between 5.9 and 18.8 μM. Elastase was inhibited by micropeptin KR1030 and micropeptin KR1002 with IC_{50} values of 28.0 μM each. Micropeptin KR998 did not inhibit elastase at a concentration up to 50 μM. The three micropeptins did not inhibit trypsin at a concentration up to 45.5 μM. Additionally, the three micropeptins were tested towards CLL cells though without activity at concentrations up to 72 nM. The results of biological activity induced by the three micropeptins are compiled in Table 9.

Table 9. The inhibitory activity [IC_{50}] of micropeptin KR1030, KR1002, and KR998 screened towards serine protease chymotrypsin, elastase and trypsin as well as CLL cells.

	Chymotrypsin	Elastase	Trypsin	CLL
Micropeptin KR1030	13.9 μM	28.0 μM	Inactive	Inactive
Micropeptin KR1002	18.8 μM	28.0 μM	Inactive	Inactive
Micropeptin KR998	5.9 μM	Inactive	Inactive	Inactive

The nature of the fifth position from the C-termini of the micropeptins has been reported to be display selectivity between trypsin and chymotrypsin types of enzyme inhibition. Selective trypsin inhibition is induced by basic amino acids where selective chymotrypsin inhibition is induced by lipophilic or aromatic amino acids [119,127]. The inhibitory activity of micropeptins towards chymotrypsin observed in this study was in accordance with the lipophilic nature of the amino acids next to the Ahp moiety, which usually are potent chymotrypsin inhibitors [119,127]. One of the most potent proteases inhibitor reported among the micropeptins with IC_{50} values in picomolar and low nanomolar range is Cyanopeptolin 1020 [142]. Cyanopeptolin 1020 differ from micropeptin KR1030, KR1002, and KR998 in the fifth position and in the side chain. This indicates some very important binding sites in these positions of micropeptins in serine proteases.

The conformation of the micropeptins is important for the inhibition of proteases. The NOE correlations between the hydroxy proton in Ahp and protons in Val indicate a U-shaped conformation where Ahp and Val are close in space. This conformation of micropeptins is found in a X-ray crystal structure of micropeptin A9072A/bovine trypsin complex and has been associated to inhibiting activity of micropeptins [143].

5.3 Conclusion

This study describes the isolation of micropeptin KR1030, KR1002, and KR998 together with the known microcyclamide GL546A from a water bloom material of the cyanobacterium *Microcystis* sp. The three new micropeptins displayed inhibitory activity towards chymotrypsin with IC_{50} values between 5.9 and 18.8 μM. The awareness of proteases influence on development of cancer is increasing and protease inhibitors develop as an interesting new class of anticancer agents [119,144]. The presence of non-proteogenic amino acids (Ahp and HcAla) in the three new micropeptins allows the expansion of the library of micropeptins that are biosynthesized by cyanobacteria. Non-proteogenic amino acids in peptides might be incorporated to avoid recognition by proteolytic enzymes or enable recognition by receptors in the immune system.

Chapter 6

Overall Discussion and Perspectives

Fungal extracts usually contain multiple bioactive compounds with high structural complexity. Historically, NPs have been a very important source in drug discovery yet untapped biodiversity [145] and knowledge from full genomes sequences [146] indicates that new compounds are still to be discovered within even well-characterized fungal species (**paper 1**) [70]. The aim of this PhD project has been to uncover unknown NPs that target CLL cells or other biological targets and additionally to identify novel bioactivities in previously described compounds. During the course of this PhD 11 compounds have been identified with activity towards CLL cells. Four of the compounds, ophiobolin A, B, C and K, induced apoptosis in CLL cells with LC_{50} values between 1 and 8 nM and a narrow therapeutic window. Additionally proxiphomin displayed cytotoxic effect towards CLL cells with a LC_{50} value of ca 20 μM.

SAR study has indicated the pharmacophore of the ophiobolins. One new ophiobolin U was isolated and the structure fully characterized by 1D and 2D NMR and an initial. The work has added to the strategy for effective dereplication that allows quickly identification of known compounds in an active extract. The results obtained have been presented in in the four previous chapters of this thesis and peer-reviewed papers.

The challenge of avoiding rediscovering of compounds forces the NPs chemist to focus on the screening setup such as preliminary selection of producing organism, prefractionation, and early dereplication. The search for novel bioactive compounds often starts with a preliminary screen set up covering a huge biodiversity. The design of the preliminary screen affects the results of the entire campaign. In our preliminary screen 289 fungal extracts from 138 fungal strains were screened. Many of the strains were newly described and with unexplored chemodiversity. To maximize the chemical spectrum of compounds produced by the strains cultivated in accordance with the OSMAC approach were applied. The most potent strains were chosen for further investigation of the activity towards CLL.

Six of the eleven compounds targeting CLL cells, which have been discovered in this project, are penicillic acid, viridicatumtoxin, calbistrin A, brefeldin A, emestrin A, and neosolaniol monoacetate. All of them displayed cytotoxic activity towards CLL and healthy cells in the same concentration (**paper 2**). In the past, compounds like these might have been developed as a drug lead to obtain analogs that kills cancer cells more efficiently than healthy cells. One example of a cytotoxic compound that was approved for clinical use in cancer treatment despite the fact that severe side effects are induced in patients is taxol. Today, approval of new drugs is more

restricted and request tumor-specific targets to meet the demand for next generation chemotherapeutics. Accordingly, a general cytotoxic hit is not sufficient as pharmaceutical anymore.

A strategy to reveal completely new chemical scaffolds may be to stimulate the microbe to express silent gene clusters [146,147]. Methods to achieve this undiscovered chemodiversity have been developed, including co-culture, epigenetic modification experiments, and metabolic engineering [148]. In these experiments, novel bioactive compounds can be produced due to either activation of silent biosynthetic pathways or due to up-regulations of the production of certain compounds [149,150]. In co-cultures, chemical signals between organisms can provoke activation or up-regulation of biosynthetic pathways [148,151]. One example of a previously unexpressed biosynthetic pathway is the libertellenones. Libertellenones A-D were produced by a fungal *Libertella* sp. strain in a co-culture with a marine bacterium. Libertellenones A-D were isolated from the co-culture and displayed anti-cancer activity towards colon cancer [152].

Chemical epigenetic modification is another approach to stimulate production of NPs not expressed under standard laboratory conditions. Epigenetic modifications can give access to pools of novel NPs scaffolds produced in their native host. One example is the report of chaetophenol C-E, three novel polycyclic skeleton produced by the fungus *Chaetomium indicum*, directly associated to epi-genetic modification [153].

Metabolic engineering can be another route to discover novel bioactive NPs through genome mining and following expression of silent genes in stable mutants [154,155]. This was done by accurate prediction of the gene cluster of the NRP nidulanin A and following expression through a stable mutant [156]. Metabolic engineering can be a challenging task that requires knowledge of the full genome sequence and the target gene cluster. Making mutant libraries is often very time consuming and still there is no guarantee for correct expression of a target compound [155].

If I should setup a new large screening campaign I would consider including both co-culture and epigenetic experiments in the pre-screen to provoke production of novel chemical scaffolds. Co-culture and epigenetic experiments are both suitable for high through-put screening as they are fast, low-cost approaches that readily can be implanted in most labs without high expenses for new equipment [155,157] Molecular biology is a more expensive and inaccessible approach as it demand time-consuming preparation of mutant strains, making it less suitable for high through-put screening. Nevertheless, metabolic engineering can, with advantage, be included in later stages of the discovery process to gain a higher and more stable expression of target metabolites.

A high yield of a compound is needed to resupply for synthesize of analogs, e.g. for SAR studies. Alternatively design of analogs can be conducted through synthetic biology where new analogs are produced directly in the living model organism. The advantage of this approach compared to semi-synthetic derivatization is that the relative complex structures, often found in NPs, easier can be produced through genetic biosynthesis.

In this current PhD study, all extracts in the preliminary screen were small-scale crude extracts. By solely screening crude extracts it is hard to distinguish between selective activity and

general cytotoxicity even if the extracts are screened towards healthy cells as well. This is due to various bioactive compounds in the crude extract and consequently, it is not possible to know if all active compounds likewise have activity towards healthy cells. Prefractionation at the preliminary screening can be beneficial and might increase the efficiency of the assay compared to screening of crude extracts. By the screening of fractions with lower complexity in an orthogonal screenings setup consisting of both target cells and healthy cells it may be possible to distinguish between fractions containing selective active compounds and general cytotoxic compounds, thus giving a more realistic hit rate. E-SPE has been the method of choice for prefractionation in this project, yet first at a later stage in the screening. These fractions could have provided the needed reduction in complexity for the initial screen. Even with all the benefits gained by prefractionation it is still worth to combine the preliminary screen with crude extracts as well. Sometimes activity is lost in a prefractionation due to disruption of potential synergisms, the active compounds may be trapped on the column, or be instable. To distinguish between these possibilities it would be valuable to recombine a small amount from each fraction and include this in the screening as well. One example of lost activity by fractionation is the *P. pinicola* extract containing the statins (section 2.3).

Dereplication is a very powerful tool to tentatively identify known compounds in a crude extract to save time isolate and structure elucidate already known compounds [86]. Dereplication can be introduced in many stages of the drug discovery process. Based on my experience in this PhD study, dereplication should be introduced very early in the drug discovery process where it functions as an early stop-or-go message and continually through the whole discovery process. Comparative dereplication of small-scale E-SPE fractions often provides a strong indication of the candidate responsible for the activity. If the potential candidate is a known compound or potential analog of a known compound, I think that the project needs to be closed before any scale up. This very conservative approach entails that more time is spent in the preliminary screen including prefractionation and a highly increased number of samples for prescreening. This might have caused rejection of the majority of the 61 active fungal extracts in this project. The problem by this conservative decision-making can be that none or only very few extracts satisfy the requirements for scale up. Nevertheless, I believe that this approach increase the possibility of discovering novel bioactive scaffolds from the extracts that are scaled up.

The performance of mass spectrometers is continuously improving, including easy access to both positive and negative ionization spectra even during fast UHPLC. Integration of these massive amounts of data; however, might represent a major challenge in the near future. In order to manage fast dereplication of the massive data flow generated, multivariate data analysis becomes a necessary tool. Recent initiatives of e.g. molecular networking based on MSMS fragmentation libraries [158] and bioassay results might in the future enable fast dereplication. The implantation of such a setup might focus a targeted screening procedure and speed up the process from observed activity to identification of compound.

During my external stay with Professor Shmuel Carmeli at Tel Aviv University, I got the opportunity to work with NPs produced by cyanobacteria with the focus of discovering novel bioactive peptides (**paper 4**). Here, the discovery process was a target-guided isolation based on NMR spectroscopy where the method of choice at DTU Systems Biology is bio-guided combined with UV and MS techniques. The project based on NMR provided three new micropeptins that inhibited chymotrypsin.

To select the most ideal separations strategy it is very important to consider the aim and type of the project. The approach with NMR as reference point is based on selection of fractions for further separation that contain a specific target compound or compound family for further purification [159], primarily based on 1D ^{1}H NMR experiments for fast and non-destructive structural information. Target-guided separation based on LC-HRMS supports the separation strategy by providing information on the number of compounds in a fraction and molecular formula.

NMR spectroscopy has a high signal richness and consequently the ^{1}H NMR spectra from crude extract and fractions tend to be filled with overlapping signals especially in the more shielded region at chemical shifts below 3 ppm [160]. Among compounds reported from cyanobacteria so far, there seems to be a prevalence of small peptides [161]. The characteristic chemical shifts of peptides originating from the more deshielded amide-(NH) and α-protons (H_α). NH chemical shifts are mostly recognized as doublets between δ_{NH} 7.0 and 9.0 ppm where H_α chemical shifts are found more upfield between $\delta_{H\alpha}$ 3.5 and 5.0 ppm [162]. These chemical shifts are easy to identify and NMR-based isolation targeting peptides is accordingly a favored method of choice. Fractions that contain secondary metabolites with no deshielded proton are not suited for NMR-based separation. For example fungal extracts that often contain a high amount of polyketides with low proton density or terpenoids that contain many shielded protons.

LC-HRMS is very sensitive method and with the access to both positive and negative ionization spectra most small molecules are detectable even in very low amounts. This very beneficial quality decreases the chance of overlooking interesting molecules although some of the compounds detected are inaccessible for preparative purification. NMR is more insensitive, especially regarding mixtures, and target-guided separation based on NMR mainly leads to compounds present in high amounts with the risk of overlook interesting compounds. Target-guided separation based on neither NMR- nor LC-HRMS provides any security that the compounds isolated are bioactive and solely these approaches can lead to discovery of inactive compounds. Consequently both approaches need to be combined with bio-guided isolation when the aim of a project is to discover compounds with a given bioactivity. Bio-guided isolation is, depended on the bioassay, often a very sensitive approach allowing discovery of bioactive compounds present only in small amounts. The sensitivity of many assays holds a duality for the NPs chemist as low-amount compounds are more unexplored but also more inaccessible. The disadvantage of solely bio-guided separation is the continual challenge of rediscovery of compounds. Furthermore bio-guided separation is limited by the choice of bioassay since NPs with other bioactivities are overlooked. None of these approaches are appropriate alone and needs

to be combined to increase the effectiveness of isolation and identification of novel biological interesting compounds.

NPs drug discovery today balance between promise and reality. The promise related to NPs as an enormous reservoir of novel chemistry with biological activities. The opportunities is abundant due to the huge unexplored diversity in the fungal kingdom (**paper 1**) [145]. Yet, the reality is that only 13 commercial NPs has been approved as pharmaceuticals between 2000 and 2010 [4]. In recent years, the pharmaceutical industry has assigned a lower priority to discovery of bioactive small molecules [163,164].

The development and approval of a new drug cost approx. US$ 1,778 million [165], which is unrealistic to conduct within academia [82]. The high cost combined with the low priority from the pharmaceutical industry makes it important for the NPs chemist to give relevance to a compound for ultimately enter into clinical trials. This requires strong collaboration within academia where interdisciplinary clusters between NPs chemistry, synthetic chemistry, biology, molecular biology, fermentation etc. are needed. Before a hit in the discovery process is interesting as a drug lead suitable for the pharmaceutical industry, the compound need to fulfill some of the items listed below [166].

- A specific and selective activity
- Target a novel biological mechanism
- Reasonably bioavailability

Specific and selective activity: As demonstrated in this PhD project many compounds display anti-cancer activity as well as antifungal activity (**paper 1 and 2**). This observation might be a consequence of general cytotoxic molecules maybe because they target eukaryote cells in general. General cytotoxicity is a huge problem in development of pharmaceuticals because it often results in severe side effects for the patients. Consequently, a bioactive compound must be superior potent with a therapeutic window or the first agent of its class before it can advance into the discovery pipeline in the pharmaceutical industry.

Target a novel biological mechanism: To be relevant for the pharmaceutical industry it is important that the compound target a novel biological mechanism [167]. Pharmaceuticals developed today only target 483 out of the estimated 3,000-10,000 therapeutic targets leaving a huge potential for novel pharmaceuticals [168]. The molecular and cellular mechanisms can be investigated within academia through for example fluorescent probes. The bioactive NPs are labeled with a single fluorescent dye through a linker resulting in a fluorescent probe. It is important the linker do not revoke the binding of the NPs to the cellular receptor [169]. The fluorescent probe is subsequently incubated with the cancer cells. It is possible to visualize the therapeutic mode of action of the bioactive NPs through LED fluorescence microscopy [170,171]. This approach provide valuable information but can be complicated to execute due to the lack of selective mono-functionalization reactions and that bioactive NPs often are isolated in limited quantities [169].

Reasonably bioavailability. The awareness of the importance of bioavailability has increased in NPs chemistry and is important to consider already at an early stage in the drug discovery [172]. Lipinski's 'rule-of-five' [173] can be a measurement for oral bioavailability. The use of Lipinski's 'rule-of-five' in NPs is a highly discussed topic among NPs chemists from the pure rejection of the concept to a narrowing of the rules. The basis of the rejection is that the 'rule-of-five' can be counter-productive due to an overemphasizing of bioavailability that exclude interesting bioactive NPs [172]. The narrowing of the rules is a more conservative opinion leaving room for developed development of synthetic analogs that satisfy the 'rule-of-five'. The discussion of Lipinski's 'rule-of-five' moving in a grey area where the rejection of the rules allows more compounds to be developed but probably fewer compounds that are approved for clinical use. In contrast, many potential leads might be excluded too early in the process.

In the discussion on the gap between academia and the pharmaceutical industry it is important to address our role as universities, which may include discovery of novel scaffolds to inspire the pharmaceutical industry or develop new methods. For academia to discover novel bioactive compounds and make them relevant for the industry requires: a strong cross-disciplinary cooperation in academia, the right contact to industry, understand the marked, and funding for industrial cooperation. Nevertheless, the final development of new drugs, including clinical trials and approval, must lie with the industry. This synergism can lead to discovery of novel pharmaceutical in the future.

Concluding Remarks

Filamentous fungi have an amazing ability to synthesize incredible structural diverse molecules. In this PhD study we pursued bioactive NPs targeting CLL cells through a combined approach of LC-DAD-HRMS-based dereplication, E-SPE, and a co-culture platform of CLL and stromal cells. A screening campaign of 289 crude fungal extracts resulted in identification of 11 compounds with activity towards CLL cells. Four of the compounds, ophiobolin A, B, C and K, induced apoptosis in CLL cells with LC_{50} values between 1 and 8 nM and a narrow therapeutic window. Proxiphomin displayed cytotoxic activity towards CLL cells with a LC_{50} value of 20 μM. The remaining six compounds responsible for the activity towards CLL cells were regarded as general cytotoxic compounds.

These low hit-rate of finding novel bioactive compounds in this project indicate that bioactive compounds produced by the genera *Penicillium* and *Aspergillus* are already well studied. New methods might be needed to achieve the goal of discovering new scaffolds. Strategies including co-culture cultivation, epigenetic modification, and molecular biology can provoke expression of some of the often more than 50 % silent gene clusters present in filamentous fungi, thereby enhancing the chance to discover novel scaffolds and biosynthetic pathways. Alternatively, isolation of microorganisms originating from more underexplored habitats e.g. the deep sea may demonstrate to be rich sources of novel bioactive NPs.

The work performed in this PhD study has demonstrated that the combined use of E-SPE and comparative dereplication assist fast identification of bioactive NPs. This approach can be sharpened with the aim of decrease rediscovery of general cytotoxic compounds. This might be done by introduction of prefractionation and dereplication combined with an orthogonal screening already at the preliminary stage. By this approach projects needs to be closed before large scale incubation, if comparative dereplication indicates a known compound as the potential candidate for activity. Future research in dereplication supported by molecular networking based on MSMS fragmentation libraries and bioassay results might add to discovery of bioactive compounds. A conservative approach like this requires more time spend with preliminary screening and no guarantee for success within the time period of one PhD project. Though this approach a more solid foundation might be provided for discovery of novel scaffolds in the extracts selected for large scale incubation.

References

1. American Cancer Society *Cancer Facts & Figures 2013*; American Cancer Society: Atlanta, 2013.

2. Hirsch, J. An anniversary for cancer chemotherapy. *J. Am. Med. Assoc.* **2006**, *296*, 1518–1520.

3. Goodman, L. S.; Wintrobe, M. M.; Dameshek, W.; Goodman, M. J.; Gilman, M. A. Nitrogen mustard therapy. Use of methyl-bis(beta-chloroethyl)amine hydrochloride and tris(beta-chloroethyl)amine hydrochloride for Hodgkin's disease, lymphosarcoma, leukemia and certain allies and miscellaneous disorders. *J. Am. Med. Assoc.* **1946**, *132*, 263–271.

4. Newman, D. J.; Cragg, G. M. Natural products as sources of new drugs over the 30 years from 1981 to 2010. *J. Nat. Prod.* **2012**, *75*, 311–335.

5. Aly, A. H.; Debbab, A.; Proksch, P. Fifty years of drug discovery from fungi. *Fungal Divers.* **2011**, *50*, 3–19.

6. Pangalis, G. A.; Vassilakopoulos, T. P.; Dimopoulou, M. N.; Siakantaris, M. P.; Kontopidou, F. N.; Angelopoulou, M. K. B-chronic lymphocytic leukemia: practical aspects. *Hematol. Oncol.* **2002**, *20*, 103–146.

7. Zenz, T.; Mertens, D.; Küppers, R.; Döhner, H.; Stilgenbauer, S. From pathogenesis to treatment of chronic lymphocytic leukaemia. *Nat. Rev. Cancer* **2010**, *10*, 37–50.

8. Kimby, E.; Brandt, L.; Nygren, P.; Glimelius, B. A systematic overview of chemotherapy effects in B-cell chronic lymphocytic leukaemia. *Acta Oncol.* **2001**, *40*, 224–230.

9. Dighiero, G.; Hamblin, T. J. Chronic lymphocytic leukaemia. *Lancet* **2008**, *371*, 1017–1029.

10. Ghia, P.; Granziero, L.; Chilosi, M.; Caligaris-Cappio, F. Chronic B cell malignancies and bone marrow microenvironment. *Semin. Cancer Biol.* **2002**, *12*, 149–155.

11. Burger, J. A.; Tsukada, N.; Burger, M.; Zvaifler, N. J.; Aquila, M. D.; Kipps, T. J. Blood-derived nurse-like cells protect chronic lymphocytic leukemia B cells from spontaneous apoptosis through stromal cell-derived factor-1. *Blood* **2000**, *96*, 2655–2663.

12. Munk Pedersen, I.; Reed, J. Microenvironmental interactions and survival of CLL B-cells. *Leuk. Lymphoma* **2004**, *45*, 2365–2372.

13. Lagneaux, L.; Delforge, A.; Bron, D.; De Bruyn, C.; Stryckmans, P. Chronic lymphocytic leukemic B cells but not normal B cells are rescued from apoptosis by contact with normal bone marrow stromal cells. *Blood* **1998**, *91*, 2387–2396.

14. Seiffert, M.; Stilgenbauer, S.; Döhner, H.; Lichter, P. Efficient nucleofection of primary human B cells and B-CLL cells induces apoptosis, which depends on the microenvironment and on the structure of transfected nucleic acids. *Leukemia* **2007**, *21*, 1977–1983.

15. Cheson, B. D.; Bennett, J. M.; Grever, M.; Kay, N.; Keating, M. J.; O'Brien, S.; Rai, K. R. National cancer institute-sponsored working group guidelines for chronic lymphocytic leukemia: revised guidelines for diagnosis and treatment. *Blood* **1996**, *87*, 4990–4997.

16. Evans, J.; Ziebland, S.; Pettitt, A. R. Incurable, invisible and inconclusive: watchful waiting for chronic lymphocytic leukaemia and implications for doctor-patient communication. *Eur. J. Cancer Care* **2012**, *21*, 67–77.

17. Desai, S.; Pinilla-Ibarz, J. Front-line therapy for chronic lymphocytic leukemia. *Cancer Control* **2012**, *19*, 26–36.

18. Terasawa, T.; Trikalinos, N. A.; Djulbegovic, B.; Trikalinos, T. A. Comparative efficacy of first-line therapies for advanced-stage chronic lymphocytic leukemia: a multiple-treatment meta-analysis. *Cancer Treat. Rev.* **2013**, *39*, 340–349.

19. Delgado, J.; Baumann, T.; Ghita, G.; Montserrat, E. Chronic lymphocytic leukemia therapy: Beyound chemoimmunotherapy. *Curr. Pharm. Des.* **2012**, *18*, 3356–3362.

20. Williams, D. H.; Stone, M. J.; Hauck, P. R.; Rahman, S. K. Why are secondary metabolites (natural products) biosynthesized? *J. Nat. Prod.* **1989**, *52*, 1189–1208.

21. Nicoletti, R.; Ciavatta, M. L.; Buommino, E.; Tufano, M. A. Antitumor extrolites produced by *Penicillium* species. *Int. J. Biomed. Pharm. Sci.* **2008**, *2*, 1–23.

22. Wani, M. C.; Taylor, L. H.; Wall, M. E.; Coggon, P.; McPhail, A. T. Plant antitumor agents. VI. The isolation and structure of taxol, a novel antileukemic and antitumor agent from *Taxus brevifolia*. *J. Am. Chem. Soc.* **1971**, *93*, 2325–2327.

23. Stierle, A.; Strobel, G.; Stierle, D. Taxol and taxane production by *Taxomyces andreanae*, an endophytic fungus of Pacific yew. *Science (80-.).* **1993**, *260*, 214–216.

24. Niedens, B. R.; Parker, S. R.; Stierle, D. B.; Stierle, A. A. First fungal aromatic L-amino acid decarboxylase from a paclitaxel-producing *Penicillium raistrickii*. *Mycologia* **2013**, *91*, 619–626.

25. Kohler, D. R.; Goldspiel, B. R. Paclitaxel (taxol). *Pharmacotherapy* **1994**, *14*, 3–34.

26. Visalakchi, S.; Muthumary, J. Taxol (anticancer drug) producing endophytic fungi: An overview. *Int. J. Pharm. Bio Sci.* **2010**, *1*, 1–9.

27. Jordan, M. A.; Wilson, L. Microtubules as a target for anticancer drugs. *Nat. Rev. Cancer* **2004**, *4*, 253–265.

28. Ghisalberti, E. L.; Narbey, M. J.; Rowland, C. Y. Metabolites of *Aspergillus terreus* antagonistic towards the take-all fungus. *J. Nat. Prod.* **1990**, *53*, 520–522.

29. Raistrick, H.; Smith, G. LXXI . Studies in the biochemistry of micro-organisms. XLII. The metabolic products of *Aspergillus terreus* Thom. A new mould metabolic product-terrein. *Biochem. J.* **1935**, *29*, 606–611.

30. Liao, W.-Y.; Shen, C.-N.; Lin, L.-H.; Yang, Y.-L.; Han, H.-Y.; Chen, J.-W.; Kuo, S.-C.; Wu, S.-H.; Liaw, C.-C. Asperjinone, a nor-neolignan, and terrein, a suppressor of ABCG2-expressing breast cancer cells, from thermophilic *Aspergillus terreus*. *J. Nat. Prod.* **2012**, *75*, 630–635.

31. Härri, E.; Loeffler, W.; Sigg, H. P.; Stähelin, H.; Tamm, C. Über die isolierung neuer stoffwechselprodukte aus *Penicillium brefeldianum*. *Helv. Chim. Acta* **1963**, *46*, 1235–1246.

32. Betina, V.; Nemec, P.; Dobias, J.; Barath, Z. Cyanein, a new antibiotic from *Penicillium cyaneum*. *Folia Biol.* **1962**, *7*, 353–357.

33. Singleton, V.; Bohonos, N.; Ullstrup, A. Decumbin, a new compound from a species of *Penicillium*. *Nature* **1958**, *181*, 1072–1073.

34. Shao, R. G.; Shimizu, T.; Pommier, Y. Brefeldin A is a potent inducer of apoptosis in human cancer cells independently of p53. *Exp. Cell Res.* **1996**, *227*, 190–196.

35. Chapman, J. R.; Tazaki, H.; Mallouh, C.; Konno, S. Brefeldin A-induced apoptosis in prostatic cancer DU-145 cells: a possible p53-independent death pathway. *BJU Int.* **1999**, *83*, 703–708.

36. Wang, J.; Huang, Y.; Fang, M.; Zhang, Y.; Zheng, Z.; Zhao, Y.; Su, W. Brefeldin A, a cytotoxin produced by *Paecilomyces* sp. and *Aspergillus clavatus* isolated from *Taxus mairei* and *Torreya grandis*. *FEMS Imunol. Med. Mic.* **2002**, *34*, 51–57.

37. Chinworrungsee, M.; Wiyakrutta, S.; Sriubolmas, N.; Chuailua, P.; Suksamrarn, A. Cytotoxic activities of trichothecenes isolated from an endophytic fungus belonging to order Hypocreales. *Arch. Pharmacal Res.* **2008**, *31*, 611–616.

38. Brian, P. W. Studies on the biological activity of griseofulvin. *Ann. Bot.* **1949**, *13*, 59–77.

39. Hector, R. F. An overview of antifungal drugs and their use for treatment of deep and superficial mycoses in animals. *Clin. Tech. Small Anim. Pr.* **2005**, *20*, 240–249.

40. Oxford, A. E.; Raistrick, H.; Simonart, P. XXIX. Studies in the biochemistry of microorganisms. LX. Griseofulvin, C17H17O6Cl, a metabolic product of *Penicillium griseofulvum* Dierckx. *Bioch. J.* **1939**, *33*, 240–248.

41. Grisham, L. M.; Wilson, L.; Bensch, K. G. Antimitotic action of griseofulvin does not involve disruption of microtubules. *Nature* **1973**, *224*, 294–296.

42. Panda, D.; Rathinasamy, K.; Santra, M. K.; Wilson, L. Kinetic suppression of microtubule dynamic instability by griseofulvin: implications for its possible use in the treatment of cancer. *Proc. Natl. Acad. Sci. USA* **2005**, *102*, 9878–9883.

43. Rebacz, B.; Larsen, T. O.; Clausen, M. H.; Rønnest, M. H.; Löffler, H.; Ho, A. D.; Krämer, A. Identification of griseofulvin as an inhibitor of centrosomal clustering in a phenotype-based screen. *Cancer Res.* **2007**, *67*, 6342–6350.

44. Rønnest, M. H.; Rebacz, B.; Markworth, L.; Terp, A. H.; Larsen, T. O.; Krämer, A.; Clausen, M. H. Synthesis and structure-activity relationship of griseofulvin analogues as inhibitors of centrosomal clustering in cancer cells. *J. Med. Chem.* **2009**, *52*, 3342–3347.

45. Borthwick, A. D. 2,5-Diketopiperazines: Synthesis, reactions, medicinal chemistry, and bioactive natural products. *Chem. Rev.* **2012**, *112*, 3641–3716.

46. Numata, A.; Takahashi, C.; Miyamoto, T.; Matsushita, T.; Kawai, K.; Usami, Y.; Matsumura, E.; Inoue, M.; Ohishi, H.; Shingu, T. Structures of cytotoxic substances and new quinazoline derivatives produced by a fungus from a saltwater fish. *Tennen Yuki Kagobutsu Toronkai Koen Yoshishu* **1991**, *33*, 723–730.

47. Wang, Y.; Li, Z.-L.; Bai, J.; Zhang, L.-M.; Wu, X.; Zhang, L.; Pei, Y.-H.; Jing, Y.-K.; Hua, H.-M. 2,5-diketopiperazines from the marine-derived fungus *Aspergillus fumigatus* YK-7. *Chem. Biodivers.* **2012**, *9*, 385–393.

48. Kanoh, K.; Kohno, S.; Asari, T.; Harada, T.; Katada, J.; Muramatsu, M.; Kawashima, H.; Sekiya, H.; Uno, I. (-)-phenylahistin: A new mammalian cell cycle inhibitor produced by *Aspergillus ustus*. *Bioorg. Med. Chem. Lett.* **1997**, *7*, 2847–2852.

49. Kanoh, K.; Kohno, S.; Katada, J.; Hayashi, Y.; Muramatsu, M.; Uno, I. Antitumor activity of phenylahistin *in vitro* and *in vivo*. *Biosci.* **1999**, *63*, 1130–1133.

50. Yamazaki, Y.; Tanaka, K.; Nicholson, B.; Deyanat-Yazdi, G.; Potts, B.; Yoshida, T.; Oda, A.; Kitagawa, T.; Orikasa, S.; Kiso, Y.; Yasui, H.; Akamatsu, M.; Chinen, T.; Usui, T.; Shinozaki, Y.; Yakushiji, F.; Miller, B. R.; Neuteboom, S.; Palladino, M.; Kanoh, K.; Lloyd, G. K.; Hayashi, Y. Synthesis and structure−Activity relationship study of antimicrotubule agents phenylahistin derivatives with a didehydropiperazine-2,5-dione structure. *J. Med. Chem.* **2012**, *55*, 1056–1071.

51. Seya, H.; Nozawa, K.; Nakajima, S.; Kawai, K.-I.; Udagawa, S.-I. Studies on fungal products. Part 8. Isolation and structure of emestrin, a novel antifungal macrocyclic epidithiodioxopiperazine from *Emericeella striata*. X-Ray molecular structure of emestrin. *J. Chem. Soc. Perk. T. 1* **1986**, *67*, 109–116.

52. Ueno, Y.; Umemori, K.; Nilmi, E.; Tanuma, S.; Nagata, S.; Sugamata, M.; Ihara, T.; Sekljlma,, M.; Kawai, K.-I.; Ueno, I.; Takhiro, F. Induction of apoptosis by T-2 toxin

and other natural toxins in HL-60 human promyelotic leukemia cells. *Nat. Toxins* **1995**, *3*, 129–137.

53. Onodera, H.; Hasegawa, A.; Tsumagari, N.; Nakai, R.; Ogawa, T.; Kanda, Y. MPC1001 and its analogues: new antitumor agents from the fungus *Cladorrhinum* species. *Org. Lett.* **2004**, *6*, 4101–4104.

54. Krizsán, K.; Bencsik, O.; Nyilasi, I.; Galgóczy, L.; Vágvölgyi, C.; Papp, T. Effect of the sesterterpene-type metabolites, ophiobolins A and B, on zygomycetes fungi. *FEMS Microbiol. Lett.* **2010**, *313*, 135–140.

55. Zhang, D.; Fukuzawa, S.; Satake, M.; Li, X.; Kuranaga, T.; Niitsu, A.; Yoshizawa, K.; Tachibana, K. Ophiobolin O and 6-epi-ophiobolin O, two new cytotoxic sesterterpenes from the marine derived fungus *Aspergillus* sp. *Nat. Prod. Commun.* **2012**, *7*, 1411–1414.

56. Yang, T.; Lu, Z.; Meng, L.; Wei, S.; Hong, K.; Zhu, W.; Huang, C. The novel agent ophiobolin O induces apoptosis and cell cycle arrest of MCF-7 cells through activation of MAPK signaling pathways. *Bioorg. Med. Chem. Lett.* **2012**, *22*, 579–585.

57. Wang, Q.-X.; Yang, J.-L.; Qi, Q.-Y.; Bao, L.; Yang, X.-L.; Liu, M.-M.; Huang, P.; Zhang, L.-X.; Chen, J.-L.; Cai, L.; Liu, H.-W. 3-Anhydro-6-hydroxy-ophiobolin A, a new sesterterpene inhibiting the growth of methicillin-resistant *Staphylococcus aureus* and inducing the cell death by apoptosis on K562, from the phytopathogenic fungus *Bipolaris oryzae*. *Bioorgan. Med. Chem. Lett.* **2013**, *23*, 3547–3550.

58. Wang, Q.-X.; Bao, L.; Yang, X.-L.; Liu, D.-L.; Guo, H.; Dai, H.-Q.; Song, F.-H.; Zhang, L.-X.; Guo, L.-D.; Li, S.-J.; Liu, H.-W. Ophiobolins P-T, five new cytotoxic and antibacterial sesterterpenes from the endolichenic fungus *Ulocladium* sp. *Fitoterapia* **2013**, *90*, 220–227.

59. Au, T. K.; Chick, W. S.; Leung, P. C. The biology of ophiobolins. *Life Sci.* **2000**, *67*, 733–742.

60. De Vries-van Leeuwen, I. J.; Kortekaas-Thijssen, C.; Mandouckou, J. A. N.; Kas, S.; Evidente, A.; de Boer, A. H. Fusicoccin-A selectively induces apoptosis in tumor cells after interferon-alpha priming. *Cancer Lett.* **2010**, *293*, 198–206.

61. Shen, X.; Krasnoff, S. B.; Lu, S. W.; Dunbar, C. D.; O'Neal, J.; Turgeon, B. G.; Yoder, O. C.; Gibson, D. M.; Hamann, M. T. Characterization of 6-epi-3-anhydroophiobolin B from *Cochliobolus heterostrophus*. *J. Nat. Prod.* **1999**, *62*, 895–897.

62. Schümann, J.; Hertweck, C. Molecular basis of cytochalasan biosynthesis in fungi: gene cluster analysis and evidence for the involvement of a PKS-NRPS hybrid synthase by RNA silencing. *J. Am. Chem. Soc.* **2007**, *129*, 9564–9565.

63. Sekita, S.; Yoshihira, K.; Natori, S.; Kuwano, H. Structures of chaetoglobosin A and B, cytotoxic metabolites of *Chaetomium globosum*. *Tetrahedron Lett.* **1973**, *14*, 2109–2112.

64. Wagenaar, M. M.; Corwin, J.; Strobel, G.; Clardy, J. Three new cytochalasins produced by an endophytic fungus in the genus *Rhinocladiella*. *J. Nat. Prod.* **2000**, *63*, 1692–1695.

65. Liu, R.; Gu, Q.; Zhu, W.; Cui, C.; Fan, G.; Fang, Y.; Zhu, T.; Liu, H. 10-Phenyl-[12]-cytochalasins Z7, Z8, and Z9 from the marine-derived fungus *Spicaria elegans*. *J. Nat. Prod.* **2006**, *69*, 871–875.

66. Thohinung, S.; Kanokmedhakul, S.; Kanokmedhakul, K.; Kukongviriyapan, V.; Tusskorn, O.; Soytong, K. Cytotoxic 10-(indol-3-yl)-[13]cytochalasans from the fungus *Chaetomium elatum* ChE01. *Arch. Pharm. Res.* **2010**, *33*, 1135–1141.

67. Knudsen, P. B.; Hanna, B.; Ohl, S.; Sellner, L.; Zenz, T.; Stilgenbauer, S.; Larsen, T. O.; Lichter, P.; Seiffert, M. Chaetoglobosin A preferentially induces apoptosis in chronic lymphocytic leukemia cells by targeting the cytoskeleton. *Leukemia* **2013**, *in revisio*.

68. Kharwar, R. N.; Mishra, A.; Gond, S. K.; Stierle, A.; Stierle, D. Anticancer compounds derived from fungal endophytes: their importance and future challenges. *Nat. Prod. Rep.* **2011**, *28*, 1208–1228.

69. Roth, B. L.; Sheffler, D. J.; Kroeze, W. K. Magic shotguns versus magic bullets: selectively non-selective drugs for mood disorders and schizophrenia. *Nat. Rev. Drug Discov.* **2004**, *3*, 353–359.

70. Frisvad, J. C.; Smedsgaard, J.; Larsen, T. O.; Samson, R. A. Mycotoxins, drugs and other extrolites produced by species in *Penicillium* subgenus *Penicillium*. *Stud. Mycol.* **2004**, *49*, 201–241.

71. Frisvad, J. C.; Andersen, B.; Thrane, U. The use of secondary metabolite profiling in chemotaxonomy of filamentous fungi. *Mycol. Res.* **2008**, *112*, 231–240.

72. Rasmussen, R. R.; Rasmussen, P. H.; Larsen, T. O.; Bladt, T. T.; Binderup, M. L. *In vitro* cytotoxicity of fungi spoiling maize silage. *Food Chem. Toxicol.* **2011**, *49*, 31–44.

73. Bugni, T. S.; Harper, M. K.; McCulloch, M. W. B.; Reppart, J.; Ireland, C. M. Fractionated marine invertebrate extract libraries for drug discovery. *Molecules* **2008**, *13*, 1372–1383.

74. Lee, J. A.; Uhlik, M. T.; Moxham, C. M.; Tomandl, D.; Sall, D. J. Modern phenotypic drug discovery is a viable, neoclassic pharma strategy. *J. Med. Chem.* **2012**, *55*, 4527–4538.

75. Zhou, M.; Luo, H.; Li, Z.; Wu, F.; Huang, C.; Ding, Z.; Li, R. Recent advances in screening of natural products for antimicrobial agents. *Comb. Chem. High T. Scr.* **2012**, *15*, 306–315.

76. Van Engeland, M.; Nieland, L. J.; Ramaekers, F. C.; Schutte, B.; Reutelingsperger, C. P. Annexin V-affinity assay: A review on an apoptosis detection system based on phosphatidylserine exposure. *Cytometry* **1998**, *31*, 1–9.

77. Elmore, S. Apoptosis: a review of programmed cell death. *Toxicol. Pathol.* **2007**, *35*, 495–516.

78. Ormerod, M. G. The study of apoptotic cells by flow cytometry. *Leukemia* **1998**, *12*, 1013–1025.

79. Larsen, T. O.; Smedsgaard, J.; Nielsen, K. F.; Hansen, M. E.; Frisvad, J. C. Phenotypic taxonomy and metabolite profiling in microbial drug discovery. *Nat. Prod. Rep.* **2005**, *22*, 672–695.

80. Leão, P. N.; Ramos, V.; Gonçalves, P. B.; Viana, F.; Lage, O. M.; Gerwick, W. H.; Vasconcelos, V. M. Chemoecological screening reveals high bioactivity in diverse culturable Portuguese marine cyanobacteria. *Mar. Drugs* **2013**, *11*, 1316–1335.

81. Smedsgaard, J.; Nielsen, J. Metabolite profiling of fungi and yeast: from phenotype to metabolome by MS and informatics. *J. Exp. Bot.* **2005**, *56*, 273–286.

82. Bode, H. B.; Bethe, B.; Höfs, R.; Zeeck, A. Big effects from small changes: possible ways to explore nature's chemical diversity. *ChemBioChem* **2002**, *3*, 619–627.

83. Månsson, M.; Phipps, R. K.; Gram, L.; Munro, M. H. G.; Larsen, T. O.; Nielsen, K. F. Explorative solid-phase extraction (E-SPE) for accelerated microbial natural product discovery, dereplication, and purification. *J. Nat. Prod.* **2010**, *73*, 1126–1132.

84. Keller, N. P.; Turner, G.; Bennett, J. W. Fungal secondary metabolism - from biochemistry to genomics. *Nat. Rev. Microbiol.* **2005**, *3*, 937–947.

85. Fox, E. M.; Howlett, B. J. Secondary metabolism: regulation and role in fungal biology. *Curr. Opin. Microbiol.* **2008**, *11*, 481–487.

86. Nielsen, K. F.; Månsson, M.; Rank, C.; Frisvad, J. C.; Larsen, T. O. Dereplication of microbial natural products by LC-DAD-TOFMS. *J. Nat. Prod.* **2011**, *74*, 2338–2348.

87. Laatsch, H. *AntiBase 2012*; Http://eu.wiley.com/WileyCDA/WileyTitle/productCd-3527334068.html, Ed.; Wiley-VCH: Weinheim, Germany, 2012.

88. Rojas-Chertó, M.; Kasper, P. T.; Willighagen, E. L.; Vreeken, R. J.; Hankemeier, T.; Reijmers, T. H. Elemental composition determination based on MS(n). *Bioinformatics* **2011**, *27*, 2376–83.

89. Frisvad, J. C.; Thrane, U. Standardized high-performance liquid chromatography 0f 182 mycotoxins and other fungal metabolites based on alkylphenone retention indices and UV-VIS spectra (diode array detedtion). *J. Chromatogr.* **1987**, *404*, 195–214.

90. Hansen, M. E.; Smedsgaard, J.; Larsen, T. O. X-Hitting: an algorithm for novelty detection and dereplication by UV spectra of complex mixtures of natural products. *Anal. Chem.* **2005**, *77*, 6805–6817.

91. Larsen, T. O.; Petersen, B. O.; Duus, J. Ø.; Sørensen, D.; Frisvad, J. C.; Hansen, M. E. Discovery of new natural products by application of X-hitting, a novel algorithm for automated comparison of full UV spectra, combined with structural determination by NMR spectroscopy. *J. Nat. Prod.* **2005**, *68*, 871–874.

92. Appleton, D. R.; Buss, A. D.; Butler, M. S. A simple method for high-throughput extract prefractionation for biological screening. *Chimia (Aarau).* **2007**, *61*, 327–331.

93. Schmid, I.; Sattler, I.; Grabley, S.; Thiericke, R. Natural Products in High Throughput Screening: Automated High-Quality Sample Preparation. *J. Biomolec. Screen.* **1999**, *4*, 15–25.

94. Nielsen, K. F.; Dalsgaard, P. W.; Smedsgaard, J.; Larsen, T. O. Andrastins A-D, *Penicillium roqueforti* metabolites consistently produced in blue-mold-ripened cheese. *J. Agr. Food Chem.* **2005**, *53*, 2908–2913.

95. Salotto, A. W.; Weiser, E. L.; Caffey, K. P.; Carty, R. L.; Racine, S. C.; Snyder, L. R. Relative retention and column selectivity for the common polar bonded-phase columns. *J. Chromatogr.* **1990**, *498*, 55–65.

96. Smedsgaard, J. Micro-scale extraction procedure for standardized screening of fungal metabolite production in cultures. *J. Chromatogr. A* **1997**, *760*, 264–270.

97. Raju, M. S.; Wu, G.-S.; Gard, A.; Rosazza, J. P. Microbial transformations of natural antitumor agents. 20. Glucosylation of viridicatumtoxin. *J. Nat. Prod.* **1982**, *45*, 321–327.

98. Bladt, T. T.; Frisvad, J. C.; Knudsen, P. B.; Larsen, T. O. Anticancer and antifungal compounds from *Aspergillus*, *Penicillium* and other filamentous fungi. *Molecules* **2013**, *18*, 11338–11376.

99. Seya, H.; Nakajima, S.; Kawai, K.-I.; Udagawa, S.-I. Structure and absolute configuration of emestrin, a new macrocyclic epidithiodioxopiperazine from *Emericella striata*. *J. Chem. Soc. Chem. Comm.* **1985**, *739*, 657–658.

100. Terao, K.; Ito, E.; Kawai, K.; Nozawa, K.; Udagawa, S. Experimental acute poisoning in mice induced by emestrin, a new mycotoxin isolated from *Emericella* species. *Mycopathologia* **1990**, *112*, 71–79.

101. Lansden, J. A.; Cole, R. J.; Dorner, J. W.; Cox, R. H.; Cutler, H. G.; Clark, J. D. A new trichothecene mycotoxin isolated from *Fusarium tricinctum*. *J. Agr. Food Chem.* **1978**, *26*, 242–244.

102. Pohland, A. E.; Schuller, P. L.; Steyn, P. S. Physicochemical data for some selected mycotoxins. *Pure Appl. Chem.* **1982**, *54*, 2219–2284.

103. Endo, A.; Kuroda, M.; Tsujita, Y. ML-236B, and ML-236C, new inhibitors of cholesterogenesis produced by *Penicillium citrinum*. *J. Antibiot.* **1976**, *29*, 1346–1348.

104. Larsen, T. O.; Lange, L.; Schnorr, K.; Stender, S.; Frisvad, J. C. Solistatinol, a novel phenolic compactin analogue from *Penicillium solitum*. *Tetrahedron Lett.* **2007**, *48*, 1261–1264.

105. Vitols, S.; Angelin, B.; Juliusson, G. Simvastatin impairs mitogen-induced proliferation of malignant B-lymphocytes from humans--*in vitro* and *in vivo* studies. *Lipids* **1997**, *32*, 255–262.

106. Lorenz, R. T.; Parks, L. W. Effects of lovastatin (mevinolin) on sterol levels and of azoles in *Saccharomyces cerevisiae*. *Antimicrob. Agents Chemother.* **1990**, *34*, 1660–1665.

107. Chamilos, G.; Lewis, R. E.; Dimitrios, P.; Kontoyiannis, D. P. Lovastatin has significant activity against zygomycetes and interacts synergistically with voriconazole. *Antimicrob. Agents Chemother.* **2006**, *50*, 96–103.

108. Singh, S. B.; Smith, J. L.; Sabnis, G. S.; Dombrowski, A. W.; Schaeffer, J. M.; Goetz, M. A.; Bills, G. F. Structure and conformation of ophiobolin K and 6-epiophiobolin K from *Aspergillus ustus* as a nematocidal agent . *Tetrahedron* **1991**, *47*, 6931–6938.

109. Samson, R. A.; Varga, J.; Meijer, M.; Frisvad, J. C. New taxa in *Aspergillus* section *Usti*. *Stud. Mycol.* **2011**, *69*, 81–97.

110. Cutler, H. G.; Crumley, F. G.; Cox, R. H.; Springer, J. P.; Arrendale, R. F.; Cole, R. J.; Cole, P. D. Ophiobolins G and H: new fungal metabolites from a novel source, *Aspergillus ustus*. *J. Agr. Food Chem.* **1984**, *32*, 778–782.

111. Wei, H.; Itoh, T.; Kinoshita, M.; Nakai, Y.; Kurotaki, M.; Kobayashi, M. Cytotoxic sesterterpenes, 6-epi-ophiobolin G and 6-epi-ophiobolin N, from marine derived fungus *Emericella variecolor* GF10. *Tetrahedron* **2004**, *60*, 6015–6019.

112. Nozoe, S.; Hirai, K.; Tusda, K. The structure of zizanin-A and -B, C25-terpenoids isolated from Helminthosporium zizaniae. *Tetrahedron Lett.* **1966**, *20*, 2211–2216.

113. Li, E.; Clark, A. M.; Rotella, D. P.; Hufford, C. D. Microbial metabolites of ophiobolin A and antimicrobial evaluation of ophiobolins. *J. Nat. Prod.* **1995**, *58*, 74–81.

114. Tsipouras, A.; Adefarati, A. A.; Tkacz, J. S.; Frazier, E. G.; Rohrer, S. P.; Birzin, E.; Rosegay, A.; Zink, D. L.; Goetz, M. A.; Singh, S. B.; Schaeffer, J. M. Ophiobolin M and analogues, noncompetitive inhibitors of ivermectin binding with nematocidal activity. *Bioorgan. Med. Chem.* **1996**, *4*, 531–536.

115. Canonica, L.; Fiecchi, A.; Galli Kienle, M.; Ranzi, B. M.; Scala, A. The biosynthesis of ophiobolins. *Tetrahedron Lett.* **1967**, 3371–3376.

116. Chiba, R.; Minami, A.; Gomi, K.; Oikawa, H. Identification of Ophiobolin F synthase by a genome mining approach: A sesterterpene synthase from *Aspergillus clavatus*. *Org. Lett.* **2013**, *15*, 594–597.

117. Evidente, A.; Andolfi, A.; Cimmino, A.; Vurro, M.; Fracchiolla, M.; Charudattan, R. Herbicidal potential of ophiobolins produced by *Drechslera gigantea*. *J. Agr. Food Chem.* **2006**, *54*, 1779–1783.

118. Binder, M.; Tarnrn, C. Proxiphomin und orotophomin, zwei neue cytochalasane. *Helv. Chim. Acta* **1973**, *7*, 2387–2396.

119. Linington, R. G.; Edwards, D. J.; Shuman, C. F.; McPhail, K. L.; Matainaho, T.; Gerwick, W. H. Symplocamide A, a potent cytotoxin and chymotrypsin inhibitor from the marine cyanobacterium *Symploca* sp. *J. Nat. Prod.* **2008**, *71*, 22–27.

120. Seife, C. Blunting Nature's swiss army knife. *Science*, **1997**, *277*, 1602–1603.

121. Yoshizawa, S.; Matsushima, R.; Watanabe, M. F.; Harada, K.; Ichihara, A.; Carmichael, W. W.; Fujiki, H. Inhibition of protein phosphatases by microcystis and nodularin associated with hepatotoxicity. *J. Cancer Res. Clini. Oncol.* **1990**, *116*, 609–614.

122. Sano, T.; Kaya, K. Oscillapeptin G, a tyrosinase inhibitor from toxic *Oscillatoria agardhii*. *J. Nat. Prod.* **1996**, *59*, 90–92.

123. Murakami, M.; Okita, Y.; Okind, T. Aeruginosin 298-A, A thrombin and trypsin inhibitor from the blue-green alga *Microcystis acruginosa* (NIES-298). *Tetrahedron Lett.* **1994**, *35*, 3129–3132.

124. Matsuda, H.; Murakami, M.; Yamaguchi, K. Microginin, an angiotensin-converting enzyme inhibitor from the blue-green alga *Microcystis aeruginosa*. *Tetrahedron Lett.* **1993**, *34*, 501–504.

125. Harada, K.; Fujii, K.; Shimada, T.; Suzuki, M.; Carmichael, W. W. Two cyclic peptides, anabaenopeptins, a third group of bioactive compounds from the cyanobacterium *Anabaena flos-aquae* NRC 525-17. *Tetrahedron Lett.* **1995**, *36*, 1511–1514.

126. Reshef, V.; Carmeli, S. New microviridins from a water bloom of the cyanobacterium *Microcystis aeruginosa*. *Tetrahedron* **2006**, *62*, 7361–7369.

127. Vegman, R.; Carmeli, S. Eight micropeptins from a Microcystis spp. bloom collected from a fishpond near Kibbutz Lehavot HaBashan, Israel. *Tetrahedron* **2013**, *in press*, DOI: 10.1016/j.tet.2013.09.054.

128. Nishizawa, T.; Ueda, A.; Nakano, T.; Nishizawa, A.; Miura, T.; Asayama, M.; Fujii, K.; Harada, K.; Shirai, M. Characterization of the locus of genes encoding enzymes producing heptadepsipeptide micropeptin in the unicellular cyanobacterium Microcystis. *J. Biochem.* **2011**, *149*, 475–485.

129. Zafrir, E.; Carmeli, S. Micropeptins from an Israeli fishpond water bloom of the cyanobacterium *Microcystis* sp. *J. Nat. Prod.* **2010**, *73*, 352–358.

130. Pettit, G. R.; Kamano, Y.; Herald, C. L.; Dufresne, C.; Cerny, R. L.; Herald, D. L.; Schmidt, J. M.; Kizu, H. Isolation and structure of the cytostatic depsipeptide dolastatin 13 from the sea hare *Dolabella auricularia*. *J. Am. Chem. Soc.* **1989**, *111*, 5015–5017.

131. Rouhiainen, L.; Paulin, L.; Suomalainen, S.; Hyytiäinen, H.; Buikema, W.; Haselkorn, R.; Sivonen, K. Genes encoding synthetases of cyclic depsipeptides, anabaenopeptilides, in *Anabaena* strain 90. *Mol. Microbiol.* **2000**, *37*, 156–167.

132. Ishida, K.; Christiansen, G.; Yoshida, W. Y.; Kurmayer, R.; Welker, M.; Valls, N.; Bonjoch, J.; Hertweck, C.; Börner, T.; Hemscheidt, T.; Dittmann, E. Biosynthesis and structure of aeruginoside 126A and 126B, cyanobacterial peptide glycosides bearing a 2-carboxy-6-hydroxyoctahydroindole moiety. *Chem. Biol.* **2007**, *14*, 565–576.

133. Hymer, C. B.; Montes-Bayon, M.; Caruso, J. A. Marfey's reagent: Past, present, and future uses of 1-fluoro-2,4-dinitrophenyl-5-L-alanine amide. *J. Sep. Sci.* **2003**, *26*, 7–19.

134. Marfey, P. Determination of D-amino acids. II. Use of a bifunctional reagent, 1,5-difluro-2,4-dinitrobenzene. *Carlsb. Res. Commun.* **1984**, *49*, 591–596.

135. Raveh, A.; Moshe, S.; Evron, Z.; Flescher, E.; Carmeli, S. Novel thiazole and oxazole containing cyclic hexapeptides from a waterbloom of the cyanobacterium *Microcystis* sp. *Tetrahedron* **2010**, *66*, 2705–2712.

136. Ishida, K.; Matsuda, H.; Okino, T.; Murakami, M. Aeruginosins, protease inhibitors from the cyanobacterium *Microcystis aeruginosa*. *Tetrahedron* **1999**, *55*, 10971–10988.

137. Harada, K.; Mayumi, T.; Shimada, T.; Suzuki, M.; Kondo, F.; Watanabe, M. F. Occurrence of four depsipeptides, aeruginopeptins, together with microcystins from toxic cyanobacteria. *Tetrahedron Lett.* **1993**, *34*, 6091–6094.

138. Ishida, K.; Matsuda, H.; Murakami, M. Micropeptins 88-A to 88-F, chymotrypsin inhibitors from the cyanobacterium *Microcystis aeruginosa* (NIES-88). *Tetrahedron* **1998**, *54*, 5545–5556.

139. Itou, Y.; Ishida, K.; Shin, H. J.; Murakami, M. Oscillapeptins A to F, serine protease inhibitors from the three strains of *Oscillatoria agardhii*. *Tetrahedron* **1999**, *55*, 6871–6882.

140. Adiv, S.; Aharonv-Nadborny, R.; Carmeli, S. Micropeptins from *Microcystis aeruginosa* collected in Dalton reservoir, Israel. *Tetrahedron* **2010**, *66*, 7429–7436.

141. Bowden, K.; Heilbron, I. M.; Jones, E. R. H.; Weedon, B. C. L. Researches on acetylenic compounds. Part I. The preparation of acetylenic ketones by oxidation of acetylenic carbinols and glycols. *J. Chem. Soc.* **1946**, 39–45.

142. Gademann, K.; Portmann, C.; Blom, J. F.; Zeder, M.; Jüttner, F. Multiple toxin production in the cyanobacterium *Microcystis*: isolation of the toxic protease inhibitor cyanopeptolin 1020. *J. Nat. Prod.* **2010**, *73*, 980–984.

143. Gademann, K.; Portmann, C. Secondary metabolites from cyanobacteria: Complex structures and powerful bioactivities. *Curr. Org. Chem.* **2008**, *12*, 326–341.

144. Decock, J.; Paridaens, R.; Cufer, T. Proteases and metastasis: clinical relevance nowadays? *Curr. Opin. Chem. Oncol.* **2005**, *17*, 545–550.

145. Hawksworth, D. L. Global species numbers of fungi: are tropical studies and molecular approaches contributing to a more robust estimate? *Biodivers. Conserv.* **2012**, *21*, 2425–2433.

146. Klejnstrup, M. L.; Frandsen, R. J. N.; Holm, D. K.; Nielsen, M. T.; Mortensen, U. H.; Larsen, T. O.; Nielsen, J. B. Genetics of polyketide metabolism in *Aspergillus nidulans*. *Metabolites* **2012**, *2*, 100–133.

147. Souza, A. C. S.; de Fatima, A.; da Silveira, R. B.; Justo, G. Z. Seek and destroy: The use of natural compounds for targeting the molecular roots of cancer. *Curr. Drug Targets* **2012**, *13*, 1072–1082.

148. Knight, V.; Sanglier, J.-J.; DiTullio, D.; Braccili, S.; Bonner, P.; Waters, J.; Hughes, D.; Zhang, L. Diversifying microbial natural products for drug discovery. *Appl. Microbiol. Biot.* **2003**, *62*, 446–58.

149. Bertrand, S.; Schumpp, O.; Bohni, N.; Bujard, A.; Azzollini, A.; Monod, M.; Gindro, K.; Wolfender, J.-L. Detection of metabolite induction in fungal co-cultures on solid media by high-throughput differential ultra-high pressure liquid chromatography-time-of-flight mass spectrometry fingerprinting. *J. Chromatogr. A* **2013**, *1292*, 219–28.

150. Pettit, R. K. Mixed fermentation for natural product drug discovery. *Appl. Microbiol. Biot.* **2009**, *83*, 19–25.

151. Bertrand, S.; Schumpp, O.; Bohni, N.; Monod, M.; Gindro, K.; Wolfender, J.-L. *De novo* production of metabolites by fungal co-culture of *Trichophyton rubrum* and *Bionectria ochroleuca*. *J. Nat. Prod.* **2013**, *76*, 1157–1165.

152. Oh, D.-C.; Jensen, P. R.; Kauffman, C. a; Fenical, W. Libertellenones A-D: induction of cytotoxic diterpenoid biosynthesis by marine microbial competition. *Bioorg. Med. Chem.* **2005**, *13*, 5267–5273.

153. Asai, T.; Yamamoto, T.; Shirata, N.; Taniguchi, T.; Monde, K.; Fujii, I.; Gomi, K.; Oshima, Y. Structurally diverse chaetophenol productions induced by chemically mediated epigenetic manipulation of fungal gene expression. *Org. Lett.* **2013**, *15*, 3346–3349.

154. Demain, A. L.; Vaishnav, P. Natural products for cancer chemotherapy. *Microb. Biotechnol.* **2011**, *4*, 687–699.

155. Cichewicz, R. H. Epigenome manipulation as a pathway to new natural product scaffolds and their congeners. *Nat. Prod. Rep.* **2010**, *27*, 11–22.

156. Andersen, M. R.; Nielsen, J. B.; Klitgaard, A.; Petersen, L. M.; Zachariasen, M.; Hansen, T. J.; Blicher, L. H.; Gotfredsen, C. H.; Larsen, T. O.; Nielsen, K. F.; Mortensen, U. H. Accurate prediction of secondary metabolite gene clusters in filamentous fungi. *PNAS* **2013**, *110*, 24–25.

157. Williams, R. B.; Henrikson, J. C.; Hoover, A. R.; Lee, A. E.; Cichewicz, R. H. Epigenetic remodeling of the fungal secondary metabolome. *Org. Biomol. Chem.* **2008**, *6*, 1895–1897.

158. Yang, J. Y.; Sanchez, L. M.; Rath, C. M.; Liu, X.; Boudreau, P. D.; Bruns, N.; Glukhov, E.; Wodtke, A.; de Felicio, R.; Fenner, A.; Wong, W. R.; Linington, R. G.; Zhang, L.; Debonsi, H. M.; Gerwick, W. H.; Dorrestein, P. C. Molecular networking as a dereplication strategy. *J. Nat. Prod.* **2013**, *76*, 1686–1699.

159. Johansen, K. T.; Wubshet, S. G.; Nyberg, N. T. HPLC-NMR revisited: Using time-slice high-performance liquid chromatography-solid-phase extraction-nuclear magnetic resonance with database-assisted dereplication. *Anal. Chem.* **2013**, *85*, 3183–3189.

160. Seger, C.; Sturm, S.; Stuppner, H. Mass spectrometry and NMR spectroscopy: modern high-end detectors for high resolution separation techniques - state of the art in natural product HPLC-MS, HPLC-NMR, and CE-MS hyphenations. *Nat. Prod. Rep.* **2013**, *30*, 970–987.

161. Welker, M.; von Döhren, H. Cyanobacterial peptides - Nature's own combinatorial biosynthesis. *FEMS Microbiol. Rev.* **2006**, *30*, 530–563.

162. Bross-Walch, N.; Kühn, T.; Moskau, D.; Zerbe, O. Strategies and tools for structure determination of natural products using modern methods of NMR spectroscopy. *Chem. Biodivers.* **2005**, *2*, 147–177.

163. Wolfender, J.-L.; Queiroz, E. F. New approaches for studying the chemical diversity of natural resources and the bioactivity of their constituents. *Chimia (Aarau).* **2012**, *66*, 324–329.

164. Walsh, C. T.; Fischbach, M. A. Natural products version 2.0: connecting genes to molecules. *J. Am. Chem. Soc.* **2010**, *132*, 2469–2493.

165. Paul, S. M.; Mytelka, D. S.; Dunwiddie, C. T.; Persinger, C. C.; Munos, B. H.; Lindborg, S. R.; Schacht, A. L. How to improve R&D productivity: the pharmaceutical industry's grand challenge. *Nat. Rev. Drug Discov.* **2010**, *9*, 203–214.

166. Overy, D. The challenge of industrializing natural product discovery in an academic lab. In *Oral presentation at: Marine Microbial Biotechnology Symposium*; DTU Systems Biology: Kgs. Lyngby, 2012.

167. Hughes, C. C.; Yang, Y.-L.; Liu, W.-T.; Dorrestein, P. C.; La Clair, J. J.; Fenical, W. Marinopyrrole A target elucidation by acyl dye transfer. *J. Am. Chem. Soc.* **2009**, *131*, 12094–12096.

168. Meisner, N.-C.; Hintersteiner, M.; Uhl, V.; Weidemann, T.; Schmied, M.; Gstach, H.; Auer, M. The chemical hunt for the identification of drugable targets. *Curr. Opin. Chem. Biol.* **2004**, *8*, 424–431.

169. Peddibhotla, S.; Dang, Y.; Liu, J. O.; Romo, D. Simultaneous arming and structure/activity studies of natural products employing O-H insertions: an expedient and versatile strategy for natural products-based chemical genetics. *J. Am. Chem. Soc.* **2007**, *129*, 12222–12231.

170. Alexander, M. D.; Burkart, M. D.; Leonard, M. S.; Portonovo, P.; Liang, B.; Ding, X.; Joullié, M. M.; Gulledge, B. M.; Aggen, J. B.; Chamberlin, A. R.; Sandler, J.; Fenical, W.; Cui, J.; Gharpure, S. J.; Polosukhin, A.; Zhang, H.-R.; Evans, P. A.; Richardson, A. D.; Harper, M. K.; Ireland, C. M.; Vong, B. G.; Brady, T. P.; Theodorakis, E. a; La Clair, J. J. A central strategy for converting natural products into fluorescent probes. *ChemBioChem* **2006**, *7*, 409–416.

171. Hughes, C. C.; MacMillan, J. B.; Gaudêncio, S. P.; Fenical, W.; La Clair, J. J. Ammosamides A and B target myosin. *Angew. Chem. Int. Ed.* **2009**, *48*, 728–732.

172. Zhang, M.-Q.; Wilkinson, B. Drug discovery beyond the "rule-of-five". *Curr. Opin. Biotechnol.* **2007**, *18*, 478–488.

173. Lipinski, C. A.; Lombardo, F.; Dominy, B. W.; Feeney, P. J. Experimental and computational approaches to estimate solubility and permeability in drug discovery and development settings. *Adv. Drug Deliv. Rev.* **1997**, *23*, 3–25.

Chemical biology of microbial anticancer natural products

Appendix

Tanja Thorskov Bladt
Chemical biology of microbial anticancer natural products - appendix

Paper 1

Anticancer and Antifungal Compounds from *Aspergillus*, *Penicillium* and other Filamentous Fungi

Bladt, T.T.; Frisvad, J.C.; Knudsen, P.B.; and Larsen, T.O.

Accepted in *Molecules* **2013**, *18*, 11338–11376

Tanja Thorskov Bladt
Chemical biology of microbial anticancer natural products - appendix

Molecules **2013**, *18*, 11338-11376; doi:10.3390/molecules180911338

OPEN ACCESS

molecules

ISSN 1420-3049

www.mdpi.com/journal/molecules

Review

Anticancer and Antifungal Compounds from *Aspergillus*, *Penicillium* and Other Filamentous Fungi

Tanja Thorskov Bladt, Jens Christian Frisvad, Peter Boldsen Knudsen and Thomas Ostenfeld Larsen *

Department of Systems Biology, Technical University of Denmark, Søltofts Plads, Building 221, DK-2800 Kgs. Lyngby, Denmark; E-Mails: ttb@bio.dtu.dk (T.T.B.); jcf@bio.dtu.dk (J.C.F.); pebok@bio.dtu.dk (P.B.K.)

* Author to whom correspondence should be addressed; E-Mail: tol@bio.dtu.dk; Tel.: +45-4525-2632; Fax: +45-4588-4148.

Received: 3 July 2013; in revised form: 23 August 2013 / Accepted: 3 September 2013 / Published: 13 September 2013

Abstract: This review covers important anticancer and antifungal compounds reported from filamentous fungi and in particular from *Aspergillus*, *Penicillium* and *Talaromyces*. The taxonomy of these fungi is not trivial, so a focus of this review has been to report the correct identity of the producing organisms based on substantial previous in-house chemotaxonomic studies.

Keywords: anticancer; polyketides; non-ribosomal peptides; terpenoids; fungi; natural products; taxonomy

1. Introduction

Filamentous fungi such as *Aspergillus*, *Penicillium* and *Talaromyces* are some of the most incredible chemical factories known today. Accordingly, numerous bioactives such as mycotoxins, antifungal and anticancer agents have been reported in the literature within the last more than 100 years [1]. Despite this many new compounds revealing remarkable new bioactivities are still being discovered, including well-known metabolites such as griseofulvin [2–5]. This, combined with the fact that large combinatorial libraries have not provided the anticipated number of new chemical entities explains why the field of natural products is currently assuming new prominence. Thus, natural products are

still used as scaffolds for synthetic organic chemistry, although nowadays primarily for designing smaller and more focused diversity oriented synthesis-derived libraries [6].

It has been estimated that approximately 1.5 million or likely as many as 3 million fungal species exist on Earth, of which only around 100,000 species have been described so far [7]. A multitude of new species are likely to be discovered from diverse habitats, such as tropical forest plants and soils, associated to insects and in the marine environment. In addition to untapped biodiversity recent sequencing of complete fungal genomes has revealed that many gene clusters are silent, suggesting the possibility for many more compounds [8]. Despite several efforts to stimulate such pathways using epigenetic modifiers [9,10], it is evident that we still do not know the full biosynthetic potential even of well studied model organisms such as *Aspergillus nidulans*, altogether strongly indicating Nature's potential as source of new promising bioactive small molecule scaffolds.

The renewed interest in natural product discovery is further enhanced with the new strategies and methodologies for fast dereplication that have been developed within the last decade. Thus chromatographic and spectroscopic methods are combined with database searching in for example Antibase, which is a comprehensive database for natural products from microorganisms [11]. The performance of mass spectrometers is continuously improving, including easy access to both positive and negative ionization spectra even during fast ultra-high-performance liquid chromatography (UHPLC). Altogether the use of accurate mass measurements for dereplication of unknown compounds reduces the number of predicted elemental compositions, ensuring that database searches are conducted with the fewest possible candidates [12]. The use of UV spectral information is often important in the dereplication process for prioritizing between the MS-generated candidates, as well as for UV-guided discovery of novel compounds [13,14].

This article reviews anticancer and often also antifungal natural products primarily produced by *Aspergillus*, *Penicillium* and *Talaromyces*. For practical reasons the compounds have been grouped into major biosynthetic classes, according to the biosynthetic origin of the core part of the structures, despite that many compounds are actually of mixed biosynthetic origin (e.g., prenylated). This review is broader in scope than other recent reviews only focusing on endophytes [15,16], and a strong focus has been on giving the correct identity of the species reported in the literature, where many may previously have been misidentified or names have been changed according to the 2011 Amsterdam Declaration on Fungal Nomenclature [17].

2. Polyketide-Derived Anticancer Compounds

Polyketides represents one of the major classes of natural products of which many are biological active [1]. Today much is known about the enzymes involved in the biosynthesis of a huge diversity of both non-reduced (aromatic), partly reduced and highly reduced polyketides [8].

Some famous fungal polyketides with anticancer activity belong to the statin family. The statins are well known cholesterol synthesis inhibitors that are used in clinical treatment of hypercholesterolemia and cardiovascular diseases [18–21]. Moreover, members the statin family are known to have antifungal properties against *Aspergillus* spp. and *Candida* spp. [18,22–24]. The statin family includes a long list of both natural and synthetic compounds, for example the naturally derived compactin, lovastatin and pravastatin. The statin structure is based on a dicyclohexene ring system connected to a

dicyclohexene ring system connected to a side chain with a closed lactone ring or an open acid form [21]. The compactins are primarily produced by *P. solitum* and *P. hirsutum* [20,25] (first misidentified as *P. brevicompactum* [18] and a fungus identified as *P. citrinum* [19]). Another group of statins that has an extra methyl group attached on the dicyclohexene ring system are produced by *A. terreus* [26] and *Monascus* spp. [27]. Several *in vitro* activities of the statins have been published throughout the years. Reports showed that compactin (Figure 1a) inhibited acute myeloid leukemia (AML) cells with a full inhibitory concentration (IC_{100}) of 2.6 μM [28]. The analogs lovastatin (Figure 1b) and simvastatin (Figure 1c) have been shown to be even more potent.

Figure 1. Statins: (**a**) Compactin, (**b**) Lovastatin and (**c**) Simvastatin.

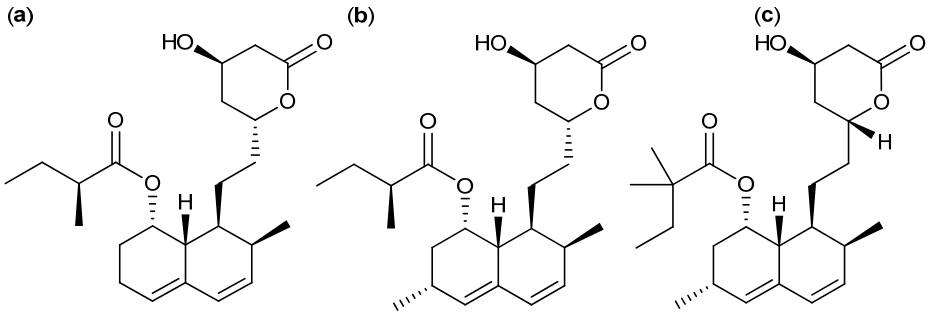

Lovastatin and the synthetic simvastatin selectively inhibited colony growth of primary AML cells with 75%–95% effectiveness. No effect was seen on normal bone marrow [29]. The more recent reported activities includes reduction of proliferation by lovastatin in four lung cancer cell lines with median inhibitory concentration (IC_{50}) values between 1.5 and 30 μM [30]. In 2010 it was shown that lovastatin induced apoptosis in ten ovarian cancer cell lines tested, with IC_{50} values between 2 and 39 μM [31], and recently lovastatin was found to inhibit breast cancer MCF-7, liver cancer HepG2, and cervical cancer HeLa cell lines with IC_{50} values of 0.7, 1.1 and 0.6 μg/mL, respectively [32]. Simvastatin inhibited two lung cancer, three melanoma, and four breast cancer cell lines with IC_{50} values between 0.8 and 5.4 μM and induced apoptosis with reduced tumor growth in hepatic cancer cells [33,34]. Encouraged by these results simvastatin has entered clinical trials as an anticancer drug [35].

The three small polyketides terrein, brefeldin A, and asperlin are examples of well-known metabolites that a couple of decades after they were discovered were shown to exhibit novel anticancer activities. The small antifungal [36] polyketide terrein (Figure 2a) produced by *A. terreus* has been known since 1935 [37]. Almost 80 years later it was found that terrein inhibits breast cancer by induction of apoptosis with an IC_{50} value of 1.1 nM in MCF-7 cell line. That makes terrein 100-fold more potent than taxol against this cell line. Additionally terrein was found active against pancreatic and liver cancer cell lines PANC-1 (IC_{50} 9.8 μM) and HepG2 (IC_{50} 66.8 μM) [38].

Figure 2. Small polyketides: (**a**) Terrein, (**b**) Brefeldin A, and (**c**) Asperlin.

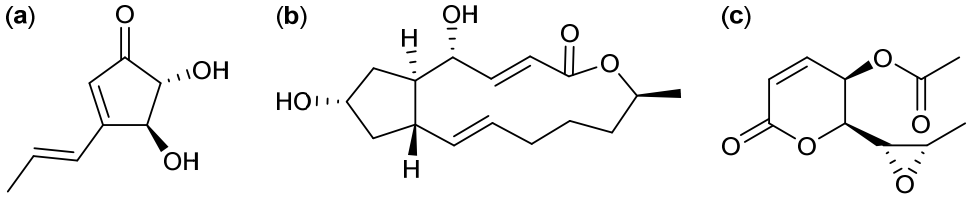

Brefeldin A (Figure 2b), another small antifungal [39,40] polyketide isolated in 1958 from *P. brefeldianum* [41] was identified almost 40 years later as inducer of apoptosis in leukemia (HL-60 and K-582), colon (HT-29), prostate (DU-145), cervical (KB and HeLa), breast (MCF-7 and BC-1), and lung (SPC-A-1 and NCI-H187) cancer cell lines [42–45]. The inhibiting effect of brefeldin A was demonstrated with IC_{50} values 35.7 nM (HL-60), 32 nM (KB), 6.4 nM (HeLa), 7.1 nM (MCF-7), 40 nM (BC-1), 6.3 nM (SPC-A-1), and 110 nM (NCI-H187) [44,45].

Asperlin (Figure 2c) was isolated from *A. nidulans* in 1966 [46]. In 2011 it was discovered that asperlin reduces cell proliferation and induce G_2/M cell cycle arrest in the human cervical carcinoma HeLa cell line [47].

Filamentous fungi are known to produce anticancer polyketides with different spiro ring structures. One of the more well-known is the antifungal [48,49] compound griseofulvin (Figure 3a) from *P. griseofulvum* [50]. Griseofulvin was introduced commercially in 1965 and first considered for cancer treatment in 1973 [49,51]. Later it was shown to induce cell proliferation and mitosis in the human cervical cancer cell line HeLa with an IC_{50} value of 20 μM, as well as it inhibits centrosomal clustering in human squamous cancer SCC-114 cell line with an IC_{50} value of 35 μM [2,3]. The synthetic analog GF-15 increased the inhibitory effect of centrosomal clustering in SCC-114 cells 25-fold with an IC_{50} value of 0.9 μM [5]. It was further shown that combined treatment of griseofulvin and the cancer chemotherapeutic agent nocodazole *in vivo* improved the effect of nocodazole and arrested tumor growth in mice infected with COLO 205 tumors [4].

Other examples of fungal anticancer polyketides with spiro ring structures are sequoiamonascin A (Figure 3b) and B from *A. parasiticus* [52]. Sequoiamonascin A demonstrated selective cytotoxicity against six leukemia cell lines and two melanoma cell lines with a median growth inhibitory (GI_{50}) $\log_{10}$ value of -6.00 [52]. Furthermore, sequoiamonascin A shows cytotoxic activity against breast cancer MCF-7, lung cancer NCI-H460 and central nervous system (CNS) cancer SF-268 cell lines where cell growth can be reduced to 1%–2% when treated with 10 μM sequoiamonascin A [52].

Figure 3. Spiro compounds: (**a**) Griseofulvin, and (**b**) Sequoiamonascin A.

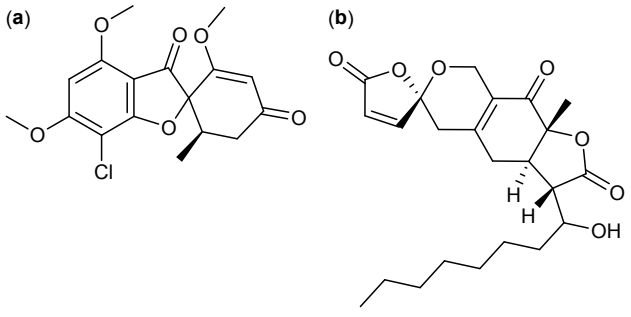

A group of fungal γ-pyrones were found to have activity against cancer. An example of these is the antifungal [48,49] 3-*O*-methylfunicone (Figure 4a) produced by *T. pinophilus* (originally published as *P. pinophlium*) [1,48]. It induced apoptosis and affects cell proliferation in various cancer cell lines including HeLa, MCF-7, A-375P and A-375M [50–53]. Another structurally related compound is penisimplicissin (Figure 4b) isolated from *T. pinophilus* (originally published as *P. simplicissimum*) [54]. It displayed selective cytotoxicity towards leukemia HL-60 and CCRF-CEM cell lines with $\log_{10}$ GI_{50} −6.7 and −5.8, respectively [55].

Figure 4. γ-Pyrones: (**a**) 3-*O*-Methylfunicone and (**b**) Penisimplicissin.

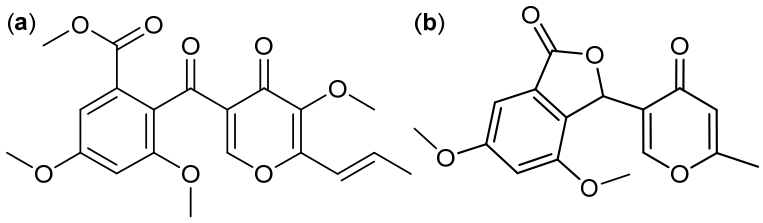

A group of more than 20 closely related azaphilones, namely the antifungal [56] chaetomugilin family, has been isolated within the last five years from marine fish-derived *Chaetomium globosum* [57–64]. The chaetomugilins C, I, P and 11-epichaetomugilin I (Figure 5) showed significant inhibition of two human leukemia P-388, HL-60 and one murine leukemia L-1210, as well as human cervical cancer cell line, KB with 11-epichaetomugilin I as the more potent with IC_{50} values of 0.7 μM (P-388), 1.0 μM (HL-60), 1.6 μM (L-1210), and 1.2 μM (KB) [62].

Figure 5. 11-Epichaetomugilin I.

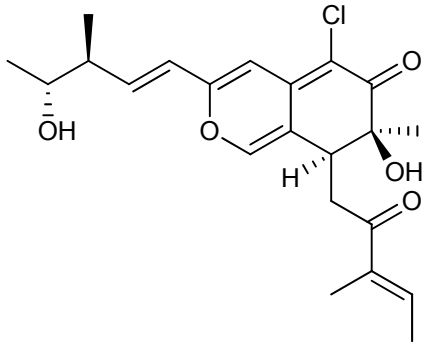

The fungal metabolite norsolorinic acid (Figure 6a) with a tricyclic structure is produced by *A. parasiticus* and *A. nidulans* [65–68]. Norsolorinic acid selectively induced cell cycle arrest in G_0/G_1 phase of the cell cycle and consequently induced apoptosis in human bladder cancer T-24 and human breast cancer MCF-7 with IC_{50} values of 10.5 and 12.7 μM, respectively [67,68].

Figure 6. (**a**) Norsolorinic acid and (**b**) Austocystin D.

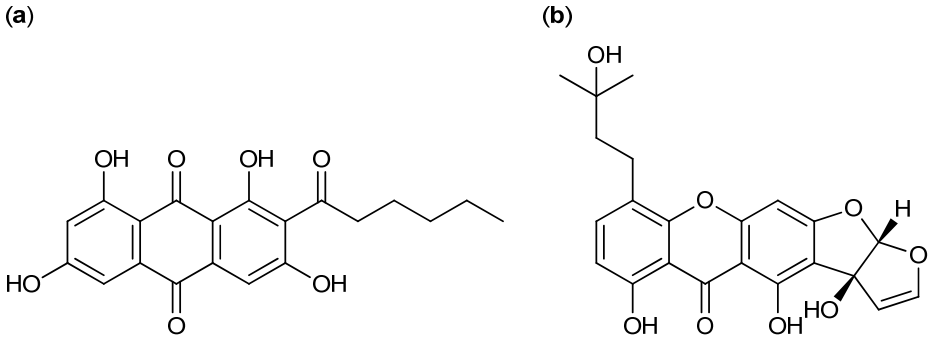

Austocystin D (Figure 6b) was isolated from *A. pseudoustus* [69] in 1974 (originally misidentified as *A. ustus* [70]). Austocystin D was shown to selectively inhibit growth of human colon carcinoma LS174T cells in mice and tumor cell lines that overexpress the multidrug resistance-associated protein [71].

Additionally, austocystin D inhibited a number of cancer cell lines: SR (leukemia, GI_{50} 16 nM), U-87 (brain, GI_{50} 4946 nM), MCF-7 (breast, GI_{50} < 1 nM), MDA-MB-231 (breast, GI_{50} 549 nM), PC-3 (prostate, GI_{50} 3 nM), SW-620 (colon, GI_{50} 27 nM), HCT-15 (colon, GI_{50} 42 nM), and MX-2 (uterine, GI_{50} 3358 nM) [72]. Although, displaying diverse activities towards many types of cancer lines, austocystin D never entered clinical trials due to a low safety window [71].

The two epimers chloctanspirone A and B (Figure 7a) are probably produced by *P. chrysogenum* or *P. rubens* [73,74] (originally published incorrectly as *P. terrestre* [75]). Chloctanspirone A and B were the first chlorinated sorbicillinoids isolated from a natural source and the first to be identified with their very unique ring structure. Chloctanspirone A was the more active analog and inhibited human leukemia HL-60 and lung cancer cell line A-549 cell lines with IC_{50} values of 9.2 and 39.7 μM, respectively [76]. Chloctanspirone B however, only showed moderately or no activity against the same cell lines. Interestingly, the two precursors terrestrols K and L (Figure 7b) that contain the epicenter, which dissociates chloctanspirone A from B were inactive. This points to the conclusion that the cyclohexenone moiety has an impact on the activity though it is not the pharmacophore [76].

Figure 7. (**a**) Chloctanspirone A, B and (**b**) Precursors terrestrols K, L.

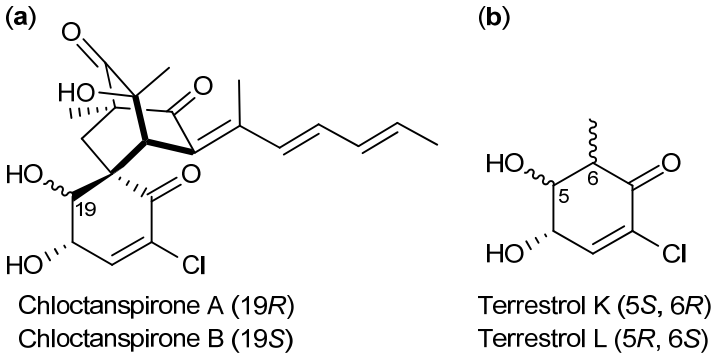

A group of around 20 *p*-terphenyls were isolated from *A. candidus* and found to be cytotoxic against the human cervical cancer cell line HeLa [77]. Thirty years later a new group of prenylated-*p*-terphenyls, called prenylterphenyllins (Figure 8a), terprenins (Figure 8b), and prenylcandidusins (Figure 8c) were isolated from *A. candidus* and *A. taichungensis* [78,79]. The activity of these compounds were studied against lung cancer cell line A-549, human leukemia cell lines HL-60 and P-388, and human epidermoid cancer cell lines KB3-1 [78,79]. Prenylterphenyllin A was found to be the more active against A-549 and HL-60 with IC_{50} values of 8.3 and 1.5 μM, respectively [79], whereas 4″-deoxyisoterprenin displayed higher activity towards KB3-1 with an IC_{50} value of 6.2 μM [78], and finally prenylcandidusin B showed higher activity against P-388 with an IC_{50} value of 1.6 μM [79].

Figure 8. Prenylterphenyllins: (**a**) Prenylterphenyllin A, (**b**) 4″-Deoxyisoterprenin, and (**c**) Prenylcandidusin B.

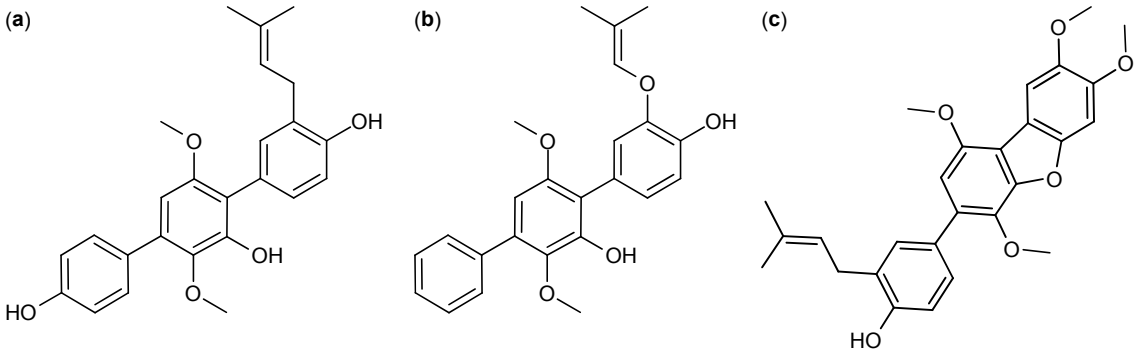

In 2011 five new di- and tricitrinols were added to the known citrinin family from *P. citrinum* [80]. All five of them showed cytotoxic activity against human leukemia HL-60, colon cancer HCT-116, and cervical cancer KB cell lines. The more potent was tricitrinol B (Figure 9), with IC_{50} values of 3.2, 4.8 and 3.9 μM, respectively [80].

Figure 9. Tricitrinol B.

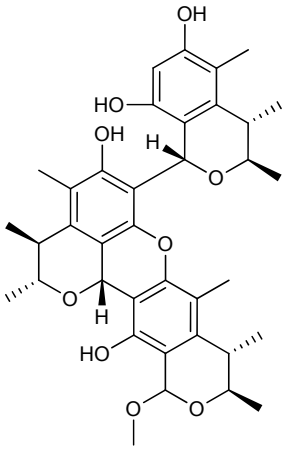

The class of perylenequinones has been used for centuries in Chinese herbal medicine, but fungal production of several perylenequinones has likewise been reported [81]. The calphostins were isolated from *Cladosporium cladosporioides* and shown to inhibit cervical cancer HeLa-S_3 and breast cancer MCF-7 cell lines. Most potent was calphostin C (Figure 10a) with IC_{50} values of 0.23 and 0.18 μM, respectively [82]. Furthermore, calphostin C induced apoptosis in acute lymphoblastic leukemia [83]. The hypocrellins, another branch, of the perylenequinone family was isolated from *Hypocrella bambusae*, originally published incorrectly as *Shira bambusicola* [84,85]. Hypocrellin D was one of the more potent analogs and inhibited liver (Bel-7721) and lung (A-549 and Anip-973) cancer cell lines, with IC_{50} values, 1.8, 8.8, 38.4 μg/ml, respectively [85]. Additionally, the hypocrellins had a photodynamic effect on a wide range of tumor cell lines. Due to their insolubility in water several analogs have been synthesized to improve the pharmacokinetics and drug delivery. Two of the more successful analogs were carboxylate salt derivatives of hypocrellin B (Figure 10b) with increased water solubility and activity against human breast cancer MCF-7 when photodynamic therapy was

used [81,86]. In 2012 a new group of perylenequinones called the phaeosphaerins were isolated from *Phaeosphaeria* sp. with phaeosphaerin B (Figure 10c) as the more potent against prostate PC-3, DU-145, LNCaP cancer cell lines with IC_{50} values of 2.4 μM, 9.5 μM and 2.7 μM, respectively [87].

Figure 10. Perylenequinones: (**a**) Calphostin C, (**b**) Hypocrellin B and (**c**) Phaeosphaerin B.

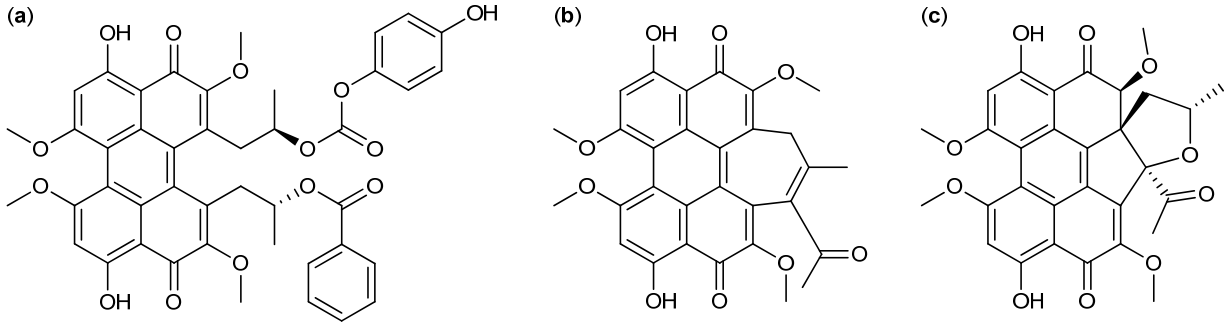

3. Nitrogen-Containing Anticancer Compounds

Fungal nitrogen containing compounds represent another large group of natural products, of which many have famous bioactivities. In general these types of compounds incorporate amino acid building blocks into often complex heteroaromatic compounds such as diketopiperazines, quinazolines and benzodiazepines [1]. Often these compounds are referred to as alkaloids, due to their basic nature, when containing primary, secondary or tertiary amine functionalities. However, compounds only containing amide bonds, that are essentially neutral, are often also referred to as alkaloids. In recent years it has become clear that many nitrogen containing compounds are biosynthesized by multifunctional enzymes (non-ribosomal peptide synthases, NRPS) with modular arrangements comparable to that seen for some polyketide synthases. In such contexts these compounds are usually referred to as non-ribosomal peptides (NRPs) even though they are also called alkaloids [88]. In the following section no attempt has been made to differentiate between the different naming of the numerous amino acid-derived metabolites.

The antifungal [89] xanthocillin X (Figure 11) was first isolated from *Dichotomomyces albus* ascribed to *D. cejpii* [90], but is produced by *P. chrysogenum* as well [1]. In 1968 xanthocillin X was found active against a Ehrlich ascites carcinoma-mouse strain with median lethal dose (LD_{50}) of 40 mg/kg [91]. Approximately 40 years later it was shown that xanthocillin X inhibited leukemia K-562, human cervical cancer HeLa, breast cancer MCF-7 and MDA-MB-231, liver cancer HepG2, lung cancer NCI-H460, and prostate cancer DU-145 cell lines with IC_{50} values between 0.4 and 12 μg/ml [89,92]. Two structural analogs named BU-4704 and xanthocillin X di-methoxy were found more potent than xanthocillin X. Instead of the two hydroxy groups BU-4704 contains a methoxy and a sulfonic acid group and xanthocillin X di-methoxy contains two methoxy groups. BU-4704 inhibited human colon HCT-116 and murine melanoma B16-F10 with IC_{50} values of 0.6 and 4.3 μg/mL, respectively [93]. Xanthocillin X di-methoxy inhibited HepG2, MCF-7 and KB cancer cell lines with IC_{50} values of 0.18, 0.38 and 0.44 μg/mL, respectively [94].

Figure 11. Xanthocillin X.

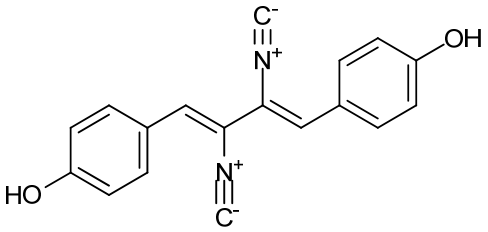

Asperphenamate (Figure 12) was first isolated from *A. flavipes* [95] and later found to be produced by several of *Penicillium* spp. as well [96]. Asperphenamate displayed moderate cytotoxic activity against several cancer cell lines [97]. Due to the low activity and a low water solubility asperphenamate was used as a lead for synthetic structurally isomers. It was found that the (*R,S*) stereoisomers were more potent than the (*S,R*) stereoisomers [98]. The more active asperphenamate derivate was N-benzoyl-O-(N′-(1-benzyloxycarbonyl-4-piperidiylcarbonyl)-D-phenylalanyl)-D-phenyl-alaninol (BBP). BBP was approx. 20-fold more active than asperphenamate against breast cancer (MCF-7, T47D and MDA-MB231), hepatic (BEL-4702), lung (A-549), and cervical (HeLa) cancer as well as leukemia (HL-60) cell lines, with IC_{50} values between 3.0 and 18.3 μM [99].

Figure 12. Asperphenamate.

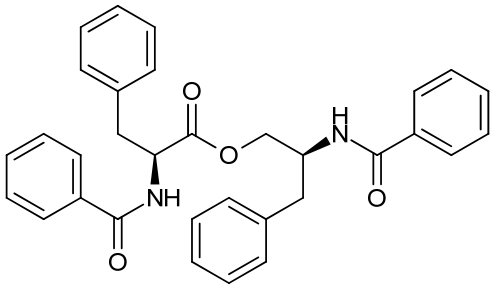

Cyclic di-peptides called diketopiperazines are in general known as cell cycle inhibitors of the G2/M phase [100]. Tryptophan/proline diketopiperazines covers the compound groups fumitremorgins, stephacidins, notoamides, tryprostatins, *etc*. This group of compounds is produced by a long range of *Aspergilli* [101–110]. The fumitremorgins are produced by *A. fumigatus* and *A. fischeri* [101–103,111]. Fumitremorgin C (Figure 13a) was found active against human leukemia P-388 with an ED_{50} value of 3.9 μg/mL and the analog 12,13-dihydroxyfumitremorgin C has antiproliferative effects on human leukemia U-937 and human prostate cancer PC-3, with IC_{50} values of 1.8 and 6.6 μM, respectively [111,112]. Furthermore fumitremorgin C was specifically and potently cytotoxic against multi-drug resistant breast- and colon cancer [113,114].

Two other tryptophan/proline diketopiperazines are stephacidin A (Figure 13b) and B produced by *A. ochraceus* and *A. westerdijkiae* [106,107]. Stephacidin B is the dimeric form of stephacidin A and was approximate 10-fold more potent. Stephacidin B exhibited inhibitory effect on prostate, ovarian, colon, breast and lung cancer cell lines with IC_{50} values between 0.06 and 0.4 μM [106].

The notoamides (Figure 13c) produced by *A. amoenus* are close analogs to the stephacidins, but with a spiro ring structure [115]. Contrary to the stephacidins the notoamides only showed low to moderate inhibition of two leukemic cell lines with IC_{50} values 22–52 μg/mL [116].

Figure 13. Tryptophan/proline diketopiperazines: (**a**) Fumitremorgin C, (**b**) Stephacidin A, (**c**) Notoamide A, (**d**) 18-Oxotryprostatin A and (**e**) Spirotryprostatin E.

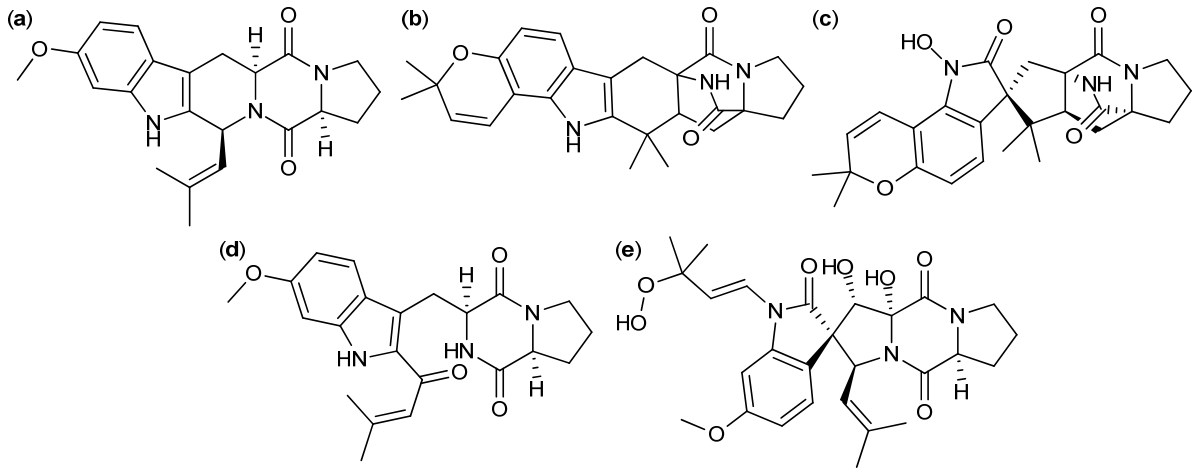

Finally, the tryprostatins (Figure 13d) and spirotryprostatins (Figure 13e) isolated from *A. fumigatus* where found active against lung (NCI-H-522 and A-549), breast (MCF-7) and prostate (PC-3) cancer as well as leukemia (HL-60 and MOLT-4). The more potent analogs were Ds1-tryprostatin B with GI_{50} values of 15.8 μM (NCI-H-522), 15.9 μM (MCF-7), and 11.9 μM (PC-3) and 18-oxotryprostatin A with an IC_{50} value of 1.3 μM (A-549) [108,110]. Spirotryprostatin E was the more potent of the spirotryprostatins, with IC_{50} values of 3.1 μM (MOLT-4), 2.3 μM (HL-60) and 3.1 μM (A-549) [109].

Other diketopiperazines originating from histidine are phenylahistin (Figure 14a) and aurantiamine (Figure 14b). Phenylahistin was first isolated from *A. ustus* in 1997 as a mixture of enantiomers [117]. (−)-Phenylahistin was more active than (+)-phenylahistin against dermal (A-431), lung (A-549), ovary (HeLa), leukemia (K-562 and P-388), breast (MCF-7), CNS (TE-671) and colon (WiDr) cancer cell lines with IC_{50} between 0.18 and 3.7 μM [118]. A synthetic analog plinabulin (NPI-2358) displays very potent activity against human prostate carcinoma cell line DU-145 and has now entered phase II clinical trials [119]. Recently, more than 60 synthetic analogs of plinabulin have been designed and synthesized. The more active analog with a benzoyl group coupled on the phenylalanine unit was 10-fold more active than plinabulin with an IC_{50} value of 1.4 nM [119]. The activity of phenylahistin was also compared to the diketopiperazine aurantiamine and other synthetic analogues [120], originally isolated by Larsen *et al*. [121].

Figure 14. (**a**) Phenylahistin and (**b**) Aurantiamine.

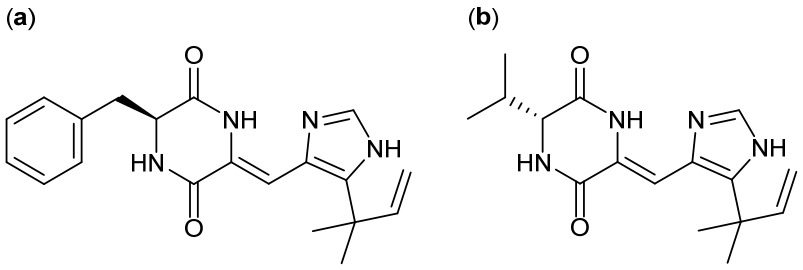

Another group of diketopiperazines with anticancer activity contain a di-sulfide bridge in the diketopiperazine ring. One of them the antifungal, immunosuppressive and antimicrobial compound gliotoxin (Figure 15a) that was isolated from *A. fumigatus*, and *D. cejpii* [122–124]. Already in 1947 the anticancer activity of gliotoxin was suggested and in 2004 it was found that gliotoxin was a very potent inhibitor of six breast cancer cell lines with IC_{50} values between 38 and 985 nM [125,126]. In 2012, gliotoxin was found active against human leukemia U-937 and human prostate cancer PC-3 cell lines with IC_{50} values of 0.2 and 0.4 μM, respectively [112].

Figure 15. Diketopiperazines with a di-sulfide bridge: (**a**) Gliotoxin, (**b**) Emestrin A and (**c**) Acetylapoaranotin.

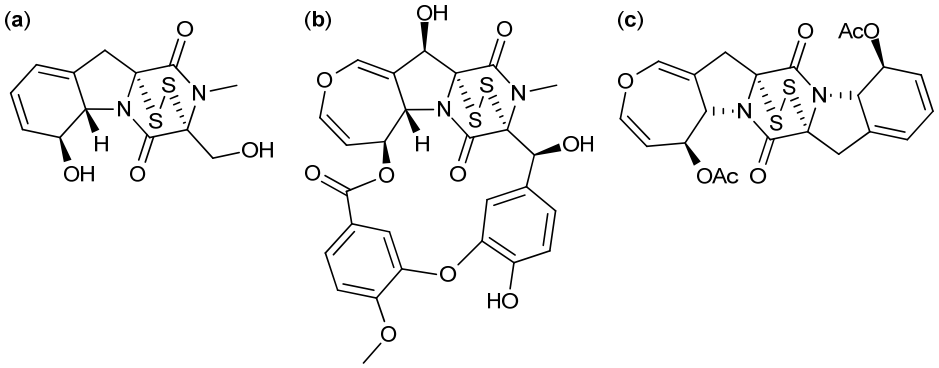

Another diketopiperazine with a di-sulfide bridge is the antifungal [127] compound emestrin A (Figure 15b) that was isolated from *Emericella striata*, now called *A. striatus* [128]. Emestrin A inhibits human leukemia (HL-60) with an IC_{50} value of 83.5 nM [129]. Eight structural analogs of emestrin A were isolated from *Cladorrhinum* sp. and found to have strong antiproliferative effects on the human prostate DU-145 cancer cell line with an IC_{50} value of 9.3 nM for the more potent emestrin C. Furthermore, it was proven that the activity decreased when the macro cyclic ring was opened and the polysulfide bridge in the diketopiperazine was absent [130].

Recently, a new diketopiperazine with a di-sulfide bridge named acetylapoaranotin (Figure 15c) produced by a marine *Aspergillus* sp. was discovered and found active against colon (HCT-116), gastric (AGS), lung (A-549), and breast (MCF-7) cancer cell lines with IC_{50} values of 13.8, 12, 2 and 10 μM, respectively [131].

The peptide leucinostatin A (Figure 16) was first isolated in 1973 from *Purpureocillium lilacinum* (originally published as *Penicillium lilacinum* or *Paecilomyces lilacinus*) [132,133]. It was found active against a number of fungi and Gram-positive bacteria, as well as Ehrlich solid carcinoma of mice with an ED_{50} value of 1.6 mg/kg [132,134]. Furthermore leucinostatin A inhibited a long range of breast, melanoma, lung, ovary, colon and laryngeal cancers as well as eight leukemia cell lines with IC_{50} values between 4 nM and 12 μM [132,135,136]. Leucinostatin A inhibited growth of prostate cancer DU-145 cells *in vitro* and *in vivo* [137]. A natural analog leucinostatin A β di-*O*-glycoside displayed active against breast cancer BT-20 cell line, though not as potent as leucinostatin A [138].

Figure 16. Leucinostatin A.

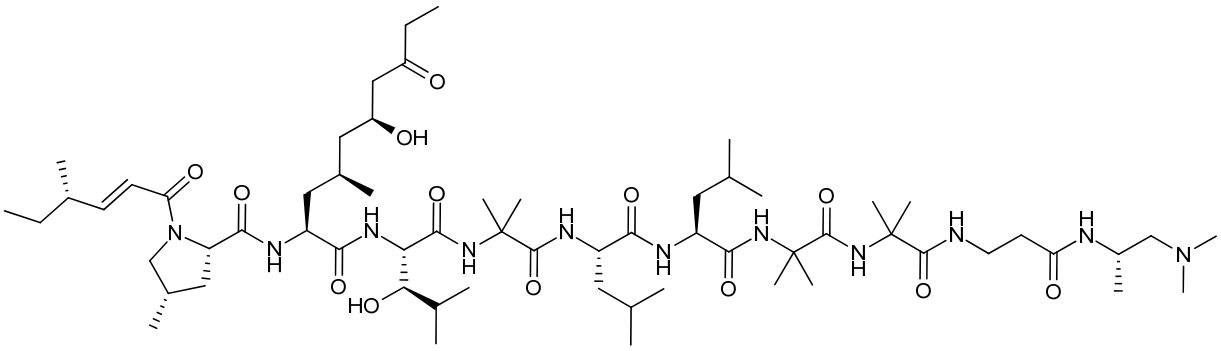

4. Terpenoid-Derived Anticancer Compounds

Terpenoids form a third large and structurally diverse biosynthetic family of natural products derived from C_5 isoprene units. Until now active anticancer terpenoids mostly belong to the sesqui- or diterpenoids [15].

Taxol, also known as paclitaxel (Figure 17), is one of the best known anticancer drugs produced by fungi, though it originally was isolated from the bark of yew tree *Taxus brevifolia* [139]. Clinical development of taxol was delayed due to problems with production of large enough quantities of the compound. This problem was solved 20 years later when it was demonstrated that taxol was also produced by the fungus *Taxomyces andreanea* [140] and later including *P. raistrickii* [141].

Figure 17. Taxol.

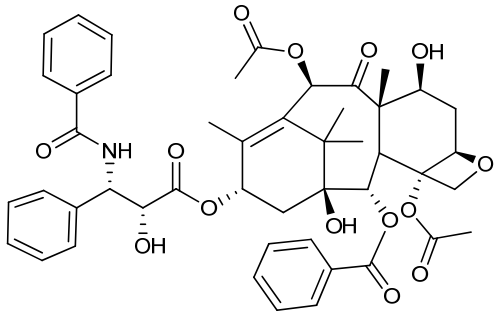

Taxol was approved as anticancer drug against a wide range of tumors in the 1990s and is the first billion dollar drug against cancer [142,143]. Taxol functions by inducing cell cycle arrest in G_2/M phase as well as apoptosis through a unique mode-of-action by promotion and stabilization of tubulin polymerization [144]. Today, taxol is routinely used to treat ovarian, breast and lung tumors as well as Kaposi's sarcoma [145]. Besides its anticancer activity taxol displays antifungal activity as well [146].

Many sesquiterpenes have been found active against cancer. Two of these are the drimane sesquiterpenes fudecadione A and B (Figure 18a) that were isolated in 2011 from *Penicillium* sp. BCC 17468. Fudecadione A was found active against human lung cancer NCI-H187, human breast cancer MCF-7, and human oral epidermoid carcinoma KB cell lines, with IC_{50} values of 24.9, 12.6 and 22.6 μM, respectively. Fudecadione B, on the other hand, was inactive against all three cancer call lines [147]. The activity of the two compounds suggests that the pharmacophore is located around the carbon at position 13, where fudecadione B is more branched [147].

Figure 18. (**a**) Fudecadione A, (**b**) Terrecyclic acid A and (**c**) a novel unnamed chloro-trinoreremophilane sesquiterpene.

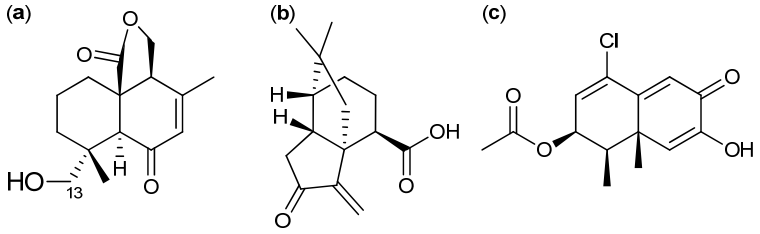

Another active sesquiterpene is the antifungal terrecyclic acid A (Figure 18b), which was isolated from *A. terreus* in 1986 [148]. Terrecyclic acid A exhibit cytotoxic activity against human lung cancer NCI-H460, human breast cancer MCF-7, and human CNS cancer SF-268 cell lines with IC_{50} values of 10.6, 24.1 and 14.7 μM, respectively, and against leukemia in mice P-388 with LD_{50} values of 63–125 mg/kg [148,149].

In 2013 a novel and as yet unnamed chlorotrinoreremophilane sesquiterpene (Figure 18c) was isolated from *Penicillium* sp. PR19N-1 [150]. This novel sesquiterpene exhibited cytotoxic activity against human leukemia HL-60 and lung cancer A-549 cell lines with IC_{50} values of 11.8 and 12.2 μM, respectively [150].

A large group of mycotoxins called the trichothecenes cover more than 150 analogs and are mainly produced by a number of *Fusarium* spp. [151]. All the trichothecenes contain a sesquiterpenoid ring structure with an epoxide. The epoxide is often responsible for the cytotoxic activity by binding to the 60S ribosomal subunit in eukaryote cells thereby inhibiting protein synthesis [152,153]. Many of the trichothecenes exhibit cytotoxic activity against both fungi and cancer cell lines [154–156]. One of the more potent is AETD (Figure 19a) that inhibits HL-60, U-937, HeLa, MCF-7 and Hep-G2 cell lines with IC_{50} values of 10, 22, 45, 53 and 170 nM [157]. Other bioactive groups are the roridins where a macrocyclic ring is connected to the sesquiterpenoid unit. One of the more active compounds of this group is 12′-hydroxyroridin E (Figure 19b), which inhibits leukemia L-1210 with an IC50 value of 0.2 μM [158]. Another trichothecene called anguidine even entered clinical trials against cancer, but did not progress beyond phase II due to a lack of therapeutic efficacy [152,159].

Figure 19. Trichothecenes (**a**) AETD and (**b**) 12′-Hydroxyroridin E.

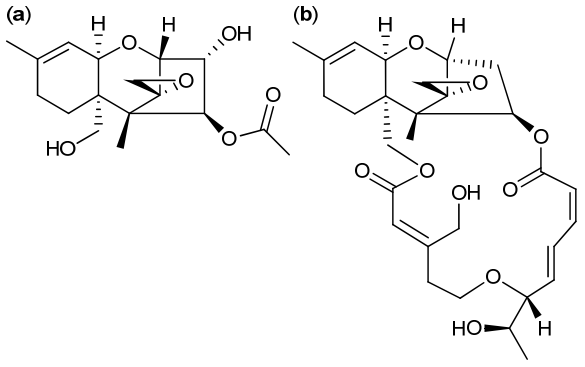

Wentilactone A and B (Figure 20a) were isolated from *A. wentii* in 1980 [160]. In 2012 it was reported that wentilactone B induced apoptosis and inhibited proliferation in human hepatoma cancer cell line SMMC-7721, with an IC_{50} value of 19 μM [161].

Figure 20. (**a**) Wentilactone B and (**b**) Wortmannin.

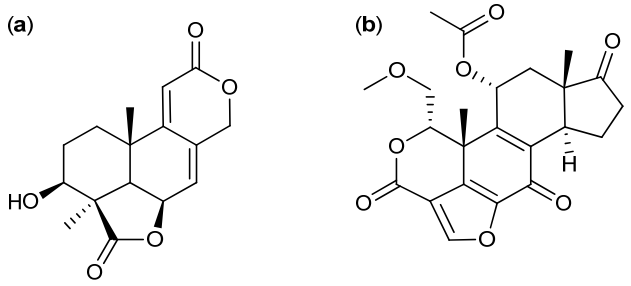

The antifungal compound wortmannin (Figure 20b) is produced by *T. wortmannii* originally published as *P. wortmannii* [162] or a related species. Wortmannin inhibit the activity of leukemia HL-60 and K-562 cell lines with IC_{50} values of 30 and 25 nM, respectively [163,164], including the breast cancer MCF-7 cell line that was inhibited by 51.3% after 48 h with a concentration of 25 nM [165]. In human pancreatic cancer cells lines PK1 and PK8 wortmannin induces apoptosis both *in vitro* and *in vivo* [166,167]. Finally, wortmannin has been shown to inhibit proliferation in lung cancer cell lines KNS-62 and Colo-699 both *in vitro* and *in vivo*, with IC_{50} values between 100 and 200 nM [168].

The ophiobolins are sesterterpenes mainly isolated from the fungal genus *Bipolaris* [169,170], but are also found in *Aspergillus* [171], *Sarocladium* [172,173], and *Drechslera* [174]. Isolation of ophiobolins from *Aspergillus* spp. misidentified as *A. ustus* were later ascribed to the three different species: *A. calidoustus*, *A. insuetus*, and *A. keveii* from the *Aspergillus* section *Usti* [69]. Ophiobolin A (Figure 21) exhibit inhibitory activity against cancer cell lines includes lung cancer A-549, colon cancer HT-29, melanoma Mel-20, leukemia P-388, and ovarian cancer OVCAR-3 with IC_{50} values of 0.1, 0.1, 0.1, 0.06 and 0.3 μM, respectively [175,176]. In 2012 the novel ophiobolin O was discovered and it was found to inhibit breast cancer MCF-7 and leukemia P-388 cell lines with IC_{50} values of 17.9 and 4.7 μM, respectively [177,178]. Most recently in 2013 the novel 3-anhydro-6-hydroxyophiobolin A was isolated and found active against lung cancer (HepG2) and leukemia (K-562) cell lines with IC_{50} values of 6.5 and 4.1 μM, respectively [179]. Besides anticancer activity the ophiobolin family show antifungal activity against a wide range of fungi [180,181].

Figure 21. Ophiobolin A.

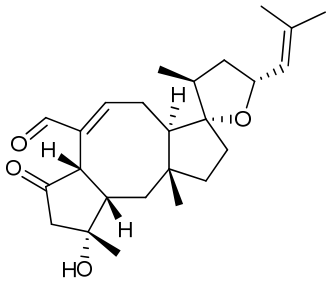

5. Anticancer Natural Products of Mixed or Unresolved Biosynthetic Origin

Filamentous fungi are capable of producing secondary metabolites of mixed biosynthetic origin. This includes both compounds such as meroterpenoids that comprise a huge class of compounds that integrate a polyketide part with a terpenoid part [182], in addition to the cytochalasins [183] and

chaetoglobosins that are biosynthesized by incorporation of amino acids into a core polyketide part. The cytochalasins contains a phenylalanine coupled to the polyketide chain where the chaetoglobosins have an tryptophan moiety [183,184]. Both the cytochalasins and the chaetoglobosins exhibit antifungal activities against a broad range fungal species [56,185,186]. The cytochalasins are produced by many fungal genera including *Aspergillus*, *Hypoxylon*, *Metarrhizium*, *Zygosporium*, *Hypocrella* and *Phoma* [90,187–190]. Many of the cytochalasins have shown inhibitory activities towards lung cancer A-549. One of the more potent is cytochalasin E (Figure 22a) which inhibited human ovarian A-2780S, human colon HCT-116 and SW-620, and lung A-549 cancer as well as human leukemia P-388 with IC_{100} values of 0.02, 1.0, and 0.2 μg/ml and IC_{50} values of 0.006 and 0.09 μM, respectively [191,192].

Figure 22. (**a**) Cytochalasin E and (**b**) Chaetoglobosin B.

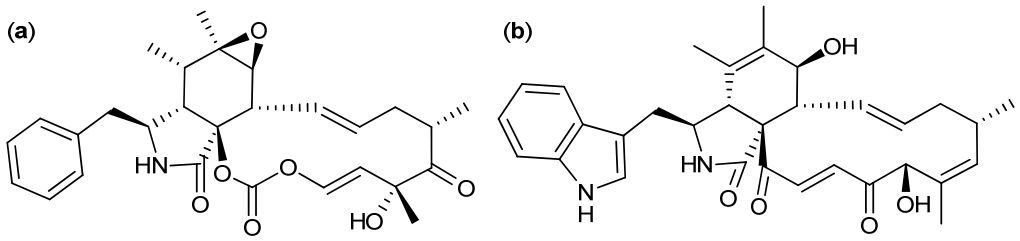

The chaetoglobosins were originally isolated from *Chaetomium globosum* in 1973 [184]. Several chaetoglobosins have been isolated over the years from *P. discolor* and *P. expansum* among others [1] and many of them showed activity against cancer cell lines. Of the more potent ones was chaetoglobosin B (Figure 22b) that inhibited human breast BC cancer cell line with an IC_{50} value of 3.0 μM [193] and chaetoglobosin D that inhibited adenocarcinoma KKU-100 and KKU-OCA17 cancer cell lines with IC_{50} values of 3.4 and 12.2 μM, respectively [193]. Chaetoglobosin U showed activity as well against KB tumor cell line with an IC_{50} value of 16.0 μM [194], and chaetoglobosin X with activity against murine hepatic cancer H-22 cell line with an IC_{50} value of 7.5 μM [195].

Another group of compounds with mixed a biosynthetic pathway are the pseurotins (Figure 23) containing phenylalanine coupled to a polyketide and with a spiro ring structure. The pseurotins were first isolated from the bacteria *Pseudeurotium ovalis* and later from the fungus *A. fumigatus* [196,197]. In 2012 four pseurotin analogs were proven active against a human breast cancer cell line MCF-7 with the more active pseurotin D inhibiting MCF-7 with an IC_{50} value of 15.6 μM [198].

Figure 23. Pseurotin A.

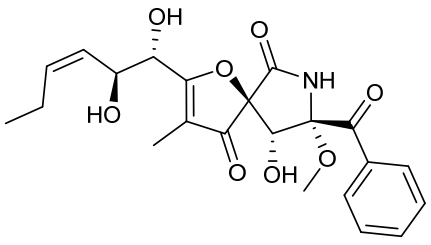

The γ-pyridone alkaloids, penicidone A–C (Figure 24a) were isolated from an endophytic *Talaromyces* sp. The biosynthesis of penicidones probably happens through the polyketide pathway

similar to penisimplicissin (Figure 24b), but with a unique introduction of nitrogen [199]. The penicidones were showed to be active against human colon cancer SW1116, human AML (K-562), and human cervical cancer (KB and HeLa) cell lines with penicidone B being the more potent analog. Penicidone B inhibited the four cancer cell lines with IC_{50} values of 54.2 μM (SW1116), 21.1 μM (K-562), 29.6 μM (KB), and 35.2 μM (HeLa) [199]. Two other γ-pyridone alkaloids called penicinoline (Figure 24b) and methylpenicinoline were isolated from an endophytic *Penicillium* sp. and *Auxarthron reticulatum* in 2010 and 2011, respectively [200,201]. Penicinoline and methylpenicinoline were shown to inhibit the lung cancer HepG2 cell line with IC_{50} values of 13.2 and 11.3 μM, respectively [202].

Figure 24. (**a**) Penicidone B and (**b**) Penicinoline.

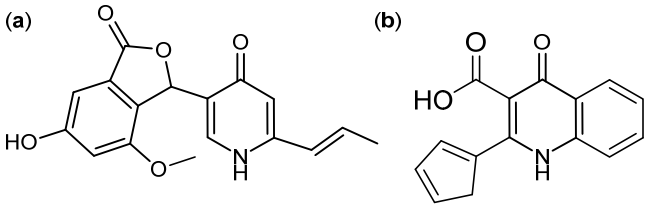

Communesins are fungal metabolites produced in *P. marinum*, *P. expansum*, *P. buchwaldii* and *P. rivulorum* [96,203–205]. The group is of highly mixed biosynthetic origin with structures combining a nitrogen-containing part, a polyketide chain and isoprene. Communesin B (Figure 25) displays the highest activity of them all against leukemia P-338, U-937, THP-1, NAMALWA, MOLT-3 and SUP-B15 cell lines with ED_{50} values of 0.5, 10.4, 11.4, 9.9, 8.1 and 7.2 μg/mL, respectively [206,207].

Figure 25. Communesin B.

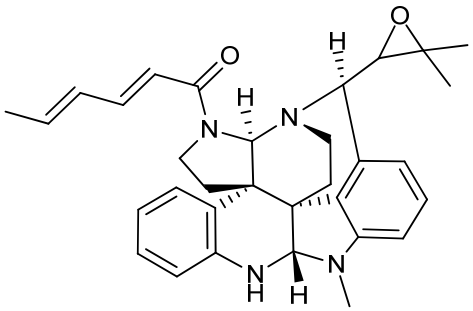

The antibiotic compound fumagillin (Figure 26a) has been one of the more potent and interesting compounds associated with anticancer activity produced by fungi. Fumagillin, classified as a meroterpenoid, was first isolated from *A. fumigatus* in 1951 [208] and further produced by *P. scabrosum* [209]. The antitumor activity of fumagillin is caused by its potent angiogenesis-inhibiting effect. Unfortunately, fumagillin had some unpleasant side effects and consequentially investigations into structural analogs have been conducted [210]. The synthetic fumagillin analog TNP-470 (Figure 26b) contains an amine and chlorine in the side chain, which led to a highly increased angiogenesis—inhibiting effect. Furthermore, TNP-470 is less toxic to normal cells compared to fumagillin [210,211]. *In vitro* and *in vivo* tests showed that TNP-470 inhibited tumor growth in

prostate (PC-3) and breast cancer (MDA-MB-231). TNP-470 entered preclinical trails in 1992 and phase I and II in 2000 but did not progress into phase III, due to a very short systemic half-live and observed neurotoxicity in patients [212–214]. Recently, in 2013, a novel natural fumagillin analog namely ligerin (Figure 26c) was isolated from a marine-derived *Penicillium* sp.[215]. Ligerin inhibited lung cancer POS1 cell line with an IC_{50} value of 117 nM [215].

Figure 26. (**a**) Fumagillin, (**b**) Synthetic analog TNP-470 and (**c**) Ligerin.

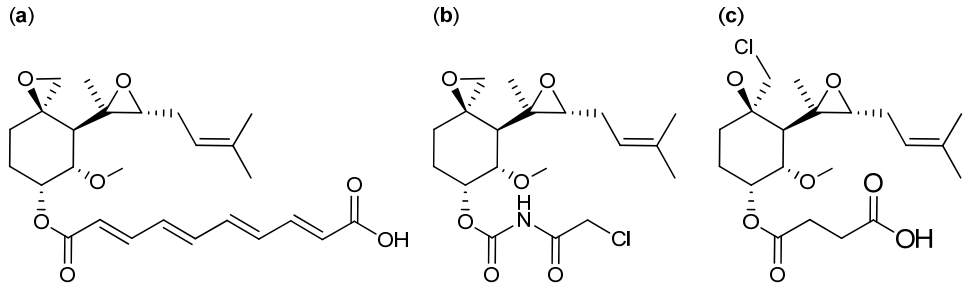

A strain so far identified as *Talaromyces purpurogenus* (earlier *P. purpurogenum*) is known to produce another group of meroterpenoids namely purpurogemutantin (Figure 27a), purpurogemutantidin (Figure 27b), and the known antifungal macrophorin A (Figure 27c) [216,217]. All three compounds inhibit human leukemia K-562 and HL-60, human cervical cancer HeLa, human gastric adenocarcinoma BGC-823 and human breast cancer MCF-7 cell lines. Purpurogemutantidin (Figure 27a) was the more potent, with IC_{50} values of 0.9, 2.4, 16.6, 31.0, and 26.3 μM, respectively. The only exception is macrophorin A that displayed higher activity towards the HL-60 cell line with an IC_{50} value of 0.9 μM [216].

Figure 27. (**a**) Purpurogemutantin, (**b**) Purpurogemutantidin and (**c**) Macrophorin A.

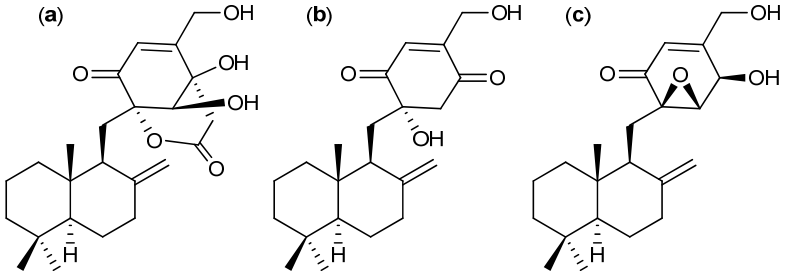

Botryodiplodin (PSX-1), a small antifungal [218] compound of unresolved biosynthetic origin (Figure 28), was isolated from *T. stipitatus* (originally named *P. stipitatum*) [219] and exhibits activity against Ehrlich ascites carcinoma, leukemia L-5178, Sarcoma 37, and cervical cancer Hela cell lines with a median effective dose (ED_{50}) values of approximately 1 μg/mL [219,220].

Figure 28. Botryodiplodin (PSX-1).

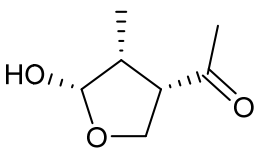

The atpenins A4, A5 and B (Figure 29) of unresolved biosynthetic pathway were first isolated from *P. atramentosum* in 1988 and shown to possess antifungal activities [221]. Twenty years later the first three atpenins were isolated again from the same fungi along with two new analogs, NBRI23477 A and B [222]. The activities of the five atpenins were examined individually against human prostate cancer cell line DU-145 and in a stromal co-cultured assay. Growth of the DU-145 cells was inhibited more effectively in the co-cultured setup, with atpenin A5 being the more potent analog with an IC_{50} value of 0.02 μg/mL [222]. All the reviewed compounds are summarized in Table 1 with their individual organisms of origin, biosynthetic pathways, target cancer cells, IC_{50} (if available), and whether the compounds exhibit antifungal activity too.

Figure 29. Atpenin A5.

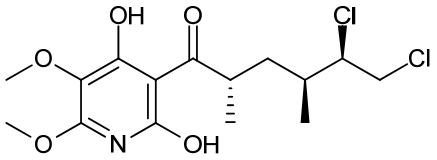

Table 1. List of fungal anticancer natural products primarily produced by *Aspergillus*, *Penicillium* and *Talaromyces* summarizing producing organisms, biosynthetic origin, target cancer cells, IC_{50} (if available), and if the compounds exhibit antifungal activity.

Species (original published)	Compound	Type	Target cell	IC_{50}	Anti-fungal (+/−)
T. pinophilus [1] (*P. pinophilum* [48])	3-O-methylfunicone [50–53]	Polyketide	HeLa	-	+ [48,49]
			MCF-7	-	
			A-375P	-	
			A-375M	-	
A. nidulans [46]	Asperlin [47]	Polyketide	HeLa	-	−
A. flavus [95] *Penicillium* spp. [96]	Asperphenamate	NPR	-	-	−
A. flavus [95] *Penicillium* spp. [96]	BBP [99]	NPR	MCF-7	3.0 μM	
			T47D	4.7 μM	
			MDA-MB231	5.2 μM	
			BEL-4702	12.7 μM	
			A-549	15.1 μM	
			HeLa	17.0 μM	
			HL-60	18.3 μM	
Aspergillus sp. [131]	Acetylapoaranotin [131]	NPR	HCT-116	13.8 μM	−
			AGS	12 μM	
			A-549	2 μM	
			MCF-7	10 μM	
P. atramentosum [222]	Atpenin A5 [222]	Unresolved biosynthetic origin	DU-145 (co-culture)	0.02 μg/mL	+ [221]
A. puniceus [69] *A. turkensis* [69] *A. pseudoustus* [69] *A. ustus* [70]	Austocystin D [71,72]	Polyketide	SR	16 nM (GI_{50})	−
			U-87	4946 nM (GI_{50})	
			MCF-7	<1 nM (GI_{50})	
			MDA-MB-231	549 nM (GI_{50})	
			PC-3	3 nM (GI_{50})	
			SW-620	27 nM (GI_{50})	
			HCT-15	42 nM (GI_{50})	
			MX-2	3358 nM (GI_{50})	
P. brevicompactum [20] *P. paneum* [223] *T. stipitatus* [1] (*P. stipitatum* [220])	Botryodiplodin [219,220]	Unresolved biosynthetic origin	EAC	0.6 μg/mL (ED_{50})	+ [218]
			L-5178	0.8 μg/mL (ED_{50})	
			Sarcoma 37	1.5 μg/mL (ED_{50})	
			HeLa	2.0 μg/mL (ED_{50})	

Table 1. *Cont.*

Species (original published)	Compound	Type	Target cell	IC_{50}	Anti-fungal (+/−)
P. brefeldianum [39]	Brefeldin A [42–45]	Polyketide	HL-60	35.7 nM	+ [39,40]
			KB	32 nM	
			HeLa	6.4 nM	
			MCF-7	7.1 nM	
			SPC-A-1	3.6 nM	
			BC-1	40 nM	
			NCI-H187	110 nM	
Cladosporium cladosporioides [82]	Calphostin C [82,83]	Polyketide	HeLa S3	0.2–8.5 μM	−
			MCF-7	0.2–2.7 μM	
			ALL	-	
Chaetomium globosum [184] *P. discolor* [1] *P. expansum* [1]	Chaetoglobosin B [193]	Mixed biosynthetic origin	BC	3.0 μM	+ [56,186]
Chaetomium globosum [184] *P. discolor* [1] *P. expansum* [1]	Chaetoglobosin D [193]	Mixed biosynthetic origin	KKU-100	3.4 μM	
			KKU-OCA17	12.2 μM	
Chaetomium globosum [184] *P. discolor* [1] *P. expansum* [1]	Chaetoglobosin U [194]	Mixed biosynthetic origin	KB	16.0 μM	
Chaetomium globosum [184] *P. discolor* [1] *P. expansum* [1]	Chaetoglobosin X [195]	Mixed biosynthetic origin	H-22	7.5 μM	
Chaetomium globosum [57–61,63,64] *T. pinophilus* [1]	11-epichaetomugilin I [62]	Polyketide	P-388	0.7 pM	+ [56]
			HL-60	1.0 pM	
			L-1210	1.6 pM	
			KB	1.2 pM	
P. chrysogenum [74] *P. rubens* [73] (*P. terrestre* [76])	Chloctanspirone A [76]	Polyketide	HL-60	9.2 μM	−
			A-549	39.7 μM	
P. buchwaldii [96] *P. marinum* [1] *P. expansum* [204] *P. rivulorum* [205]	Communesin B [206,207]	Mixed biosynthetic origin	P-388	0.5 μg/mL (ED_{50})	−
			U-937	10.4 μg/mL (ED_{50})	
			THP-1	11.4 μg/mL (ED_{50})	
			NAMALWA	9.9 μg/mL (ED_{50})	
			MOLT-3	8.1 μg/mL (ED_{50})	
			SUP-B15	7.2 μg/mL (ED_{50})	
Mariannaea elegans (*Spicaria elegans* [192]) *A. clavatus* [190] *A. rhizopodus* [90] *Hypoxylon terricola* [187]	Cytochalasin E [191,192]	Mixed biosynthetic origin	A-2780	0.02 μg/mL (IC_{100})	+ [185]
			HCT-116	1.0 μg/mL (IC_{100})	
			SW-620	0.2 μg/mL (IC_{100})	
			A-549	0.006 μM	
			P-388	0.09 μM	
A. striatus (*Emericella striata* [128]) *Cladorrhinum* sp.	Emestrin A [129]	NPR	HL-60	83.5 nM	+ [127]
A. striatus (*Emericella striata* [128]) *Cladorrhinum* sp.	Emestrin C [130]	NPR	DU-145	9.3 nM	
Penicillium sp. BCC 17468 [147]	Fudecadione A [147]	Terpene	MCF-7	12.6 μg/mL	−
			KB	22.3 μg/mL	
			NCI-H187	24.9 μg/mL	
A. fumigatus [208] *P. scabrosum* [209]	Fumagillin [210]	Mixed biosynthetic origin	Angiogenesis inhibitor	-	−
	TNP-470 [210–214]	Synthetic	PC-3	-	
			MDA-MB-231	-	
Penicillium sp. [215]	Linerin [215]	Mixed biosynthetic origin	POS1	117 nM	

Table 1. *Cont.*

Species (original published)	Compound	Type	Target cell	IC_{50}	Anti-fungal (+/−)
A. fumigatus [101,102] *A. fischeri* [103]	Fumitremorgin C [111,113,114]	NPR	P-388	3.9 μg/mL (ED_{50})	+ [224]
A. fumigatus [101,102] *A. fischeri* [103]	12,13-dehydroxyfumitremorgin C [112]	NPR	U-937	1.8 μM	
			PC-3	6.6 μM	
A. fumigatus [122] *D. cejpii* [123]	Gliotoxin [112,125,126]	NPR	MCF-7	985 nM	+ [124]
			T47D	365 nM	
			BT-474	102 nM	
			ZR75-1	158 nM	
			MDA MB231	38 nM	
			MDA MB435	87 nM	
			U-937	0.2 μM	
			PC-3	0.4 μM	
P. griseofulvum [225]	Griseofulvin [2–4,226,227]	Polyketide	HeLa	20 μM	+ [226,228]
			SCC-114	35 μM	
	GF-15 [5]	Synthetic	SCC-114	0.9 μM	
Hypocrella bambusae (*Shiraia bambusicola* [84,85])	Hypocrellin D [85]	Polyketide	Bel-7721	1.8 μg/mL	+ [229]
			A-549	8.8 μg/mL	
			Anip-973	38.4 μg/mL	
	Synthetic analog [86]	Synthetic	MCF-7 (PDT)	-	
Purpureocillium lilacinum[133] (*P. lilacinum* [132])	Leucinostatin A [132,135–138]	NPR	Ehrlich	1.6 mg/kg (LD_{50})	+ [132,134]
			L-1210	410.3 nM (IC_{100})	
			BT-20	2.3 nM	
			MCF-7	4 nM	
			G-361	7 nM	
			HT-144	6 nM	
			A-549	16 nM	
			A-427	59 nM	
			SK-MES-1	12 μM	
			Caov-3	17 nM	
			Caov-4	53 nM	
			SKOV-3	1,236 nM	
			HT-29	119 nM	
			LoVo	114 nM	
			HEp-2	40 nM	
			HL-60	12 nM	
			HSB-2	5 nM	
			K-562	6 nM	
			KG-1	46 nM	
			RPMI-1788	158 nM	
			SKW-6.4	6 nM	
			U-937	319 nM	
			Raji	11 nM	
A. parasiticus [65,66] *A. nidulans* [67,68]	Norsolorinic acid [67,68]	Polyketide	T-24	10.5 μM	−
			MCF-7	12.7 μM	
A. amoenus [115]	Notoamides [116,230]	NPR	HeLa/L-1210	22–52 μg/mL	−
Bipolaris sp.[169,170] *A. calidoustus* [69] *A. insuetus* [69] *A. keveii* [69] (*A. ustus* [171]) *Sarocladium oryzae* [173] (*Cephalosporium caerulens* [172]) *D. maydis* [174] *D. sorghicola* [174]	Ophiobolin A [175,176]	Terpene	A-549	0.1 μM	+ [180,181]
			HT-29	0.1 μM	
			Mel-20	0.1 μM	
			P-388	0.06 μM	
			OVCAR-3	0.3 μM	
Bipolaris oryzae [179]	3-anhydro-6-hydroxyophiobolin A [179]	Terpene	HepG2	6.5 μM	
			K-562	4.1 μM	
Aspergillus section *Usti* [69] (*A. ustus* [177])	Ophiobolin O [177,178]	Terpene	MFC-7	17.9 μM	
			P-388	4.7 μM	

Table 1. *Cont.*

Species (original published)	Compound	Type	Target cell	IC_{50}	Anti-fungal (+/−)
Talaromyces sp. (*Penicillium* sp.) [199]	Penicidone B [199]	Mixed biosynthetic origin	SW1116	54.2 μM	−
			K-562	21.1 μM	
			KB	29.6 μM	
			HeLa	35.2 μM	
Penicillium sp. [200] *Auxarthron reticulatum* [201]	Penicinoline [202]	Mixed biosynthetic origin	HepG2	13.2 μM	−
Penicillium sp. [200] *Auxarthron reticulatum* [201]	Methyl-penicinoline [202]	Mixed biosynthetic origin	HepG2	11.3 μM	
T. pinophilus [1] (*P. simplicissimum* [54])	Penisimplicissin [55]	Polyketide	HL-60	−6.7 (log10 GI_{50})	−
			CCRF-CEM	−5.8 (log10 GI_{50})	
Phaeosphaeria sp. [87]	Phaeosphaerin B [87]	Polyketide	PC-3	2.4 μM	−
			DU-145	9.5 μM	
			LNCaP	2.7 μM	
A. ustus [117]	Phenylahistin [118]	NPR	A-431	0.22 μM	−
			A-549	0.30 μM	
			HeLa	0.20 μM	
			K-562	0.19 μM	
			P-388	0.33 μM	
			MCF-7	3.7 μM	
			TE-671	0.18 μM	
A. taichungensis [79]	Prenylterphenyllin A [79]	Polyketide	A-549	8.3 μM	−
			HL-60	1.5 μM	
A. candidus [77,78]	4”-deoxyisoterprenin [78]	Polyketide	KB3-1	6.2 μM	
A. taichungensis [79]	Prenylcandidusin B [79]	Polyketide	P-388	1.6 μM	
Pseudeurotium ovalis [196] *A. fumigatus* [197]	Pseurotin D [198]	Mixed biosynthetic origin	MFC-7	15.6 μM	−
T. purpurogenus mutant BD-1-6 [1] (*P. purpurogenum* [216])	Purpurogemutantidin [216]	Mixed biosynthetic origin	K-562	0.9 μM	+ [217]
			HeLa	16.6 μM	
			BGC-823	31.0 μM	
			MCF-7	26.3 μM	
T. purpurogenus mutant BD-1-6 [1] (*P. purpurogenum* [216])	Macrophorin A [216]	Mixed biosynthetic origin	HL-60	0.9 μM	
A. parasiticus [231]	Sequoiamonascin A [231]	Polyketide	MCF-7	1%	−
			NCI-H460	1%	
			SF-268	2%	
				Percent cell growth compared to untreated cells at 10 μM	
P. solitum [20,25] (*P. brevicompactum* [18]) *P. hirsutum* [20] (*P. citrinum* [19])	Compactin [28]	Polyketide	AML	2.6 μM (IC_{100})	+ [18]

Table 1. *Cont.*

Species (original published)	Compound	Type	Target cell	IC_{50}	Anti-fungal (+/−)
A. terreus [26] *Monascus sp.*[27]	Lovastatin [29–32]	Polyketide	OVHS-1	39 μM	+ [22–24]
			Calu-1	3 μM	
			H-460	3 μM	
			A-549	10 μM	
			H-441	30 μM	
			Ovca-432	2 μM	
			A-2780	3 μM	
			Hey	3 μM	
			Ovca-429	5 μM	
			HOC-7	10 μM	
			DOV-13	11 μM	
			Skov-3	21 μM	
			A-2780-ADR	21 μM	
			A-2780-CIS	22 μM	
			MCF-7	1.7 μM	
			HepG2	2.7 μM	
			HeLa	1.5 μM	
			AML	-	
	Simvastatin [1,20,29,33,34]	Synthetic	DLRP	0.9 μM	+ [23,24]
			H-1299	1.3 μM	
			HT-144	1.0 μM	
			MI-14	0.8 μM	
			SK-MEL-28	0.8 μM	
			BT-474A	4.2 μM	
			SKBR-3	2.2 μM	
			MDA-MB-453	5.4 μM	
			BT-20	1.7 μM	
			AML	-	
A. ochraceus [106] *A. westerdijkiae* [107]	Stephacidin B [106]	NPR	PC-3	0.4 μM	−
			LNCaP	0.06 μM	
			A-2780	0.3 μM	
			A-2780/DDP	0.4 μM	
			A-2780/Tax	0.3 μM	
			HCT-116	0.5 μM	
			HCT-116/mdr+	0.5 μM	
			HCT-116/topo	0.4 μM	
			MCF-7	0.3 μM	
			SKBR-3	0.3 μM	
			LX-1	0.4 μM	
Taxomyces andreanea [140] *P. raistrickii* [141]	Taxol [139,142–145]	Terpene	Clinical use: Ovarian tumors Breast tumors Lung tumors Kaposi's sarcoma	-	+ [146]
A. terreus [148]	Terrecyclic acid A [148,149,232]	Terpene	NCI-H460	10.6 μM	+ [148]
			MCF-7	24.1 μM	
			SF-268	14.7 μM	
			P-388	63–125 mg/kg (LD_{50})	
A. terreus [37]	Terrein [38]	Polyketide	MCF-7	1.1 nM	+ [36]
			PANC-1	9.8 μM	
			HepG2	66.8 μM	
Fusarium spp. [151] *Isaria japonica* [157]	4-Acetyl-12,13-epoxy-9-trichothecene- 3,15-diol (AETD) [157]	Terpene	HL-60	10 nM	+ [154]
			U-937	22 nM	
			HeLa	45 nM	
			MCF-7	53 nM	
			Hep-G2	170 nM	
Fusarium spp. [151] *Myrothecium roridum* [158]	12'hydroxyroridin E [158]	Terpene	L-1210	0.2 μM	
			BC-1	0.9 μM	
			NCI-H187	1.5 μM	

Table 1. *Cont.*

Species (original published)	Compound	Type	Target cell	IC_{50}	Anti-fungal (+/−)
P. citrinum [80]	Tricitrinol B [80]	Polyketide	HL-60	3.2 μM	−
			HCT-116	4.8 μM	
			KB	3.9 μM	
A. fumigatus [104,105,108,109]	Ds2-tryprostatin B [108]	NPR	NCI-H-522	15.8 μM (GI_{50})	−
			MCF-7	15.9 μM (GI_{50})	
			PC-3	11.9 μM (GI_{50})	
A. fumigatus [104,105,108,109]	18-oxotryprostatin A [110]	NPR	A-549	1.3 μM	
A. fumigatus [104,105,108,109]	Spirotryprostatin E [109]	NPR	MOLT-4	3.1 μM	
			HL-60	2.3 μM	
			A-549	3.1 μM	
Penicillium sp. [150]	Unnamed chloro-trinoreremophilane sesquiterpene [150]	Terpene	HL-60	11.8 μM	−
			A-549	12.2 μM	
A. wentii [160]	Wentilactones [161]	Terpene	SMMC-7721	19 μM	+ [233]
T. wortmannii [1] (*P. wortmannii* [162]) Or similar species.	Wortmannin [163–168]	Terpene	HL-60	30 nM	+ [162]
			K-562	25 nM	
			KNS-62	100–200 nM	
			Colo-699	100–200 nM	
P. chrysogenum [1] *D. cejpii* [90] (*D. albus*[90])	Xanthocillin X [89,91,92]	NPR	Ehrlich ascites carcinoma-mouse strain	40 mg/kg (LD_{50})	+ [89]
			K-562	0.4 μg/mL	
			HeLa	1.2 μg/mL	
			MCF-7	12 μg/mL	
			HepG2	7 μg/mL	
			NCI-H460	10 μg/mL	
			Du-145	8 μg/mL	
			MDA-MB-231	8 μg/mL	
Aspergillus sp. [93]	BU-4704 [93]	NPR	HCT-116	0.6 μg/mL	
			B16-F10	4.3 μg/mL	
P. chrysogenum [1]	Xanthocillin X di-methoxy [94]	NPR	HepG2	0.2 μg/mL	
			MCF-7	0.4 μg/mL	
			KB	0.4 μg/mL	

6. Conclusions

In this article we have reviewed 50 compounds or compound families with anticancer and often also antifungal activities, primarily produced by *Aspergillus*, *Penicillium* and *Talaromyces*. Mycologists predict that less than 10% of all fungal species have been isolated so far, indicating a huge potential for further discovery of novel bioactive chemical scaffolds, if these fungi can be cultured in the laboratory. New strategies such as the application of epigenetic modifiers may help to uncover the full biosynthetic potential of fungi and other microorganisms. Development and improvement of screening methods and assays will further assist revealing new bioactivities of already known compounds. Additionally, ongoing progress in fast dereplication, including improvement of the performance of mass spectrometers and high resolution of UHPLC chromatograms, will ensure that database searches will lead to fewer possible candidates thereby advancing the drug discovery process. Altogether the future seems promising for discovery of many more bioactive small molecules to be used either as scaffolds for: (i) diversity oriented synthesis, or (ii) as a starting point for cloning and engineering of whole biosynthetic gene clusters towards novel engineered bioactive natural products.

Acknowledgments

We thank the Danish Cancer Society (grant number R-20-A1157-10-52) for their support.

Conflicts of Interest

The authors declare no conflict of interest.

References

1. Frisvad, J.C.; Smedsgaard, J.; Larsen, T.O.; Samson, R.A. Mycotoxins, drugs and other extrolites produced by species in *Penicillium* subgenus *Penicillium*. *Stud. Mycol.* **2004**, *49*, 201–241.
2. Panda, D.; Rathinasamy, K.; Santra, M.K.; Wilson, L. Kinetic suppression of microtubule dynamic instability by griseofulvin: implications for its possible use in the treatment of cancer. *Proc. Natl. Acad. Sci. USA* **2005**, *102*, 9878–9883.
3. Rebacz, B.; Larsen, T.O.; Clausen, M.H.; Rønnest, M.H.; Löffler, H.; Ho, A.D.; Krämer, A. Identification of griseofulvin as an inhibitor of centrosomal clustering in a phenotype-based screen. *Cancer Res.* **2007**, *67*, 6342–6350.
4. Ho, Y.-S.; Duh, J.-S.; Jeng, J.-H.; Wang, Y.-J.; Liang, Y.-C.; Lin, C.-H.; Tseng, C.-J.; Yu, C.-F.; Chen, R.-J.; Lin, J.-K. Griseofulvin potentiates antitumorigenesis effects of nocodazole through induction of apoptosis and G2/M cell cycle arrest in human colorectal cancer cells. *Int. J. Cancer* **2001**, *91*, 393–401.
5. Rønnest, M.H.; Rebacz, B.; Markworth, L.; Terp, A.H.; Larsen, T.O.; Krämer, A.; Clausen, M.H. Synthesis and structure-activity relationship of griseofulvin analogues as inhibitors of centrosomal clustering in cancer cells. *J. Med. Chem.* **2009**, *52*, 3342–3347.
6. Newman, D.J.; Cragg, G.M. Natural products as sources of new drugs over the 30 years from 1981 to 2010. *J. Nat. Prod.* **2012**, *75*, 311–335.
7. Hawksworth, D.L. Global species numbers of fungi: are tropical studies and molecular approaches contributing to a more robust estimate? *Biodivers. Conserv.* **2012**, *21*, 2425–2433.
8. Klejnstrup, M.L.; Frandsen, R.J.N.; Holm, D.K.; Nielsen, M.T.; Mortensen, U.H.; Larsen, T.O.; Nielsen, J.B. Genetics of polyketide metabolism in *Aspergillus nidulans*. *Metabolites* **2012**, *2*, 100–133.
9. Williams, R.B.; Henrikson, J.C.; Hoover, A.R.; Lee, A.E.; Cichewicz, R.H. Epigenetic remodeling of the fungal secondary metabolome. *Org. Biomol. Chem.* **2008**, *6*, 1895–1897.
10. Henrikson, J.C.; Hoover, A.R.; Joyner, P.M.; Cichewicz, R.H. A chemical epigenetics approach for engineering the in situ biosynthesis of a cryptic natural product from *Aspergillus niger*. *Org. Biomol. Chem.* **2009**, *7*, 435–438.
11. Laatsch, H. *AntiBase 2012*. Available online: http://eu.wiley.com/WileyCDA/WileyTitle/productCd-3527334068.html/ (accessed on 5 September 2013).
12. Nielsen, K.F.; Månsson, M.; Rank, C.; Frisvad, J.C.; Larsen, T.O. Dereplication of microbial natural products by LC-DAD-TOFMS. *J. Nat. Prod.* **2011**, *74*, 2338–2348.

13. Hansen, M.E.; Smedsgaard, J.; Larsen, T.O. X-hitting: an algorithm for novelty detection and dereplication by UV spectra of complex mixtures of natural products. *Anal. Chem.* **2005**, *77*, 6805–6817.
14. Larsen, T.O.; Petersen, B.O.; Duus, J.Ø.; Sørensen, D.; Frisvad, J.C.; Hansen, M.E. Discovery of new natural products by application of X-hitting, a novel algorithm for automated comparison of full UV spectra, combined with structural determination by NMR spectroscopy. *J. Nat. Prod.* **2005**, *68*, 871–874.
15. Wang, L.-W.; Zhang, Y.-L.; Lin, F.-C.; Hu, Y.-Z.; Zhang, C.-L. Natural products with antitumor activity from endophytic fungi. *Mini-Rev. Med. Chem.* **2011**, *11*, 1056–1074.
16. Kharwar, R.N.; Mishra, A.; Gond, S.K.; Stierle, A.; Stierle, D. Anticancer compounds derived from fungal endophytes: Their importance and future challenges. *Nat. Prod. Rep.* **2011**, *28*, 1208–1228.
17. Hawksworth, D.L.; Crous, P.W.; Redhead, S.A.; Reynolds, D.R.; Samson, R.A.; Seifert, K.A.; Taylor, J.W.; Wingfield, M.J.; Abaci, O.; Aime, C.; *et al.* The Amsterdam declaration on fungal nomenclature. *IMA Fungus* **2011**, *2*, 105–112.
18. Brown, A.G.; Smale, T.C.; King, T.J.; Hasenkamp, R.; Thompson, R.H. Crystal and molecular structure of compactin, a new antifungal metabolite from *Penicillium brevicompactum*. *J. Chem. Soc. Perk. T. 1* **1976**, *1976*, 1165–1173.
19. Endo, A.; Kuroda, M.; Tsujita, Y. ML-236B, and ML-236C, new inhibitors of cholesterogenesis produced by *Penicillium citrinum*. *J. Antibiot.* **1976**, *29*, 1346–1348.
20. Frisvad, J.C.; Filtenborg, O. Terverticillate penicillia: Chemotaxonomy and mycotoxin production. *Mycologia* **1989**, *81*, 837–861.
21. Wong, W.-L.; Dimitroulakos, J.; Minden, M.; Penn, L. HMG-CoA reductase inhibitors and the malignant cell: the statin family of drugs as triggers of tumor-specific apoptosis. *Leukemia* **2002**, *16*, 508–519.
22. Qiao, J.; Kontoyiannis, D.P.; Wan, Z.; Li, R.; Liu, W. Antifungal activity of statins against *Aspergillus* species. *Med. Mycol.* **2007**, *45*, 589–593.
23. Chamilos, G.; Lewis, R.E.; Dimitrios, P.; Kontoyiannis, D.P. Lovastatin has significant activity against zygomycetes and interacts synergistically with voriconazole. *Antimicrob. Agents Chemother.* **2006**, *50*, 96–103.
24. Macreadie, I.G.; Johnson, G.; Schlosser, T.; Macreadie, P.I. Growth inhibition of *Candida* species and *Aspergillus fumigatus* by statins. *FEMS Microbiol. Lett.* **2006**, *262*, 9–13.
25. Larsen, T.O.; Lange, L.; Schnorr, K.; Stender, S.; Frisvad, J.C. Solistatinol, a novel phenolic compactin analogue from *Penicillium solitum*. *Tetrahedron Lett.* **2007**, *48*, 1261–1264.
26. Alberts, A.W.; Chen, J.; Kuron, G.; Hunt, V.; Huff, J.; Hoffman, C.; Rothrock, J.; Lopez, M.; Joshua, H.; Harris, E.; *et al.* Mevinolin: A highly potent competitive inhibitor of hydroxymethylglutaryl-coenzyme A reductase and a cholesterol-lowering agent. *Proc. Natl. Acad. Sci. USA* **1980**, *77*, 3957–61.
27. Endo, A.; Monacolin, K. A new hypocholesterolemic agent produced by a *Monascus* speicies. *J. Antibiot.* **1979**, *32*, 852–854.

28. Sharma, S.; Hulcher, F.; Dodge, W. Effects of cholesterol synthesis inhibitor on the proliferation of avian granulocytic and monocytic progenitor cells and primary acute monocytic leukemia cells. *J. Nutr.* **1984**, *2*, 65–69.
29. Newman, A.; Clutterbuck, R.D.; Powles, R.L.; Catovsky, D.; Millar, J.L. A comparison of the effect of the 3-hydroxy-3-methylglutaryl coenzyme A (HMG-CoA) reductase inhibitors simvastatin, lovastatin and pravastatin on leukaemic and normal bone marrow progenitors. *Leukemia Lymphoma* **1997**, *24*, 533–537.
30. Maksimova, E.; Yie, T.-A.; Rom, W.N. *In vitro* mechanisms of lovastatin on lung cancer cell lines as a potential chemopreventive agent. *Lung* **2008**, *186*, 45–54.
31. Martirosyan, A.; Clendening, J.W.; Goard, C.A.; Penn, L.Z. Lovastatin induces apoptosis of ovarian cancer cells and synergizes with doxorubicin: potential therapeutic relevance. *BMC Cancer* **2010**, *10*, 103.
32. Mahmoud, A.M.; Al-Abd, A.M.; Lightfoot, D.A.; El-Shemy, H.A. Anti-cancer characteristics of mevinolin against three different solid tumor cell lines was not solely p53-dependent. *J. Enzym. Inhib. Med. Ch.* **2012**, *27*, 673–679.
33. Relja, B.; Meder, F.; Wilhelm, K.; Henrich, D.; Marzi, I.; Lehnert, M. Simvastatin inhibits cell growth and induces apoptosis and G0/G1 cell cycle arrest in hepatic cancer cells. *Int. J. Mol. Med.* **2010**, *26*, 735–741.
34. Glynn, S.A.; O'Sullivan, D.; Eustace, A.J.; Clynes, M.; O'Donovan, N. The 3-hydroxy-3-methylglutaryl-coenzyme A reductase inhibitors, simvastatin, lovastatin and mevastatin inhibit proliferation and invasion of melanoma cells. *BMC Cancer* **2008**, *8*, 9.
35. Osmak, M. Statins and cancer: Current and future prospects. *Cancer Lett.* **2012**, *324*, 1–12.
36. Ghisalberti, E.L.; Narbey, M.J.; Rowland, C.Y. Metabolites of *Aspergillus terreus* antagonistic towards the take-all fungus. *J. Nat. Prod.* **1990**, *53*, 520–522.
37. Raistrick, H.; Smith, G. LXXI. Studies in the biochemistry of micro-organisms. XLII. The metabolic products of *Aspergillus terreus* Thom. A new mould metabolic product-terrein. *Biochem. J.* **1935**, *29*, 606–611.
38. Liao, W.-Y.; Shen, C.-N.; Lin, L.-H.; Yang, Y.-L.; Han, H.-Y.; Chen, J.-W.; Kuo, S.-C.; Wu, S.-H.; Liaw, C.-C. Asperjinone, a nor-neolignan, and terrein, a suppressor of ABCG2-expressing breast cancer cells, from thermophilic *Aspergillus terreus*. *J. Nat. Prod.* **2012**, *75*, 630–635.
39. Härri, E.; Loeffler, W.; Sigg, H.P.; Stähelin, H.; Tamm, C. Über die isolierung neuer stoffwechselprodukte aus *Penicillium brefeldianum*. *Helv. Chim. Acta* **1963**, *46*, 1235–1246.
40. Betina, V.; Nemec, P.; Dobias, J.; Barath, Z. Cyanein, a new antibiotic from *Penicillium cyaneum*. *Folia Biol.* **1962**, *7*, 353–357.
41. Singleton, V.; Bohonos, N.; Ullstrup, A. Decumbin, a new compound from a species of *Penicillium*. *Nature* **1958**, *181*, 1072–1073.
42. Shao, R.G.; Shimizu, T.; Pommier, Y. Brefeldin A is a potent inducer of apoptosis in human cancer cells independently of p53. *Exp. Cell Res.* **1996**, *227*, 190–196.
43. Chapman, J.R.; Tazaki, H.; Mallouh, C.; Konno, S. Brefeldin A-induced apoptosis in prostatic cancer DU-145 cells: A possible p53-independent death pathway. *BJU Int.* **1999**, *83*, 703–708.

44. Wang, J.; Huang, Y.; Fang, M.; Zhang, Y.; Zheng, Z.; Zhao, Y.; Su, W. Brefeldin A, a cytotoxin produced by *Paecilomyces* sp. and *Aspergillus clavatus* isolated from *Taxus mairei* and *Torreya grandis*. *FEMS Imunol. Med. Mic.* **2002**, *34*, 51–57.
45. Chinworrungsee, M.; Wiyakrutta, S.; Sriubolmas, N.; Chuailua, P.; Suksamrarn, A. Cytotoxic activities of trichothecenes isolated from an endophytic fungus belonging to order Hypocreales. *Archi. Pharmacal Res.* **2008**, *31*, 611–616.
46. Argoudelia, A.D.; Zieserl, J.F. The structure of U-13,933, a new antibiotic. *Tetrahedron Lett.* **1966**, *7*, 1969–1973.
47. He, L.; Nan, M.-H.; Oh, H.C.; Kim, Y.H.; Jang, J.H.; Erikson, R.L.; Ahn, J.S.; Kim, B.Y. Asperlin induces G2/M arrest through ROS generation and ATM pathway in human cervical carcinoma cells. *Biochem. Bioph. Res. Co.* **2011**, *409*, 489–493.
48. Brian, P.W. Studies on the biological activity of griseofulvin. *Ann. Bot.* **1949**, *13*, 59–77.
49. Hector, R.F. An overview of antifungal drugs and their use for treatment of deep and superficial mycoses in animals. *Clin. Tech. Small Anim. Pract.* **2005**, *20*, 240–249.
50. Oxford, A.E.; Raistrick, H.; Simonart, P. XXIX. Studies in the biochemistry of microorganisms. LX. Griseofulvin, C17H17O6Cl, a metabolic product of *Penicillium griseofulvum* Dierckx. *Bioch. J.* **1939**, *33*, 240–248.
51. Grisham, L.M.; Wilson, L.; Bensch, K.G. Antimitotic action of griseofulvin does not involve disruption of microtubules. *Nature* **1973**, *224*, 294–296.
52. Stierle, D.B.; Stierle, A.A.; Bugni, T. Sequoiamonascins A–D: Novel anticancer metabolites isolated from a redwood endophyte. *J. Org. Chem.* **2003**, *68*, 4966–4969.
53. De Stefano, S.; Nicoletti, R.; Milone, A.; Zambardino, S. 3-O-Methylfunicone, a fungitoxic metabolite produced by the fungus *Penicillium pinophilum*. *Phytochemistry* **1999**, *52*, 1399–1401.
54. Stammati, A.; Nicoletti, R.; De Stefano, S.; Zampaglioni, F.; Zucco, F. Cytostatic properties of a novel compound derived from *Penicillium pinophilum*: An *in vitro* study. *Altern. Lab. Anim.* **2002**, *30*, 69–75.
55. Buommino, E.; Nicoletti, R.; Gaeta, G.M.; Orlando, M.; Ciavatta, M.L.; Baroni, A.; Tufano, M.A. 3-*O*-methylfunicone, a secondary metabolite produced by *Penicillium pinophilum*, induces growth arrest and apoptosis in HeLa cells. *Cell Proliferat.* **2004**, *37*, 413–426.
56. Buommino, E.; Boccellino, M.; de Filippis, A.; Petrazzuolo, M.; Cozza, V.; Nicoletti, R.; Ciavatta, M.L.; Quagliuolo, L.; Tufano, M.A. 3-*O*-methylfunicone produced by *Penicillium pinophilum* affects cell motility of breast cancer cells, downregulating avb5 integrin and inhibiting metalloproteinase-9 secretion. *Mol. Carcinogen.* **2007**, *46*, 930–940.
57. Baroni, A.; de Luca, A.; de Filippis, A.; Petrazzuolo, M.; Manente, L.; Nicoletti, R.; Tufano, M.A.; Buommino, E. 3-*O*-methylfunicone, a metabolite of *Penicillium pinophilum*, inhibits proliferation of human melanoma cells by causing G(2)+M arrest and inducing apoptosis. *Cell Proliferat.* **2009**, *42*, 541–553.
58. Buommino, E.; Tirino, V.; de Filippis, A.; Silvestri, F.; Nicoletti, R.; Ciavatta, M.L.; Pirozzi, G.; Tufano, M. A 3-*O*-methylfunicone, from *Penicillium pinophilum*, is a selective inhibitor of breast cancer stem cells. *Cell Proliferat.* **2011**, *44*, 401–409.

59. Komai, S.-I.; Hosoe, T.; Itabashi, T.; Nozawa, K.; Yaguchi, T.; Fukushima, K.; Kawai, K.-I. New vermistatin derivatives isolated from *Penicillium simplicissimum*. *Heterocycles* **2005**, *65*, 2771–2776.
60. Stierle, A.A.; Stierle, D.B.; Girtsman, T. Caspase-1 inhibitors from an extremophilic fungus that target specific leukemia cell lines. *J. Nat. Prod.* **2012**, *75*, 344–350.
61. Qin, J.-C.; Zhang, Y.-M.; Gao, J.-M.; Bai, M.-S.; Yang, S.-X.; Laatsch, H.; Zhang, A.-L. Bioactive metabolites produced by *Chaetomium globosum*, an endophytic fungus isolated from *Ginkgo biloba*. *Bioorgan. Med. Chem. Lett.* **2009**, *19*, 1572–1574.
62. Yamada, T.; Doi, M.; Shigeta, H.; Muroga, Y.; Hosoe, S.; Numata, A.; Tanaka, R. Absolute stereostructures of cytotoxic metabolites, chaetomugilins A–C, produced by a *Chaetomium* species separated from a marine fish. *Tetrahedron Lett.* **2008**, *49*, 4192–4195.
63. Yasuhide, M.; Yamada, T.; Numata, A.; Tanaka, R. Chaetomugilins, new selectively cytotoxic metabolites, produced by a marine fish-derived *Chaetomium* species. *J. Antibiot.* **2008**, *61*, 615–622.
64. Yamada, T.; Yasuhide, M.; Shigeta, H.; Numata, A.; Tanaka, R. Absolute stereostructures of chaetomugilins G and H produced by a marine-fish-derived *Chaetomium* species. *J. Antibiot.* **2009**, *62*, 353–357.
65. Muroga, Y.; Yamada, T.; Numata, A.; Tanaka, R. Chaetomugilins I–O, new potent cytotoxic metabolites from a marine-fish-derived *Chaetomium* species. Stereochemistry and biological activities. *Tetrahedron* **2009**, *65*, 7580–7586.
66. Muroga, Y.; Yamada, T.; Numata, A.; Tanaka, R. 11- and 4'-epimers of chaetomugilin A, novel cytostatic metabolites from marine fish-derived fungus *Chaetomium globosum*. *Helv. Chim. Acta* **2010**, *93*, 542–549.
67. Yamada, T.; Muroga, Y.; Jinno, M.; Kajimoto, T.; Usami, Y.; Numata, A.; Tanaka, R. New class azaphilone produced by a marine fish-derived *Chaetomium globosum*. The stereochemistry and biological activities. *Bioorgan. Med. Chem.* **2011**, *19*, 4106–4113.
68. Yamada, T.; Jinno, M.; Kikuchi, T.; Kajimoto, T.; Numata, A.; Tanaka, R. Three new azaphilones produced by a marine fish-derived *Chaetomium globosum*. *J. Antibiot.* **2012**, *65*, 413–417.
69. Chen, G.-D.; Li, Y.-J.; Gao, H.; Chen, Y.; Li, X.-X.; Li, J.; Guo, L.-D.; Cen, Y.-Z.; Yao, X.-S. New azaphilones and chlorinated phenolic glycosides from *Chaetomium elatum* with caspase-3 inhibitory activity. *Planta Med.* **2012**, *78*, 1683–1689.
70. Lee, L.; Bennett, J.W.; Goldblatt, L.A.; Lundin, R.E. Norsolorinic acid from a mutant strain of *Aspergillus parasiticus*. *J. Am. Oil Chemi. Soc.* **1971**, *48*, 93–94.
71. Bennett, J.W.; Lee, L.S.; Vinnett, C. The correlation of aflatoxin and norsolorinic acid production. *J. Am. Oil Chem. Soc.* **1971**, *48*, 368–370.
72. Wang, C.C.C.; Chiang, Y.-M.; Kuo, P.-L.; Chang, J.-K.; Hsu, Y.-L. Norsolorinic acid inhibits proliferation of T24 human bladder cancer cells by arresting the cell cycle at the G0/G1 phase and inducing a Fas/membrane-bound Fas ligand-mediated apoptotic pathway. *Clini. Exp. Pharmacol. P.* **2008**, *35*, 1301–1308.
73. Wang, C.C.C.; Chiang, Y.-M.; Kuo, P.-L.; Chang, J.-K.; Hsu, Y.-L. Norsolorinic acid from *Aspergillus nidulans* inhibits the proliferation of human breast adenocarcinoma MCF-7 cells via Fas-mediated pathway. *Basic Clin. Pharmacol.* **2008**, *102*, 491–497.

74. Samson, R.A.; Varga, J.; Meijer, M.; Frisvad, J.C. New taxa in *Aspergillus* section. *Usti*. *Stud. Mycol.* **2011**, *69*, 81–97.
75. Steyn, P.S.; Vleggaar, R. Austocystins. Six novel dihydrofuro (3',2':4,5)furo(3,2-b)xanthenones from *Aspergillus ustus*. *J. Chem. Soc. Perk. T. 1* **1974**, *1974*, 2250–2256.
76. Ireland, C.; Aalbersberg, W.; Andersen, R.; Ayral-Kaloustian, S.; Berlinck, R.; Bernan, V.; Carter, G.; Churchill, A.; Clardy, J.; Concepcion, G.; *et al.* Anticancer agents from unique natural products sources. *Pharm. Biol.* **2003**, *41*, 15–38.
77. Marks, K.M.; Park, E.S.; Arefolov, A.; Russo, K.; Ishihara, K.; Ring, J.E.; Clardy, J.; Clarke, A.S.; Pelish, H.E. The selectivity of austocystin D arises from cell-line-specific drug activation by cytochrome P450 enzymes. *J. Nat. Prod.* **2011**, *74*, 567–573.
78. Houbraken, J.; Frisvad, J.C.; Samson, R. A. Fleming's penicillin producing strain is not *Penicillium chrysogenum* but *P. rubens*. *IMA Fungus* **2011**, *2*, 87–95.
79. Houbraken, J.; Frisvad, J.C.; Seifert, K.A.; Overy, D.P.; Tuthill, D.M.; Valdez, J.G.; Samson, R.A. New penicillin-producing *Penicillium* species and an overview of section *Chrysogena*. *Persoonia* **2012**, *29*, 78–100.
80. Liu, W.; Gu, Q.; Zhu, W.; Cui, C.; Fan, G.; Zhu, T.; Liu, H.; Fang, Y. Chloctanspirones A and B, novel chlorinated polyketides with an unprecedented skeleton, from marine sediment derived fungus *Penicillium terrestre*. *Tetrahedron Lett.* **2005**, *46*, 4993–4996.
81. Li, D.; Chen, L.; Zhu, T.; Kurtán, T.; Mándi, A.; Zhao, Z.; Li, J.; Gu, Q. Chloctanspirones A and B, novel chlorinated polyketides with an unprecedented skeleton, from marine sediment derived fungus *Penicillium terrestre*. *Tetrahedron* **2011**, *67*, 7913–7918.
82. Takahashi, C.; Yoshihira, K.; Natori, S.; Umeda, M. The structures of toxic metabolites of *Aspergillus candidus*. I. The compounds A and E, cytotoxic *p*-terphenyls. *Chem. Pharm. Bull.* **1976**, *24*, 613–620.
83. Wei, H.; Inada, H.; Hayashi, A.; Higashimoto, K.; Pruksakorn, P.; Kamada, S.; Arai, M.; Ishida, S. Prenylterphenyllin and its dehydroxyl analogs, new cytotoxic substances from a marine-derived fungus *Aspergillus candidus* IF10. *J. Antibiot.* **2007**, *60*, 586–590.
84. Cai, S.; Sun, S.; Zhou, H.; Kong, X.; Zhu, T.; Li, D.; Gu, Q. Prenylated polyhydroxy-*p*-terphenyls from *Aspergillus taichungensis* ZHN-7-07. *J. Nat. Prod.* **2011**, *75*, 1106–1110.
85. Du, L.; Liu, H.-C.; Fu, W.; Li, D.-H.; Pan, Q.-M.; Zhu, T.-J.; Geng, M.-Y.; Gu, Q.-Q. Unprecedented citrinin trimer tricitinol B functions as a novel topoisomerase IIα inhibitor. *J. Med. Chem.* **2011**, *54*, 5796–5810.
86. Mulrooney, C.A.; O'Brien, E.M.; Morgan, B.J.; Kozlowski, M.C. Perylenequinones: Isolation, synthesis, and biological activity. *Eur. J. Org. Chem.* **2012**, *2012*, 3887–3904.
87. Kobayashi, E.; Ando, K.; Nakano, H.; Iida, T.; Ohno, H.; Morimoto, M.; Tamaoki, T. Calphostins (UCN-1028), novel and specific inhibitors of protein kinase C. I. Fermentation, isolation, physico-chemical properties and biological activities. *J. Antibiot.* **1989**, *42*, 1470–1474.
88. Zhu, D.M.; Narla, R.K.; Fang, W.H.; Chia, N.C.; Uckun, F.M. Calphostin C triggers calcium-dependent apoptosis in human acute lymphoblastic leukemia cells. *Clini. Cancer Res.* **1998**, *4*, 2967–2976.
89. Wu, H.; Lao, X.-F.; Wang, Q.-W.; Lu, R.-R. The shiraiachromes: novel fungal perylenequinone pigments from *Shiraia bambusicola*. *J. Nat. Prod.* **1989**, *52*, 948–951.

90. Fang, L.; Qing, C.; Shao, H.; Yang, Y.; Dong, Z.; Wang, F.; Zhao, W.; Yang, W.; Liu, J. Hypocrellin D, a cytotoxic fungal pigment from fruiting bodies of the ascomycete *Shiraia bambusicola*. *J. Antibiot.* **2006**, *59*, 351–354.
91. Zhang, Y.; Song, L.; Xie, J.; Qiu, H.; Gu, Y.; Zhao, J. Novel surfactant-like hypocrellin derivatives to achieve simultaneous drug delivery in blood plasma and cell uptake. *Photochem. Photobiol.* **2010**, *86*, 667–672.
92. Li, G.; Wang, H.; Zhu, R.; Sun, L.; Wang, L.; Li, M.; Li, Y.; Liu, Y.; Zhao, Z.; Lou, H. Phaeosphaerins A−F, cytotoxic perylenequinones from an endolichenic fungus, *Phaeosphaeria* sp. *J. Nat. Prod.* **2012**, *75*, 142–147.
93. Gao, X.; Chooi, Y.-H.; Ames, B.D.; Wang, P.; Walsh, C.T.; Tang, Y. Fungal indole alkaloid biosynthesis: Genetic and biochemical investigation of the tryptoquialanine pathway in *Penicillium aethiopicum*. *J. Am. Chem. Soc.* **2011**, *133*, 2729–2741.
94. Shang, Z.; Li, X.; Meng, L.; Li, C.; Gao, S.; Huang, C.; Wang, B. Chemical profile of the secondary metabolites produced by a deep-sea sediment-derived fungus *Penicillium commune* SD-118. *Chin. J. Oceanol. Limn.* **2012**, *30*, 305–314.
95. Varga, J.; Due, M.; Frisvad, J.C.; Samson, R.A. Taxonomic revision of *Aspergillus* section *Clavati* based on molecular, morphological and physiological data. *Stud. Mycol.* **2007**, *59*, 89–106.
96. Ando, K.; Suzuki, S.; Takatsuki, A.; Arima, K.; Tamura, G. A new antibiotic, 1-(*p*-hydroxyphenyl)-2,3-diisocyano-4-(*p*-methoxyphenyl)-buta-1,3-diene. I. Isolation and biological properties. *J. Antibiot.* **1968**, *21*, 582–586.
97. Kozlovskiĭ, A.G.; Zhelifonova, V.P.; Antipova, T.V; Adanin, V.M.; Novikova, N.D.; Deshevaia, E.A.; Schlegel, B.; Dahse, H.M.; Gollmick, F.A.; Grafe, U. *Penicillium expansum*, a resident fungal strain of the orbital complex Mir, producing xanthocillin X and questiomycin A. *Prikl. Biokhim. Mikrobiol.* **2004**, *40*, 344–349.
98. Tsunkawa, M.; Ohkusa, N.; Kobaru, S.; Narita, Y.; Mirate, S.; Sawada, Y.; Oki, T. BU-4704, a new member of the xanthocillin class. *J. Antibiot.* **1993**, *46*, 687–688.
99. Zhan, X.; Zhao, H.; Guan, Y.; Xiao, C.; He, Q. Mechanism of inhibiting proliferation by xanthocillin X dimethyl in tumor cells. *Zhongguo Xinyao Zazhi* **2010**, *19*, 832–836.
100. Clark, A.M.; Hufford, C.D.; Robertson, L.W. Two metabolites from *Aspergillus flavipes*. *Lloydia* **1977**, *40*, 146–151.
101. Frisvad, J.C.; Houbraken, J.; Popma, S.; Samson, R.A. Two new *Penicillium* species *Penicillium buchwaldii* and *Penicillium spathulatum*, producing the anticancer compound asperphenamate. *FEMS microbiol. Lett.* **2013**, *339*, 77–92.
102. Wu, P.-L.; Lin, F.-W.; Wu, T.-S.; Kuoh, C.-S.; Lee, K.-H.; Lee, S.-J. Cytotoxic and anti-HIV principles from the rhizomes of *Begonia nantoensis*. *Chem. Pharm. Bull.* **2004**, *52*, 345–349.
103. Yuan, L.; Wang, J.H.; Sun, T.M. Total synthesis and anticancer activity studies of the stereoisomers of asperphenamate and patriscabratine. *Chin. Chem. Lett.* **2010**, *21*, 155–158.
104. Li, Y.; Luo, Q.; Yuan, L.; Miao, C.; Mu, X.; Xiao, W.; Li, J.; Sun, T.; Ma, E. JNK-dependent Atg4 upregulation mediates asperphenamate derivative BBP-induced autophagy in MCF-7 cells. *Toxicol. Appl. Pharm.* **2012**, *263*, 21–31.
105. Borthwick, A.D. 2,5-Diketopiperazines: Synthesis, reactions, medicinal chemistry, and bioactive natural products. *Chem. Rev.* **2012**, *112*, 3641–3716.

106. Yamazaki, M.; Suzuki, S.; Miyaki, K. Tremorgenic toxins from *Aspergillus fumigatus* Fres. *Chem. Pharm. Bull.* **1971**, *19*, 1739–1740.
107. Abraham, W.-R.; Arfmann, H. 12,13-Dihydroxy-fumitremorgin C from *Aspergillus fumigatus*. *Phytochemistry* **1990**, *29*, 1025–1026.
108. Samson, R.A.; Hong, S.; Peterson, S.W.; Frisvad, J.C.; Varga, J. Polyphasic taxonomy of *Aspergillus* section *Fumigati* and its teleomorph *Neosartorya*. *Stud. Mycol.* **2007**, *59*, 147–203.
109. Cui, C.-B.; Kakeya, H.; Okada, G.; Onose, R.; Ubukata, M.; Takahashi, I.; Isono, K.; Osada, H. Tryprostatins A and B, novel mammalian cell cycle inhibitors produced by *Aspergillus fumigatus*. *J. Antibiot.* **1995**, *48*, 1382–1384.
110. Cui, C.; Kakeya, H.; Osada, H. Novel mammalian cell cycle inhibitors, spirotryprostatins A and B, produced by *Aspergillus fumigatus*, which inhibit mammalian cell cycle at G2/M phase. *Tetrahedron* **1996**, *52*, 12651–12666.
111. Qian-Cutrone, J.; Huang, S.; Shu, Y.-Z.; Vyas, D.; Fairchild, C.; Menendez, A.; Krampitz, K.; Dalterio, R.; Klohr, S.E.; Gao, Q. Stephacidin A and B: two structurally novel, selective inhibitors of the testosterone-dependent prostate LNCaP cells. *J. Am. Chem. Soc.* **2002**, *124*, 14556–14557.
112. Finefield, J.M.; Frisvad, J.C.; Sherman, D.H.; Williams, R.M. Fungal origins of the bicyclo[2.2.2]diazaoctane ring system of prenylated indole alkaloids. *J. Nat. Prod.* **2012**, *75*, 812–833.
113. Zhao, S.; Smith, K.S.; Deveau, A.M.; Dieckhaus, C.M.; Johnson, M.A.; Macdonald, T.L.; Cook, J.M. Biological activity of the tryprostatins and their diastereomers on human carcinoma cell lines. *J. Med. Chem.* **2002**, *45*, 1559–1562.
114. Wang, F.; Fang, Y.; Zhu, T.; Zhang, M.; Lin, A.; Gu, Q.; Zhu, W. Seven new prenylated indole diketopiperazine alkaloids from holothurian-derived fungus *Aspergillus fumigatus*. *Tetrahedron* **2008**, *64*, 7986–7991.
115. Zhang, M.; Wang, W.-L.; Fang, Y.-C.; Zhu, T.-J.; Gu, Q.-Q.; Zhu, W.-M. Cytotoxic alkaloids and antibiotic nordammarane triterpenoids from the marine-derived fungus *Aspergillus sydowi*. *J. Nat. Prod.* **2008**, *71*, 985–989.
116. Numata, A.; Takahashi, C.; Miyamoto, T.; Matsushita, T.; Kawai, K.; Usami, Y.; Matsumura, E.; Inoue, M.; Ohishi, H.; Shingu, T. Structures of cytotoxic substances and new quinazoline derivatives produced by a fungus from a saltwater fish. *Tennen Yuki Kagobutsu Toronkai Koen Yoshishu* **1991**, *33*, 723–730.
117. Wang, Y.; Li, Z.-L.; Bai, J.; Zhang, L.-M.; Wu, X.; Zhang, L.; Pei, Y.-H.; Jing, Y.-K.; Hua, H.-M. 2,5-diketopiperazines from the marine-derived fungus *Aspergillus fumigatus* YK-7. *Chem. Biodivers.* **2012**, *9*, 385–393.
118. Rabindran, S.K.; He, H.; Singh, M.; Brown, E.; Collins, K.I.; Annable, T.; Greenberger, L.M. Reversal of a novel multidrug resistance mechanism in human colon carcinoma cells by fumitremorgin C. *Cancer Res.* **1998**, *1998*, 5850–5858.
119. Rho, M.C.; Hayashi, M.; Fukami, A.; Obata, R.; Sunazuka, T.; Tomoda, H.; Komiyama, K.; Omura, S. Reversal of multidrug resistance by 7-*O*-benzoylpyripyropene A in multidrug-resistant tumor cells. *J. Antibiot.* **2000**, *53*, 1201–1206.

120. Jurjevic, Z.; Peterson, S.W.; Horn, B.W. *Aspergillus* section *Versicolores*: nine new species and multilocus DNA sequence based phylogeny. *IMA Fungus* **2012**, *3*, 59–79.
121. Kato, H.; Yoshida, T.; Tokue, T.; Nojiri, Y.; Hirota, H.; Ohta, T.; Williams, R.M.; Tsukamoto, S. Notoamides A–D: Prenylated indole alkaloids isolated from a marine-derived fungus, *Aspergillus* sp. *Angew. Chem. Int. Edit.* **2007**, *46*, 2254–2256.
122. Kanoh, K.; Kohno, S.; Asari, T.; Harada, T.; Katada, J.; Muramatsu, M.; Kawashima, H.; Sekiya, H.; Uno, I. (−)-phenylahistin: A new mammalian cell cycle inhibitor produced by *Aspergillus ustus*. *Bioorg. Med. Chem. Lett.* **1997**, *7*, 2847–2852.
123. Kanoh, K.; Kohno, S.; Katada, J.; Hayashi, Y.; Muramatsu, M.; Uno, I. Antitumor activity of phenylahistin *in vitro* and *in vivo*. *Biosci.* **1999**, *63*, 1130–1133.
124. Yamazaki, Y.; Tanaka, K.; Nicholson, B.; Deyanat-Yazdi, G.; Potts, B.; Yoshida, T.; Oda, A.; Kitagawa, T.; Orikasa, S.; Kiso, Y.; *et al.* Synthesis and structure−Activity relationship study of antimicrotubule agents phenylahistin derivatives with a didehydropiperazine-2,5-dione structure. *J. Med. Chem.* **2012**, *55*, 1056–1071.
125. Hayashi, Y.; Orikasa, S.; Tanaka, K.; Kanoh, K.; Kiso, Y. Total synthesis of anti-microtubule diketopiperazine derivatives: phenylahistin and aurantiamine. *J. Org. Chem.* **2000**, *65*, 8402–8405.
126. Larsen, T.O.; Frisvad, J.C.; Jensen, S.R. Aurantiamine, a diketopiperazine from two varieties of *Penicillium aurantiogriseum*. *Phytochemistry* **1992**, *31*, 1613–1615.
127. Menzel, A.O.; Wintersteiner, O.; Hoogerheide, J.O. The isolation of gliotoxin and fumigacin from culture filtrates of *Aspergillus fumigatus*. *J. Biol. Chem.* **1944**, *152*, 419–429.
128. Kaouadji, M. Gliotoxin: Uncommon 1H couplings and revised ^{1}H- and ^{13}C-NMR assignments. *J. Nat. Prod.* **1990**, *53*, 717–719.
129. Carberry, S.; Molloy, E.; Hammel, S.; O'Keeffe, G.; Jones, G.W.; Kavanagh, K.; Doyle, S. Gliotoxin effects on fungal growth: Mechanisms and exploitation. *Fungal Genet. Biol.* **2012**, *49*, 302–312.
130. Kidd, J.G. Effects of an antibiotic from *Aspergillus fumigatus* Fresenius on tumor cells *in vitro*, and its possible identity with gliotoxin. *Science* **1947**, *105*, 511–513.
131. Vigushin, D.M.; Mirsaidi, N.; Brooke, G.; Sun, C.; Pace, P.; Inman, L.; Moody, C.J.; Coombes, R.C. Gliotoxin is a dual inhibitor of farnesyltransferase and geranylgeranyltransferase I with antitumor activity against breast cancer *in vivo*. *Med. Mycol.* **2004**, *21*, 21–30.
132. Seya, H.; Nozawa, K.; Nakajima, S.; Kawai, K.-I.; Udagawa, S.-I. Studies on fungal products. Part 8. Isolation and structure of emestrin, a novel antifungal macrocyclic epidithiodioxopiperazine from *Emericeella striata*. X-Ray molecular structure of emestrin. *J. Chem. Soc. Perk. T. 1* **1986**, *1986*, 109–116.
133. Seya, H.; Nakajima, S.; Kawai, K.-I.; Udagawa, S.-I. Structure and absolute configuration of emestrin, a new macrocyclic epidithiodioxopiperazine from *Emericella striata*. *J. Chem. Soc. Chem. Comm.* **1985**, *739*, 657–658.
134. Ueno, Y.; Umemori, K.; Nilmi, E.; Tanuma, S.; Nagata, S.; Sugamata, M.; Ihara, T.; Sekljlma,, M.; Kawai, K.-I.; Ueno, I.; Takhiro, F. Induction of apoptosis by T-2 toxin and other natural toxins in HL-60 human promyelotic leukemia cells. *Nat. Toxins* **1995**, *3*, 129–137.

135. Onodera, H.; Hasegawa, A.; Tsumagari, N.; Nakai, R.; Ogawa, T.; Kanda, Y. MPC1001 and its analogues: New antitumor agents from the fungus *Cladorrhinum* species. *Org. Lett.* **2004**, *6*, 4101–4104.
136. Choi, E.J.; Park, J.-S.; Kim, Y.-J.; Jung, J.-H.; Lee, J.K.; Kwon, H.C.; Yang, H.O. Apoptosis-inducing effect of diketopiperazine disulfides produced by *Aspergillus* sp. KMD 901 isolated from marine sediment on HCT116 colon cancer cell lines. *J. Appl. Microbiol.* **2011**, *110*, 304–313.
137. Arai, T.; Mikami, Y.; Fukushima, K.; Utsumi, T.; Yazawa, K. A new antibiotic, leucinostatin, derived from *Penicillium lilacinum*. *J. Antibiot.* **1973**, *26*, 157–161.
138. Luangsa-Ard, J.; Houbraken, J.; van Doorn, T.; Hong, S.-B.; Borman, A.M.; Hywel-Jones, N.L.; Samson, R.A. *Purpureocillium*, a new genus for the medically important *Paecilomyces lilacinus*. *FEMS microbiol. Lett.* **2011**, *321*, 141–149.
139. Fukushima, K.; Arai, T.; Mori, Y.; Tsuboi, M.; Suzuki, M. Studies on peptide antibiotics, leucinostatins. I. Separation, physico- chemical properties and biological activities of leucinostatins A and B. *J. Antibiot.* **1983**, *36*, 1606–1612.
140. Strobel, G.A.; Torczynski, R.; Bollon, A. *Acremonium* sp.—A leucinostatin A producing endophyte of European yew (*Taxus baccata*). *Plant Sci.* **1997**, *128*, 97–108.
141. Ishiguro, K.; Arai, T. Action of the peptide antibiotic leucinostatin. *Antimicrobi. Agents Chemither.* **1976**, *9*, 893–898.
142. Kawada, M.; Inoue, H.; Ohba, S.-I.; Masuda, T.; Momose, I.; Ikeda, D. Leucinostatin A inhibits prostate cancer growth through reduction of insulin-like growth factor-I expression in prostate stromal cells. *Int. J. Cancer* **2010**, *126*, 810–818.
143. Strobel, G.A.; Hess, W.M. Glucosylation of the peptide leucinostatin A, produced by an endophytic fungus of European yew, may protect the host from leucinostatin toxicity. *Chem. Biol.* **1997**, *4*, 529–536.
144. Wani, M.C.; Taylor, L.H.; Wall, M.E.; Coggon, P.; McPhail, A.T. Plant antitumor agents. VI. The isolation and structure of taxol, a novel antileukemic and antitumor agent from *Taxus brevifolia*. *J. Am. Chem. Soc.* **1971**, *93*, 2325–2327.
145. Stierle, A.; Strobel, G.; Stierle, D. Taxol and taxane production by *Taxomyces andreanae*, an endophytic fungus of Pacific yew. *Science* **1993**, *260*, 214–216.
146. Niedens, B.R.; Parker, S.R.; Stierle, D.B.; Stierle, A.A. First fungal aromatic L-amino acid decarboxylase from a paclitaxel-producing *Penicillium raistrickii*. *Mycologia* **2013**, *91*, 619–626.
147. Kohler, D.R.; Goldspiel, B.R. Paclitaxel (taxol). *Pharmacotherapy* **1994**, *14*, 3–34.
148. Visalakchi, S.; Muthumary, J. Taxol (anticancer drug) producing endophytic fungi: An overview. *Int. J. Pharm. Bio Sci.* **2010**, *1*, 1–9.
149. Schiff, P.B.; Fant, J.; Horwitz, S.B. Promotion of microtubule assembly *in vitro* by taxol. *Nature* **1979**, *277*, 665–667.
150. Jordan, M.A.; Wilson, L. Microtubules as a target for anticancer drugs. *Nat. Rev. Cancer* **2004**, *4*, 253–265.
151. Young, D.H.; Michelotti, E.L.; Swindell, C.S.; Krauss, N.E. Antifungal properties of taxol and various analogues. *Experientia* **1992**, *48*, 882–885.

152. Pittayakhajonwut, P.; Dramae, A.; Intaraudom, C.; Boonyuen, N.; Nithithanasilp, S.; Rachtawee, P.; Laksanacharoen, P. Two new drimane sesquiterpenes, fudecadiones A and B, from the soil fungus *Penicillium* sp. BCC 17468. *Planta Med.* **2011**, *77*, 74–76.
153. Hirota, A.; Nakagawa, M.; Hirota, H.; Takahashi, T. Terrecylic acid A, a new antibiotic from *Aspergillus terreus* IV. Absolute stereochemistry of terrecyclic acid A. *J. Antibiot.* **1986**, *39*, 1–4.
154. Wijeratne, E.M.K.; Turbyville, T.J.; Zhang, Z.; Bigelow, D.; Pierson, L.S.; VanEtten, H.D.; Whitesell, L.; Canfield, L.M.; Gunatilaka, A.A.L. Cytotoxic constituents of *Aspergillus terreus* from the rhizosphere of *Opuntia versicolor* of the Sonoran desert. *J. Nat. Prod.* **2003**, *66*, 1567–1573.
155. Wu, G.; Lin, A.; Gu, Q.; Zhu, T.; Li, D. Four new chloro-eremophilane sesquiterpenes from an antarctic deep-sea derived fungus, *Penicillium* sp. PR19N-1. *Mar. Drugs* **2013**, *11*, 1399–1408.
156. Woloshuk, C.P.; Shim, W.-B. Aflatoxins, fumonisins, and trichothecenes: a convergence of knowledge. *FEMS Microbiol. Rev.* **2013**, *37*, 94–109.
157. Sudakin, D. Trichothecenes in the environment: relevance to human health. *Toxicol. Lett.* **2003**, *143*, 97–107.
158. Shifrin, V.I.; Anderson, P. Trichothecene mycotoxins trigger a ribotoxic stress response that activates c-Jun N-terminal kinase and p38 mitogen-activated protein kinase and induces apoptosis. *J. Biol. Chem.* **1999**, *274*, 13985–13992.
159. Campos, F.F.; Johann, S.; Cota, B.B.; Alves, T.M.A.; Rosa, L.H.; Caligiorne, R.B.; Cisalpino, P.S.; Rosa, C.A.; Zani, C.L. Antifungal activity of trichothecenes from *Fusarium* sp. against clinical isolates of *Paracoccidioides brasiliensis*. *Mycoses* **2011**, *54*, E122–E129.
160. Sun, T.; Zheng, W.; Peng, H.; Zhang, A.; Chen, Y.; Tan, R.; Shen, P. A small molecule IFB07188 inhibits proliferation of human cancer cells by inducing G2/M cell cycle arrest and apoptosis. *Biomedi. Pharmacother.* **2012**, *66*, 512–518.
161. Pae, H.O.; Oh, G.S.; Choi, B.M.; Seo, E.A.; Oh, H.; Shin, M.K.; Kim, T.H.; Kwon, T.O.; Chung, H.T. Induction of apoptosis by 4-acetyl-12,13-epoxyl-9-trichothecene-3,15-diol from *Isaria japonica* Yasuda through intracellular reactive oxygen species formation and caspase-3 activation in human leukemia HL-60 cells. *Toxicol. in Vitro* **2003**, *17*, 49–57.
162. OH, G.-S.; Hong, K.-H.; OH, H.; Pae, H.-O.; Kim, I.-K.; Kwon, T.-O.; Shin, M.-K.; Chung, H.-T. 4-Acetyl-12,13-epoxyl-9-trichothecene-3 ,15-diol isolated from the fruiting bodies of *Iaria japonica* YASUDA induces apoptosis of human leukemia cells (HL-60). *Biol. Pharm. Bull.* **2001**, *24*, 785–789.
163. Xu, J.; Takasaki, A.; Kobayashi, H.; Oda, T.; Yamada, J.; Mangindaan, R.E.P.; Ukai, K.; Nagai, H.; Namikoshi, M. Four new macrocyclic trichothecenes from two strains of marine-derived fungi of the genus *Myrothecium*. *J. Antibiot.* **2006**, *59*, 451–455.
164. Goodwin, W.; Haas, C.D.; Fabian, C.; Heller-Bettinger, I.; Hoogstraten, B. Phase I clinical evaluation of anguidine (diacetoxyscirpenol, NSC-141537). *Cancer* **1977**, *42*, 23–26.
165. Dornera, J.W.; Colea, R.J.; Springerb, J.P.; Coxc, R.H.; Cutlerd, H.; Wicklow, D.T. Isolation and identification of two new biologically active norditerpene dilactones from *Aspergillus wentii*. *Phytochemistry* **1980**, *19*, 1157–1161.
166. Zhang, Z.; Miao, L.; Sun, W.; Jiao, B.; Wang, B.; Yao, L.; Huang, C. Wentilactone B from *Aspergillus wentii* induces apoptosis and inhibits proliferation and migration of human hepatoma SMMC-7721 cells. *Bio. Pharm. Bull.* **2012**, *35*, 1964–1971.

167. Brian, P.W.; Curtis, P.J.; Hemming, H.G.; Norris, G.L.F. Wortmannin, an antibiotic produced by *Penicillium wortmanni*. *Trans. Br. Mycol. Soc.* **1957**, *40*, 365–368.
168. Nakamura, M.; Nakashima, S.; Katagiri, Y.; Ajozawa, Y. Effect of wortmannin and 2-(4-Morpholinyl)-8-phenyl-4*H*-1-benzopyran-4-one (LY294002) on *N*-formyl-methionyl-leucyl-phenylalanine-induced phospholipase D activation in differentiated HL60 Cells. *Biochem. Pharmacol.* **1997**, *53*, 1929–1936.
169. Wang, X.; Wu, Q.; Zhang, L.; Wu, Y.; Shu, Y. Wortmannin induced apoptosis of leukemia cells by reducing PI3K/Akt. *Chin. German J. Clin.Oncol.* **2010**, *9*, 734–738.
170. Yun, J.; Lv, Y.G.; Yao, Q.; Wang, L.; Li, Y.P.; Yi, J. Wortmannin inhibits proliferation and induces apoptosis of MCF-7 breast cancer cells. *Eur. J. Gynaecol. Oncol.* **2012**, *33*, 367–369.
171. Ng, S.S.W.; Tsao, M.; Chow, S.; Hedley, D.W. Inhibition of phosphatidylinositide 3-kinase enhances gemcitabine-induced apoptosis in human pancreatic cancer cells. *Cancer Res.* **2000**, *60*, 5451–5455.
172. Ng, S.S.W.; Tsao, M.; Nicklee, T.; Hedley, D.W. Wortmannin inhibits PKB/Akt phosphorylation and promotes gemcitabine antitumor activity in orthotopic human pancreatic cancer xenografts in immunodeficient mice. *Clini. Cancer Res.* **2001**, *7*, 3269–3275.
173. Boehle, A.S.; Kurdow, R.; Boenicke, L.; Schniewind, B.; Faendrich, F.; Dohrmann, P.; Kalthoff, H. Wortmannin inhibits growth of human non-small-cell lung cancer *in vitro* and *in vivo*. *Langenbeck Arch. Surg.* **2002**, *387*, 234–239.
174. Au, T.K.; Chick, W.S.; Leung, P.C. The biology of ophiobolins. *Life Sci.* **2000**, *67*, 733–742.
175. Ahn, J.-W.; Lee, M.-K.; Choi, S.-U.; Lee, C.-O.; Kim, B.-S. Cytotoxic ophiobolins produced by *Bipolaris* sp. *J. Microbiol. Biotechn.* **1998**, *8*, 406–408.
176. Singh, S.B.; Smith, J.L.; Sabnis, G.S.; Dombrowski, A.W.; Schaeffer, J.M.; Goetz, M.A.; Bills, G.F. Structure and conformation of ophiobolin K and 6- epiophiobolin K from *Aspergillus ustus* as a nematocidal agent. *Tetrahedron* **1991**, *47*, 6931–6938.
177. Nozoe, S.; Itai, A.; Tsuda, K.; Okuda, S. The chemical transformation of cephalonic acid. *Tetrahedron Lett.* **1967**, *42*, 4113–4117.
178. Bills, G.F.; Platas, G.; Gams, W. Conspecificity of the cerulenin and helvolic acid producing "Cephalosporium caerulens", and the hypocrealean fungus Sarocladium oryzae. *Mycolo. Res.* **2004**, *108*, 1291–1300.
179. Sugawara, F.; Strobel, G.; Strange, R.N.; Siedow, J.N.; Van Duyne, G.D.; Clardy, J. Phytotoxins from the pathogenic fungi *Drechslera maydis* and *Drechslera sorghicola*. *Proc. Natl. Acad. Sci. USA* **1987**, *84*, 3081–3085.
180. De Vries-van Leeuwen, I. J.; Kortekaas-Thijssen, C.; Mandouckou, J.A.N.; Kas, S.; Evidente, A.; de Boer, A.H. Fusicoccin—A selectively induces apoptosis in tumor cells after interferon-alpha priming. *Cancer Lett.* **2010**, *293*, 198–206.
181. Shen, X.; Krasnoff, S.B.; Lu, S.W.; Dunbar, C.D.; O'Neal, J.; Turgeon, B.G.; Yoder, O.C.; Gibson, D.M.; Hamann, M.T. Characterization of 6-epi-3-anhydroophiobolin B from *Cochliobolus heterostrophus*. *J. Nat. Prod.* **1999**, *62*, 895–897.
182. Yang, T.; Lu, Z.; Meng, L.; Wei, S.; Hong, K.; Zhu, W.; Huang, C. The novel agent ophiobolin O induces apoptosis and cell cycle arrest of MCF-7 cells through activation of MAPK signaling pathways. *Bioorgan. Med. Chem.* **2012**, *22*, 579–585.

183. Zhang, D.; Fukuzawa, S.; Satake, M.; Li, X.; Kuranaga, T.; Niitsu, A.; Yoshizawa, K.; Tachibana, K. Ophiobolin O and 6-epi-ophiobolin O, two new cytotoxic sesterterpenes from the marine derived fungus *Aspergillus* sp. *Nat. Prod. Commun.* **2012**, *7*, 1411–1414.
184. Wang, Q.-X.; Yang, J.-L.; Qi, Q.-Y.; Bao, L.; Yang, X.-L.; Liu, M.-M.; Huang, P.; Zhang, L.-X.; Chen, J.-L.; Cai, L.; *et al.* 3-Anhydro-6-hydroxy-ophiobolin A, a new sesterterpene inhibiting the growth of methicillin-resistant *Staphylococcus aureus* and inducing the cell death by apoptosis on K562, from the phytopathogenic fungus *Bipolaris oryzae*. *Bioorgan. Med. Chem. Lett.* **2013**, *23*, 3547–3550.
185. Li, E.; Clark, A.M.; Rotella, D.P.; Hufford, C.D. Microbial metabolites of ophiobolin A and antimicrobial evaluation of ophiobolins. *J. Nat. Prod.* **1995**, *58*, 74–81.
186. Krizsán, K.; Bencsik, O.; Nyilasi, I.; Galgóczy, L.; Vágvölgyi, C.; Papp, T. Effect of the sesterterpene-type metabolites, ophiobolins A and B, on zygomycetes fungi. *FEMS Microbiol. Lett.* **2010**, *313*, 135–140.
187. Geris, R.; Simpson, T.J. Meroterpenoids produced by fungi. *Nat. Prod. Rep.* **2009**, *26*, 1063–1094.
188. Schümann, J.; Hertweck, C. Molecular basis of cytochalasan biosynthesis in fungi: gene cluster analysis and evidence for the involvement of a PKS-NRPS hybrid synthase by RNA silencing. *J. Am. Chem. Soc.* **2007**, *129*, 9564–9565.
189. Sekita, S.; Yoshihira, K.; Natori, S.; Kuwano, H. Structures of chaetoglobosin A and B, cytotoxic metabolites of *Chaetomium globosum*. *Tetrahedron Lett.* **1973**, *14*, 2109–2112.
190. Fu, J.; Zhou, Y.; Li, H.; Ye, Y.; Guo, J. Antifungal metabolites from *Phomopsis* sp By254, an endophytic fungus in *Gossypium hirsutum*. *Afr. J. Microbiol. Res.* **2011**, *5*, 1231–1236.
191. Wicklow, D.T.; Rogers, K.D.; Dowd, P.F.; Gloer, J.B. Bioactive metabolites from *Stenocarpella maydis*, a stalk and ear rot pathogen of maize. *Fungal Biol.* **2011**, *115*, 133–142.
192. Frisvad, J.C.; Andersen, B.; Thrane, U. The use of secondary metabolite profiling in chemotaxonomy of filamentous fungi. *Mycol. Res.* **2008**, *112*, 231–240.
193. Cimmino, A.; Andolfi, A.; Berestetskiy, A.; Evidente, A. Production of phytotoxins by *Phoma exigua* var. *exigua*, a potential mycoherbicide against perennial thistles. *J. Agr. Food Chem.* **2008**, *56*, 6304–6309.
194. Xu, H.; Fang, W.-S.; Chen, X.-G.; He, W.-Y.; Cheng, K.-D. Cytochalasin D from *Hypocrella Bambusae*. *J. Asian Nat. Prod. Res.* **2001**, *3*, 151–155.
195. Demain, A.L.; Hunt, N.A.; Malik, V.; Kobbe, B.; Hawkins, H.; Matsuo, K.; Wogan, G.N. Improved procedure for production of cytochalasin E and tremorgenic mycotoxins by *Aspergillus clavatus*. *Appl. Environ. Microbiol.* **1976**, *31*, 138–140.
196. Wagenaar, M.M.; Corwin, J.; Strobel, G.; Clardy, J. Three new cytochalasins produced by an endophytic fungus in the genus *Rhinocladiella*. *J. Nat. Prod.* **2000**, *63*, 1692–1695.
197. Liu, R.; Gu, Q.; Zhu, W.; Cui, C.; Fan, G.; Fang, Y.; Zhu, T.; Liu, H. 10-Phenyl-[12]-cytochalasins Z7, Z8, and Z9 from the marine-derived fungus *Spicaria elegans*. *J. Nat. Prod.* **2006**, *69*, 871–875.
198. Thohinung, S.; Kanokmedhakul, S.; Kanokmedhakul, K.; Kukongviriyapan, V.; Tusskorn, O.; Soytong, K. Cytotoxic 10-(indol-3-yl)-[13]cytochalasans from the fungus *Chaetomium elatum* ChE01. *Arch. Pharm. Res.* **2010**, *33*, 1135–1141.

199. Ding, G.; Song, Y.C.; Chen, J.R.; Xu, C.; Ge, H.M.; Wang, X.T.; Tan, R.X. Chaetoglobosin U, a cytochalasan alkaloid from endophytic *Chaetomium globosum* IFB-E019. *J. Nat. Prod.* **2006**, *69*, 302–304.
200. Wang, Y.; Xu, L.; Ren, W.; Zhao, D.; Zhu, Y.; Wu, X. Bioactive metabolites from *Chaetomium globosum* L18, an endophytic fungus in the medicinal plant *Curcuma wenyujin*. *Phytomedicine* **2012**, *19*, 364–368.
201. Bloch, P.; Tamm, C.; Bollinger, P.; Petcher, T.J.; Weber, H.P. 13. Pseurotin, a new metabolite of *Pseudeurotium ovalis* Stolk having an unusual hetero-spirocyclic system. *Helv. Chim. Acta* **1976**, *59*, 133–137.
202. Wenke, J.; Anke, H.; Sterner, O. Pseurotin A and 8-*O*-demethylp-seurotin A from *Aspergillus fumigatus* and their inhibitory activities on chitin synthase. *Biosci. Biotechnol. Biochem.* **1993**, *57*, 961–964.
203. Martinez-Luis, S.; Cherigo, L.; Arnold, E.; Spadafore, C.; Gerwick, W.H.; Cubilla-Rios, L. Antiparasitic and anticancer constituentd of the endophytic fungus *Aspergillus* sp. strain F1544. *Nat. Prod. Commun.* **2012**, *7*, 165–168.
204. Ge, H.M.; Shen, Y.; Zhu, C.H.; Tan, S.H.; Ding, H.; Song, Y.C.; Tan, R.X. Penicidones A-C, three cytotoxic alkaloidal metabolites of an endophytic *Penicillium* sp. *Phytochemistry* **2008**, *69*, 571–576.
205. Shao, C.-L.; Wang, C.-Y.; Gu, Y.-C.; Wei, M.-Y.; Pan, J.-H.; Deng, D.-S.; She, Z.-G.; Lin, Y.-C. Penicinoline, a new pyrrolyl 4-quinolinone alkaloid with an unprecedented ring system from an endophytic fungus *Penicillium* sp. *Bioorg. Med. Chem. Lett.* **2010**, *20*, 3284–3286.
206. Elsebai, M.F.; Rempel, V.; Schnakenburg, G.; Kehraus, S.; Christa, E.M.; Gabriele, M.K. Identification of a potent and selective cannabinoid CB1 receptor antagonist from *Auxarthron reticulatum*. *ACS Med. Chem. Lett.* **2011**, *2*, 866–869.
207. Gao, H.; Zhang, L.; Zhu, T.; Gu, Q.; Li, D. Unusual pyrrolyl 4-quinolinone alkaloids from the marine-derived fungus *Penicillium* sp. ghq208. *Chem. Pharm. Bull.* **2012**, *60*, 1458–1460.
208. Frisvad, J.C.; Samson, R.A. Polyphasic taxonomy of *Penicillium* subgenus *Penicillium* A guide to identification of food and air-borne terverticillate Penicillia and their mycotoxins. *Stud. Mycol.* **2004**, *49*, 1–173.
209. Larsen, T.O.; Frisvad, J.C.; Ravn, G.; Skaaning, T. Mycotoxin production by *Penicillium expansum* on blackcurrant and cherry juice. *Food Addit. Contam.* **1998**, *15*, 671–675.
210. Dalsgaard, P.W.; Blunt, J.W.; Munro, M.H.G.; Frisvad, J.C.; Christophersen, C. Communesins G and H, new alkaloids from the psychrotolerant fungus *Penicillium rivulum*. *J. Nat. Prod.* **2005**, *68*, 258–261.
211. Numata, A.; Takahashi, C.; Ito, Y.; Takada, T.; Kawai, K.; Usami, Y.; Matsumura, E.; Imachia, M.; Ito, T.; Hasegawa, T. Communesins, cytotoxic metabolites of a fungus isolated from a marine alga. *Tetrahedron* **1993**, *34*, 2355–2358.
212. Jadulco, R.; Edrada, R.A.; Ebel, R.; Berg, A.; Schaumann, K.; Wray, V.; Steube, K.; Proksch, P. New communesin derivatives from the fungus *Penicillium* sp. derived from the Mediterranean sponge *Axinella verrucosa*. *J. Nat. Prod.* **2004**, *67*, 78–81.
213. Eble, T.E.; Hanson, F.R. Fumagillin, an antibiotic from *Aspergillus fumigatus* H-3. *Antibiot. Chemother.* **1951**, *1*, 54–58.

214. Frisvad, J.C.; Samson, R.A.; Stolk, A.C. A new species of *Penicillium*, *P. scabrosum*. *Persoonia* **1990**, *14*, 177–182.
215. Ingber, D.; Fujita, T.; Kishimoto, S.; Sudo, K.; Kanamaru, T.; Brem, H.; Folkman, J. Synthetic analogues of fumagillin that inhibit angiogenesis and suppress tumour growth. *Nature* **1990**, *348*, 555–557.
216. Kusaka, M.; Sudo, K.; Fujita, T.; Marui, S.; Itoh, F.; Ingber, D.; Folkman, J. Potent anti-angiogenic action of AGM-1470: comparison to the fumagillin parent. *Biochem. Bioph. Res. Co.* **1991**, *174*, 1070–1076.
217. Yamaoka, M.; Yamamoto, T.; Ikeyama, S.; Sudo, K.; Fujita, T. Angiogenesis inhibitor TNP-470 (AGM-1470) potently inhibits the tumor growth of hormone-independent human breast and prostate carcinoma cell lines. *Cancer Res.* **1993**, *51*, 5233–5236.
218. Kruger, E.A.; Figg, W.D. TNP-470: An angiogenesis inhibitor in clinical development for cancer. *Expert Opin. Inv. Drug* **2000**, *9*, 1383–1396.
219. Bhargava, P.; Marshall, J.L.; Rizvi, N.; Dahut, W.; Yoe, J.; Figuera, M.; Phipps, K.; Ong, V.S.; Kato, A.; Hawkins, M.J. A Phase I and pharmacokinetic study of TNP-470 administered weekly to patients with advanced cancer. *Clin. Cancer Res.* **1999**, *5*, 1989–1995.
220. Vansteelandt, M.; Blanchet, E.; Egorov, M.; Petit, F.; Toupet, L.; Bondon, A.; Monteau, F.; le Bizec, B.; Thomas, O.P.; Pouchus, Y.F.; *et al.* Ligerin, an antiproliferative chlorinated sesquiterpenoid from a marine-derived *Penicillium* strain. *J. Nat. Prod.* **2013**, *76*, 297–301.
221. Fang, S.-M.; Cui, C.-B.; Li, C.-W.; Wu, C.-J.; Zhang, Z.-J.; Li, L.; Huang, X.-J.; Ye, W.-C. Purpurogemutantin and purpurogemutantidin, new drimenyl cyclohexenone derivatives produced by a mutant obtained by diethyl sulfate mutagenesis of a marine-derived *Penicillium purpurogenum* G59. *Mar. Drugs* **2012**, *10*, 1266–1287.
222. Sassa, T.; Ishizaki, A.; Nukina, M.; Ikeda, M.; Sugiyama, T. Isolation and identification of new antifungal macrophorins E, F and G as malonyl meroterpenes from *Botryosphaeria berengeriana*. *Biosci. Biotechnol. Biochem.* **1998**, *62*, 2260–2262.
223. Cabedo, N.; López-Gresa, M.P.; Primo, J.; Ciavatta, M.L.; González-Mas, M.C. Isolation and structural elucidation of eight new related analogues of the mycotoxin (−)-botryodiplodin from *Penicillium coalescens*. *J. Agr. Food Chem.* **2007**, *55*, 6977–6983.
224. Fuska, J.; Proksa, B.; Uhrín, D. The antibiotic PSX-1 produced by *Penicillium stipitatum* is identical with botryodiplodin. *Folia Microbiol.* **1988**, *33*, 238–240.
225. Fuska, J.; Kuhr, I.; Nemec, P.; Fuskova, A. Antitumor antibiotics produced by *Penicillium stipitatum* THOM. *J. Antibiot.* **1973**, *27*, 123–127.
226. Omura, S.; Tomoda, H.; Kimura, K.; Zhen, D.-Z.; Kumagai, H.; Igarashi, K.; Imamura, N.; Takahashi, Y.; Tanaka, Y.; Iwai, Y. Atpenins, new antifungal antibiotics produced by *Penicillium* sp. *J. Antibiot.* **1988**, *41*, 1769–1773.
227. Kawada, M.; Momose, I.; Someno, T.; Tsujiuchi, G.; Ikeda, D. New atpenins, NBRI23477 A and B, inhibit the growth of human prostate cancer cells. *J. Antibiot.* **2009**, *62*, 243–246.
228. Boysen, M.; Skouboe, P.; Frisvad, J.; Rossenl, L. Reclassification of the *Penicillium roqueforti* group into three species on the basis of molecular genetic and biochemical profiles. *Microbiology* **1996**, *142*, 541–549.

229. Li, X.-J.; Zhang, Q.; Zhang, A.-L.; Gao, J.-M. Metabolites from *Aspergillus fumigatus*, an endophytic fungus associated with *Melia azedarach*, and their antifungal, antifeedant, and toxic activities. *J. Agr. Food Chem.* **2012**, *60*, 3424–3431.
230. Ma, G.; Khan, S.I.; Jacob, M.R.; Babu, L.; Li, Z.; Pasco, D.S.; Walker, L.A.; Khan, I.A.; Tekwani, B.L. Antimicrobial and antileishmanial activities of hypocrellins A and B. *Antimicrob. Agents Ch.* **2004**, *48*, 4450–4452.
231. Tsukamoto, S.; Kato, H.; Samizo, M.; Nojiri, Y.; Onuki, H.; Hirota, H.; Ohta, T. Notoamides F-K, prenylated indole alkaloids isolated from a marine-derived *Aspergillus* sp. *J. Nat. Prod.* **2008**, *71*, 2064–2067.
232. Nakagawa, M.; Hirota, A.; Sakai, H. Terrecyclic acid A, a new antibiotic from *Aspergillus terreus*. I. Taxonomy, production, and chemical and biological properties. *J. Antibiot.* **1982**, *35*, 778–782.
233. Sun, H.-F.; Li, X.-M.; Meng, L.; Cui, C.-M.; Gao, S.-S.; Li, C.-S.; Huang, C.-G.; Wang, B.-G. Asperolides A-C, tetranorlabdane diterpenoids from the marine alga-derived endophytic fungus *Aspergillus wentii* EN-48. *J. Nat. Prod.* **2012**, *75*, 148–152.

Tanja Thorskov Bladt
Chemical biology of microbial anticancer natural products - appendix

Paper *2*

Bio-Activity and Dereplication Based Discovery of Ophiobolins and Other Fungal Secondary Metabolites Targeting Chronic Lymphocytic Leukemia Cells

Bladt, T.T.; Dürr, C.; Knudsen, P.B.; Kildgaard, S.; Frisvad, J.C.; Gotfredsen, C.H.; Seiffert, M.; Larsen, T.O.

Molecules, **2013**, *18*, 14629-14650

Tanja Thorskov Bladt
Chemical biology of microbial anticancer natural products - appendix

Molecules **2013**, *18*, 14629-14650; doi:10.3390/molecules181214629

OPEN ACCESS

molecules

ISSN 1420-3049

www.mdpi.com/journal/molecules

Article

Bio-Activity and Dereplication-Based Discovery of Ophiobolins and Other Fungal Secondary Metabolites Targeting Leukemia Cells

Tanja Thorskov Bladt [1,†], Claudia Dürr [2,†], Peter Boldsen Knudsen [1], Sara Kildgaard [1], Jens Christian Frisvad [1], Charlotte Held Gotfredsen [3], Martina Seiffert [2,*] and Thomas Ostenfeld Larsen [1,*]

[1] Department of Systems Biology, Technical University of Denmark, Søltofts Plads, Building 221, Kgs. Lyngby DK-2800, Denmark; E-Mails: ttb@bio.dtu.dk (T.T.B.); pebok@bio.dtu.dk (P.B.K.); sarki@bio.dtu.dk (S.K.); jcf@bio.dtu.dk (J.C.F.)

[2] German Cancer Research Center, Molecular Genetics, Im Neuenheimer Feld 280, Heidelberg D-69120, Germany; E-Mail: C.Duerr@dkfz-heidelberg.de

[3] Department of Chemistry, Technical University of Denmark, Kemitorvet, Building 201, Kgs. Lyngby DK-2800, Denmark; E-Mail: chg@kemi.dtu.dk

† These authors contributed equally to this work.

* Authors to whom correspondence should be addressed; E-Mails: M.Seiffert@dkfz-heidelberg.de (M.S.); tol@bio.dtu.dk (T.O.L.); Tel.: +49-6221-42-4586 (M.S.); Fax: +49-6221-42-2995 (M.S.); Tel.: +45-4525-2632 (T.O.L.); Fax: +45-4588-4148 (T.O.L.).

Received: 12 October 2013; in revised form: 15 November 2013 / Accepted: 21 November 2013 / Published: 26 November 2013

Abstract: The purpose of this study was to identify and characterize fungal natural products (NPs) with *in vitro* bioactivity towards leukemia cells. We based our screening on a combined analytical and bio-guided approach of LC-DAD-HRMS dereplication, explorative solid-phase extraction (E-SPE), and a co-culture platform of CLL and stromal cells. A total of 289 fungal extracts were screened and we tracked the activity to single compounds in seven of the most active extracts. The novel ophiobolin U was isolated together with the known ophiobolins C, H, K as well as 6-epiophiobolins G, K and N from three fungal strains in the *Aspergillus* section *Usti*. Ophiobolins A, B, C and K displayed bioactivity towards leukemia cells with induction of apoptosis at nanomolar concentrations. The remaining ophiobolins were mainly inactive or only slightly active at micromolar

concentrations. Dereplication of those ophiobolin derivatives possessing different activity in combination with structural analysis allowed a correlation of the chemical structure and conformation with the extent of bioactivity, identifying the hydroxy group at C3 and an aldehyde at C21, as well as the A/B-*cis* ring structure, as indispensible for the strong activity of the ophiobolins. The known compounds penicillic acid, viridicatumtoxin, calbistrin A, brefeldin A, emestrin A, and neosolaniol monoacetate were identified from the extracts and also found generally cytotoxic.

Keywords: natural products; ophiobolin U; dereplication; explorative solid phase extraction (E-SPE); filamentous fungi; cytotoxic; cancer; leukemia

1. Introduction

Screening and discovery of compounds that act against chronic lymphocytic leukemia (CLL) cells are crucial since CLL is considered as an incurable disease and currently applied treatment strategies primarily aim at prolonging patient survival [1,2]. Filamentous fungi have proven to be an incredible source of diverse bioactive compounds. The continuous improvements of analytical instruments and new approaches for fast dereplication have resulted in an increased interest in natural products discovery [3–5]. CLL is the most common type of leukemia among adults in the Western World. Even though most patients initially show a good response to therapy, relapse of disease is very frequent, with a subsequent increase in chemoresistance [6]. Consequently, there is a great need for discovery and development of new agents. Treatment strategies used today are based on small-molecule alkylating agents such as chlorambucil and fludarabine. These agents are often used in combination with monoclonal antibodies, or more recently inhibitors that target essential signaling pathways in CLL [7,8]. In contrast to other cancer cells, the majority of CLL cells is non-proliferating, arrested in G_0/G_1 phase of the cell cycle and accumulates in the patients due to apoptosis resistance [1]. *In vivo*, CLL cells are associated with a survival-inducing microenvironment of stromal cells, non-malignant leukocytes, so-called nurse-like cells, as well as growth and differentiation factors [9,10]. Removed from their natural microenvironment, the CLL cells rapidly undergo apoptosis *in vitro*, even though they are long-living cells *in vivo* [11]. However, viability of CLL cells can be maintained *in vitro* by co-cultivation with stromal cells, for example the bone marrow-derived cell line HS-5 [12,13]. Such co-cultures mimic the microenvironment of CLL cells *in vivo*, they are ideally suited for screening of natural products (NPs) [14]. We have already demonstrated that fungal NPs are a proper source for discovering compounds with activity towards CLL cells *in vitro*. This was done by identification of chaetoglobosin A from *P. aquamarinum*. Chaetoglobosin A induced apoptosis in CLL cells more selectively compared to healthy cells with a median lethal dose (LC_{50}) of 2.8 μM [15].

Novel secondary metabolites produced by filamentous fungi such as *Penicillium* and *Aspergillus* are being discovered continuously [4,16]. With the increase in target-based specific biological assays, previously described compounds might display novel bioactivities [17,18], justifying their presence in novel screening efforts. Testing all known as well as novel NPs against all disease targets is an impracticable approach, why setting up a suitable strategy is essential to any screening program [19].

Targeted screening strategies in NPs-based drug discovery rely on identifying compounds targeting a specific disease or biological mechanism. In such screening campaigns, the selection of fungi is essential and needs to represent as wide a biodiversity as possible, with the hope of an equally high chemodiversity [19]. One strategy to increase chemodiversity for rapid bio-testing is to select strains representing a wide variety of species with a limited number of strains from each species [19,20]. The spectrum of compounds produced by the individual strains can further be diversified or maximized by the 'one strain-many compounds' (OSMAC) approach, through variation of culture conditions [16].

Dereplication is the tentative identification of known NPs in complex mixtures, before unnecessary time is spent on isolating already known compounds. One dereplication approach is based on liquid chromatography-diode array detection-high resolution mass spectrometry (LC-DAD-HRMS) and database searching, which ensures a high throughput and reproducibility [3]. Subsequent to dereplication a separation strategy for preparative isolation of NPs is necessary. Here a small scale preliminary chemical characterization focusing on identification of functional groups is helpful. Co-eluting interferences often experienced in traditional reverse phase (RP) chromatography can be reduced or even completely removed by choosing orthogonal purifications strategies [21]. One approach for prefractionation is explorative solid-phase-extraction (E-SPE) [21] that relies on ion-exchanger columns such as strong anion-exchanger (SAX), mixed mode anion-exchanger (MAX), and strong cation-exchanger (SCX). This method has proven to be very powerful for separating fungal NPs due to the relative high percentages of ionizable functional groups [21].

In this current paper we describe our screening efforts of discovering fungal NPs with bio-activity in a co-culture platform of chronic lymphocytic leukemia (CLL) cells and stromal cells and their retesting in CLL cells cultures in conditioned media of stromal cells [12]. The fungal NPs were tentatively identified by LC-DAD-HRMS based dereplication and extracts were fractionated in order to assign the activity to single compounds [3]. Confidence in this identification was improved by using an E-SPE strategy based on an array of orthogonal separation techniques [19,21]. Thereby among others, ophiobolins were identified and further structural studies were performed by dereplicating different ophiobolin dervatives leading to the identification of chemical moieties and conformations that are indispensable for strong bioactivity. Ophiobolins lacking these moieties possessed either low or no bioactivity.

2. Results and Discussion

A total of 289 fungal extracts were prepared from cultivation of 137 fungal strains (Figure 1 and Table S1) on a selection of solid media at variable temperatures in accordance with the OSMAC approach [16]. The extracts were prepared by the micro-extraction method developed by Smedsgaard [22]. To obtain a representative sample of the fungal colonies the plugs were taken across the colony. Sixty one (61) extracts showed activity towards CLL cells (Table S2). Seven of the candidates that displayed the highest level of activity (Figure 1) were selected for further bio-testing. Large-scale extracts were prepared from incubation on the media supporting the highest level of bioactivity, and the extracts were prefractionated before further testing.

Figure 1. Screening set-up. Two hundred and eighty nine (289) fungal extracts (from 137 fungal strains) were tested for cell death-inducing activity for CLL cells but not for stromal cells. From the 61 active extracts the seven candidates that displayed the highest bio-assay activity were selected for single compound isolation in a large scale and further bio testing.

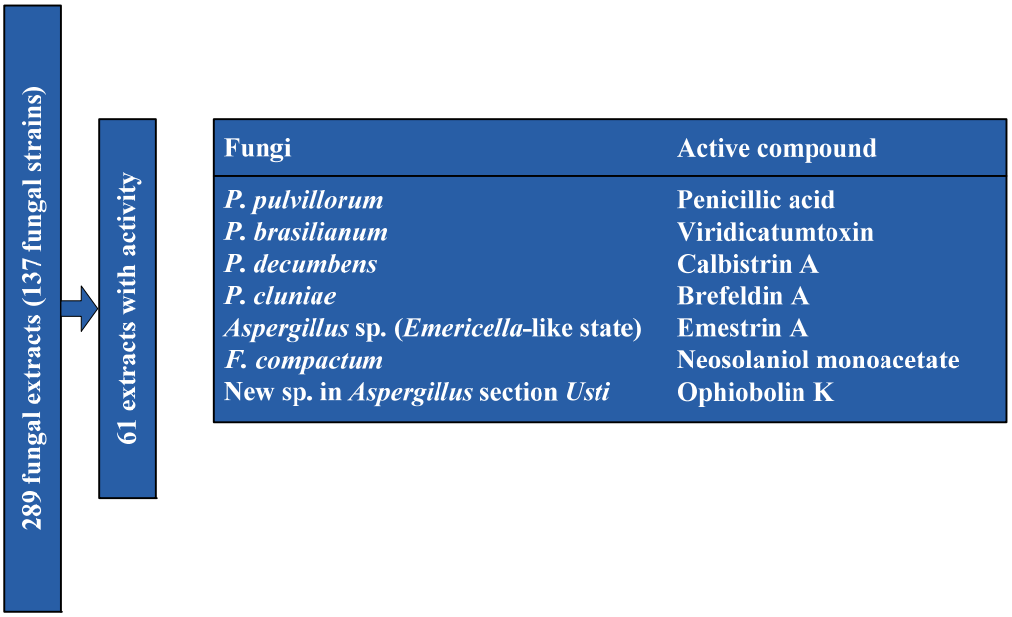

2.1. MS Based Dereplication of Penicillium pulvillorum Extract

The extract of *P. pulvillorum* (IBT 22393) was among the candidates that displayed the highest level of activity (≈1.25 µg/mL). The first five flash fractions (ranging from 15%–40% organic) were tested active against CLL cells *in vitro*. LC-DAD-HRMS revealed one major component shared between these fractions, with an elementary composition of $C_8H_{10}O_4$ (−0.7 ppm mass accuracy) (Figure 2). AntiBase2012 [23] revealed penicillic acid as a likely candidate responsible for the observed activity. The tentative identification of penicillic acid was confirmed by comparison of the retention time to a standard from our in-house metabolite database (1,559 standards) as well as comparison of ^{1}H- and ^{13}C-NMR chemical shifts to the literature data [24].

Figure 2. Dereplication of penicillic acid from *P. pulvillorum* mass spectrum of penicillic acid [23]. The mass spectrum shows a widespread adduct pattern that besides $[M+H]^+$ contains ions that corresponds to neutral loss of water $[M+H-H_2O]^+$ and the sodiated adduct $[M+Na]^+$, as well as the corresponding dimeric ions $[2M+H]^+$, $[2M+H-H_2O]^+$, and $[2M+Na]^+$.

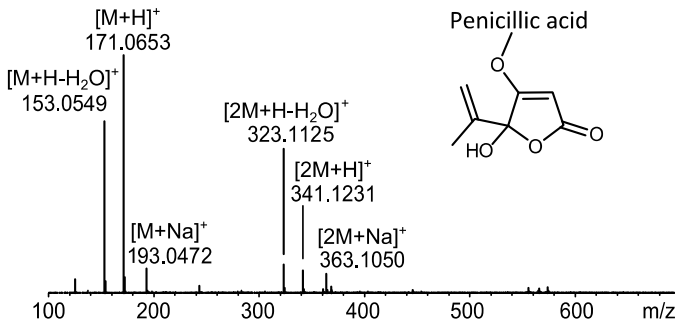

To verify the observed anti-leukemic activity in the extract, penicillic acid was purified and tested on CLL cells, resulting in induced cell death in both CLL and stromal (HS-5) cells. No further work on this extract was done as penicillic acid is regarded as a generally cytotoxic compound [24].

2.2. Comparative Dereplication Based on Explorative Solid Phase Extraction (E-SPE)

The E-SPE strategy was applied to a series of highly complex extracts, *i.e.*, *P. brasilianum* (IBT 22244), *P. decumbens* (IBT 11843), *P. cluniae* (IBT 21051), *Aspergillus* sp. (*Emericella*-like state) (IBT 22838), and *Fusarium compactum* (IBT 9034). The extract of *P. brasilianum* (IBT 22244) was very potent against CLL cells *in vitro* (≈5 ng/mL) with the active compound retained on both anion-exchangers (SAX and MAX) as well as the two normal-phase columns (diol and amino), while unretained on the cation-exchanger (SCX). The combined biological and chromatographic information lead to the conclusion that the bioactive compound contained a strong anion. The large scale extract was fractionated on a SAX column. Comparison of chromatographic peaks from the fraction that contained neutral/basic compounds (Figure 3a) and the fraction with acidic compounds (Figure 3b), showed that the anion-exchange was extremely selective, removing the majority of inactive compounds from the extract.

Figure 3. E-SPE strategy based on a SAX column to separate co-eluting compounds in the crude extract of *P. brasilianum*. (**a**) UHPLC chromatograms of the SAX fraction that contained neutral/basic compounds. The ion trace of compound I (*m/z* 462.2387) is marked with red; (**b**) UHPLC chromatogram of the SAX fraction that contained acidic compounds. The ion trace of compound IV (*m/z* 548.1916) is marked with blue; (**c**) In the crude extract compound I and IV were co-eluting on a RP C_{18} column.

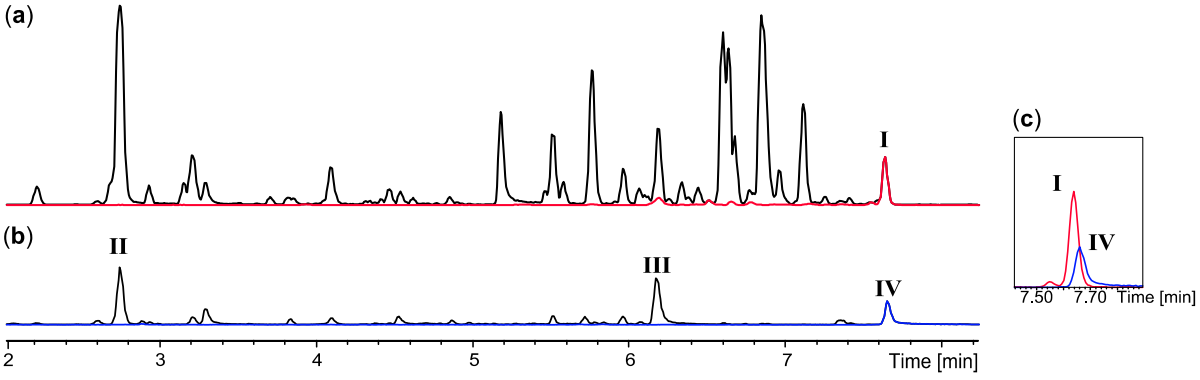

In the initial extract, the two compounds **I** and **IV** co-eluted on a C_{18} RP column (Figure 3c). These were easily and quantitatively separated on the SAX column due to the difference in charged functionalities. Only three major acidic compounds were left in the bioactive fraction (Figures 3b and 4a), significantly simplifying the subsequent dereplication and purification process. Based on comparative HRMS analysis, compound **II** was immediately eliminated due to its presence in the inactive neutral/basic fraction. The molecular formula of compounds **III** and **IV** were established as $C_{15}H_{10}O_9$ (−0.7 ppm) and $C_{30}H_{31}NO_{10}$ (−0.2 ppm), respectively. These were used as queries in AntiBase2012 (Figure 4b) [23]. Compound **II** had no hits in AntiBase2012 that contained a strong anion, thus likely being a novel compound or novel analogue of a known compound. Compound **IV** had two hits in

AntiBase2012. One of the candidates had no strong anion and was consequently eliminated, which left viridicatumtoxin as the only candidate (Figure 4b).

Figure 4. Dereplication of the *P. brasilianum extract* (**a**) UHPLC chromatogram of the active SAX fraction that contained the acidic compounds as well as UV and MS spectra of the potential candidates; (**b**) Hits in Antibase2012.

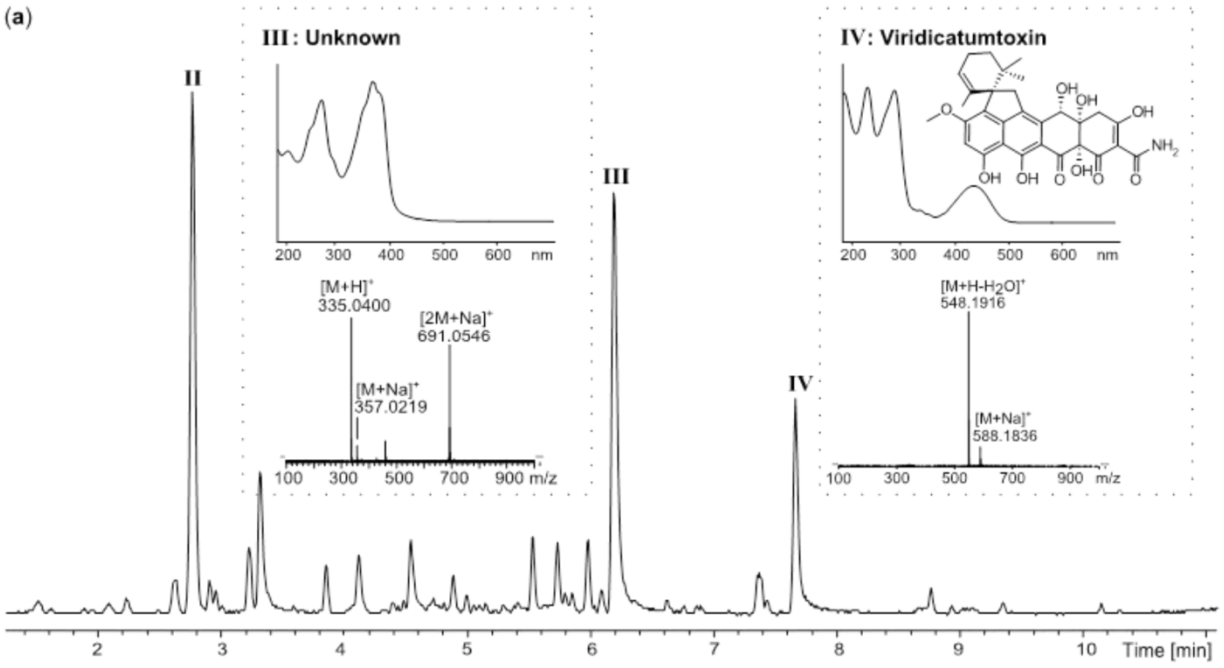

(**b**)

III: Unknown			**IV: Viridicatumtoxin**	
Query	No. of candidates		Query	No. of candidates
$C_{15}H_{10}O_9$	1		$C_{30}H_{31}NO_{10}$	2
Strong anion	0		Strong anion	1

The identity of viridicatumtoxin as compound **IV** was confirmed: (1) by comparison to the retention time and UV spectrum of an in-house standard; (2) by the fact that it held a strong anion; and (3) by having similar ^{1}H-NMR chemical shifts as published for viridicatumtoxin [25]. Viridicatumtoxin was isolated as one of the most cytotoxic compounds tested towards CLL cells in this screening campaign with a median lethal concentrations (LC_{50}) value between 0.7 and 3.5 nM. Further testing revealed that the activity was not specific, as both CLL and stromal cells were targeted.

One flash fraction (70% organic) from the *P. decumbens* (IBT 11843) extract was found active towards CLL cells (≈200 ng/mL). Further E-SPE analysis showed that the active compound was retained on SAX and MAX columns indicating the presence of a strong anion. By comparative dereplication tentative identifications of calbistrin A (Figure 5a) and B as well as their precursor (or decomposition product) versiol (Figure 5c) were established within the fraction. The MS based dereplication was complicated by the fact that the $[M+H]^+$ ion was absent in the mass spectra of calbistrin A and B. The presences of strong adduct- and fragmentation patterns consisting of the sodiated, $[M+Na]^+$, and the ammoniated, $[M+NH_4]^+$, adducts as well as neutral loss of one and two

water molecules assisted the establishment of the monoisotopic masses and hereby the molecular formulas of calbistrin A and B. The identity of calbistrin A was confirmed by the presence of a carboxylic acid and by comparison of retention time and UV spectrum to an in-house standard. The tentative identity of calbistrin B was confirmed by comparison of the UV spectrum to that of calbistrin A (Figure 5a). Testing of calbistrin A from our in-house metabolite collection showed general cytotoxic activity towards CLL and healthy cells. Comparative experiments with calbistrin C (Figure 5b) from the metabolite collection did not induce cell death, indicating that the pharmacophore is located in the versiol part (Figure 5c) of the molecule.

Figure 5. Structure of (**a**) Calbistrin A, (**b**) Calbistrin C, and (**c**) Versiol.

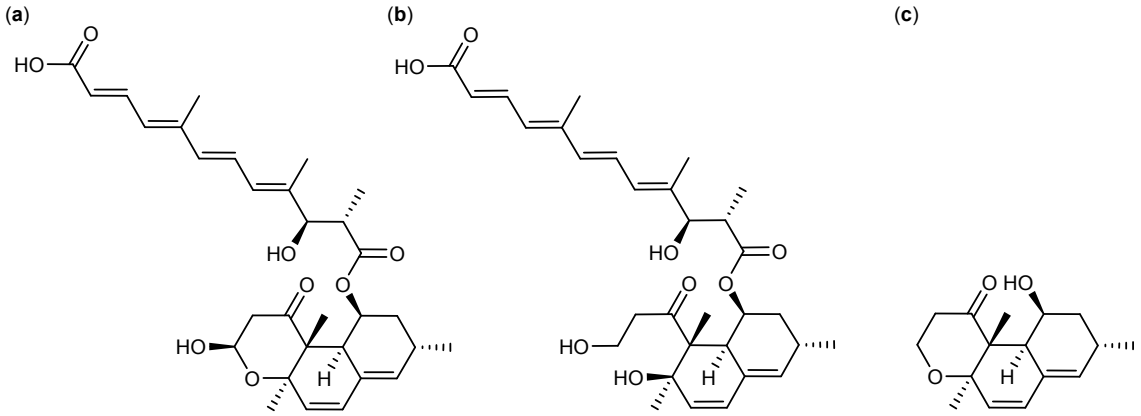

A bioactive flash fraction (activity approx. 100 ng/mL) from a *Penicillium cluniae* (IBT 21051) extract was likewise subjected to E-SPE. Here, the bioactivity profiled revealed that the active compound was a medium to apolar compound with no charged functionalities. By comparative dereplication, the active compound was tentatively identified as brefeldin A (Figure 6a), which was in accordance with the profile revealed by E-SPE. The identity of brefeldin A was confirmed by its retention time and UV spectrum compared to an in-house standard. Brefeldin A is a known anticancer compound [5,26] and commercially available, thus the activity was easily confirmed in the CLL assay. The compound displayed general cytotoxic activity for CLL cells (0.39–1.56 μM) and stromal cells.

Figure 6. Examples of E-SPE and comparative dereplication (**a**) Brefeldin produced by *P. cluniae*, (**b**) Emestrin A produced by *Aspergillus* sp. (*Emericella*-like state), and (**c**) Neosolaniol monoacetate produced by *F. compactum*.

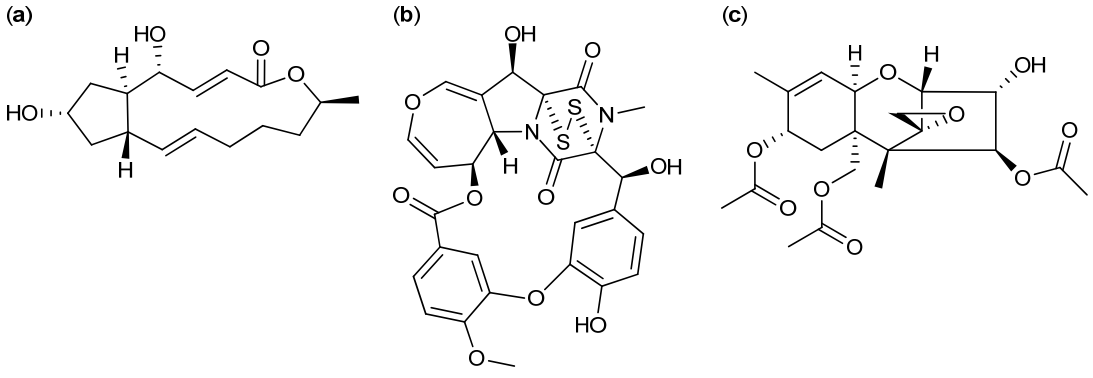

The E-SPE strategy of the bioactive extract (≈40 ng/mL) from *Aspergillus* sp. (*Emericella*-like state, IBT 22838) resulted in retention of the bioactive compound on the amino normal phase SPE column. Fast comparative dereplication based on UV spectra and retention times of in-house standards as well as comparison of ^{1}H-NMR chemical shifts [27] led to an identification of the known antifungal and anticancer compound, emestrin A (Figure 6b) [5,28,29]. The pure emestrin A isolated form the active fractions showed cytotoxic activity towards CLL cells and stromal cells at the same concentration levels. Accordingly, emestrin A is regarded as a generally cytotoxic compound with no therapeutic window [30]. No further work was pursued on the *Aspergillus* sp. (*Emericella*-like state) extract.

The last example of bio-guided isolation based on E-SPE is demonstrated by the *F. compactum* (IBT 9034) extract with an activity at approximately 200 ng/mL. The bioactive compound from *F. compactum* was retained on both the diol and amino columns in the E-SPE pre-fractionation experiment. Comparative dereplication revealed only one candidate that might be responsible for the activity. The compound was tentatively identified as the known trichothecene, neosolaniol monoacetate (Figure 6c). The compound was isolated and the ^{1}H-NMR data was compared to the literature for final identification of neosolaniol monoacetate [31]. Neosolaniol monoacetate was tested in the CLL assay and found as a generally cytotoxic why no further work was performed on the *F. compactum* extract. The E-SPE approach with the optimized collection of ion-exchangers and normal phase SPE columns has turned out to be a good combination to evaluate and follow bioactivity of fungal extracts.

2.3. Biological Structure-Activity Relationship of Ophiobolins

The bioactive extract from a new species in *Aspergillus* section *Usti* (IBT 18591) was more selective than the above mentioned active extracts and in consequence selected for more detailed investigations. MS- and UV-based dereplication led to the tentative identification of the ophiobolin family of compounds. Ophiobolin K and 6-epiophiobolin K (Figure 7) [32] were isolated and ophiobolin K was found very potent against CLL cells *in vitro*.

The ophiobolins are a family of naturally occurring sesterterpenoids, currently comprising more than 35 known analogues [33–37]. They all consist of a C_{25} skeleton with a dicyclopenta[a,d]cyclooctane ring system. Some ophiobolins have an extra ring incorporated, as observed in ophiobolin A and H (Figure 7), forming two different types of tetra-cyclic structures [38]. The absolute configuration of ophiobolin A and G have been determined by X-ray crystallography [39,40] and the conformations of all stereocenters except C6 is expected to be conserved based on the biosynthetic production of ophiobolins demonstrated by the first sesterterpene synthase described in 2013 [41]. Ophiobolins exhibit a broad spectrum of inhibitory activity against cancer cell lines, including lung cancer A549, breast cancer MCF7, colon cancer HT29, melanoma Mel20, leukemia P388 and L1210 cell lines [5,34,35,42–45].

Further investigations of the anti-leukemic activity and pharmacophore of the ophiobolins in the CLL/stromal cell co-culture platform were performed with the purpose of isolating a high number of naturally occurring analogs as well as identification of novel analogues. Taking advantage of the huge biodiversity available in the IBT culture collection [19], we expanded the biodiversity and hereby the expected chemodiversity with 12 closely related *Aspergilli* from the section *Usti* (Table S7) [46]. Cultures of the 12 new strains were extracted in micro-scale [22] to explore their potential for

producing ophiobolins. *A. insuetus* (IBT 28266) and *A. calidoustus* (IBT 25726) were identified as potent ophiobolin producers with one likely novel and more known ophiobolins analogs compared to the original strain (Figure 8).

The novel ophiobolin U (Figure 9) was isolated together with ophiobolin H [40] (Figure 7) and the rare 6-epiophiobolin N [43] (Figure 7) from the *A. insuetus* extract, while ophiobolin C [47] (Figure 7) and 6-epiophiobolin G [43] (Figure 7) were isolated from the *A. calidoustus* extract.

The structure of the novel ophiobolin U was elucidated by 1D and 2D NMR spectroscopy. The ^{1}H-NMR spectrum of ophiobolin U was closely related to that of ophiobolin K with many practically identical chemical shifts (Table S8 and S9). The most remarkable difference between ophiobolin U and ophiobolin K was found at C5 that shifted 143.9 ppm upfield from 217.0 to 73.1 ppm in the carbon spectrum, indicating the disappearance of a ketone group. C5 had an additional HSQC correlation to a signal at 4.91 ppm (H5). This significant change indicated a reduction of the ketone (C5) in ophiobolin K to a secondary alcohol in ophiobolin U. This reduction was confirmed by the identification of a COSY spin system between H1-H2-H6 in ophiobolin K that in ophiobolin U was expanded with a vicinal coupling between the protons at 3.02 (H6) and 4.91 (H5) and further a vicinal coupling between H5 and the diastereotopic protons at 1.87 (H4a) and 2.68 ppm(H4b) (Figure 10a).

Figure 7. Structures of ophiobolin A, 3-anhydro-ophiobolin A, 3-anhydro-6-epiophiobolin A, ophiobolin B, ophiobolin C, 6-epiophiobolin G, ophiobolin H, 6-epiophiobolin K, ophiobolin K, 6-epiophiobolin N, and ophiobolin U.

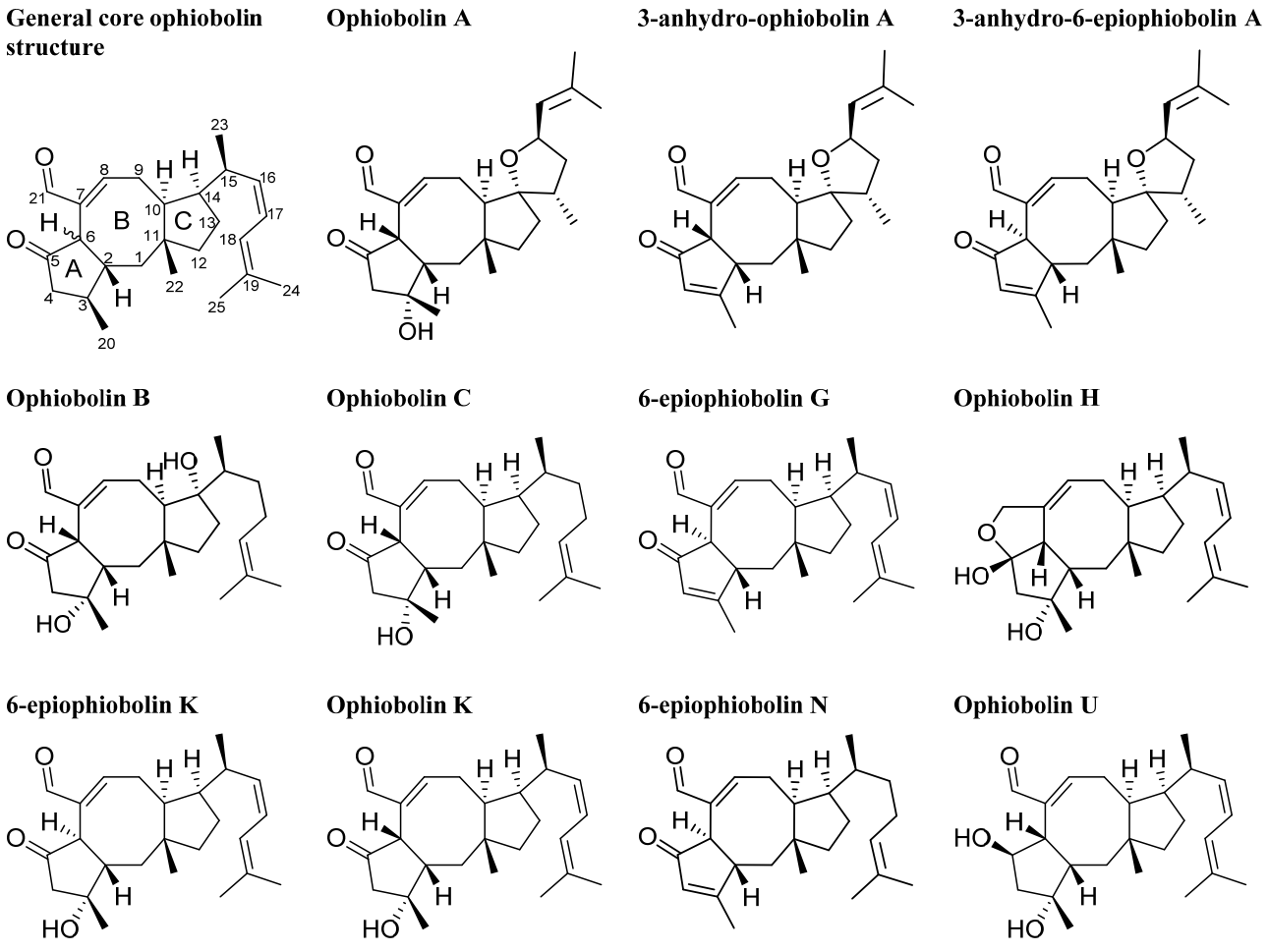

Figure 8. UHPLC chromatograms of (**a**) the new species in *Aspergillus* section *Usti* (IBT 18591) producing ophiobolin K and 6-epiophiobolin K, (**b**) *A. insuetus* (IBT 28266) producing the novel ophiobolin U together with ophiobolin H, K, C as well as 6-epiophiobolin K and N and (**c**) *A. calidoustus* (IBT 25726) producing ophiobolin K and C as well as 6-epiophiobolin K and G.

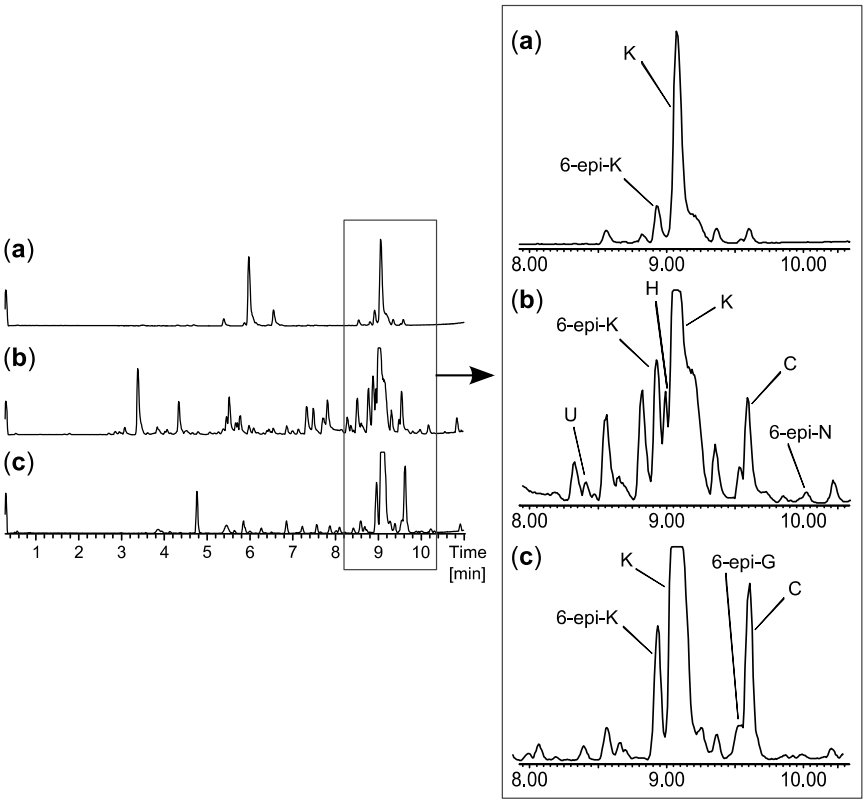

Figure 9. Structure of ophiobolin U.

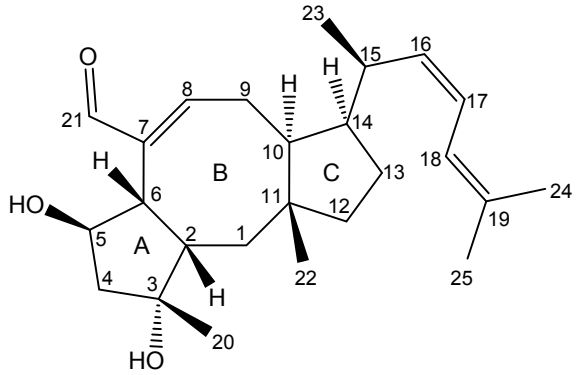

The spin systems identified in the DQF-COSY spectrum of ophiobolin U were assembled through HMBC correlations, which also enabled the identification of the quaternary carbon atoms. The most important HMBC correlations are shown in Figure 10b. The COSY spin systems were connected by HMBC connectivities further confirming the presence of the eight-membered ring. HMBC connectivities were found from H5 to the quaternary carbons at 81.9 (C3) and 142.1 ppm (C7), from the diastereotopic protons at 1.03 (H1a) and 1.58 ppm (H1b) to C3 and the carbon at 54.0 ppm (C10), and finally from H9 to C7 and the quaternary carbon at 44.1 ppm (C11). The reduction at C5 changed

the chemical environment of the surrounding carbons (C2, C3, C6, C8 and C21) that were more deshielded and therefore shifted 1.8–6.5 ppm downfield compared to ophiobolin K (Table S8). The remaining chemical shifts in ophiobolin U matched the chemical shifts of ophiobolin K (Tables S8 and S9).

Figure 10. (**a**) Important DQF-COSY couplings and (**b**) important HMBC connectivities in the novel compound ophiobolin U.

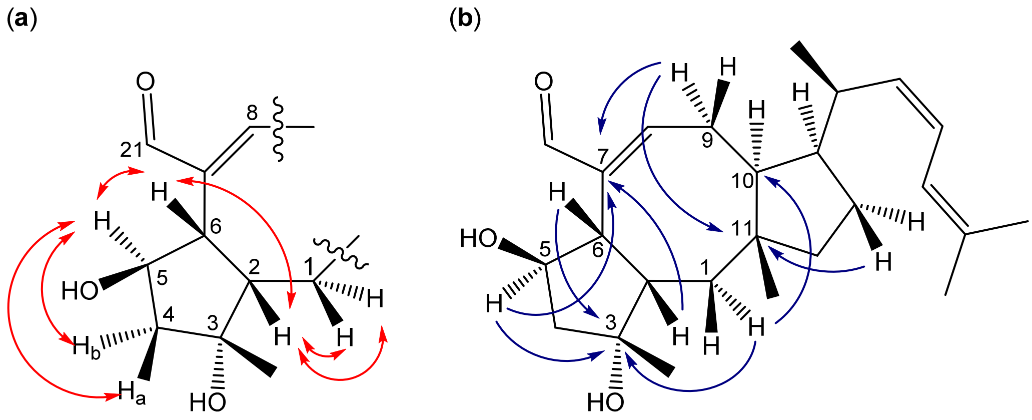

The stereochemistry of the A/B ring system in ophiobolin U (Figure 9) was assigned based on NOE correlations and chemical shifts. The A/B-*cis* ring system was established by the NOE correlations found between the protons at 2.30 (H2) and 3.02 ppm (H6), as demonstrated in Figure 11. The stereochemistry of C-5 was tentatively assigned through strong NOE correlations of the diastereotopic protons at 1.87 (H4a) and 2.68 ppm (H4b). H4a had NOE correlations to the protons at 1.26 ppm (H20) and H2, while H4b had a NOE correlation to H5, which indicated that the hydroxy group at C5 was *cis* to H6. Other important NOE correlations are shown in Figure 11.

Figure 11. Important NOE correlations in ophiobolin U.

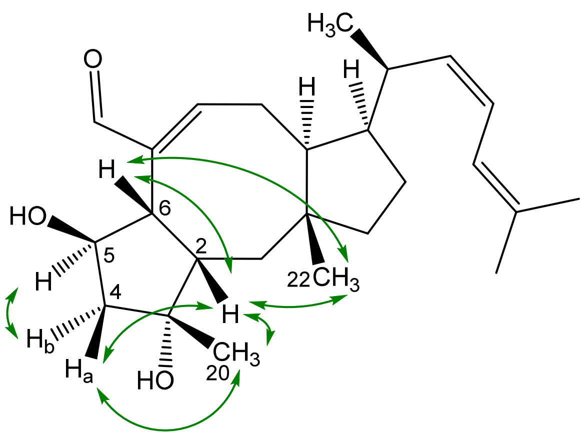

The A/B-*cis* was confirmed by chemical shifts. Earlier reports showed that C1 and C22 in ophiobolins with A/B-*cis* ring structure are more upfield compared to ophiobolins with A/B-*trans* ring structure [48]. In ophiobolin U and ophiobolin K, the chemical shifts of C1 and C22 were more upfield compared to 6-epiophiobolin K, which indicate a A/B-*cis* ring structure in ophiobolin U. Other reports have showed that the A/B-*cis* ring structure in ophiobolins causes a small deshielding (0.2–0.3 ppm)

for H2 and H8 as well as a small shielding (0.3–0.6 ppm) for H4 [49]. The ^{1}H chemical shifts for ophiobolin U were inconclusive regarding conformation of the A/B ring system. The residual stereocenters of ophiobolin U were the same as in the known ophiobolins due to the stereospecificity of the biosynthetic pathway of the ophiobolins [41,50].

The stereochemistry of the A/B ring system of the remaining six ophiobolins (ophiobolin K, 6-epiophiobolin K, 6-epiophiobolin N, 6-epiophiobolin G, ophiobolin H, and ophiobolin C) isolated in this study were confirmed by NOE correlations. Together with the general trend that C1 and C22 in the ophiobolins with A/B-*cis* ring structure were more upfield compared to ophiobolins with A/B-*trans* ring structure [43,48]. The shifting of chemical shifts for H2, H4, and H8 for the A/B-*cis* ring system were more ambiguous due to the small deshielding/shielding in chemical shifts and inconclusive for the seven ophiobolins. A comparison of the ^{13}C and ^{1}H chemical shifts of all the seven ophiobolins are found in Tables S8 and S9, respectively.

Besides the seven purified ophiobolins: ophiobolin A, ophiobolin B, 3-anhydroophiobolin A, and 3-anhydro-6-epiophiobolin A (Figure 7) were bought as standards with the aim of obtaining a broader understanding of the SAR of the ophiobolin family against CLL cells. Ophiobolin U was unstable and therefore not applied in any bioassay, but the remaining ten ophiobolins were tested for their cytotoxic activity towards CLL cells. Ophiobolin A, B, C, and K showed the strongest effects with LC_{50} values between 1 and 8 nM (results compiled in Table 1 and Figure 12a). Testing of normal lung fibroblasts revealed that ophiobolin A and B displayed cytotoxic effects at 10 nM concentration indicating a slight difference in bio-activity for CLL cells in comparison to healthy fibroblasts. Ophiobolin C and K displayed no effect towards normal lung fibroblasts in concentrations up to 10 nM (Figure S17). Interestingly, 3-anhydroophiobolin A, 3-anhydro-6-epiophiobolin A, 6-epiophiobolin G, ophiobolin H, 6-epiophiobolin K, and 6-epiophiobolin N exhibited low or no activity towards CLL cells. In fact, 6-epiophiobolin K targeted CLL cell viability only when applied at a 100-fold higher concentration than ophiobolin K (Figure 12b). Ophiobolin-treated cells were further stained with PE-labelled Annexin-V and 7-AAD, or antibodies for activated caspase-3 prior to flow cytometric analyses. Thereby, apoptosis was identified as the mode of killing of CLL cells as demonstrated recently for chaetoglobosin A [15].

Table 1. Apoptosis inducing activity (LC_{50} [nM]) of the 10 ophiobolins towards CLL cells.

Compound	LC_{50}
Ophiobolin A	1 nM
3-anhydro-ophiobolin A	Inactive
3-anhydro-6-epiophiobolin A	Inactive
Ophiobolin B	2 nM
Ophiobolin C	8 nM
6-epiophiobolin G	Inactive
Ophiobolin H	Inactive
Ophiobolin K	4 nM
6-epiophiobolin K	Inactive
6-epiophiobolin H	Inactive

Figure 12. Effects of different ophiobolins on CLL cell viability. (**a**) CLL cells cultured in HS-5 conditioned media were treated for 24 h with increasing concentrations of ophiobolin A, ophiobolin B, ophiobolin C, ophiobolin K, and 6-epiophiobolin K, and cell viability was analyzed by CellTiter-Glo® assay measuring each data point as duplicate. Relative cell viability compared to DMSO control (0.1%) is depicted as mean values +SD of 3 independent CLL samples; (**b**) As 6-epiophiobolin K treatment did not decrease cell viability in the concentration range tested in (a), CLL cells were treated with up to 900 nM of 6-epiophiobolin K, and cell viability was determined and compared to the active ophiobolin B.

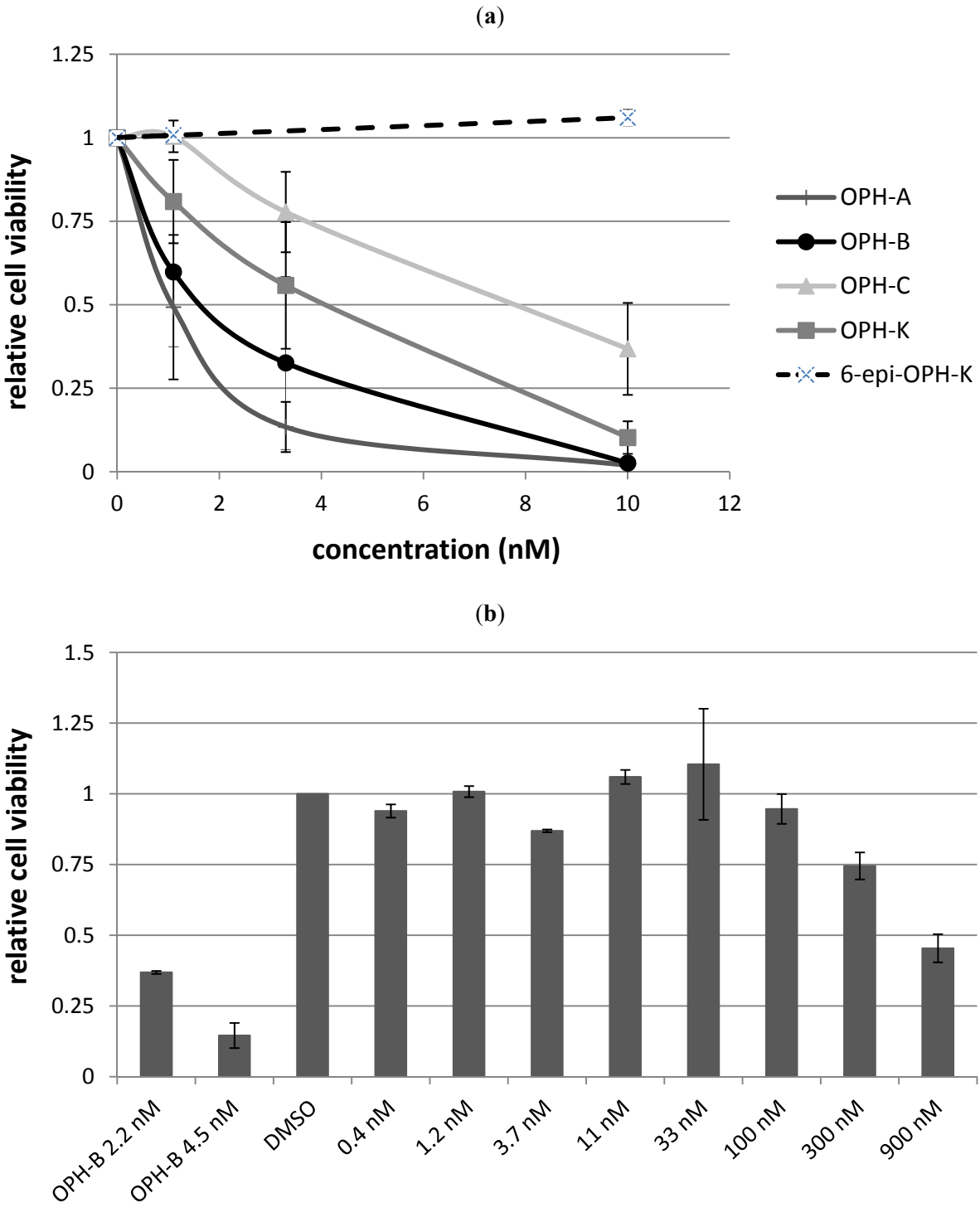

The results displayed in Table 1 and Figure 12a indicates that presence of a hydroxy group at C3 and an aldehyde at C21 is crucial for the activity of the ophiobolins. Our findings are thus in agreement with previous studies that have shown that these two groups covalently bind to calmodulin [51,52]. None of the 6-epiophiobolins tested were active against the CLL cells. To earn a broader understanding of the importance of this small steric change at C6, 3D-modeling of ophiobolin K (blue) and 6-epiophiobolin K (red) were done to give a visual representation of their lowest energy conformations (Figure 13).

Figure 13. Modulated 3D structures of ophiobolin K (blue) and 6-epiophiobolin K (red) in their lowest energy conformations overlaid. H6 protons are marked in ophiobolin K (cyan) and 6-epiophiobolin K (orange). The chain extending from C14 in ring C is not displayed to get a better clarity of the structures (the cut-off point is marked with *).

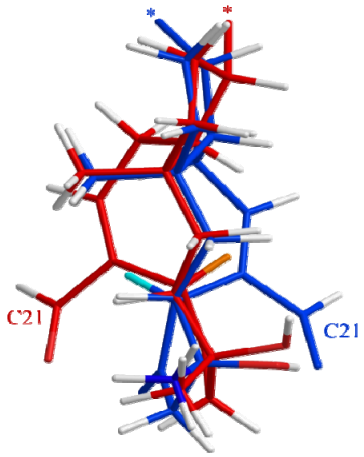

The difference in conformation between ophiobolin K and 6-epiophiobolin K involves a flipping of the eight-membered ring that result in a change of position of the C21 aldehyde from one to the other side of the plane observed in the figure. This conformational change is likely preventing the binding of calmodulin by the C21 aldehyde due to steric hindrance, resulting in the lack of activity for 6-epiophiobolin K contrasting ophiobolin K.

3. Experimental

3.1. General

The fungal strains used are from the IBT culture collection at Department of Systems Biology, Technical University of Denmark. The LC-MS analyses were performed on a maXis quadrupole time of flight (qTOF) mass spectrometer (Bruker Daltonics, Bremen, Germany) with an electrospray ionization (ESI) ion source. The maXis was calibrated using sodium formate automatically infused prior to each analytical run, providing a mass accuracy of below 1 ppm. The mass spectrometer was linked to an Ultimate 3000 UHPLC system (Dionex, Sunnyvale, CA, USA) with DAD. Separation was achieved on a Kinetex C_{18}, 2.6 µm, 2.1 × 100 mm column (Phenomenex, Torrance, CA, USA) with a flow of 0.4 mL min^{-1} at 40 °C using a linear gradient 10% acetonitrile (ACN) in Milli-Q water (MQ) with 20 µM formic acid (FA) going to 100% ACN in 10 min. All compounds were isolated by bio-guided fractionation started by flash chromatography of the crude extracts, fractionated with an Isolera

One automated flash system (Biotage, Uppsala, Sweden). The isolation of compounds were performed by a semi-preparative Gilson HPLC system (Middleton, WI, USA) with a 215 Liquid Handler, 819 Injection Module and a 172 DAD and fully controlled with Trilution LC software or on a Waters 600 chromatograph (Milford, MA, USA) attached to a Waters 600 DAD. One-dimensional and two-dimensional NMR experiments were acquired using standard pulse sequences on a 800 MHz Bruker Avance spectrometer with a 5 mm TCI cryoprobe at the Danish Instrument Centre for NMR Spectroscopy of Biological Macromolecules at Carlsberg Laboratory, alternatively on a 500 MHz Varian Unity Inova (Palo Alto, CA, USA) equipped with a HCP probe or a 400 MHz Bruker Avance III equipped a BBO Prodigy cryoprobe NMR spectrometers.

3.2. Micro Extraction for Initial Screen

Two hundred and eighty nine (289) fungal extracts were prepared from cultivation of 137 fungal strains (Table S1). All extracts were prepared in accordance with the micro-extraction method developed by Smedsgaard [22]. Five plugs were collected across the colony. The samples were subsequently extracted using (3:2:1 v/v/v) methanol (MeOH), dichloromethane (DCM) and ethyl acetate (EtOAc) with 0.5% FA.

3.3. Cultivation and Extraction

The seven extracts described here were *P. pulvillorum* (IBT 22393), *P. brasilianum* (IBT 22244), *P. decumbens* (IBT 11843), *P. cluniae* (IBT 21051), *Aspergillus* sp. (*Emericella*-like state, IBT 22838), *F. compactum* (IBT 9034), and a new species in *Aspergillus* section *Usti* (IBT 18591). Each fungus was cultivated on 50 plates (media are listed in supplementary) for 8 days at 25 °C in the dark with the exceptions of *P. brasilianum*. *P. brasilianum* (IBT 22244), *A. insuetus* (IBT 28266), and *A. calidoustus* (IBT 25726) were cultivated on 200 agar plates with Yeast Extract Sucrose (YES) for 14 days (except *A. calidoustus* that was incubated for 7 days) at 25 °C in the dark. All the fungi were extracted separately with EtOAc containing 1% FA. Unwanted carbohydrates from the media as well as fatty acids were removed from the four large extract (*P. brasilianum*, the new species in *Aspergillus* section *Usti*, *A. insuetus*, and *A. calidoustus*) by liquid-liquid extraction with water/MeOH and heptane, respectively leaving the crude extracts.

3.4. Bioassay-Guided Fractionation

The crude extract of *P. decumbens*, *P. pulvillorum*, *P. cluniae, Aspergillus* sp. (*Emericella*-like state), and *F. compactum* were fractionated on a RP C_{18} (25 g, 33 mL) column flash column with at gradient of: 15%–100% ACN in 20 min and flow rate 25 mL/min. No further fractionations were done with the bioactive flash fraction from the *P. cluniae* extract. Penicillic acid was purified from the bioactive flash fraction from the *P. pulvillorum* extract by semi-preparative HPLC LunaII C_{18} (250 × 10 mm, 5 μm) column with at gradient of: 15%–100% ACN in 20 min and flow rate 5 mL/min. ACN and MQ were added 20 mM FA.

Penicillic acid: White solid; UV (ACN) λ_{max}: 227 nm; HRMS *m/z* 170.0573 (M^+ calculated for $C_8H_{10}O_4$, *m/z* 170.0574; 0.5 ppm).

3.4.1. E-SPE

P. brasilianum, *P. decumbens*, *Aspergillus* sp. (*Emericella*-like state), and *F. compactum* extracts were prefractionated analytical in accordance with the E-SPE method developed by Månsson *et al.* [21] with SAX, MAX, and SCX ion-exchanger SPE columns though without the Sephadex LH-20 column. Additionally two normal phase (amino and diol) columns were add to the setup. For each extract, 5 mg was loaded on both the amino column (100 mg, 1 mL) and the diol column (100 mg, 1 mL). The compounds were eluted by 2 column volume (CV) heptane, 2 CV DCM, 2 CV DCM/EtOAc (1:1), 2 CV EtOAc, 2 CV EtOAc/MeOH, 2 CV MeOH, 4 CV ACN, 2 CV ACN/MQ + 2% FA (75:25), 2 CV ACN/MQ + 2% FA (50:50), 2 CV ACN/MQ + 2% FA (25:75), 2 CV ACN/MQ + 2% FA (10:90). No further fractionations were done with the bioactive flash fraction from the *P. decumbens* extract.

The bioactive C_{18} flash fraction from the *Aspergillus* sp. (*Emericella*-like state) extract was loaded on the amino column (10 g, 15 mL) and eluted by 2 CV heptane, 2 CV DCM, 2 CV DCM/EtOAc (1:1), 2 CV EtOAc, 2 CV EtOAc/MeOH, 2 CV MeOH, 4 CV ACN, 2 CV ACN/MQ + 2% FA(75:25), 2 CV ACN/MQ + 2% FA (50:50), 2 CV ACN/MQ + 2% FA (25:75), 2 CV ACN/MQ + 2% FA (10:90). Emestrin A (1.1 mg) was finally isolated by preparative HPLC on a LunaII C_{18} (250 × 10 mm, 5 μm) column with at gradient of: 50%–100% ACN in 20 min and flow rate 5 mL/min. ACN and MQ were added 50 ppm trifluoroacetic acid (TFA).

Emestrin A: White solid; $[\alpha]_{589.3nm}$: +22°; UV (ACN) λ_{max}: 230 (sh), 267 (sh), 285 (sh); HRMS *m/z* 598.0713 (M^+ calculated for $C_{27}H_{22}N_2O_{10}S_2$, *m/z* 598.0711; 0.4 ppm).

The bioactive C_{18} flash fraction from the *F. compactum* extract was loaded on a diol column (10 g, 15 mL) and eluted by 2 CV heptane, 2 CV heptanes/DCM (1:1), 2 CV DCM, 2 CV DCM/EtOAc (1:1), 2 CV EtoAc, 2 CV EtOAc/MeOH, 2 CV MeOH, 2 CV MeOH/ACN (1:1) and 2 CV ACN. Neosolaniol monoacetate was isolated with semi-preparative HPLC on a Luna II, C_{18}, 5 μm, 10 × 250 mm column with 30%–70% ACN in 20 min and flow rate 5 mL/min. ACN and MQ were added 20 mM FA.

Neosolaniol monoacetate: White solid; HRMS *m/z* 424.1728 (M^+ calculated for $C_{21}H_{28}O_9$, *m/z* 424.1728; 0 ppm).

The crude extract of *P. brasilianum* was loaded on a SAX column (100 g, 132 mL) and washed by 1 CV 70% MeOH in MQ (pH 11) and 1 CV 100% MeOH (pH 7) giving the SAX-1 fraction. Subsequently eluted by 2 CV 100% MeOH (pH 2) giving the SAX-2 fraction. Viridicatumtoxin was isolated (27.5 mg) from SAX-2 on a RP C_{18} column with at gradient of: 30%–100% ACN in 60 min and flow rate 40 mL/min. ACN and MQ were added 50 ppm TFA.

Viridicatumtoxin: Yellow solid; UV (ACN) λ_{max}: 238, 286, 435 nm; HRMS *m/z* 565.1942 (M^+ calculated for $C_{30}H_{31}NO_{10}$, *m/z* 565.1942; 0 ppm).

3.4.2. Ophiobolins

The crude extract of a new species in *Aspergillus* section *Usti* (IBT 18591) was fractionated on a RP C_{18} (25 g, 33 mL) flash column with at gradient of: 15%–100% ACN in 20 min and flow rate

25 mL/min. Subsequently the active fraction was loaded on a diol flash column and eluted with 2 CV heptane, 2 CV heptanes/DCM (1:1), 2 CV DCM, 2 CV EtOAc, 2 CV MeOH. Ophiobolin K and 6-epiophiobolin K were isolated from the active fraction by semi-preparative HPLC on a Luna II, C_{18}, 5 µm, 10 × 250 mm column by 70%–100% ACN in 25 min and flow rate 5 mL/min.

Ophiobolin K: White solid; $[\alpha]_{589.3nm}$: +161°; UV (ACN) λ_{max}: 241 nm; HRMS *m/z* 384.2658 (M^+ calculated for $C_{25}H_{36}O_3$, *m/z* 384.2659; 0.3 ppm); ^{13}C- and ^{1}H-NMR: see Tables S8 and S9, respectively.

6-Epiophiobolin K: White solid; $[\alpha]_{589.3nm}$: +53°; UV (ACN) λ_{max}: 239 nm; HRMS *m/z* 384.2658 (M^+ calculated for $C_{25}H_{36}O_3$, *m/z* 384.2659; 0.3 ppm); ^{13}C- and ^{1}H-NMR: see Tables S8 and S9, respectively.

The crude extract of *A. insuetus* (IBT 28266) was loaded on a diol flash column and eluted with 2 × 2 CV heptane, 2 CV heptanes/DCM (1:1), 2 CV DCM, 2 CV EtOAc, 2 CV MeOH. The active fraction was then loaded on a RP C_{18} flash column with at gradient of: 80%–100% ACN in 45 min and flow rate 40 mL/min. Ophiobolin U, ophiobolin H and 6-epiophiobolin N were isolated from the active fraction by semi-preparative HPLC on a Gemini, C_6-Ph, 5 µm, 10 × 250 mm column. Ophiobolin U was purified by 55%–70% ACN in 25 min and flow rate 5 mL/min. Ophiobolin H and 6-epiophiobolin N were purified by 50% ACN isocratic in 15 min, then 50–60 min ACN in 15 min, and then up to 100% ACN in 5 min. ACN and MQ were added 50 ppm TFA.

Ophiobolin U: White solid; $[\alpha]_{589.3nm}$: +3°; UV (ACN) λ_{max}: 242 nm; HRMS *m/z* 386.2813 (M^+ calculated for $C_{25}H_{38}O_3$, *m/z* 386.2816; 0.5 ppm); ^{1}H-NMR (800 MHz, $CDCl_3$): δ 0.91 (2H, d, 6.7, H23), 0.99 s (3H, s, H22), 1.03 (1H, m, H1a), 1.26 (3H, s, H20), 1.38 (2H, m, H12), 1.55 (1H, m, H10), 1.58 (1H, m, H1b), 1.58 (1H, m, H13a), 1.74 (3H, s, H24), 1.78 (1H, m, H13b), 1.82 (3H, s, H25), 1.87 (1H, dd, 4.1, 15.1, H4a), 2.09 (1H, m, H14), 2.24 (1H, m, H9a), 2.30 (1H, m, H2), 2.68 (1H, dd, 7.9, 15.1, H4b), 2.72 (1H, m, H15), 2.89 (1H, dd, 8.5, 12.5, H9b), 3.02 d (1H, d, 9.6, H6), 4.91 (1H, dd, 4.7, 7.9, H5), 5.21 (1H, t, 10.0, H16), 6.00 (1H, m, H18), 6.03 (1H, m, H17), 6.94 t (1H, d, 8.5, H8), 9.26 (1H, s, H21); ^{13}C-NMR (200 MHz, $CDCl_3$): δ 18.3 (C24), 18.6 (C22), 20.6 (C23), 25.6 (C9), 26.3 (C20), 26.7 (C13), 26.7 (C25), 35.2 (C1), 35.9 (C15), 42.0 (C12), 44.1 (C11), 47.4 (C14), 50.5 (C6), 51.0 (C2), 53.4 (C4), 54.0 (C10), 73.1 (C5), 81.9 (C3), 120.2 (C18), 122.3 (C17), 135.9 (C19), 137.7 (C16), 142.1 (C7), 164.1 (C8), 198.1 (C21). Full dataset is found in Table S10.

Ophiobolin H: White solid; $[\alpha]_{589.3nm}$: +60°; UV (ACN) λ_{max}: 241 nm; HRMS *m/z* 386.2817 (M^+ calculated for $C_{25}H_{38}O_3$, *m/z* 386.2816; −0.5 ppm); ^{13}C- and ^{1}H-NMR: see Tables S8 and S9, respectively.

6-Epiophiobolin N: White solid; $[\alpha]_{589.3nm}$: +10°; UV (ACN) λ_{max}: 232 nm; HRMS *m/z* 368.2711 (M^+ calculated for $C_{25}H_{36}O_2$, *m/z* 368.2710; −0.2 ppm); ^{13}C- and ^{1}H-NMR: see Tables S8 and S9, respectively.

The crude extract of *A. calidoustus* (IBT 25726) was loaded on a diol flash column and eluted with 2 CV heptane, 2 CV heptanes/DCM (1:1), 2 CV DCM, 2 CV EtOAc, 2 CV MeOH. Ophiobolin C and 6-epiophiobolin G were isolated from the active fraction by semi-preparative HPLC on a Luna II, C_{18}, 5 µm, 10 × 250 mm column. Ophiobolin C was purified by 80% ACN in MQ and 6-epiophiobolin G was purified by 80% MeOH in MQ both isocratic with a flow rate of 5 mL/min.

Ophiobolin C: White solid; $[\alpha]_{589.3nm}$: +298°; UV (ACN) λ_{max}: 240 nm; HRMS *m/z* 386.2813 (M^+ calculated for $C_{25}H_{38}O_3$, *m/z* 386.2816; 0.7 ppm); ^{13}C- and ^1H-NMR: see Tables S8 and S9, respectively.

6-Epiophiobolin G: White solid; $[\alpha]_{589.3nm}$: +127°; UV (ACN) λ_{max}: 234 nm; HRMS *m/z* 366.2553 (M^+ calculated for $C_{25}H_{34}O_2$, *m/z* 366.2554; 0.1 ppm); ^{13}C- and ^1H-NMR: see Tables S8 and S9, respectively.

3.5. CLL Cells, Cell Viability and Apoptosis Assays

Whole blood samples were obtained from patients that matched the standard diagnostic criteria for CLL after informed consent in accordance with the Declaration of Helsinki. All studies performed were approved by the ethics committee of the University of Ulm. Peripheral blood mononuclear cells (PBMC) were isolated by Ficoll density gradient and consisted of at least 80% $CD5^+CD19^+$ leukemic cells as determined by flow cytometry. For the initial screen, cocultures of HS-5 stromal cells and CLL cells were established as previously described [53]. For retesting of bio-active substances, CLL cells were cultured in conditioned media of HS-5 cells, which was harvested after 3–4 days of culture and 80% confluency and depleted of HS-5 cells and debris by centrifugation. CLL cells were seeded in duplicates at a density of 3×10^5 cells/well in opaque-walled 96-well plates. Fractions or pure compounds were added in different concentrations and incubated for 24 h. 0.1% DMSO was used as a negative control. Cell viability was assessed using CellTiter-Glo® assay (Promega, Madison, WI, USA) according to manufacturer's protocol. Luminescence signals were recorded using a Mithras LB940 plate reader (Berthold Technologies, Bad Wildbad, Germany). Background signals of medium were subtracted from each well as described by Knudsen *et al.* [15].

Apoptotic cell death was detected by flow cytometry using Annexin V-phycoerythrin (PE) and 7-aminoactinomycin (7-AAD) staining kit (BD Biosciences, Heidelberg, Germany) as described by Seiffert *et al.* [12]. To confirm apoptosis induction, staining for active caspase 3 was performed after fixation and permeabilization of cells using BD Cytofix/Cytoperm™ solution as described by the manufacturer by using PE-conjugated anti-active caspase 3 antibodies (clone C92-605, BD Biosciences). All flow cytometry analyses were carried out using a FACSCanto II flow cytometer equipped with FACSDiva software (BD Biosciences).

4. Conclusions

In conclusion, our combined bio-guided and dereplication based discovery approach has proven to be effective for fast dereplication and discovery of bioactive fungal natural products that target CLL cells. Comparative testing of active extracts on CLL cells as well as healthy cells identified compounds with general and selective bioactivity. The ophiobolin family showed high activity for CLL cells. The known ophiobolins A, B, C and K induced apoptosis in CLL cells with LC_{50} values of 1, 2, 8, and 4 nM, respectively with a lower bioactivity for healthy fibroblasts. The high activities for CLL cells were found only in ophiobolins with a hydroxy group at C3, an aldehyde at C21, and A/B-*cis* ring structure. In the remaining six bioactive extracts, the compounds responsible for the activity were tentatively identified by dereplication, and the activities towards CLL cells were verified by testing the pure compounds. The six active compounds, penicillic acid, viridicatumtoxin, calbistrin A, brefeldin A, emestrin A, and neosolaniol monoacetate, were all known and generally cytotoxic. In order to identify

substances that are of therapeutic value for cancer cells, selective active substances need to be retested on a large cohort of cancer and healthy cells. In general, cytotoxic compounds are only suitable as anti-cancer pharmaceuticals if they selectively target the cancer cells and not healthy cells, or at least have a higher impact on the tumor cells. Activity optimization is well exemplified with these studies demonstrating the great potential of looking into the chemistry of closely related species to obtain more analogue compounds of a promising scaffold.

Supplementary Materials

Supplementary materials can be accessed at: http://www.mdpi.com/1420-3049/18/12/14629/s1.

Acknowledgments

We acknowledge the support of The Danish Cancer Society grant # R20-A1157-10-S2. This study was additionally supported by the Helmholtz Virtual Institute "Understanding and overcoming resistance to apoptosis and therapy in leukemia" and by the research project of the German Federal Ministry of Education and Research "CancerEpiSys". We thank the Danish Instrument Center for NMR Spectroscopy of Biological Macromolecules for NMR time. Furthermore, we thank Maria Månsson for critical proof reading of the manuscript and for suggestions and Sibylle Ohl for technical support.

Conflicts of Interest

The authors declare no conflict of interest.

References

1. Zenz, T.; Mertens, D.; Küppers, R.; Döhner, H.; Stilgenbauer, S. From pathogenesis to treatment of chronic lymphocytic leukaemia. *Nat. Rev. Cancer* **2010**, *10*, 37–50.
2. Burger, J.A.; Montserrat, E. Coming full circle: 70 years of chronic lymphocytic leukemia cell redistribution, from glucocorticoids to inhibitors of B-cell receptor signaling. *Blood* **2013**, *121*, 1501–1509.
3. Nielsen, K.F.; Månsson, M.; Rank, C.; Frisvad, J.C.; Larsen, T.O. Dereplication of microbial natural products by LC-DAD-TOFMS. *J. Nat. Prod.* **2011**, *74*, 2338–2348.
4. Frisvad, J.C.; Smedsgaard, J.; Larsen, T.O.; Samson, R.A. Mycotoxins, drugs and other extrolites produced by species in *Penicillium* subgenus *Penicillium*. *Stud. Mycol.* **2004**, *49*, 201–241.
5. Bladt, T.T.; Frisvad, J.C.; Knudsen, P.B.; Larsen, T.O. Anticancer and antifungal compounds from *Aspergillus*, *Penicillium* and other filamentous fungi. *Molecules* **2013**, *18*, 11338–11376.
6. Delgado, J.; Baumann, T.; Ghita, G.; Montserrat, E. Chronic lymphocytic leukemia therapy: Beyound chemoimmunotherapy. *Curr. Pharm. Des.* **2012**, *18*, 3356–3362.
7. Tsimberidou, A.-M.; Keating, M.J. Treatment of patients with fludarabine-refractory chronic lymphocytic leukemia: need for new treatment options. *Leuk. Lymphoma* **2010**, *51*, 1188–1199.
8. Isfort, S.; Cramer, P.; Hallek, M. Novel and emerging drugs for chronic lymphocytic leukemia. *Curr. Cancer Drug Tar.* **2012**, *12*, 471–483.

9. Burger, J.A.; Tsukada, N.; Burger, M.; Zvaifler, N.J.; Aquila, M.D.; Kipps, T.J. Blood-derived nurse-like cells protect chronic lymphocytic leukemia B cells from spontaneous apoptosis through stromal cell-derived factor-1. *Blood* **2000**, *96*, 2655–2663.
10. Munk Pedersen, I.; Reed, J. Microenvironmental interactions and survival of CLL B-cells. *Leuk. Lymphoma* **2004**, *45*, 2365–2372.
11. Lagneaux, L.; Delforge, A.; Bron, D.; de Bruyn, C.; Stryckmans, P. Chronic lymphocytic leukemic B cells but not normal B cells are rescued from apoptosis by contact with normal bone marrow stromal cells. *Blood* **1998**, *91*, 2387–2396.
12. Seiffert, M.; Stilgenbauer, S.; Döhner, H.; Lichter, P. Efficient nucleofection of primary human B cells and B-CLL cells induces apoptosis, which depends on the microenvironment and on the structure of transfected nucleic acids. *Leukemia* **2007**, *21*, 1977–1983.
13. Panayiotidis, P.; Jones, D.; Ganeshaguru, K.; Foroni, L.; Hoffbrand, A.V. Human bone marrow stromal cells prevent apoptosis and support the survival of chronic lymphocytic leukaemia cells *in vitro*. *Br. J. Haematol.* **1996**, *92*, 97–103.
14. Schulz, A.; Toedt, G.; Zenz, T.; Stilgenbauer, S.; Lichter, P.; Seiffert, M. Inflammatory cytokines and signaling pathways are associated with survival of primary chronic lymphocytic leukemia cells *in vitro*: A dominant role of CCL2. *Haematologica* **2011**, *96*, 408–416.
15. Knudsen, P.B.; Hanna, B.; Ohl, S.; Sellner, L.; Zenz, T.; Stilgenbauer, S.; Larsen, T.O.; Lichter, P.; Seiffert, M. Chaetoglobosin A preferentially induces apoptosis in chronic lymphocytic leukemia cells by targeting the cytoskeleton. *Leukemia* **2013**, in press.
16. Bode, H.B.; Bethe, B.; Höfs, R.; Zeeck, A. Big effects from small changes: Possible ways to explore nature's chemical diversity. *ChemBioChem* **2002**, *3*, 619–627.
17. Rebacz, B.; Larsen, T.O.; Clausen, M.H.; Rønnest, M.H.; Löffler, H.; Ho, A.D.; Krämer, A. Identification of griseofulvin as an inhibitor of centrosomal clustering in a phenotype-based screen. *Cancer Res.* **2007**, *67*, 6342–6350.
18. Liao, W.-Y.; Shen, C.-N.; Lin, L.-H.; Yang, Y.-L.; Han, H.-Y.; Chen, J.-W.; Kuo, S.-C.; Wu, S.-H.; Liaw, C.-C. Asperjinone, a nor-neolignan, and terrein, a suppressor of ABCG2-expressing breast cancer cells, from thermophilic *Aspergillus terreus*. *J. Nat. Prod.* **2012**, *75*, 630–635.
19. Larsen, T.O.; Smedsgaard, J.; Nielsen, K.F.; Hansen, M.E.; Frisvad, J.C. Phenotypic taxonomy and metabolite profiling in microbial drug discovery. *Nat. Prod. Rep.* **2005**, *22*, 672–695.
20. Smedsgaard, J.; Nielsen, J. Metabolite profiling of fungi and yeast: From phenotype to metabolome by MS and informatics. *J. Exp. Bot.* **2005**, *56*, 273–286.
21. Månsson, M.; Phipps, R.K.; Gram, L.; Munro, M.H.G.; Larsen, T.O.; Nielsen, K.F. Explorative solid-phase extraction (E-SPE) for accelerated microbial natural product discovery, dereplication, and purification. *J. Nat. Prod.* **2010**, *73*, 1126–1132.
22. Smedsgaard, J. Micro-scale extraction procedure for standardized screening of fungal metabolite production in cultures. *J. Chromatogr. A* **1997**, *760*, 264–270.
23. Laatsch, H., Ed.; *AntiBase 2012*; Wiley-VCH: Weinheim, Germany, 2012. Available online: http://eu.wiley.com/WileyCDA/WileyTitle/productCd-3527334068.html (accessed on 5 September 2013).
24. Pohland, A.E.; Schuller, P.L.; Steyn, P.S. Physicochemical data for some selected mycotoxins. *Pure Appl. Chem.* **1982**, *54*, 2219–2284.

25. Raju, M.S.; Wu, G.-S.; Gard, A.; Rosazza, J.P. Microbial transformations of natural antitumor agents. 20. Glucosylation of viridicatumtoxin. *J. Nat. Prod.* **1982**, *45*, 321–327.
26. Shao, R.G.; Shimizu, T.; Pommier, Y. Brefeldin A is a potent inducer of apoptosis in human cancer cells independently of p53. *Exp. Cell Res.* **1996**, *227*, 190–196.
27. Seya, H.; Nakajima, S.; Kawai, K.-I.; Udagawa, S.-I. Structure and absolute configuration of emestrin, a new macrocyclic epidithiodioxopiperazine from *Emericella striata*. *J. Chem. Soc. Chem. Comm.* **1985**, *739*, 657–658.
28. Seya, H.; Nozawa, K.; Nakajima, S.; Kawai, K.-I.; Udagawa, S.-I. Studies on fungal products. Part 8. Isolation and structure of emestrin, a novel antifungal macrocyclic epidithiodioxopiperazine from *Emericeella striata*. X-Ray molecular structure of emestrin. *J. Chem. Soc. Perk. T. 1* **1986**, *67*, 109–116.
29. Ueno, Y.; Umemori, K.; Nilmi, E.; Tanuma, S.; Nagata, S.; Sugamata, M.; Ihara, T.; Sekljlma, M.; Kawai, K.-I.; Ueno, I.; *et al*. Induction of apoptosis by T-2 toxin and other natural toxins in HL-60 human promyelotic leukemia cells. *Nat. Toxins* **1995**, *3*, 129–137.
30. Terao, K.; Ito, E.; Kawai, K.; Nozawa, K.; Udagawa, S. Experimental acute poisoning in mice induced by emestrin, a new mycotoxin isolated from *Emericella* species. *Mycopathologia* **1990**, *112*, 71–79.
31. Lansden, J.A.; Cole, R.J.; Dorner, J.W.; Cox, R.H.; Cutler, H.G.; Clark, J.D. A new trichothecene mycotoxin isolated from *Fusarium tricinctum*. *J. Agric. Food Chem.* **1978**, *26*, 242–244.
32. Singh, S.B.; Smith, J.L.; Sabnis, G.S.; Dombrowski, A.W.; Schaeffer, J.M.; Goetz, M.A.; Bills, G.F. Structure and conformation of ophiobolin K and 6- epiophiobolin K from *Aspergillus ustus* as a nematocidal agent. *Tetrahedron* **1991**, *47*, 6931–6938.
33. Krizsán, K.; Bencsik, O.; Nyilasi, I.; Galgóczy, L.; Vágvölgyi, C.; Papp, T. Effect of the sesterterpene-type metabolites, ophiobolins A and B, on zygomycetes fungi. *FEMS Microbiol. Lett.* **2010**, *313*, 135–140.
34. Zhang, D.; Fukuzawa, S.; Satake, M.; Li, X.; Kuranaga, T.; Niitsu, A.; Yoshizawa, K.; Tachibana, K. Ophiobolin O and 6-epi-ophiobolin O, two new cytotoxic sesterterpenes from the marine derived fungus *Aspergillus* sp. *Nat. Prod. Commun.* **2012**, *7*, 1411–1414.
35. Yang, T.; Lu, Z.; Meng, L.; Wei, S.; Hong, K.; Zhu, W.; Huang, C. The novel agent ophiobolin O induces apoptosis and cell cycle arrest of MCF-7 cells through activation of MAPK signaling pathways. *Bioorg. Med. Chem. Lett.* **2012**, *22*, 579–585.
36. Wang, Q.-X.; Yang, J.-L.; Qi, Q.-Y.; Bao, L.; Yang, X.-L.; Liu, M.-M.; Huang, P.; Zhang, L.-X.; Chen, J.-L.; Cai, L.; *et al*. 3-Anhydro-6-hydroxy-ophiobolin A, a new sesterterpene inhibiting the growth of methicillin-resistant *Staphylococcus aureus* and inducing the cell death by apoptosis on K562, from the phytopathogenic fungus *Bipolaris oryzae*. *Bioorgan. Med. Chem. Lett.* **2013**, *23*, 3547–3550.
37. Wang, Q.-X.; Bao, L.; Yang, X.-L.; Liu, D.-L.; Guo, H.; Dai, H.-Q.; Song, F.-H.; Zhang, L.-X.; Guo, L.-D.; Li, S.-J.; *et al*. Ophiobolins P-T, five new cytotoxic and antibacterial sesterterpenes from the endolichenic fungus *Ulocladium* sp. *Fitoterapia* **2013**, *90*, 220–227.
38. Au, T.K.; Chick, W.S.; Leung, P.C. The biology of ophiobolins. *Life Sci.* **2000**, *67*, 733–742.
39. Nozoe, S.; Morisaki, M.; Tsuda, K.; Takahashi, N.; Tamura, S.; Ishibashi, K.; Schirasaka, M. The structure of ophiobolin, a C25 terpenoid having a novel skeleton. *J. Am. Chem. Soc.* **1965**, *87*, 4968–4970.

40. Cutler, H.G.; Crumley, F.G.; Cox, R.H.; Springer, J.P.; Arrendale, R.F.; Cole, R.J.; Cole, P.D. Ophiobolins G and H: New fungal metabolites from a novel source, *Aspergillus ustus*. *J. Agric. Food Chem.* **1984**, *32*, 778–782.
41. Chiba, R.; Minami, A.; Gomi, K.; Oikawa, H. Identification of Ophiobolin F synthase by a genome mining approach: A sesterterpene synthase from *Aspergillus clavatus*. *Org. Lett.* **2013**, *15*, 594–597.
42. Shen, X.; Krasnoff, S.B.; Lu, S.W.; Dunbar, C.D.; O'Neal, J.; Turgeon, B.G.; Yoder, O.C.; Gibson, D.M.; Hamann, M.T. Characterization of 6-epi-3-anhydroophiobolin B from *Cochliobolus heterostrophus*. *J. Nat. Prod.* **1999**, *62*, 895–897.
43. Wei, H.; Itoh, T.; Kinoshita, M.; Nakai, Y.; Kurotaki, M.; Kobayashi, M. Cytotoxic sesterterpenes, 6-epi-ophiobolin G and 6-epi-ophiobolin N, from marine derived fungus *Emericella variecolor* GF10. *Tetrahedron* **2004**, *60*, 6015–6019.
44. Fujiwara, H.; Matsunaga, K.; Kumagai, H.; Ishizuka, M.; Ohizumi, Y. Ophiobolin A, a novel apoptosis-inducing agent from fungus strain f-7438. *Pharm. Pharmacol. Commun.* **2000**, *6*, 427–431.
45. Bury, M.; Novo-Uzal, E.; Andolfi, A.; Cimini, S.; Wauthoz, N.; Heffeter, P.; Lallemand, B.; Avolio, F.; Delporte, C.; Cimmino, A.; *et al.* Ophiobolin A, a sesterterpenoid fungal phytotoxin, displays higher *in vitro* growth-inhibitory effects in mammalian than in plant cells and displays *in vivo* antitumor activity. *Int. J. Oncol.* **2013**, *43*, 575–585.
46. Samson, R.A.; Varga, J.; Meijer, M.; Frisvad, J.C. New taxa in *Aspergillus* section *Usti*. *Stud. Mycol.* **2011**, *69*, 81–97.
47. Nozoe, S.; Hirai, K.; Tusda, K. The structure of zizanin-A and -B, C25-terpenoids isolated from *Helminthosporium zizaniae*. *Tetrahedron Lett.* **1966**, *20*, 2211–2216.
48. Li, E.; Clark, A.M.; Rotella, D.P.; Hufford, C.D. Microbial metabolites of ophiobolin A and antimicrobial evaluation of ophiobolins. *J. Nat. Prod.* **1995**, *58*, 74–81.
49. Tsipouras, A.; Adefarati, A.A.; Tkacz, J.S.; Frazier, E.G.; Rohrer, S.P.; Birzin, E.; Rosegay, A.; Zink, D.L.; Goetz, M.A.; Singh, S.B.; *et al*. Ophiobolin M and analogues, noncompetitive inhibitors of ivermectin binding with nematocidal activity. *Bioorg. Med. Chem.* **1996**, *4*, 531–536.
50. Canonica, L.; Fiecchi, A.; Galli Kienle, M.; Ranzi, B.M.; Scala, A. The biosynthesis of ophiobolins. *Tetrahedron Lett.* **1967**, *35*, 3371–3376.
51. De Vries-van Leeuwen, I.J.; Kortekaas-Thijssen, C.; Mandouckou, J.A.N.; Kas, S.; Evidente, A.; de Boer, A.H. Fusicoccin-A selectively induces apoptosis in tumor cells after interferon-alpha priming. *Cancer Lett.* **2010**, *293*, 198–206.
52. Evidente, A.; Andolfi, A.; Cimmino, A.; Vurro, M.; Fracchiolla, M.; Charudattan, R. Herbicidal potential of ophiobolins produced by *Drechslera gigantea*. *J. Agric. Food Chem.* **2006**, *54*, 1779–1783.
53. Seiffert, M.; Schulz, A.; Ohl, S.; Döhner, H.; Stilgenbauer, S.; Lichter, P. Soluble CD14 is a novel monocyte-derived survival factor for chronic lymphocytic leukemia cells, which is induced by CLL cells *in vitro* and present at abnormally high levels *in vivo*. *Blood* **2010**, *116*, 4223–4230.

Sample Availability: Not available.

Supplementary Materials for

Bio-Activity and Dereplication Based Discovery of Ophiobolins and Other Fungal Secondary Metabolites Targeting Leukemia Cells

Contents

List of Figures

List of Tables

1. Strains tested in the initial screening against chronic lymphocytic leukemia (CLL)

Table S1. Strains tested in the initial screening.

Isolate number	Species	Isolate number	Species
21947	*Aspergillus cystallinus*	22516, 22523	*Penicillium faroense*
3234, 5265	*Aspergillus cavernicola*	21051	*Penicillium cluniae*
24813	*Aspergillus granulosus*	11843	*Penicillium decumbens*
24666	*Aspergillus conjunctus*	26291	*Penicillium bialowiezense*
10526, 18590	*Aspergillus caespitosus*	18329	*Penicillium brevicompactum*
22551	*Aspergillus diversus*	22244	*Penicillium brasillianum*
22564, 24812	*Aspergillus funiculosis*	22393	*Penicillium pulvillorum*
11054	*Aspergillus deflectus*	23856	*Penicillium svalbardense*
22568	*Aspergillus varians*	23667	*Penicillium lapatayae*
4537, 28161	*Aspergillus pseudoustus*	16536	*Penicillium alpinium*
14906, 23076	*Aspergillus subvesicolor*	14084	*Penicillium caseium*
10525	*Aspergillus neocaespitos*	16545	*Penicillium pinicola*
23282	*Aspergillus microcysticus*	22760	*Penicillium aquamarinum*
24752, 22153	*Aspergillus karnakataense*	22662	*Penicillium groenlandense*
26386, 22274	*Aspergillus janus*	24414	*Penicillium algidum*
17337	*Aspergillus aureolatus*	24411	*Penicillium jamesonlandense*
11835	*Aspergillus sydowii*	22544	*Penicillium eidiense*
10127	*Aspergillus quasivesicolor*	22356	*Penicillium monticola*
18591	New sp. in the *Aspergillus* section *Usti*	22663	*Penicillium floccosum*
21781, 22558	*Aspergillus brevis*	17760	*Penicillium artemision*
13670, 13691	*Aspergillus neopuniceus*	14073	*Penicillium wyomingense*
20587	*Aspergillus neoustus*	13954	*Penicillium minitum*
16756	*Aspergillus panamensis*	24420	*Penicillium rivulorum*
11860, 11847	*Aspergillus protuberus*	29798	*Penicillium diversicolor*
11821, 25061	*Aspergillus vesicolor*	16537	*Penicillium ribeum*
23160	*Aspergillus subsessilis*	16625	*Penicillium turcosum*
22554, 25041	*Aspergillus ustus*	22779	*Penicillium jugorum*
17674	*Aspergillus pseudoversicolor*	30014	*Penicillium galathea*
4332	*Aspergillus neovesicolor*	30013	*Penicillium nassarsuaquense*
18288	*Aspergillus arizonae*	fel 248, cml 832	*Pestalotiopsis*
13989	*Aspergillus aculeatus*	fel 64	*Arthrinium phaeospermum*
22838	*Aspergillus sp. (Emericella-like state)*	fel 192	*Ascochyta*

Table S1. *Cont.*

Isolate number	Species	Isolate number	Species
9194	*Cylindrocarpon olidum*	fell 01	*Acremonium*
8893	*Fusarium poae*	fel 240	*Paraconiothyrium*
8988	*Fusarium avenaceum*	cml 1707	*Nodulisporium*
8979, 9077, 9115	*Fusarium equiseti*	fel 89, fel 355, fel 364	*Phomopsis*
8977	*Fusarium tricinctum*	fel 302	*Cytospora*
8945, 7785	*Epicoccum nigrum*	fel 159	*Bipolaris sp.*
9034	*Fusarium compactum*	fel 06	*Glomerella cingulata*
9044	*Fusarium culmorum*	fel 307, fel 308	*Lecanicillium pasalliotae*
9063	*Fusarium cerealis*	fel 17, fel 42	*Paraconiothyrium sporulosum*
9085	*Fusarium oxysporum*	fel 05, fel 30, cml 1716	*Periconia*
9096	*Fusarium redolens*	fel 299A	*Curvularia*
9089	*Fusarium merismoides*	fel 142	*Tubercularia sp.*
9087	*Fusarium torulosum*	fel 315	*Verticillium leptobactum*
9086, 9206	*Fusarium solani*	cml 1692	*Lasiodiplodia theobromae*
9103	*Fusarium flocciferum*	cml 1709	*Collototrichum crassipes*
9112, 9121	*Fusarium pallidoroseum*	cml 1681	*Cuvularia prasadii*
9107	*Fusarium proliferatum*	cml 1671	*Libertella*
9117	*Fusarium verticillioides*	fel 58, cml 1702, cml 1703, cml 1690	*Microsphaeropsis*
1807	*Fusarium sambucinam*	cml 1670A	*Clonostachys*
9184	*Fusarium chlamydosporum*	cml 1693	*Spegazzinia deightonii*
9181	*Fusarium neohelle*	cml 1695	*Virgatospora echinofibrosa*
9182	*Fusarium neochlam*	fel 09, fel 241	*Paraconiothyrium brasiliense*

2. Strains found active against chronic lymphocytic leukemia (CLL)

Table S2. Strains found active in the initial screening.

Isolate number	Species	Maximum activity observed on media
9103	*Fusarium occiferum*	YES
9034	*Fusarium compactum*	YES
22838	*Aspergillus sp. (Emericella-like state)*	YES
13989	*Aspergillus aculeatus*	CYA
23105	*Aspergillus pseudovesicolor*	YES
3235	*Aspergillus cavernicola*	YES
18950	*Aspergillus caespitosus*	YES
22564	*Aspergillus funiculosis*	YES
22551	*Aspergillus diversus*	YES
14906	*Aspergillus subvesicolor*	CYA
23282	*Aspergillus microcysticus*	CYA
24752	*Aspergillus karnakataense*	YES
18951	New sp. in the *Aspergillus* section *Usti*	YES
20587	*Aspergillus neoustus*	YES
23160	*Aspergillus subsessilis*	CYA
26291	*Penicillium bialowienze*	YES
18329	*Penicillium brevicompactum*	YES
21051	*Penicillium cluniae*	YES
22393	*Penicillium pulvillorum*	YES
22244	*Penicillium brasilianum*	YES
11843	*Penicillium decumbens*	YES
18288	*Aspergillus arizonae*	CYA
16545	*Penicillium pinicola*	YES
22760	*Penicillium aquamarinum*	CYA
22523	*Penicillium faroense*	YES
22662	*Penicillium groenlandense*	ALK
24411	*Penicillium jamesonlandense*	CYA
22544	*Penicillium eidense*	YES
22356	*Penicillium monticola*	CYA
22663	*Penicillium occosum*	CYA
17760	*Penicillium artemision*	YES
29798	*Penicillium diversicolor*	YES
16537	*Penicillium ribeum*	YES
16625	*Penicillium turcosum*	ALK

Table S2. *Cont*.

Isolate number	**Species**	**Maximum activity observed on media**
22779	*Penicillium jugorum*	CYA
30014	*Penicillium galathea*	CYA
fel 248	*Pestalotiopsis*	MEA
fel 64	*Arthrinium phaeospermum*	MEA
fel 355	*Phomopsis*	MEA
fel 302	*Cytospora*	MEA
fel 159	*Bipolaris sp*	YES
fel 308	*Lecanicillium psalliotae*	YES
fel 240	*Paraconiothyrium brasiliense*	YES
fel 17	*Paraconiothyrium sporulosum*	YES
fel 05, fel 30 and cml 1716	*Periconia*	YES
fel 299A	*Curvularia*	YES
fel 142	*Tubercularia*	YES
cml 1692	*Lasiodiplodia theobromae*	YES
cml 1709	*Collototrichum crassipes*	YES
cml 1692	*Libertella*	YES
cml 1703, cml 1690	*Microphaeropsis*	YES
cml 1707	*Nodulisporium*	YES
cml 1670A	*Clonostachys*	YES
cml 1693	*Spegazzinia deightonii*	YES
cml 1695	*Virgatospora echinofibrosa*	YES

3. Penicillic acid isolated from *Penicillium pulvillorum* (IBT 22393)

Figure S1. ^{1}H-NMR spectrum of penicillic acid in DMSO-d_6 at 500 MHz

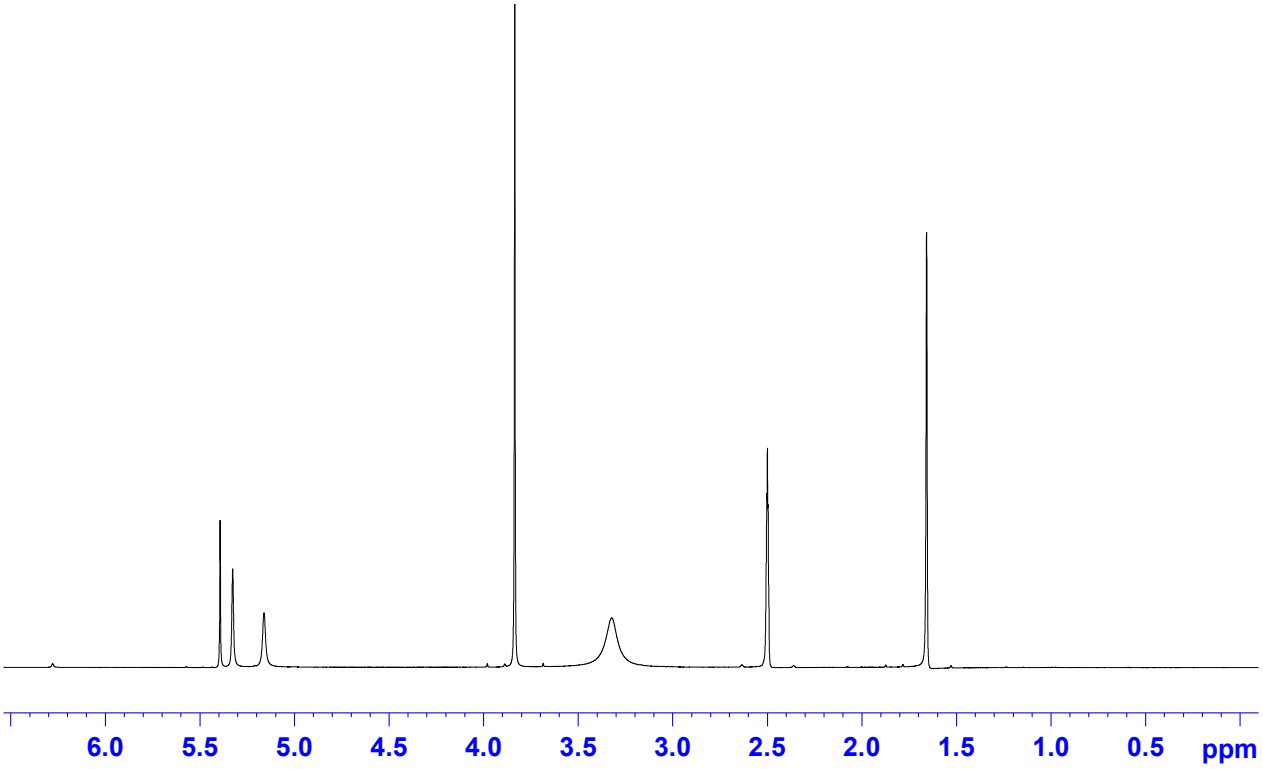

Table S3. ^{1}H and ^{13}C-NMR for penicillic acid in DMSO at 500 MHz for ^{1}H and 125 MHz for ^{13}C.

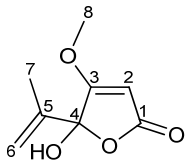

	δ_H mult. (*J* (Hz))	δ_C *
1		169.8
2	5.39 1 H, s	89.6
3		178.6
4		106.3
4-OH	3.33 1 H, br.s.	
5		140.4
6a	5.16 1 H, s	115.4
6b	5.33 1 H, br.s.	115.4
7	1.65 3 H, s	16.9
8	3.84 3 H, s	58.5

* ^{13}C-NMR chemical shifts determined from HSQC and HMBC experiments.

4. Viridicatumtoxin isolated from *P. brasilianum* (IBT 22244)

Figure S2. ^{1}H-NMR spectrum of viridicatumtoxin in DMSO-d_6 at 400 MHz.

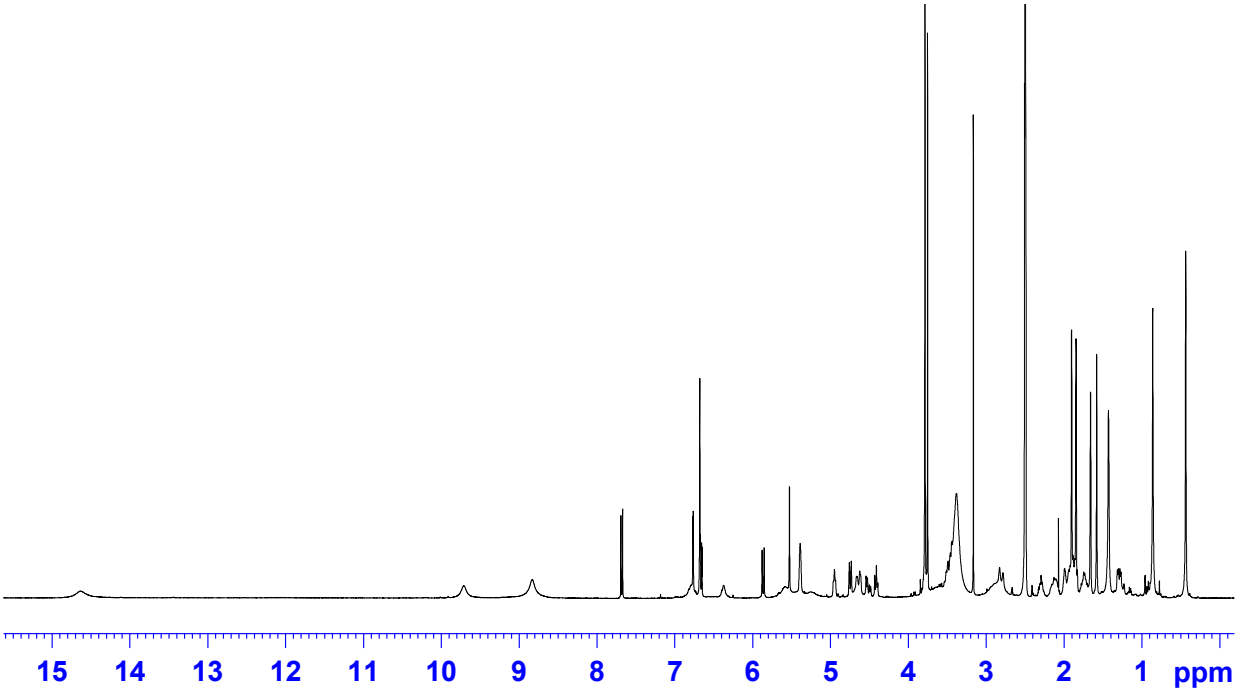

Table S4. ^{1}H-NMR for viridicatumtoxin in DMSO at 500 MHz.

	δ_H mult. (*J* (Hz))
4α	2.55 (1H, m)
4β	2.81 (1H, m)
5	4.66 (1H, br.s.)
9	6.68 (1H, s)
14α	2.91 (1H, m)
14β	3.17 (1H, m)
17	5.40 (1H, br.s.)
18α	1.98 (1H, m)
18β	2.13 (1H, m)
19α	1.30 (1H, dd, 5.6, 12.8)
19β	1.75 (1H, m)
21	0.45 (3H, s)
22	0.87 (3H, s)
23	1.43 (3H, s)
24	3.79 (3H,s)
OH	5.59 (1H, br.s.)
OH	6.79 (1H, br.s.)
OH	8.84 (1H, br.s.)
OH	9.73 (1H, br.s.)
OH	14.64 (1H, br.s.)

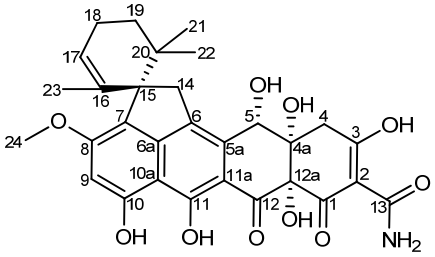

5. Emestrin A isolated from *Aspergillus* sp. (*Emericella*-like state) (IBT 22838)

Figure S3. ^{1}H-NMR spectrum of emestrin A in DMSO-d_6 at 500 MHz.

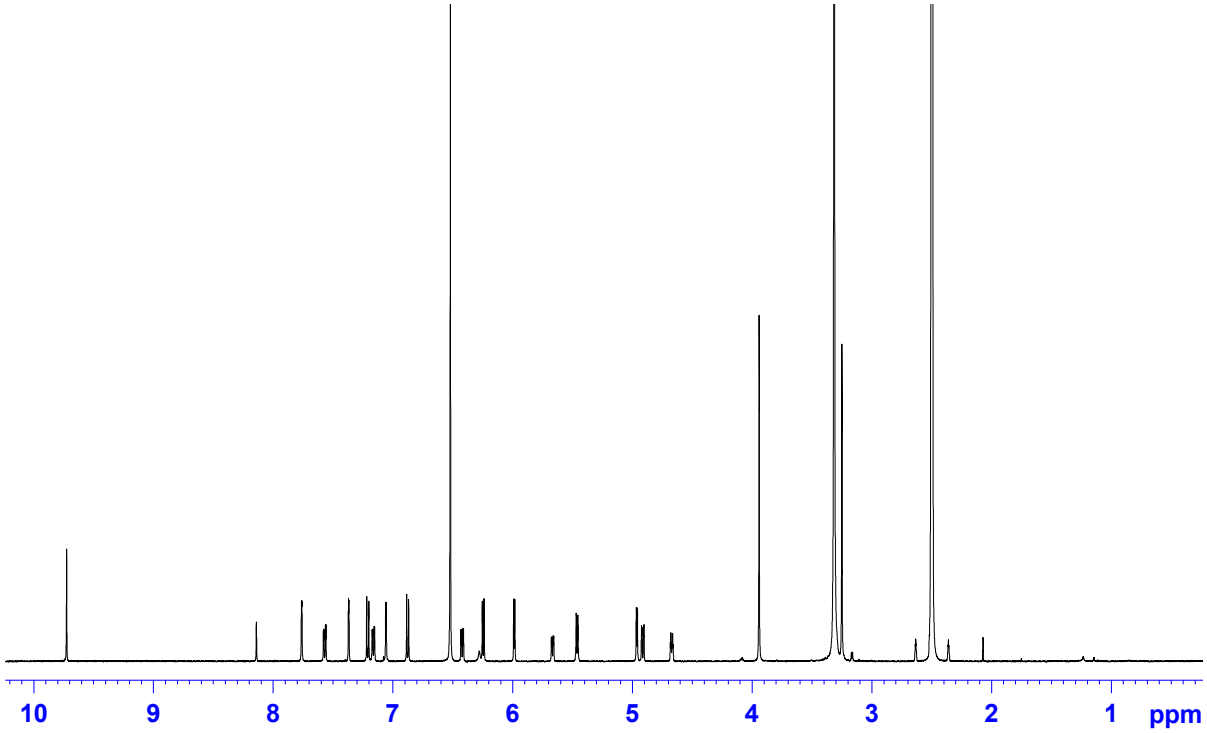

Table S5. ^{1}H and ^{13}C-NMR for emestrin A in DMSO at 500 MHz for ^{1}H and 125 MHz for ^{13}C.

	δ_H mult. (*J* (Hz))	δ_C *
1		80.8 ‡
2		164.2 †
3		80.8 ‡
4		164.2 †
5a	5.67 1 H, dd (2.5, 7.4)	59.8
5b		160.2
6	4.67 1 H, ddd (2.0, 2.5, 7.4)	74.6
7	4.91 1 H, dd (2.0, 8.5)	106.2
8	6.42 1 H, dd (2.5, 8.5)	137.1
10	7.06 1 H, d (2.5)	141.1
11	5.46 1 H, d (7.2)	72.6
11-OH	6.25 1 H, d (7.2)	
12	3.25 3 H, s	27.1
1'		127.2
2'	7.76 1 H, d (1.9)	122.5
3'		143.6
4'		149.0
4'-OH	9.73 1 H, s	
5'	6.88 1 H, d (8.3)	115.2
6'	7.16 1 H, dd (2.0, 8.3)	124.8
7'	4.96 1 H, d (4.6)	74.6
7'-OH	5.99 1 H, d (4.6)	
1"		145.6
2"		153.4
3"	7.21 1 H, d (8.6)	112.1
4"	7.57 1 H, dd (1.9, 8.6)	123.8
5"		122.0
6"	7.37 1 H, d (1.9)	120.0
7"		164.3
8"	3.94 3 H, s	55.7

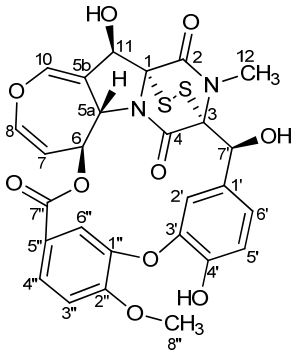

* ^{13}C-NMR chemical shifts determined from HSQC and HMBC experiments; ‡ Not possible to distinguish between C1 and C3; † Not possible to distinguish between C2 and C4.

6. Neosolaniol monoacetate isolated from *Fusarium compactum* (IBT 9034)

Figure S4. ^{1}H-NMR spectrum of neosolaniol monoacetate in DMSO-d_6 at 500 MHz.

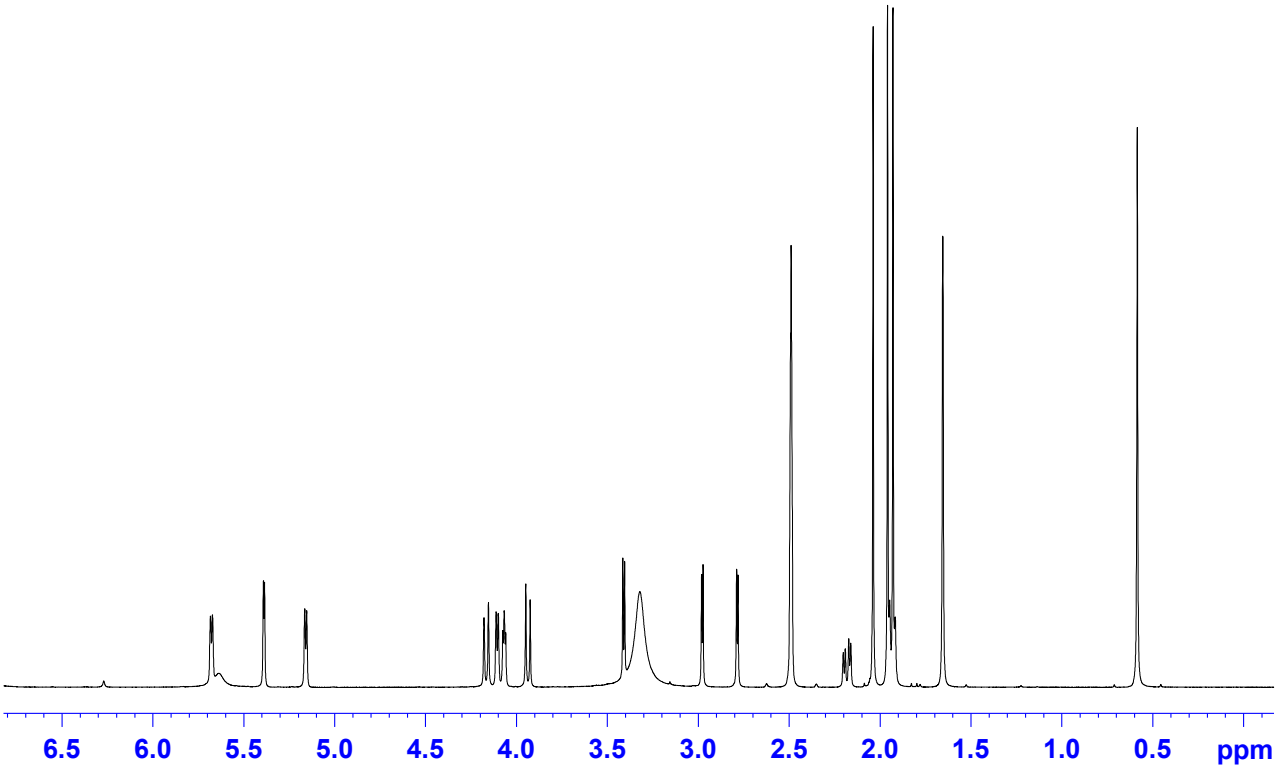

Table S6. ^{1}H-NMR for neosolaniol monoacetate in DMSO at 500 MHz.

	δ_H mult. (*J* (Hz))
2	3.41 1H, d (5.0)
3	4.07 1H, dd, (3.0; 5.0)
4	5.39 1H, d (3.2)
5	
6	
7a	2.18 1H, dd (5.3; 15.7)
7b	1.94 1H, m
8	5.15 1H, d, (5.3)
9	
10	5.67 1H, d (5.7)
11	4.1 1H, d (5.7)
12	
13a	2.78 1H, d (3.9)
13b	2.98 1H, d (3.9)
14	0.59 3H, s
15a	3.94 1H, d (12.2)
15b	4.16 1H, d (12.2)
16	1.66 3H, s
C=O C4	
C=O C8	
C=O C15	
CH3 C4	1.96 3H, s
CH3 C8	2.04 3H, s
CH3 C15	1.93 3H, s

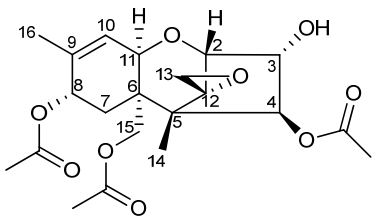

7. Ophiobolins

7.1 Potential ophiobolin producing strains from the *Aspergilli* section *Usti*

Table S7. *Aspergilli* section *Usti*.

IBT number	Species
4537	*Aspergillus ustus*
10619	
20587	
22554	
25041	
10524	*Aspergillus keveii*
24673	
24708	
28266	*Aspergillus insuetus*
28267	
13091	*Aspergillus calidoustus*
25726	

7.2 NMR data for ophiobolin U, ophiobolin K, 6-epiophiobolin K, ophiobolin C, ophiobolin H, 6-epiophiobolin H, and 6-epiophiobolin G

Table S8. ^{13}C-NMR data for ophiobolin U, ophiobolin K, 6-epiophiobolin K, ophiobolin C, ophiobolin H, 6-epiophiobolin H, and 6-epiophiobolin G. (***** 125 MHz in dimethyl sulfoxide (DMSO)-d_6, † 125 MHz in $CDCl_3$, or ‡ 200 MHz in $CDCl_3$, δ_C).

Ophiobolin	U ‡	K *	6-epi-K *	C †	H ‡	6-epi-N ‡	6-epi-G †
1	35.2	34.5	41.0	36.0	35.7	45.6	45.8
2	51.0	49.2	49.6	50.8	50.9	49.3	49.2
3	81.9	76.2	74.7	76.6	80.2	179.8	178.1
4	53.4	53.9	54.7	54.6	50.8	130.0	130.2
5	73.1	217.0	216.1	217.5	116.0	209.6	208.2
6	50.5	48.3	48.2	48.4	52.8	49.9	50.0
7	142.1	140.6	141.5	141.5	138.5	140.1	139.9
8	164.1	157.6	159.9	163.8	123.6	157.3	158.1
9	25.6	24.3	30.0	24.7	25.0	31.0	30.9
10	54.0	53.0	43.1	53.4	55.0	43.1	43.8
11	44.1	43.3	44.9	43.6	43.6	45.0	45.4
12	42.0	42.2	44.4	42.6	43.0	44.5	44.3
13	26.7	25.4	27.1	22.8	26.8	27.1	27.8
14	47.4	46.2	51.4	45.2	47.2	51.1	52.1
15	35.9	34.4	31.9	32.7	35.5	31.8	32.6
16	137.7	136.9	136.0	36.8	138.0	37.1	135.7
17	122.3	121.7	123.3	26.0	121.7	25.6	124.0
18	120.2	119.9	120.1	124.3	120.4	124.4	120.0
19	135.9	134.6	135.3	131.0	135.2	131.6	136.6
20	26.3	25.7	25.2	25.4	25.4	17.4	17.3
21	198.1	193.1	194.7	195.9	71.5	193.0	193.0
22	18.6	18.2	22.8	19.0	18.7	23.1	22.9
23	20.6	19.6	21.1	16.4	20.4	18.6	21.3
24	18.3	18.0	17.9	17.6	18.2	17.7	18.2
25	26.7	25.9	26.1	25.6	26.6	25.7	26.5

Table S9. ^{1}H-NMR data for ophiobolin U, ophiobolin K, 6-epiophiobolin K, ophiobolin C, ophiobolin H, 6-epiophiobolin H, and 6-epiophiobolin G. (* 500 MHz in DMSO-d_6, † 500 MHz in $CDCl_3$, or ‡ 800 MHz in $CDCl_3$, δ_H mult. (*J* (Hz))).

Ophiobolin	U ‡	K *	6-epi-K *	C †	H ‡	6-epi-N ‡	6-epi-G †
1a	1.03 m	1.14 m	1.58 m	1.26 m	1.36 m	1.18 m	1.15 m
1b	1.58 m	1.58 m	1.65 m	1.81 m	1.42 m	2.04 dd (3.7; 13.2)	2.03 m
2	2.30 m	2.25 m	1.91 m	2.38 m	2.26 m	2.71 m	2.66 m
3-OH			6.51 br.s.				
4a	1.87 dd (4.1, 15.1)	2.35 m	2.21 m	2.49 m	2.10 m	6.11 s	6.04 s
4b	2.68 dd (7.9, 15.1)	2.50 m	2.77 d (16.0)	2.80 m	2.18 m		
5	4.91 dd (4.7, 7.9)						
6	3.02 d (9.6)	3.22 d (9.8)	3.04 d (10.8)	3.26 m	3.17 d (9.8)	3.54 d (3.7)	3.40 m
8	6.94 t (8.5)	7.02 t (8.5)	6.96 m	7.21 m	5.64 br.s.	6.86 dd (2.0; 6.3)	6.80 m
9a	2.24 m	2.04 m	2.27 m	2.31 m	1.70 m	2.25 m	2.20 m
9b	2.89 dd (8.5, 12.5)	2.69 m	2.65 m	2.45 m	2.50 dd (8.6; 13.8)	2.71 m	2.93 m
10	1.55 m	1.56 m	2.46 m	1.67 m	1.60 m	2.72 m	2.63 m
12a	1.38 m	1.33 m	1.38 m	1.41 m	1.40 dd (7.6; 11.7)	1.42 m	1.43 m
12b		1.35 m	1.44 m	1.44 m	1.57 m	1.51 m	1.52 m
13a	1.58 m	1.54 m	1.22 m	1.46 m	1.54 m	1.23 m	1.25 m
13b	1.78 m	1.69 m	1.57 m	1.55 m	1.76 m	1.58 m	1.67 m
14	2.09 m	2.09 m	1.87 m	2.36 m	2.05 m	1.75 m	1.89 m
15	2.72 m	2.72 m	2.61 m	1.65 m	2.68 m	1.42 m	2.55 m
16a	5.21 t (10.0)	5.23 t (9.5)	5.25 t (9.3)	1.18 m	5.20 m	0.99 m	5.11 t (1.3)
16b				1.24 m		1.45 m	
17a	6.03 m	5.99 m	6.11 m	1.95 m	5.99 m	1.94 m	6.10 m
17b				2.00 m		2.07 m	
18	6.00 m	6.04 m	6.09 m	5.09 m	5.98 m	5.12 t (7.0)	6.00 m
20	1.26 s	1.19 s	1.26 s	1.36 s	1.24 s	2.10 s	2.06 s
21a	9.26 s	9.14 s	9.12 s	9.23 s	4.48 br.s.	9.30 s	9.26 s
21b					4.59 d (12.2)		
22	0.99 s	0.91 s	0.77 s	0.90 s	0.90 s	0.86 m	0.85 s
23	0.91 d (6.7)	0.85 d (6.6)	0.92 d (6.6)	0.78 d (6.8)	0.88 d (6.7)	0.91 d (6.4)	0.97 d (6.8)
24	1.74 s	1.68 s	1.70 s	1.61 s	1.73 s	1.61 s	1.76 s
25	1.82 s	1.76 s	1.79 s	1.69 s	1.80 s	1.69 s	1.83 s

7.3 Ophiobolin U isolated from *A. insuetus* (IBT 28266)

Figure S5. ^{1}H-NMR spectrum of ophiobolin U in $CDCl_3$ at 800 MHz.

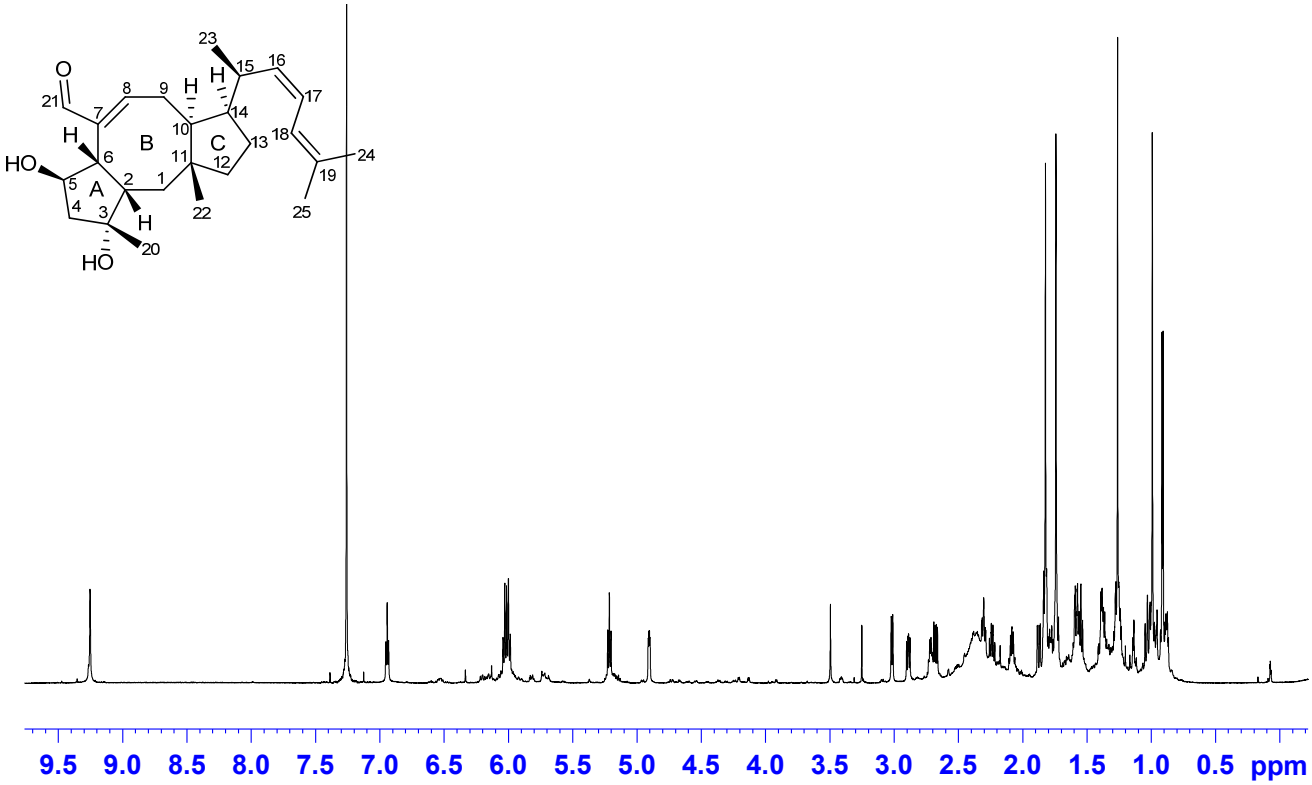

Figure S6. ^{13}C-NMR spectrum of ophiobolin U in $CDCl_3$ at 200 MHz.

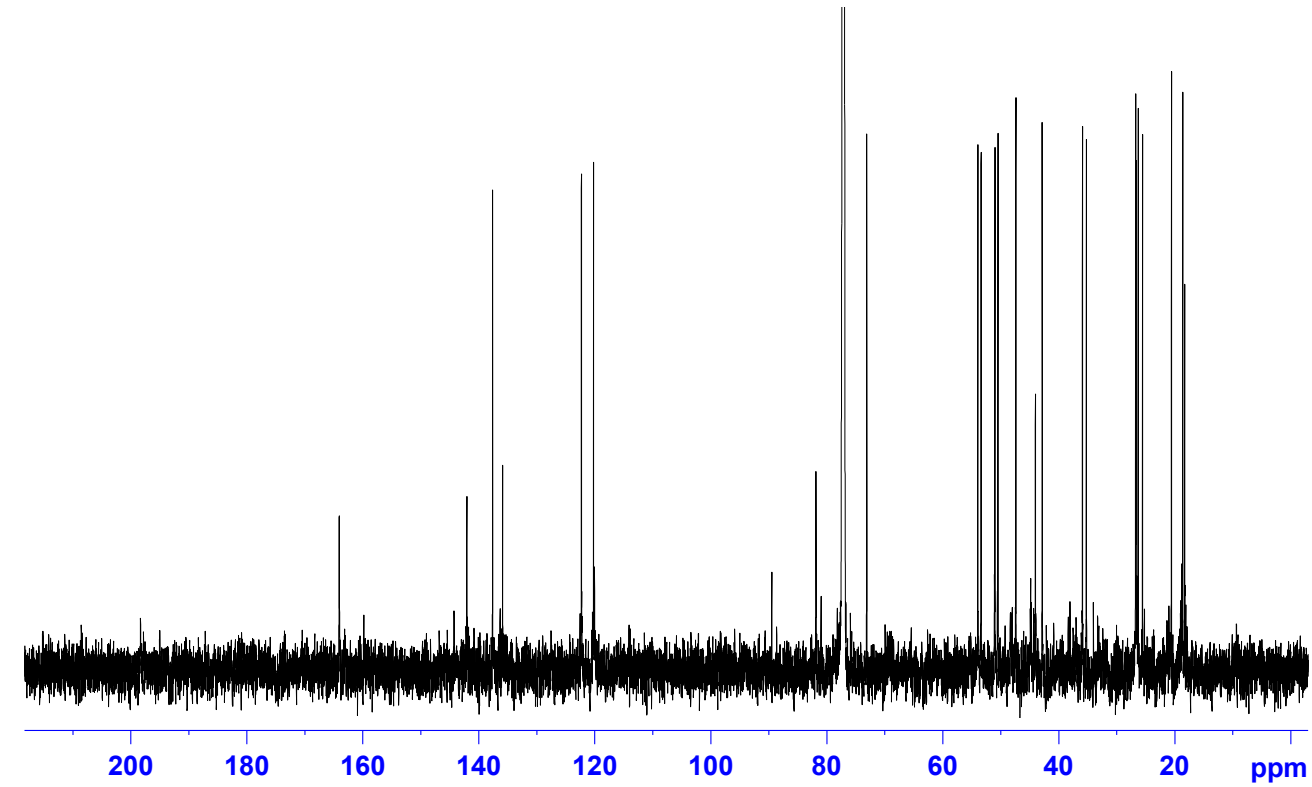

Table S10. ^{1}H- and ^{13}C-NMR for ophiobolin U in $CDCl_3$ at 800 MHz for ^{1}H and 200 MHz for ^{13}C.

	δ_H mult. (*J* (Hz))	δ_C	HMBC connectivities	NOE connectivities
1a	1.03 (1H, m)	35.2	2, 3, 10, 11, 22	1b
1b	1.58 (1H, m)	35.2	3, 10, 12	1a, 2, 15, 20, 22
2	2.30 (1H, m)	51.0	1, 3, 6, 7	6, 20, 22
3		81.9		
4a	1.87 (1H, dd, 4.1, 15.1)	53.4	3, 5	2, 4b, 20
4b	2.68 (1H, dd, 7.9, 15.1)	53.4	2, 3, 6	4a, 5
5	4.91 (1H, dd, 4.7, 7.9)	73.1	3, 6, 7	4b, 6
6	3.02 d (1H, d, 9.6)	50.5	2, 3, 5, 7, 8, 21	2, 5, 9a, 22
7		142.1	-	-
8	6.94 t (1H, d, 8.5)	164.1	6, 9, 21	9a, 9b, 10, 21
9a	2.24 (1H, m)	25.6	7, 8, 10, 11	6, 8, 9b, 22
9b	2.89 (1H, dd, 8.5, 12.5)	25.6	7, 8, 10, 11, 14	8, 9a, 10, 14, 15, 16
10	1.55 (1H, m)	54.0	8, 9, 11, 14, 15, 22	8, 9b, 14
11		44.1	-	-
12	1.38 (2H, m)	42.0	10, 11, 13, 14, 22	13a, 13b, 22
13a	1.58 (1H, m)	26.7	11, 14, 15	12, 13b, 22, 23
13b	1.78 (1H, m)	26.7	10, 11, 14, 15	12, 13a, 14
14	2.09 (1H, m)	47.4	10, 11, 13, 15, 16, 23	9b, 10, 13b, 15, 16, 23
15	2.72 (1H, m)	35.9	14, 16, 17, 23	9b, 1b, 14, 16, 18, 22, 23
16	5.21 (1H, t, 10.0)	137.7	14, 15, 18, 23	9b, 14, 15, 17, 23
17	6.03 (1H, m)	122.3	15, 19	16, 24
18	6.00 (1H, m)	120.2	24, 25	15, 25
19		135.9		
20	1.26 (3H, s)	26.3	2; 3; 4	1b, 2, 4a
21	9.26 (1H, s)	198.1	6, 7, 8	5, 8
22	0.99 s (3H, s)	18.6	1, 10, 11, 14	1b, 2, 6, 9a, 12, 13a, 15
23	0.91 (2H, d, 6.7)	20.6	14, 15, 16	13a, 14, 15, 16
24	1.74 (3H, s)	18.3	18, 19, 25	17
25	1.82 (3H, s)	26.7	18, 19, 24	18

7.4 Ophiobolin H isolated from *A. insuetus* (IBT 28266)

Figure S7. ^{1}H-NMR spectrum of ophiobolin H in $CDCl_3$ at 800 MHz.

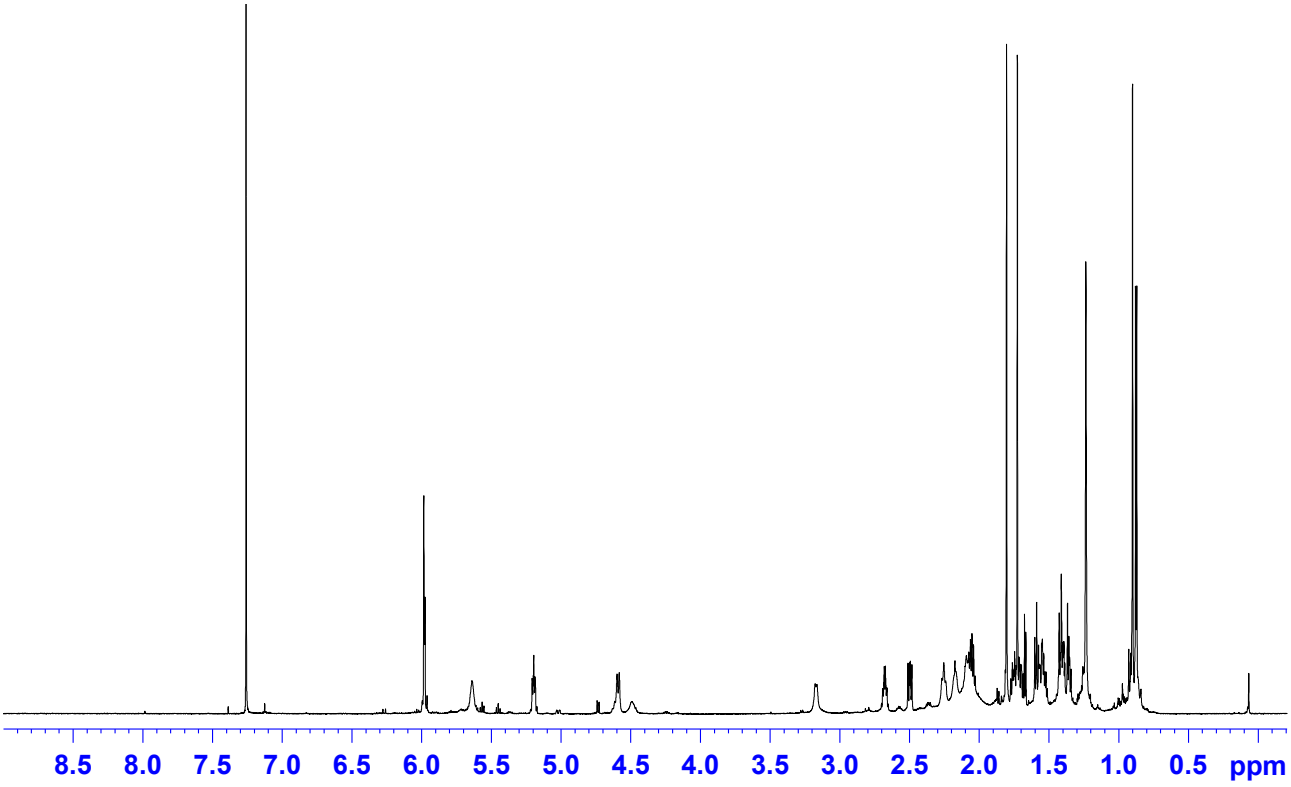

Figure S8. ^{13}C-NMR spectrum of ophiobolin H in $CDCl_3$ at 200 MHz.

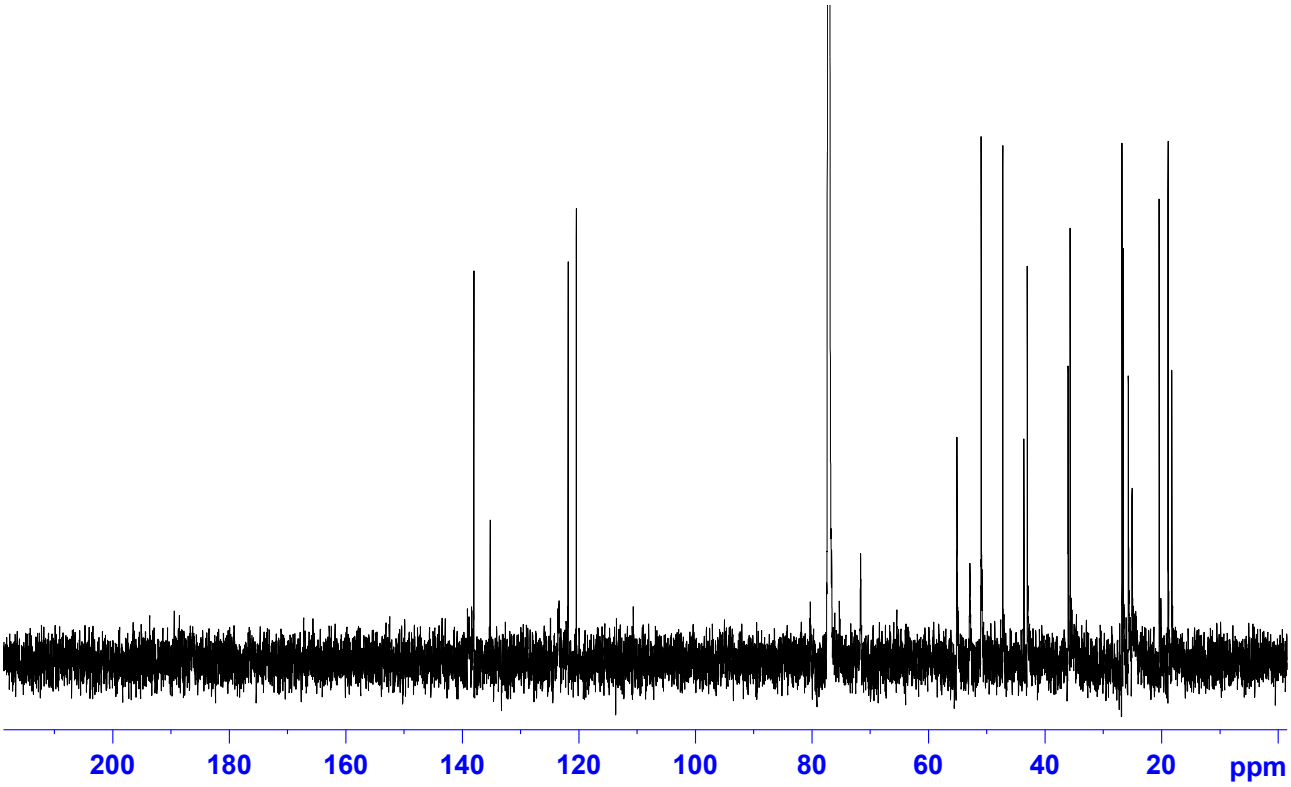

Table S11. ^{1}H- and ^{13}C-NMR for ophiobolin H in $CDCl_3$ at 800 MHz for ^{1}H and 200 MHz for ^{13}C.

	δ_H mult. (*J* (Hz))	δ_C	HMBC connectivities	NOE connectivities
1a	1.36 m	35.7	2, 6, 10, 11, 22	1b
1b	1.42 m	35.7		1a, 2, 8, 20
2	2.26 m	50.9		1b, 6, 20, 22
3		80.2		
4a	2.10 m	50.8		4b, 20
4b	2.18 m	50.8		4a
5		116.0		
6	3.17 d (9.8)	52.8		2, 9a, 22
7		138.5		
8	5.64 br.s.	123.6		1b, 9b
9a	1.70 m	25.0	8, 10, 11	6, 9b, 22
9b	2.50 dd (8.6; 13.8)	25.0	7, 8, 10, 11, 14	8, 9a, 10, 15, 16
10	1.60 m	55.0	8, 9, 11, 14, 15, 22	9b, 14
11		43.6		
12a	1.40 dd (7.6; 11.7)	43.0	10, 11, 14, 22	12b, 13a, 22
12b	1.57 m	43.0	13, 15	12a, 13b
13a	1.54 m	26.8	12, 14, 15	12a, 13b, 23
13b	1.76 m	26.8	10, 11, 14	12b, 13a, 14
14	2.05 m	47.2	10, 11, 13, 15, 16, 23	10, 13b, 16, 23
15	2.68 m	35.5	14, 16, 23	9b, 18, 22
16	5.20 m	138.0	18	9b, 14, 17, 23
17	5.99 m	121.7	15, 19	16, 24
18	5.98 m	120.4	16, 24, 25	15, 23, 25
19		135.2		
20	1.24 s	25.4	2, 3	1b, 2, 4a
21a	4.48 br.s.	71.5		
21b	4.59 d (12.2)	71.5		
22	0.90 s	18.7	1, 10, 11	2, 6, 9a, 12a, 15
23	0.88 d (6.7)	20.4	14, 15, 16	13a, 14, 16, 18
24	1.73 s	18.2	18, 19, 25	17
25	1.80 s	26.6	18, 19, 24	18

7.5 6-epiophiobolin N isolated from *A. insuetus* (IBT 28266)

Figure S9. ^{1}H-NMR spectrum of 6-epiophiobolin N in $CDCl_3$ at 800 MHz.

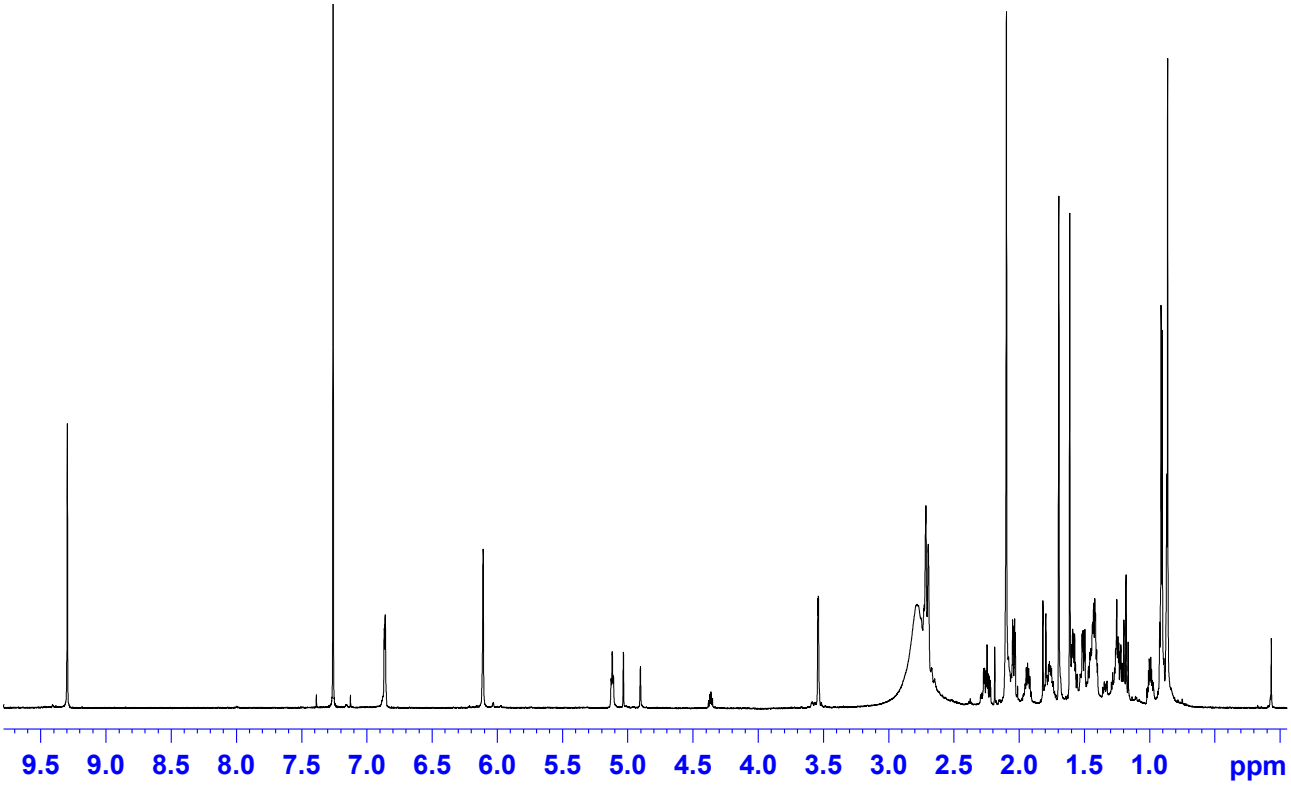

Figure S10. ^{13}C-NMR spectrum of 6-epiophiobolin N in $CDCl_3$ at 200 MHz.

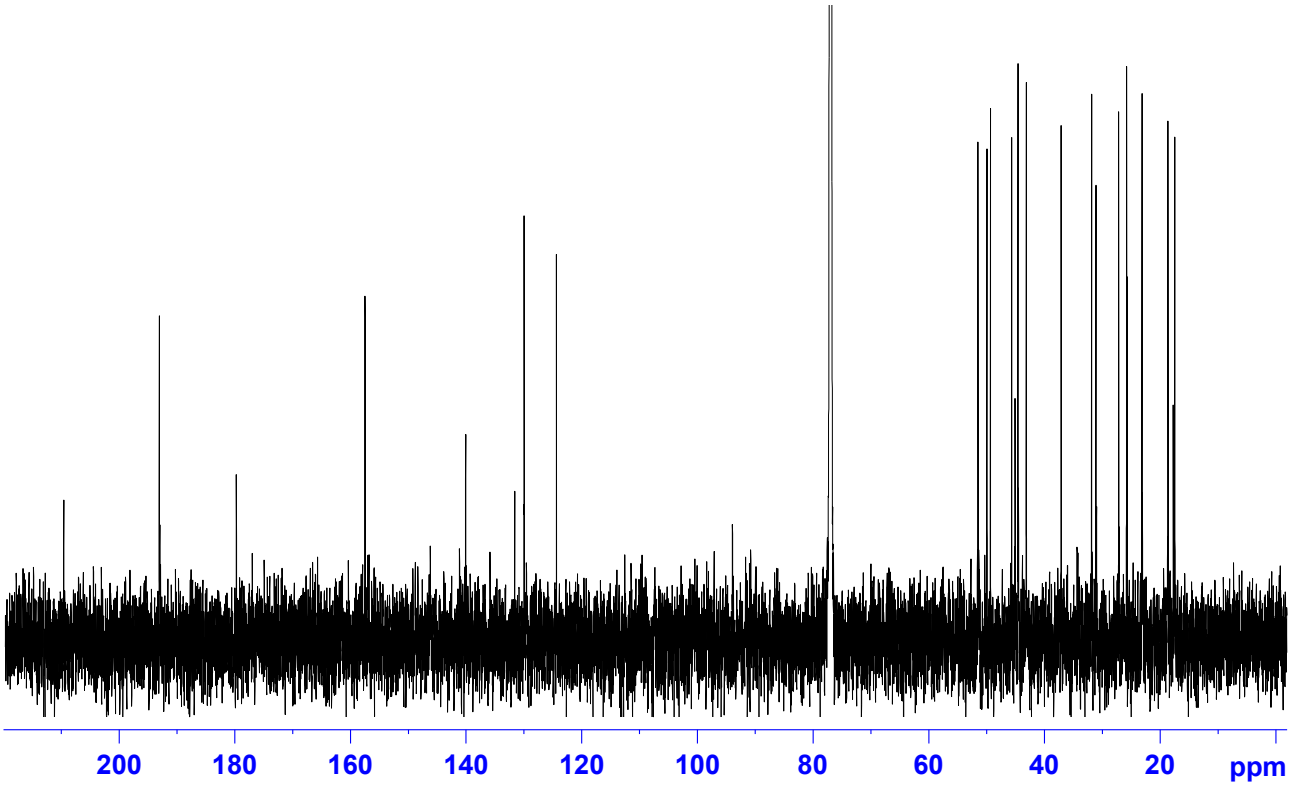

Table S12. ^{1}H and ^{13}C NMR for 6-epiophiobolin N in $CDCl_3$.at 800 MHz for ^{1}H and 200 MHz for ^{13}C.

	δ_H mult. (*J* (Hz))	δ_C	HMBC connectivities	NOE connectivities
1a	1.18 m	45.6	2; 3; 10; 12; 22	1b, 6, 10, 12a/15 *
1b	2.04 dd (3.7; 13.2)	45.6	2, 6, 10, 11	1a, 10, 12a/15 *, 12b, 22
2	2.71 m	49.3	8, 11	8. 9a, 16b, 20, 22
3		179.8		
4	6.11 s	130.0	3; 5; 6; 20	20
5		209.6		
6	3.54 d (3.7)	49.9	1; 2; 5; 7; 8; 21	1a; 2; (8); 9a, 10
7		140.1		
8	6.86 dd (2.0; 6.3)	157.3	6; 10; 21	2/9b **, (6), 9a, 21, 22
9a	2.25 m	31.0	7; 8; 10	2/9b **, 6, 8, 12a, 22
9b	2.71 m	31.0	8, 11	8. 9a, 12a/15 *, 20, 22
10	2.72 m	43.1	1, 7, 13, 14, 22	1a, 1b, 6, 14, 16b
11		45.0		
12a	1.42 m	44.5	1, 13, 22	1a, 1b, 9b, 12b, 13b, 14, 17a, 23
12b	1.51 m	44.5	10; 11; 14; 22	1b; 12a/15 *; 13a; 13b; 22
13a	1.23 m	27.1	12; 14; 15	12b; 13b; 22; 23
13b	1.58 m	27.1	10; 11	13a; 14, 12a/15 *; 23
14	1.75 m	51.1		9b, 10, 12a/15 *, 13b
15	1.42 m	31.8		1a, 1b, 9b, 12b, 13b, 14, 17a, 23
16a	0.99 m	37.1	15; 17; 18; 23	10; 17b; 18
16b	1.45 m	37.1	23	2/9b **; 10, 16a
17a	1.94 m	25.6	16; 18; 19	12a/15 *; 17b; 23
17b	2.07 m	25.6		16a; 17a; 23
18	5.12 t (7.0)	124.4	24; 25	15; 16a; 25
19		131.6		
20	2.10 s	17.4	2, 3, 4	2/9b **; 4
21	9.30 s	193.0	6, 7	8
22	0.86 m	23.1	1; 10; 12	1b; 2/9b **; 8; 9a; 12b; 13a
23	0.91 d (6.4)	18.6	14; 15; 16	10; 13a; 13b; 15; 16a; 17a; 17b
24	1.61 s	17.7	18; 19; 25	25
25	1.69 s	25.7	18; 19; 24	18; 24

* Not possible to distinguish between H12a and H15; ** Not possible to distinguish between H2 and H9b.

7.6 Ophiobolin K isolated from a new sp. in the *Aspergillus* section *Usti* (IBT 18591)

Figure S11. ^{1}H-NMR spectrum of ophiobolin K in $CDCl_3$ at 800 MHz.

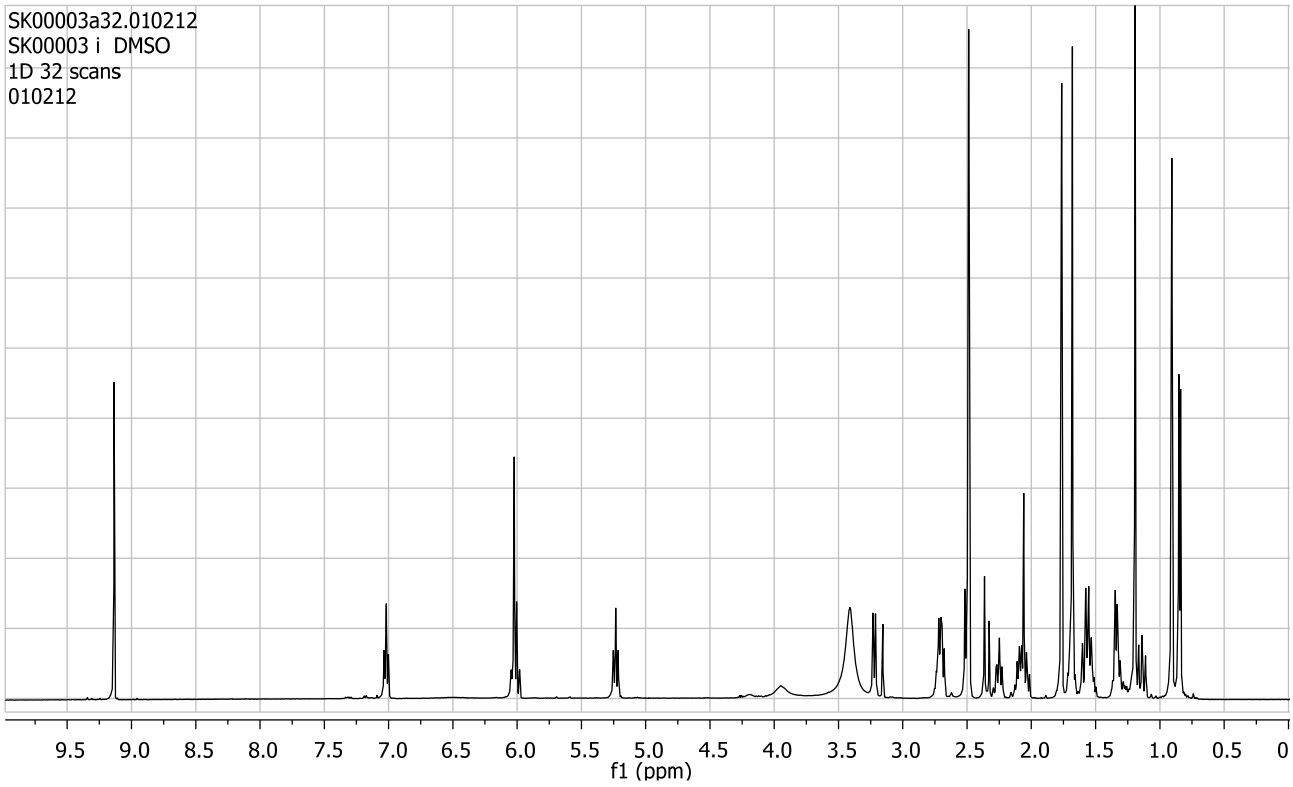

Table S13. ^{1}H and ^{13}C-NMR for ophiobolin K in DMSO-d_6 at 500 MHz for ^{1}H and 125 MHz for ^{13}C.

	δ_H mult. (*J* (Hz))	δ_C *	HMBC connectivities	NOE connectivities
1a	1.14 m	34.5	6, 10, 11, 22	
1b	1.58 m		6, 10, 11	2, 12a, 20
2	2.25 m	49.2	1, 4, 6, 7	1b, 4a, 6, 20, 22
3		76.2		
4a	2.35 m	53.9	3, 5, 20	2, 20
4b	2.50 m		2, 3, 5	
5		217.0		
6	3.22 d (9.8)	48.3	2, 3, 5, 7, 8, 21	2, 9a, 22
7		140.6		
8	7.02 t (8.5)	157.6	6, 9, 21	9b, 10, 21
9a	2.04 m	24.3	7, 8, 10, 11	6, 22
9b	2.69 m		7, 8, 10, 11, 14	8, 10, 16
10	1.56 m	53.0	1, 8, 9, 11, 14, 22	8, 9b, 12
11		43.3		
12a	1.33 m	42.2	10, 11, 13, 14, 22	1b, 13b, 22
12b	1.35 m			
13a	1.54 m	25.4	11, 15	14, 22, 23, 24
13b	1.69 m		11	12a, 14
14	2.09 m	46.2	10, 11, 13, 15, 16, 23	13a/b, 15, 16 , 23
15	2.72 m	34.4	16, 17, 23	14, 18, 22, 23
16	5.23 t (9.5)	136.9	14, 15, 18, 23	9b, 14, 17, 23
17	5.99 m	121.7	15, 18	16, 24
18	6.04 m	119.9	16, 19, 24, 25	15, 23, 25
19		134.6		
20	1.19 s	25.7	2, 3, 4	1b, 2, 4a
21	9.14 s	193.1	6, 7, 8	8
22	0.91 s	18.2	1, 10, 11	2, 6, 9a, 12a, 13a,15
23	0.85 d (6.6)	19.6	14, 15, 16	13a, 14, 15, 16, 18
24	1.68 s	18.0	18, 19, 25	13a, 17, 25
25	1.76 s	25.9	18, 19, 24	18, 24

* ^{13}C NMR chemical shifts determined from HSQC and HMBC experiments.

7.7 6-Epiophiobolin K isolated from a new sp. in the *Aspergillus* section *Usti* (IBT 18591)

Figure S12. ^{1}H-NMR spectrum of 6-epiophiobolin K in $CDCl_3$ at 800 MHz.

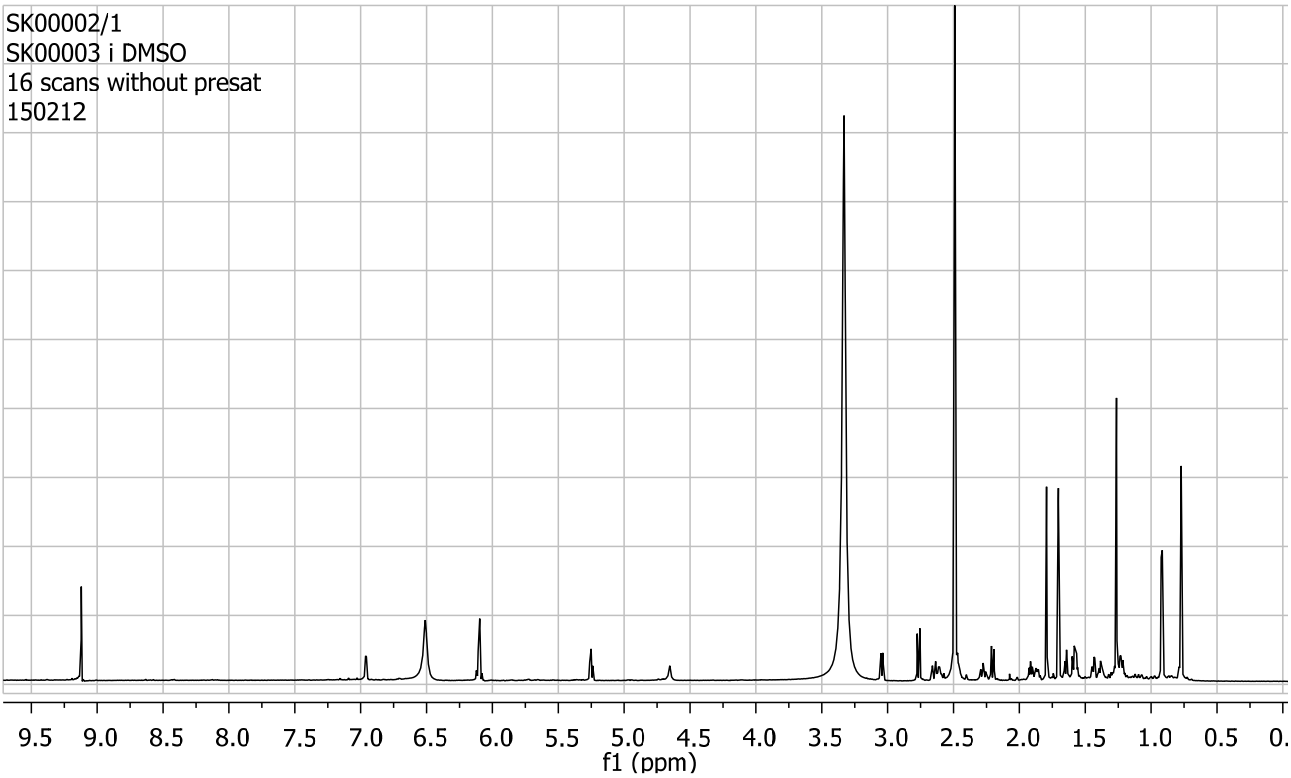

Figure S13. ^{13}C-NMR spectrum of 6-epiophiobolin K in $CDCl_3$ at 200 MHz.

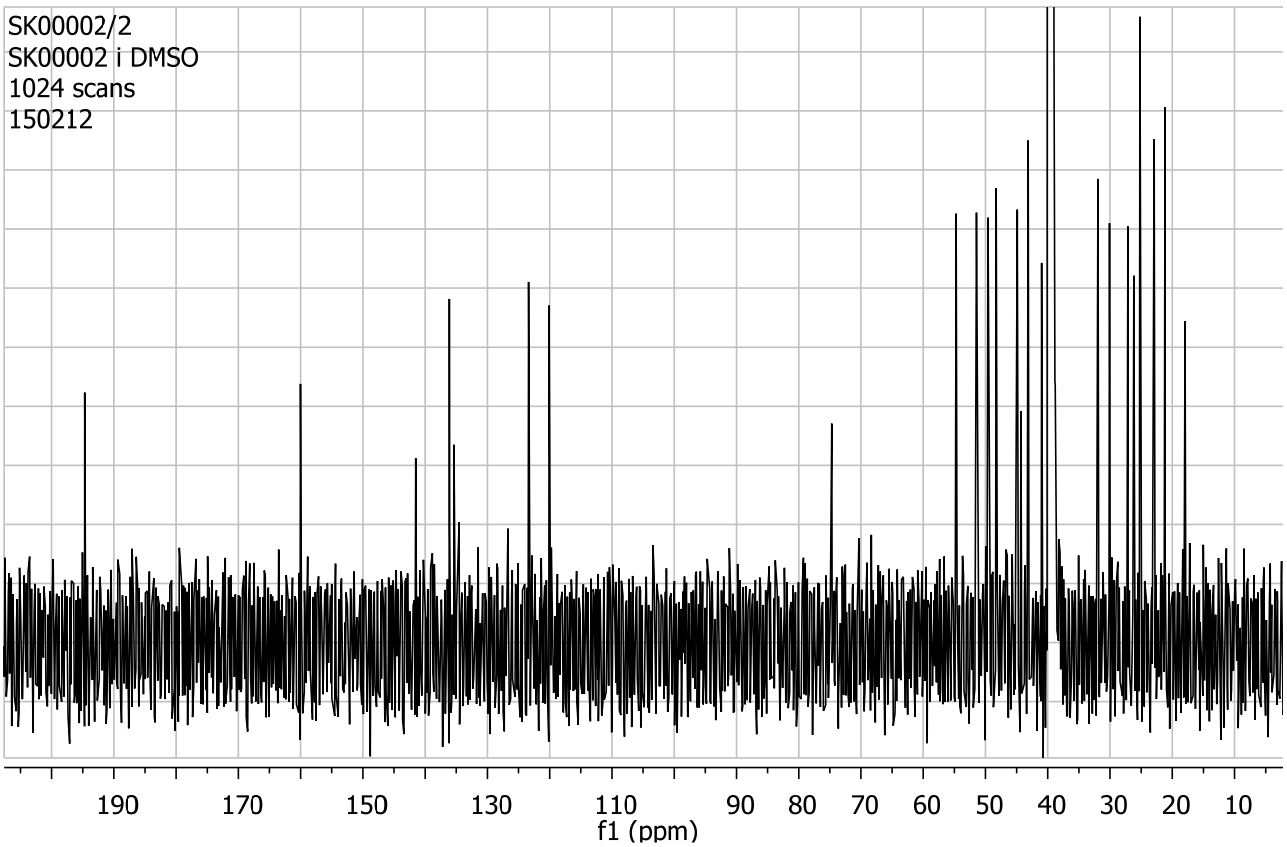

Table S14. ^{1}H and ^{13}C-NMR for 6-epiophiobolin K in DMSO-d_6 at 500 MHz for ^{1}H and 125 MHz for ^{13}C.

	δ_H mult. (*J* (Hz))	δ_C	HMBC connectivities	NOE connectivities
1a	1.58 m	41.0	2, 6, 10, 22	6, 12a
1b	1.65 m			2, 20, 22
2	1.91 m	49.6	6, 7	1a/b , 4b, 20, 22
3		74.7		
3-OH	6.51 br.s.			
4a	2.21 m	54.7	2, 3, 5	20 (w)
4b	2.77 d (16.0)		3, 5, 20	2, 20
5		216.1	-	
6	3.04 d (10.8)	48.2	1, 2, 5, 7, 21	1a, 2 (w), 10
7		141.5		
8	6.96 m	159.9	6, 10, 21	9a/b, 21, 22
9a	2.27 m	30.0	7, 8	8, 22 (w)
9b	2.65 m			8, 10
10	2.46 m	43.1		6, 9b, 14
11		44.9		
12a	1.38 m	44.4	10, 22	1a
12b	1.44 m		10, 22	22
13a	1.22 m	27.1	14, 15	22
13b	1.57 m			14, 23
14	1.87 m	51.4		10, 13b, 16, 23
15	2.61 m	31.9		17, 23
16	5.25 t (9.3)	136.0	14, 18	14, 17, 23
17	6.11 m	123.3	15, 19	16, 24
18	6.09 m	120.1	24, 25	15, 23, 25
19		135.3		
20	1.26 s	25.2	2, 3, 4	1b, 2, 4b
21	9.12 s	194.7	6, 7, 8	8
22	0.77 s	22.8	1, 10, 11	1b, 2, 8, 9a, 12b, 13a
23	0.92 d (6.6)	21.1	14, 15, 16	13b, 14, 15, 16, 17
24	1.70 s	17.9	18, 19, 25	17
25	1.79 s	26.1	18, 19, 24	17

7.8 Ophiobolin C isolated from *A. calidoustus* (IBT 25726)

Figure S14. ^{1}H-NMR spectrum of ophiobolin C in $CDCl_3$ at 800 MHz.

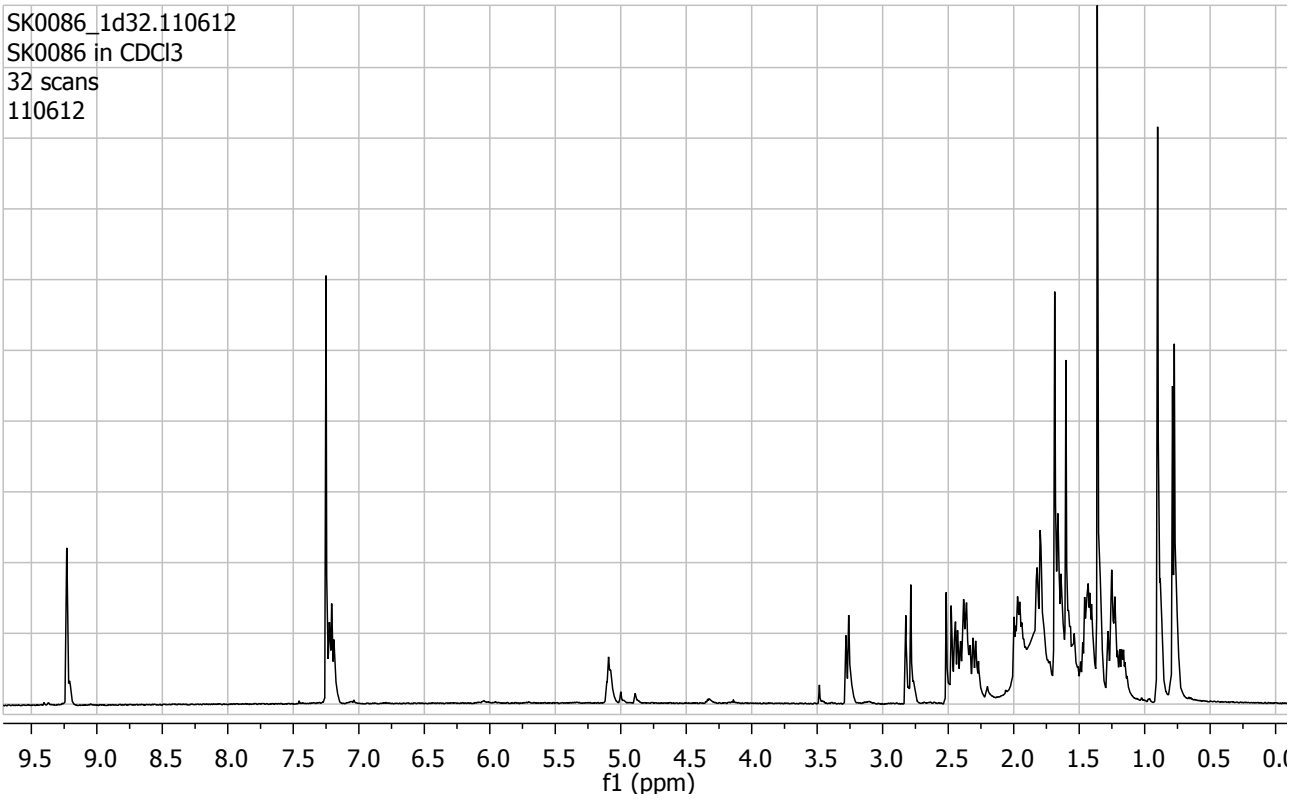

Table S15. ^{1}H and ^{13}C-NMR for ophiobolin C in $CDCl_3$ at 800 MHz for ^{1}H and 200 MHz for ^{13}C.

	δ_H mult. (*J* (Hz))	δ_C *	HMBC connectivities	NOE connectivities
1a	1.26 m	36.0	2, 10, 11	
1b	1.81 m		6, 10	2, 12a, 20
2	2.38 m	50.8		1b, 4a, 6, 20, 22
3		76.6		
4a	2.49 m	54.6	5, 20	2, 20
4b	2.80 m		2, 3, 5	20
5		217.5		
6	3.26 m	48.4	2, 3, 5, 7, 8, 21	2, 9a, 22
7		141.5		
8	7.21 m	163.8	6, 9, 21	9b, 10, 21
9a	2.31 m	24.7	7, 8, 10, 11	6, 22, 23
9b	2.45 m		7, 8, 10, 11	8, 10
10	1.67 m	53.4	8, 14, 15	8, 9b, 16b
11		43.6		
12a	1.41 m	42.6		1b, 22
12b	1.44 m			
13a	1.46 m	22.8	11	23
13b	1.55 m		10, 11	14
14	2.36 m	45.2		13b, 15, 16b, 17b
15	1.65 m	32.7	16	14, 23
16a	1.18 m	36.8	14, 15, 17, 18, 23	17a, 23
16b	1.24 m		14, 15, 17, 18, 23	1b, 10, 14,17b, 18
17a	1.95 m	26.0	15, 16, 18, 19	16a,18
17b	2.00 m		16, 18, 19	14, 16b, 23, 24
18	5.09 m	124.3	24, 25	16b, 17a, 25
19		131.0		
20	1.36 s	25.4	2, 3, 4	1b, 2, 4a/b
21	9.23 s	195.9	6, 7	8
22	0.90 s	19.0	10, 11, 12	2, 6, 9a, 12a
23	0.78 d (6.8)	16.4	14, 15, 16	9a, 13a, 15, 16a, 17b
24	1.61 s	17.6	18, 19, 25	17b
25	1.69 s	25.6	18, 19, 24	18

* ^{13}C NMR chemichal shifts determinated from HSQC and HMBC experiments.

7.9 6-epiophiobolin G isolated from *A. calidoustus* (IBT 25726)

Figure S15. ^{1}H-NMR spectrum of 6-epiophiobolin G in $CDCl_3$ at 800 MHz.

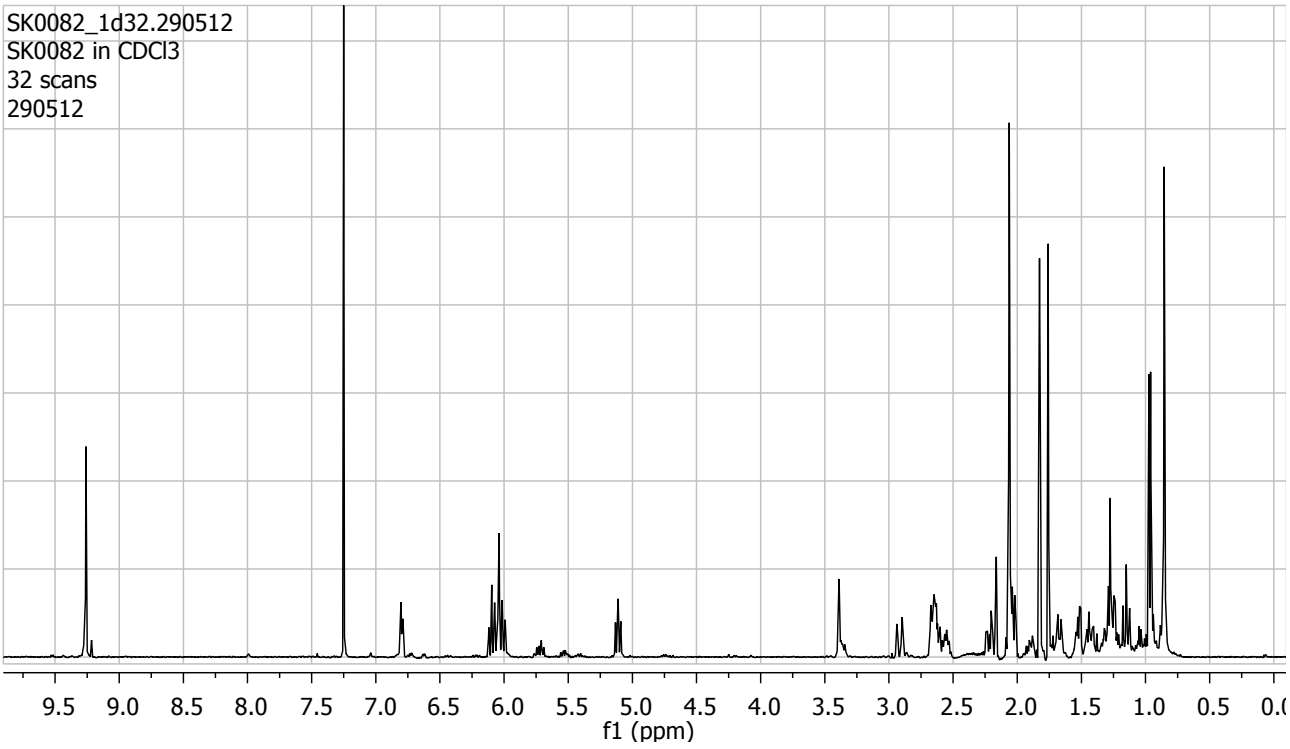

Figure S16. ^{13}C-NMR spectrum of 6-epiophiobolin G in $CDCl_3$ at 200 MHz.

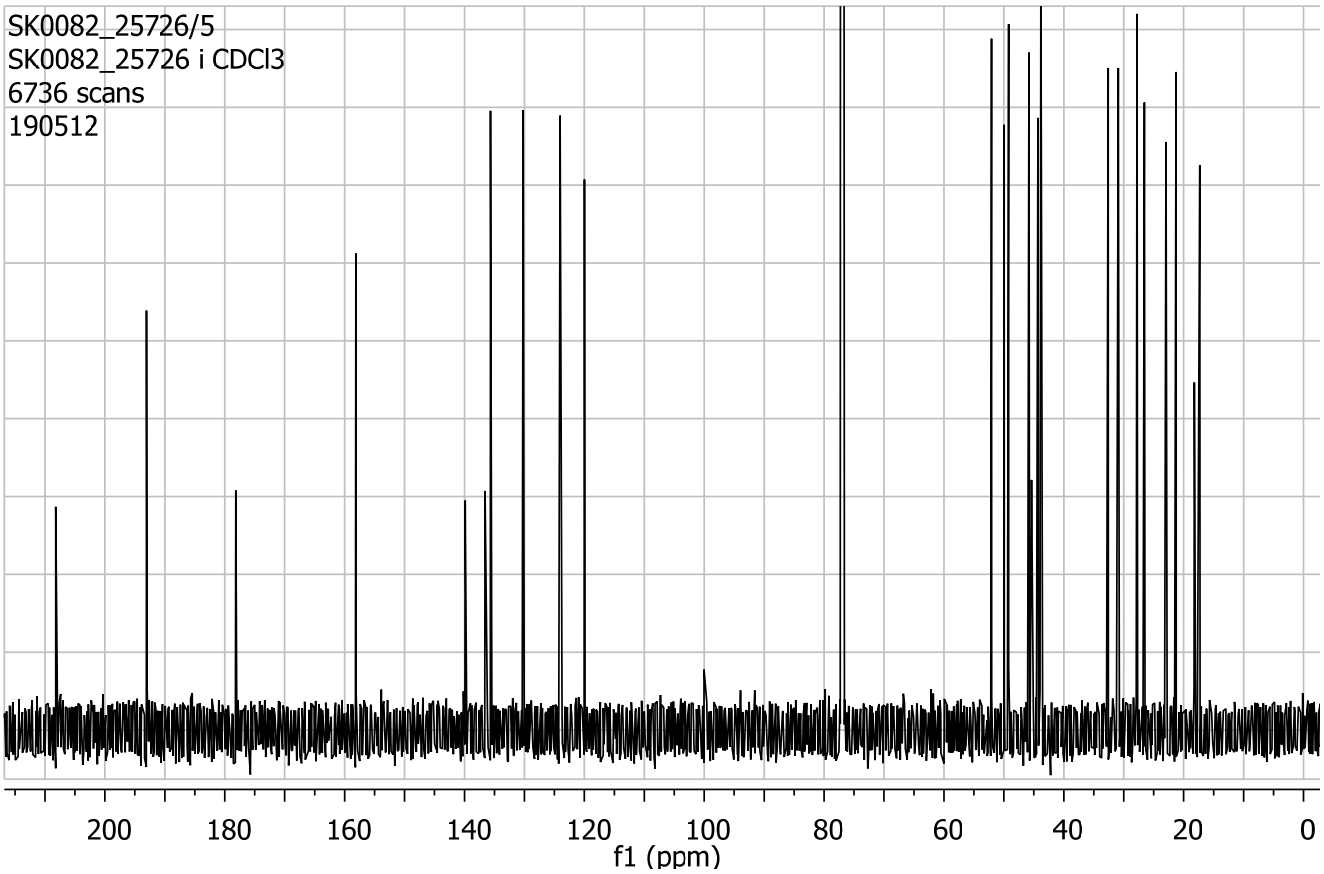

Table S16. ^{1}H and ^{13}C-NMR for 6-epiophiobolin G in $CDCl_3$ at 800 MHz for ^{1}H and 200 MHz for ^{13}C.

	δ_H mult. (*J* (Hz))	δ_C	HMBC connectivities	NOE connectivities
1a	1.15 m	45.8	2, 3, 10, 11, 22	6, 10, 12a
1b	2.03 m		3, 6, 12, 22	2, 22
2	2.66 m	49.2	1	1b, 22
3		178.1		
4	6.04 s	130.2	3, 5, 6, 20	20
5		208.2		
6	3.40 m	50.0	1, 2, 5, 7, 8, 21	1a, 10
7		139.9		
8	6.80 m	158.1	6, 9, 10, 21	9a/b, 21, 22
9a	2.20 m	30.9	7, 8, 10, 14	8, 15, 22
9b	2.93 m		7, 8, 10, 11	8, 10
10	2.63 m	43.8	8, 9, 11, 13, 14, 22	1a, 6, 9b, 14
11		45.4		
12a	1.43 m	44.3	1, 13, 14, 22	1a, 13b
12b	1.52 m		1, 10, 13, 14, 22	22
13a	1.25 m	27.8	12, 14, 15	22
13b	1.67 m		10, 11, 14	12a, 14, 23
14	1.89 m	52.1	9, 10, 13, 15, 16, 23	10, 13b, 16, 23
15	2.55 m	32.6	14, 16, 17, 23	9a/b, 18, 23
16	5.11 t (1.3)	135.7	14, 15, 17, 18, 23	14, 17, 23
17	6.10 m	124.0	15, 18, 19, 23	16, 24
18	6.00 m	120.0	16, 17, 24, 25	15, 23, 25
19		136.6		
20	2.06 s	17.3	2, 3, 4, 5	4
21	9.26 s	193.0	6, 7	8
22	0.85 s	22.9	1, 12	1b, 2, 8, 9a, 12b, 13a
23	0.97 d (6.8)	21.3	14, 15, 16	13b, 14, 15, 16,18
24	1.76 s	18.2	18,19, 25	17
25	1.83 s	26.5	18,19, 24	18

7.10 Activity of ophiobolin A, B, C and K + 6-epiophiobolin K towards healthy fibroblasts (Wi-38) cells

Figure S17. Activity of ophiobolin A, B, C and K + 6-epiophioboln K towards healthy fibroblasts (Wi-38).

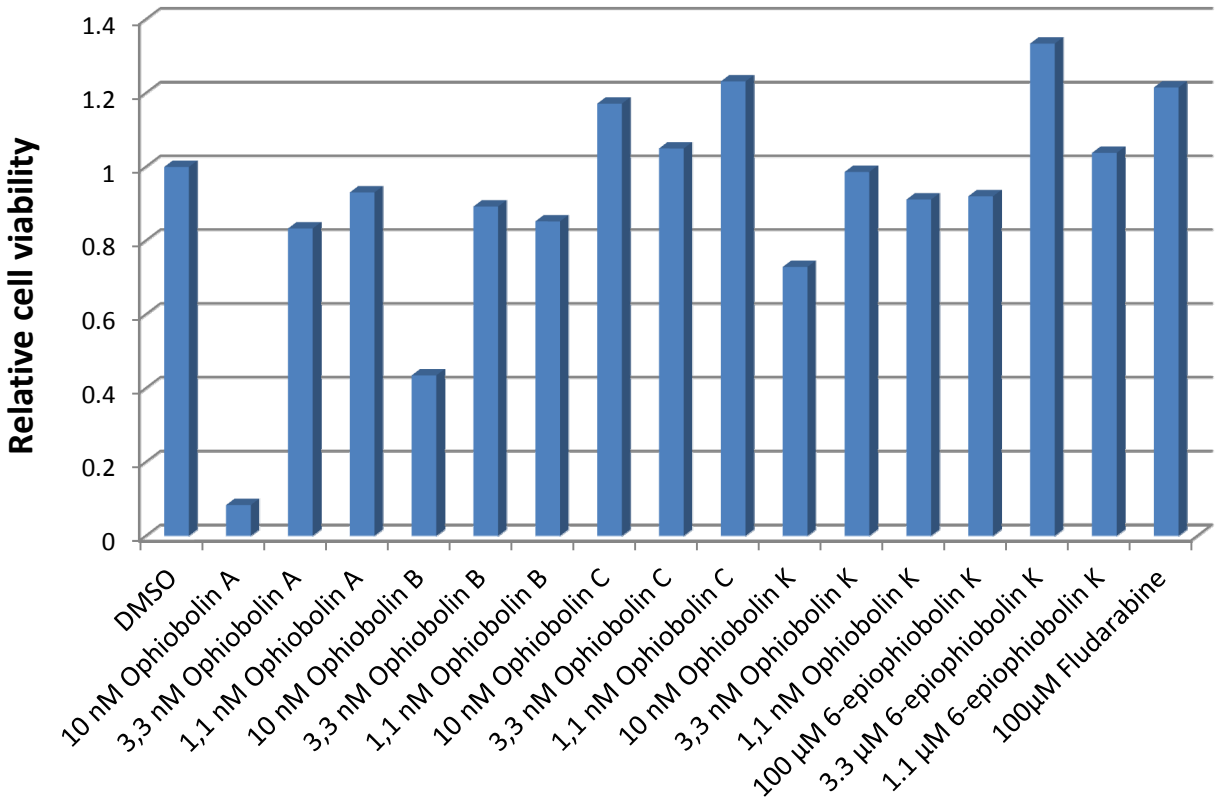

7.11 Apoptosis induction in CLL cells by different ophiobolins

Figure S18. CLL cells cultured in DMEM were treated for 24 hours with two different concentrations of ophiobolin A, ophiobolin B, ophiobolin C and ophiobolin K. In order to analyze apoptosis induction, cells of each well were divided into two parts and analyzed by flow cytometry using two different staining strategies. (**a**) cell survival was analyzed by gating on cells that were negative for Annexin V-phycoerythrin (PE) and 7-amino-actinomycin (7-AAD). Relative survival compared to DMSO control (0.1%) is depicted as mean values +SD of 4 independent CLL samples; (**b**) Caspase-3 activity is depicted as mean values +SD of 4 independent CLL samples relative to DMSO control (0.1%).

(**a**)

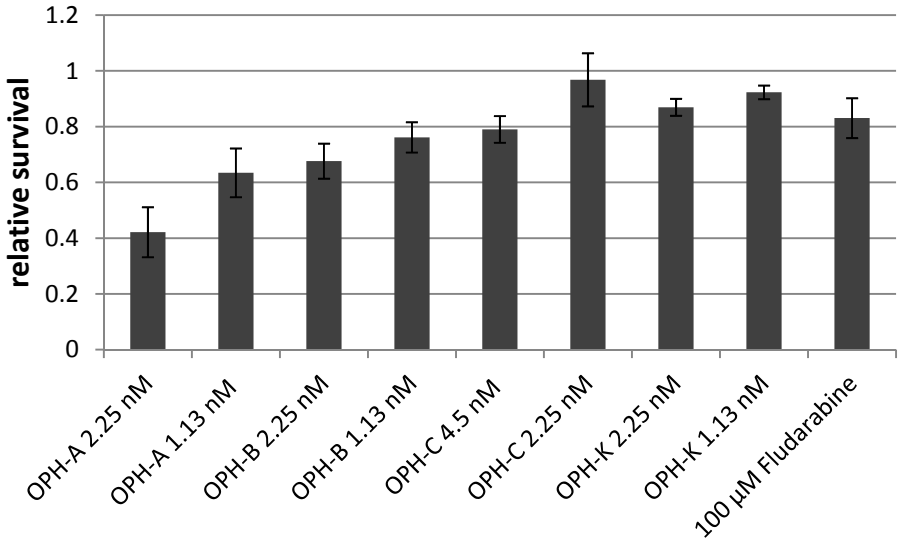

(**b**)

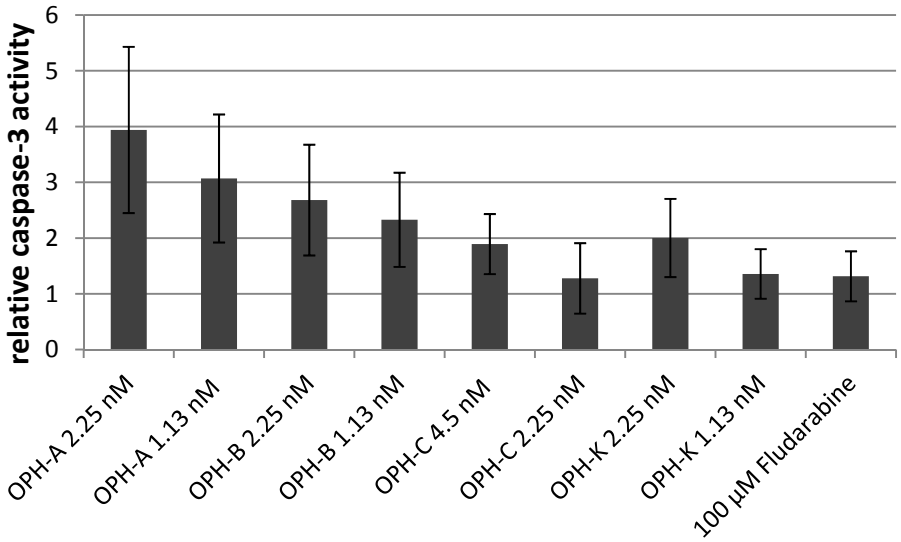

Tanja Thorskov Bladt
Chemical biology of microbial anticancer natural products - appendix

Experimental (*Penicillium jugorum* and *Penicillium pinicola*)

The *P. jugorum* (IBT 22779) and *P. pinicola* (IBT16545) extracts were prepared for initial screen in accordance with the micro-extraction method developed by Smedsgaard [Smedsgaard, J. *J. Chromatogr. A* **1997**, *760*, 264–270][1]. Five plugs were collected across the colony. The samples were subsequently extracted using (3:2:1 v/v/v) MeOH, DCM and EtOAc with 0.5 % FA.

For large scale *P. jugorum* and *P. pinicola* were cultivated on 50 plates on CYA and YES, respectively for 8 days at 25°C in the dark and extracted with EtOAc + 1 % FA. The crude extracts were fractionated on a RP C_{18} (25 g, 33 ml) column flash column with at gradient of: 15-100 % ACN in 20 min and flow rate 25 ml/min.

Both extracts were fractionated in analytical (5 mg per column) scale in accordance with the E-SPE method developed by Månsson *et al.* [2]. The E-SPE setup contained SAX, MAX, and SCX ion-exchanger SPE columns though without the Sephadex LH-20 column. Additionally two normal phase (amino and diol) columns were add to the setup. For each extract, 5 mg was loaded on both the amino column (100 mg, 1 ml) and the diol column (100 mg, 1 ml). The compounds were eluted by 2 column volume (CV) heptane, 2 CV DCM, 2 CV DCM:EtOAc (1:1), 2 CV EtOAc, 2 CV EtOAc:MeOH, 2 CV MeOH, 4 CV ACN, 2 CV ACN:MQ + 2% FA (75:25), 2 CV ACN:MQ + 2% FA (50:50), 2 CV ACN:MQ + 2% FA (25:75), 2 CV ACN:MQ + 2% FA (10:90). No further fractionations were done with the *P. jugorum* and *P. pinicola* extract.s.

References:

1. Smedsgaard, J. Micro-scale extraction procedure for standardized screening of fungal metabolite production in cultures. *J. Chromatogr. A* **1997**, *760*, 264–270.

2. Månsson, M.; Phipps, R. K.; Gram, L.; Munro, M. H. G.; Larsen, T. O.; Nielsen, K. F. Explorative solid-phase extraction (E-SPE) for accelerated microbial natural product discovery, dereplication, and purification. *J. Nat. Prod.* **2010**, *73*, 1126–1132.

Tanja Thorskov Bladt
Chemical biology of microbial anticancer natural products - appendix

Paper *3*

Sclerotionigrin A and B, two Novel Cytochalasans Targeting Chronic Lymphocytic Leukemia

Petersen, L.M.; **Bladt, T.T.**; Dürr, D.; Seiffert, M.; Gotfredsen, C.H. and Larsen, T.O.

Manuscripts intented for Organic Letters

Tanja Thorskov Bladt
Chemical biology of microbial anticancer natural products - appendix

Sclerotionigrin A and B, two Novel Cytochalasans Targeting Chronic Lymphocytic Leukemia

Lene M. Petersen[1], Tanja T. Bladt[1], Claudia Dürr[2], Martina Seiffert[2], Jens C. Frisvad[1], Charlotte H. Gotfredsen[3], Thomas O. Larsen[1,*]

[1]Technical University of Denmark, Department of Systems Biology, Søltofts Plads, Building 221, DK-2800 Kgs. Lyngby, Denmark, [2]German Cancer Research Center, Molecular Genetics, Im Neuenheimer Feld 280, D-69120 Heidelberg, Germany, [3]Technical University of Denmark, Department of Chemistry, Kemitorvet, Building 201, DK-2800 Kgs. Lyngby, Denmark.

Supporting Information Placeholder

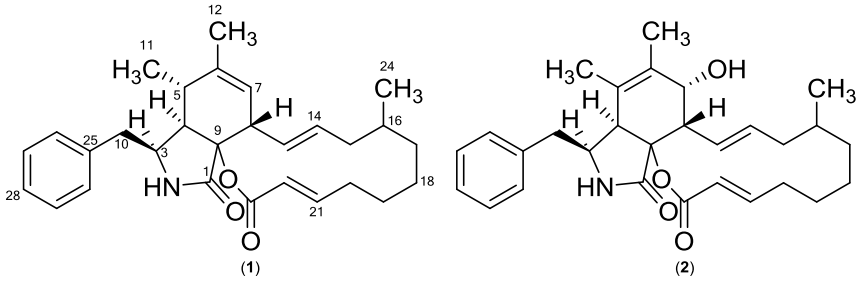

ABSTRACT: Two new cytochalasans, sclerotionigrin A (1) and B (2) were isolated together with the known proxiphomin (3) from the filamentous fungus *Aspergillus sclerotioniger*. The structures and relative stereochemistry of 1 and 2 were determined based on comparison with 3, and from extensive 1D and 2D NMR spectroscopic analysis, supported by high resolution mass spectrometry (HRMS). All three compound displayed cytotoxic activity towards chronic lymphocytic leukemia cells *in vitro*, with 3 as the most active.

Chronic lymphocytic leukemia (CLL) is the most common type of leukemia among adults in the Western World. CLL is considered as an incurable disease and todays applied treatment strategies primarily aim at prolonging patient survival[1,2]. Consequently discovery of compounds that act against CLL and other types of cancer cells is crucial. Numerous types of anticancer compounds have been reported in the literature[3,4], and with the increase in specific biological assays, both novel and previously described compounds might display promising novel bioactivities[5,6]. An important and diverse group of fungal anticancer compounds that have caught our interest are the cytochalasans due to their wide range of biological functions[7]. In particular this includes inhibitory activities towards lung, ovarian, and human colon cancer as well as human leukemia[8,9]. Recently, we have demonstrated that chaetoglobosin A, produced by *Penicillium aquamarinum*, selectively induce apoptosis in CLL cells with a median lethal dose (LD_{50}) value of 2.8 µM.[10] Encouraged by this finding we searched for potential novel cytochalasan type of compounds in black aspergilli. The only indication of production of any cytochalasans in *Aspergillus* subgenus *Circumdati* section *Nigri* is aspergillin PZ, for which the precursor aspochalasin C or D has been suggested[11,12]. However in the sister clade *Aspergillus* subgenus *Circumdati* section *Flavipedes*, many cytochalasans have been reported, including aspochalasin A-D[13], E[14], F & G[15], D & H[16], I-K[17,18], L[19], U[20] and TMC-169[21] in addition to aspochalamin A-D, aspochalasin D & Z[22], rosellichalasin[23], and cytochalasin E, 5,6-dehydro-7-hydroxy cytochalasin E, and a $\Delta^{6,12}$-5,6-dehydro-7-hydroxy cytochalasin E, 10-phenyl-[12]-cytochalasin Z16, 10-phenyl-[12]-cytochalasin Z17, cytochalasin Z11, cytochalasin Z13, Z16-Z20, and rosellichalasin[24,25,26,27,28]. In another species of *Aspergillus* subgenus *Circumdati* section *Circumdati*, *Aspergillus elegans* aspochalasin A1, B, D, H, I, J, cytochalasin Z24, zygosporin D, rosellichalasin and aspergillin PZ were found[29] supporting the view that aspochalasin D is a precursor of aspergillin PZ. Finally in the less closely related *Aspergillus clavatus* in *Aspergillus* subgenus *Fumigati* section *Clavati* cytochalasin E and K have been isolated[30,31].

Here we report the target-guided isolation and structure elucidation of the two novel cytochalasins sclerotionigrin A (**1**) and B (**2**) based on UV, MS, and NMR data. **1** and **2** were isolated from *Aspergillus sclerotioniger* (IBT 22905) together with the known cytochalasin proxiphomin (**3**)[32]. We have previously reported ochratoxin A, ochratoxin B and pyranonigrin A from this isolate[33].

A. sclerotioniger (IBT 22905) was inoculated and extracted. After work up the extract was dryloaded on diol resin and fractionated on a 50 g pre-packed diol column using an Isolera flash purification system (Biotage). The compounds were eluted using a 7 step gradient of heptane-DCM-EtOAc-MeOH

with a flow rate of 40 ml/min. Fractions were collected automatically (66 ml in each fraction). The Isolera fractions were subjected to further purification on a semi-preparative HPLC Waters 600 Controller with a 996 photodiode array detector (Waters) on a Luna II C_{18} column (250 x 10 mm, 5 µm, Phenomenex). A flowrate of 5 mL/min was used and 50 % ACN isocratic for 5 min, then to 100 % in 15 min. 50 ppm TFA was added to ACN and milliQ-water. This yielded **1** (7.8 mg), **2** (2.1 mg), and **3** (1.3 mg).

The structure of compound **3** was tentatively identified through UHPLC-DAD-HRMS based dereplication of the crude extract. The pseudomolecular ion, $[M+H]^+$, was recognized from the mass spectrum due to the presence of the sodiated adduct, $[M+Na]^+$ and the corresponding dimeric adducts $[2M+H]^+$ and $[2M+Na]^+$. The molecular formula $C_{29}H_{37}NO_2$ was established with an accuracy of 0.8 ppm through the monoisotopic mass of $[M+H]^+$ of *m/z* 432.2901. The formula was used for a query in Antibase2012[34] with one resulting hit, proxiphomin (**3**). NMR data and optical rotation of **3**[35] matched published data[32].

Compound **1** was purified as a yellow powder. The UV spectrum displayed absorption maxima at 210 nm. The ESI^+ spectrum showed a distinct adduct pattern consisting of $[M+H]^+$, $[M+Na]^+$, $[2M+H]^+$ and $[2M+Na]^+$. The molecular formula $C_{29}H_{37}NO_3$ (12 double-bond equivalents) was obtained from HRMS of $[M+H]^+$ (*m/z* 448.2843) with an accuracy of 2.3 ppm. The ^{1}H NMR spectra revealed the presence of one amide proton, 15 methines (five which were vinylic and five aromatic), six methylene, and three methyls (Table 1).

The DQF-COSY spectrum of **1** defined four spin systems. The linking between COSY spin systems and assignments of the remaining signals and quaternary carbons were accomplished through detailed analysis of HMBC experimental data (Figure 1).

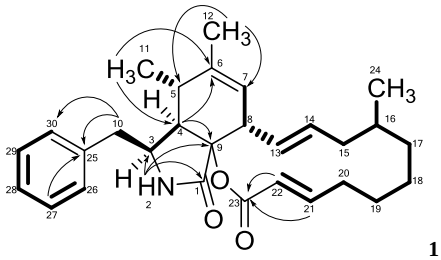

1

Figure 1. Important HMBC correlations connecting the three COSY spin systems (marked in bold) in **1**. The remaining HMBC correlations are found in Table 1.

The HMBC correlations from the protons at δ_H 1.65 ppm (H10) and 7.26 (H27 and H29) to a quaternary carbon at δ_C 137.8 (C25), together with HMBC correlations from the protons at δ_H 7.14 (H26 and H30) to the carbon at δ_C 42.6 (C10) linked two of the spin systems belonging to the Phe moiety in **1**. The amide proton at δ_H 8.00 ppm (H2) displayed HMBC correlations to the carbons at δ_C 54.2 (C3) and 170.6 ppm (C1). Combination of these HMBC correlations established the Phe moiety of **1**, which was incorporated on the polyketide (PK) part of the molecule.

Table 1. NMR data for sclerotionigrin A (1).†

No.	δ_H (integral, mult., *J* [Hz])	δ_C	HMBC	NOESY
1	-	170.6	-	-
2	8.00 (1H, s)	-	1, 3, 4, 9	3, 10
3	3.09 (1H, td, 5.8, 3.1)	54.2	-	2, 4, 10, 11, 12, 26/30
4	2.53 (1H, dd, 4.2, 3.1)	49.1	3, 5, 6, 9	3, 10, 11, 26/30
5	2.57 (1H, m)	33.6	-	7, 8, 11
6	-	140.0	-	-
7	5.25 (1H, m)	123.6	-	5,8, 12
8	3.15 (1H, m)	45.8	-	5, 7, 13, 14
9	-	85.4	-	-
10	2.82 (2H, dd, 5.8, 2.2)	42.6	3, 4, 25, 26/30	3, 4, 26/30
11	0.68 (3H, d, 7.1)	12.8	4, 5, 6	3, 4, 5, 12, 26/30
12	1.65 (3H, s)	19.4	5, 6, 7	3, 7, 11
13	5.85 (1H, ddd, 14.8, 10.0, 1.2)	128.9	15	8, 15
14	5.22 (1H, m)	132.6	8	8, 15', 16
15	1.60 (1H, d, 13.5)	40.7	13, 14, 16	13, 15'
15'	2.07 (1H, dd, 13.5, 2.1)	40.7	-	14, 15, 16, 20', 24
16	1.36 (1H, m)	31.9	-	14, 15', 19'
17	0.61 (1H, m)	33.8	-	17', 18', 24
17'	1.66 (1H, m)	33.8	-	17
18	1.14 (1H, m)	25.9	-	18'
18'	1.53 (1H, m)	25.9	-	17, 18
19	1.29 (1H, m)	25.3	-	24
19'	1.68 (1H, m)	25.3	-	16, 21
20	2.23 (1H, m)	33.1	-	20', 21
20'	2.29 (1H, m)	33.1	-	15', 20, 22
21	6.96 (1H, ddd, 15.5, 8.6, 6.8)	151.7	23	19', 20, 22
22	5.65 (1H, d, 15.5)	120.6	20, 23	20', 21
23	-	163.5	-	-
24	0.84 (3H, d, 6.3)	20.0	15, 16, 17	15', 17, 19
25	-	137.8	-	-
26‡	7.14 (1H, d, 7.5)	129.5	10, 26/30 28	3, 4, 10, 11
27‡	7.26 (1H, t, 7.4)	128.0	25, 29	-
28	7.18 (1H, t, 7.5)	126.1	26, 30	-
29‡	7.26 (1H, t, 7.5)	128.0	25, 27	-
30‡	7.14 (1H, d, 7.5)	129.5	10, 26/30, 28	3, 4, 10, 11

† ^{1}H NMR data were obtained at 500 MHz in DMSO-d_6 and ^{13}C data were obtained at 125 MHz in DMSO-d_6. ^{13}C-NMR chemical shifts determined from HSQC and HMBC experiments. ‡It was not possible to distinguish between no. 26 and 30 as well as no. 27 and 29.

The PK part of **1**, could be established through a large COSY spin system (from H7 to H22), equal to that seen in **3**. Furthermore a COSY coupling was found between the proton at δ_H 2.57 ppm (H5) and a methyl group at 0.68 ppm (C11). This part was coupled to the PK part by a week COSY coupling between H5 and H7 identified as a w-coupling. The COSY spin system could furthermore be connected via HMBC correlations to the above mentioned Phe moiety as well as the PK part. The protons at δ_H 1.65 (H12) correlated to the carbons at δ_C 33.6 (C5) and 123.6 ppm (C7) where proton at δ_H 0.68 (H11) correlated to the carbons at δ_C 49.1 (C4) and 140.0 ppm (C6). The proton at 2.53 ppm (H4) correlated to

C5, C6 and the quaternary carbon at δ_C 85.4 ppm (C9). Finally the PK chain was closed via an ester bond assigned from HMBC correlations from the vinylic protons at δ_H 5.65 (H22) and 6.96 ppm (H21) to the carbonyl carbon at δ_C 163.5 ppm (C23) supported by the high chemical shift of the quaternary carbon at δ_C 85.4 ppm (C9) indicating that C9 is bound to oxygen, and a carbonyl group, similar to what is seen in several other cytochalasans.[7]

This structure accounted for all the degree of unsaturation required by the formula allowing the assignment of **1** as sclerotionigrin A.[36] The size of the vicinal coupling constants ($^3J_{HH}$) for H13/H14 and H21/H22 were rather large (14.8 and 15.5 Hz respectively) suggestion trans stereochemistry. NOESY experiments enabled determination of the relative stereochemistry for most of the stereogenic centers of **1** to be very similar to those of **3**. NOE connectivities were found between the proton at δ_H 3.09 ppm (H3), δ_H 2.53 (H4) and the methyl at δ_H 0.68 ppm (H11) placing these protons at the same side of the central ring system. Other NOE connectivities were observed between the protons at δ_H 2.57 ppm (H5), 5.25 (H7) and 3.15 (H8), whereas no NOE connectivities could be seen to H3, H4 or H11, strongly indicating the positioning of H5, H7 and H8 on the opposite side of the central ring system compared to H3, H4 and H11. The stereocenters at C9 and C16 could not be assigned through NOESY correlations, however being biosynthesized by the same fungus we propose that the stereochemistry at these centers are identical to those of **3**. Especially we note that the extra oxidation between C9 and C23 in other cytochalasans never leads to a change in stereochemistry at C9.[7,15] We do however note that the optical rotation of **1** and **2** are positive as opposed to that of **3** and other similar cytochalasans,[15] indicating a possible difference in stereochemistry. Further experiments, e.g. X-ray crystallography or circular dichroism (CD) are needed to clarify the absolute stereochemistry of **1**.

Compound **2**, was isolated as a yellow powder, and displayed UV absorption maxima at 212 nm and the ESI^+ MS adducts $[M+H]^+$, $[M+Na]^+$, $[2M+H]^+$ and $[2M+Na]^+$. The molecular formula of **2**, $C_{29}H_{37}NO_4$ was deduced from the monoisotopic mass obtained from the $[M+H]^+$ ion (*m/z* 464.2797) with the accuracy of 1.2 ppm. Examination of the NMR spectra of **2** displayed a high similarity compared to **1**. Comparison of the NMR spectra of **1** and **2** (see Tables 1 and 2, respectively) revealed that the difference between them is located in position five, six and seven.

The Phe moiety in **2** was identified through a connection of the two COSY spin systems linked by HMBC correlations as demonstrated for **1**. The COSY spin system of the PK chain terminated with a proton at δ_H 3.68 ppm (H7), indicating a binding to a hydroxy group instead of the vinyllic methine group observed for **1** at this position. This was also evident from the carbon chemical shift moving to δ_C 69.1 ppm (C7).

Table 2. NMR data for sclerotionigrin B (2).†

No.	δ_H (integral, mult., *J* [Hz])	δ_C	HMBC	NOESY
1	-	171.2	-	-
2	8.34 (1H, br. s)	-	3, 4, 9	3, 10’
3	3.39 (1H, m)	57.7	1, 4, 5, 9	2, 10, 10’, 11, 26/30
4	3.32 (1H, m)	47.1	1, 5, 6, 9	13, 26/30
5	-	123.9	-	-
6	-	134.2	-	-
7	3.68 (1H, d, 9.7)	69.1	-	8, 12, 13
8	3.05 (1H, t, 10.0)	48.3	1, 4, 7, 9, 13, 14	7, 13, 14
9	-	83.6	-	-
10	2.55 (1H, dd, 13.0, 10.1)	42.5	3, 4, 25, 26/30	3, 10’, 26/30
10’	2.92 (1H, dd, 13.0, 5.0)	42.5	3, 4, 25, 26/30	2, 3, 10, 26/30
11	1.16 (3H, s)	16.7	4, 5, 6	3, 26/30
12	1.52 (3H, s)	14.3	5, 6, 7	7
13	6.03 (1H, dd, 15.0, 11.3)	128.4	8, 15/15’	4, 7, 8, 14, 15
14	5.00 (1H, ddd, 15.0, 10.8, 3.4)	132.7	8, 15/15’	8, 13, 15, 15’
15	1.58 (1H, dd, 24.3, 11.1)	41.6	16	13, 14, 15’, 16, 17’
15’	2.00 (1H, br. d., 11.6)	41.6	-	14, 15, 16, 24
16	1.13 (1H, m)	32.5	-	15, 15’, 17’, 18, 24
17	0.52 (1H, dd, 19.4, 11.0)	34.5	-	17’
17’	1.67 (1H, m)	34.5	24	15, 16, 17, 18, 24
18	0.86 (1H, m)	26.1	-	16, 17’, 18’
18’	1.68 (1H, m)	26.1	20	18, 19, 21
19	1.30 (1H, dd, 21.5, 10.2)	25.4	-	18’, 19’
19’	1.73 (1H, m)	25.4	-	19
20	2.11 (1H, dd, 20.8, 10.9)	33.4	-	20’, 22
20’	2.41 (1H, dd, 12.7, 4.6)	33.4	-	20, 21
21	6.89 (1H, ddd, 15.7, 10.8, 5.0)	151.4	20, 23	18’, 20’, 22
22	5.79 (1H, d, 16.1)	121.3	20, 23	20, 21
23	-	163.8	-	-
24	0.83 (3H, d, 6.6)	19.9	15, 16, 17	15’, 16, 17’
25	-	137.4	-	-
26‡	7.08 (1H, d, 7.1)	128.9	10, 28, 30	3, 4, 10, 10’, 11, 27/29
27‡	7.31 (1H, t, 7.5)	128.2	25, 29	26/30, 28
28	7.23 (1H, t, 7.4)	126.3	26, 30	27/29
29‡	7.31(1H, t, 7.5)	128.2	25, 27	26/30, 28
30‡	7.08 (1H, d, 7.1)	128.9	10, 26, 28	3, 4, 10, 10’,11, 27/29

† ^{1}H NMR data were obtained at 500 MHz in DMSO-d_6 and ^{13}C data were obtained at 125 MHz in DMSO-d_6. ^{13}C-NMR chemical shifts determined from HSQC and HMBC experiments. ‡It was not possible to distinguish between no. 26 and 30 as well as no. 27 and 29.

HMBC correlations from the three protons of the methyl group at δ_H 1.52 ppm (H12) to the carbons at δ_C 123.9 (C5), 134.2 (C6) and 69.1 (C7), combined with correlations from the protons at δ_H 1.16 ppm (H11) to the carbons at δ_C 47.1 (C4) and 123.9 ppm (C5) and 134.2 (C6) linked the Phe moiety to

the spin system in the polyketide chain (Figure 2). The remaining chemical shifts in **2** matched the chemical shifts of **1** (Table 1 and 2) and the structure of **2**[37] was established altogether giving a classic methylated cytochalasin carbon skeleton.[7]

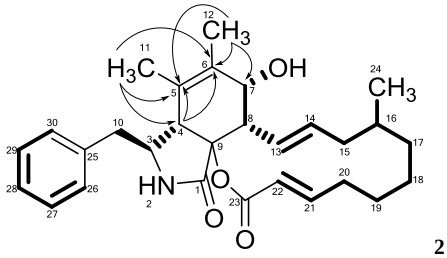

2

Figure 2. Important HMBC correlations establishing the quaternary carbon C5 and C6 in **2**. The remaining HMBC correlations are found in Table 2. Individual COSY spin systems are marked in bold.

As the optical rotation of **2** was similar to the optical rotation of **1,** the two compounds most likely have the same relative stereochemistry. The absolute stereochemistry of **2** has not yet been solved.

Biological testing of the cytotoxicity of compounds **1**-**3** towards CLL cells *in vitro* were performed using a CellTiter-Glo® assay (see Supplementary S18).[10] Compound **3** displayed the strongest effects with estimated medial lethal concentration (LC_{50}) values of ca 48 μM. Where no effect was found towards healthy B-cells in concentrations < 100 μM. Compounds **1** and **2** only showed minor activities at concentrations below 100 μM (Figure S18).

In summary the two new cytochalasins, sclerotionigrin A (**1**) and B (**2**) have been isolated from *A. sclerotioniger* together with the known proxiphomin (**3**). Compound **3** displayed the strongest cytotoxic effects towards CLL, however not as promising as recently demonstrated for chaetoglobosin A.[10] This is the first report of cytochalasan production from one of the currently more than twenty-five known black *Aspergillus* species.[16] even though cytochalasans are very common in the related yellow *Aspergillus* species such as *A. flavipes*, *A. terreus* and *A. elegans* [29,38]. Further species in *Aspergillus* section *Nigri* should be examined for cytochalasan production, as the cytochalasan related metabolite, aspergillin PZ, has also been found in this group in addition to proxiphomin, and sclerotionigrin A and B. This may be important for both drug discovery and food safety, as the black Aspergilli are common in foods.

ASSOCIATED CONTENT

Supporting Information. General experimental procedures, ^{1}H, DQF-COSY, HSQC, HMBC and NOESY spectra for all three compounds, as well as bioassay results are available in the supporting information.

AUTHOR INFORMATION

Corresponding Author

*E-mail: tol@bio.dtu.dk

Author Contributions

All authors have given approval to the final version of the manuscript.

Notes

The authors declare no conflict of interest.

ACKNOWLEDGMENT

The study was supported by the Danish Council for Independent Research, Technology, and Production Sciences (grant # 09-064967), and The Novo Nordic Foundation (grant # XXX).

REFERENCES

[1] Zenz, T.; Mertens, D.; Küppers, R.; Döhner, H.; Stilgenbauer, S. Nat. Rev. Cancer **2010**, 10, 37–50.
[2] Burger, J. A.; Montserrat, E. *Blood* **2013**, *121*, 1501–1509.
[3] Frisvad, J. C.; Smedsgaard, J.; Larsen, T. O.; Samson, R. A. *Stud. Mycol.* **2004**, *49*, 201–241.
[4] Bladt, T. T.; Frisvad, J. C.; Knudsen, P. B.; Larsen, T. O. *Molecules* **2013**, *18*, 11338–11376.
[5] Rebacz, B.; Larsen, T. O.; Clausen, M. H.; Rønnest, M. H.; Löffler, H.; Ho, A. D.; Krämer, A. *Cancer Res.* **2007**, *67*, 6342–6350.
[6] Liao, W.-Y.; Shen, C.-N.; Lin, L.-H.; Yang, Y.-L.; Han, H.-Y.; Chen, J.-W.; Kuo, S.-C.; Wu, S.-H.; Liaw, C.-C. *J. Nat. Prod.* **2012**, *75*, 630–635.
[7] Schümann, J.; Hertweck, C. *J. Am. Chem. Soc.* **2007**, *129*, 9564–9565.
[8] Wagenaar, M. M.; Corwin, J.; Strobel, G.; Clardy, J. *J. Nat. Prod.* **2000**, *63*, 1692–1695.
[9] Liu, R.; Gu, Q.; Zhu, W.; Cui, C.; Fan, G.; Fang, Y.; Zhu, T.; Liu, H. *J. Nat. Prod.* **2006**, *69*, 871–875.
[10] Knudsen, P.B.; Hanna, B.; Ohl, S.; Sellner, T.Z.; Stilgenbauer, S.; Larsen, T.O.; Lichter, P.; Seiffert, M. *Leukemia* **2013** *in revision*.
[11] Zhang, Y.; Wang, T.; Pei, Y.; Feng, B. *J. Antibiot.* **2002**, *55*, 693-695.
[12] Canham, S.M.; Overman, L.E., Tanis, P.S. *Tetrahedron* **2011**, *67*, 0837-9843.
[13] Keller-Schierlein, W.; Kupfer, E. *Helv. Chim. Acta* **1979**, *62*, 1501-1523.
[14] Naruse, N.; Yamamoto, H.,; Murata, S.; Sawada, Y.; Fukagawa, Y.; Oki, T. *J. Antibiot*. **1993**, *46*, 679-681.
[15] Fang, F.; Ui, H.; Shiomi, K.; Masuma, R.; Yamaguchi, Y.; Zhang, C.G.; Zhang, X.W.; Tanaka, Y.; Omura, S. *J. Antibiot*. **1998**, *50*; 919-925.
[16] Tomikawa, T.; Shin-Ya, K.; Seto, H.; Okusa, N.; Kajiura, T.; Hayakawa, Y. *J. Antibiot*., **2002**, *55*, 666-668.
[17] Choo, S.J.; Yun, B.S.; Ryoo, I.J.; Kim, Y.H.; Bae, K.H.; Yoo, I.D. *J. Microbiol. Biotechnol*. **2009**, *19*, 368-371.
[18] Zhou, G.X.; Wijeratne, K.; Bigelow, D.; Pierson III, L.S.;VanEtten, H.D.; Gunatilaka, A.A.L. *J. Nat. Prod*. **2004**, *67*, 328-332.
[19] Rochfort, S.; Ford, J.; Ovenden, S., Wan, S.S.; George, S., Wildman, H.; Tail, R.M.; Meurer-Grimes, B., Cox, S.; Coates, J.; Rhodes D. *J. Antibiot*. , **2005**, *58*, 279-283.
[20] Liu, J.,; Hu, Z.; Zheng, Z.; Xu, Q. *J. Antibiot*., **2012**, *65*, 49-52.
[21] Kohno, J.,; Nonaka, N.; Nishio, M., Ohnuki, T.; Kawano, K.; Okuda, T.; Komatsubara, S. *J. Antibiot*. **1999**, *52*, 575-577.
[22] Gebhardt, K.; Schimana, J.; Hötzel, A.; Dettner, K.; Draeger, S.; Beil, W.; Rheinheimer, J.; Fiedler, H.-P. *J. Antibiot.* **2004**, *57*, 707-714.
[23] Barrow, C.J.; Sedlock, D.M.; Sun, H.H.; Cooper, R.; Gillum, A.M. *J. Antibiot*. **1994**, *47*, 1182-1187.
[24] Fujishima, T.; Ichikawa, M.; Ishige, H., Yoshino, H.; Ohishi, J.; Ikegami, S. *Hakkokogaku Kaishi- J. Soc. Ferm.* **1979**, *57*, 15-19.
[25] Lin, Z.; Zhang, G.; Zhu, T.; Wei, H.; Gu, Q. *Helv. Chim. Acta* **2009**, *92*, 1538-1544.
[26] Ge, H.M.; Peng, H.; Guo, Z.K.; Cui, J.T.; Song Y.C.; Tan, R.X. *Planta Med*.,**2010**, *76*, 822-824.
[27] Zhang H.; Zhang J.; Hui, S.; Zhang, Z.; Zhu, C.-J.; Ng S.W.; Tan, R.-X., *Planta Med.*, **2010**, *76*, 1616-1621.
[28] Xiao, L.; Liu, H.; Wu, N.; Liu, M.; Wei, J.; Zhang, Y.; Lin X. *World J. Microbiol. Biotechnol*., **2013**, *29*, 11-17.
[29] Zheng, C.J.; Shao, C.L.; Wu, L.Y.; Chen, M.;Wang, K.L.; Zhao, D.L.; Sun, X.P., Chen, G.Y.; Wang C.Y. *Marine Drugs*, **2013**, *11*, 2054-2068.

[30] Büchi, G.; Kitaura, Y.; Yuan, S., Wright, H.E.; Clardy, J., Demain, A.L.; Glinsukon, T.; Hunt, N.; Wogan, G.N. *J. Amer. Chem. Soc*. **1973**, *95*, 5423-5425.
[31] Steyn, P.S.; van Heerden, F.R.; Rabie, C.J. *J. Chem. Soc. Perkin I*, **1982**, 541-544.
[32] Binder, M.; Tarnrn, C. *Helv. Chim. Acta* **1973**, *7*, 2387–2396.
[33] Samson, R.A.; Houbraken, J.A.M.P.; Kuijpers, A.F.A.; Frank, J.M.; Frisvad, J.C. *Stud. Mycol*., **2004**, *50*, 45-61.
[34] Laatsch, H. AntiBase 2012. Available online: http://eu.wiley.com/WileyCDA/WileyTitle/ productCd-3527334068.html/ (accessed on 5 September 2013).
[35] **3**: Yellow solid; $[\alpha]_{589.3nm}$: -21° (*c* 0.1, MeOH); UV (ACN) λ_{max}: 244 nm; HRMS *m/z* 432.2901 ($[M+H]^+$ calculated for $C_{29}H_{38}NO_2$, *m/z* 432.2904; 0.8 ppm); ^{13}C- and ^1H-NMR: see Supporting information.
[36] **1** was obtanied as a yellow solid; $[\alpha]_{589.3nm}$: +4° (*c* 0.8, MeOH); UV (ACN) λ_{max}: 210 nm; HRMS *m/z* 448.2843 ($[M+H]^+$ calculated for $C_{29}H_{38}NO_3$, *m/z* 448.2853; 2.3 ppm); ^{13}C- and ^1H-NMR: see Table 1.
[37] **2** Yellow solid; $[\alpha]_{589.3nm}$: +41° (*c* 0.2, MeOH); UV (ACN) λ_{max}: 212 nm; HRMS *m/z* 464.2797 ($[M+M]^+$ calculated for $C_{29}H_{38}NO_4$, *m/z* 463.2724; 1.2 ppm); ^{13}C- and ^1H-NMR: see Table 2.
[16] Varga, J.; Frisvad, J.C.; Kocsubé, S.; Brankovics, B.; Tóth, B.; Szigeti, G.; Samson, R.A. *Stud. Mycol*. **2011**, *69*, 1-17.
[38] Scherlack, K.; Boettger, D.; Remme, N.; Hertwech, C. *Nat. Prod. Rep*. **2010**, *27*, 869-886.

Tanja Thorskov Bladt
Chemical biology of microbial anticancer natural products - appendix

Supporting Information

Sclerotionigrin A and B, two Novel Cytochalasans Targeting Chronic Lymphocytic Leukemia

Lene M. Petersen,[1] Tanja T. Bladt,[1] Claudia Dürr[2], Martina Seiffert[2], Jens C. Frisvad[1], Charlotte H. Gotfredsen[3], Thomas O. Larsen[1,*]

[1]Technical University of Denmark, Department of Systems Biology, Søltofts Plads, Building 221, DK-2800 Kgs. Lyngby, Denmark, [2]German Cancer Research Center, Molecular Genetics, Im Neuenheimer Feld 280, D-69120 Heidelberg, Germany, [3]Technical University of Denmark, Department of Chemistry, Kemitorvet, Building 201, DK-2800 Kgs. Lyngby, Denmark.

tol@bio.dtu.dk

Contents

S1 General Experimental Procedures

Aspergillus sclerotieoniger (IBT 22905) is from the IBT culture collection at Department of Systems Biology, Technical University of Denmark. *A. sclerotieoniger* was inoculated as three point inoculations on czapek yeast agar (CYA) on 100 plates at 25 °C for 7 days in the dark. CYA plates were prepared as described by Frisvad and Samson.[1] The plates were harvested and extracted twice overnight with ethyl acetate (EtOAc) containing 1 % formic acid. The extracts were filtered and concentrated *in vacuo*. Work up: The combined extract was dissolved in methanol (MeOH)/milliQ-water (9:1) and an equal amount of heptane was added followed by seperation of phases. Additional milliQ-water was added to the MeOH/water phase untill a ratio of 1:1, and metabolites were extracted with dichloromethane (DCM). The phases were then concentrated separately *in vacuo*. The DCM phase was used for further fractionation.

The LC-MS analyses were performed on a maXis quadrupole time of flight (qTOF) mass spectrometer (Bruker Daltonics) with an electrospray ionization (ESI) ion source. The maXis was calibrated using sodium formate automatically infused prior to each analytical run, providing a mass accuracy of below 1 ppm. The mass spectrometer was linked to an Ultimate 3000 UHPLC system (Dionex) with DAD. Separation was achieved on a Kinetex C_{18}, 2.6µm, 2.1x100 mm column (Phenomenex) with a flow of 0.4 ml min^{-1} at 40°C using a linear gradient 10 % acetonitrile (ACN) in Milli-Q water (MQ) with 20 µM formic acid (FA) going to 100 % ACN in 10 min. All compounds were isolated started by flash chromatography of the crude extracts, fractionated with an Isolera One automated flash system (Biotage). The isolation of compounds were performed by a semi-preparative Waters 600 DAD. One-dimensional and two-dimensional NMR experiments were acquired on a 500 MHz Varian Unity Inova equipped with a HCP probe. ^{1}H, DQF-COSY, edHSQC, HMBC and NOESY experiments were acquired using standard pulse sequences. Optical rotation values were obtained on a Perkin-Elmer 241 Polarimeter at 589 nm.

S2 ^{1}H NMR spectrum for Sclerotionigrin A (1) at 500 MHz in DMSO-d_6

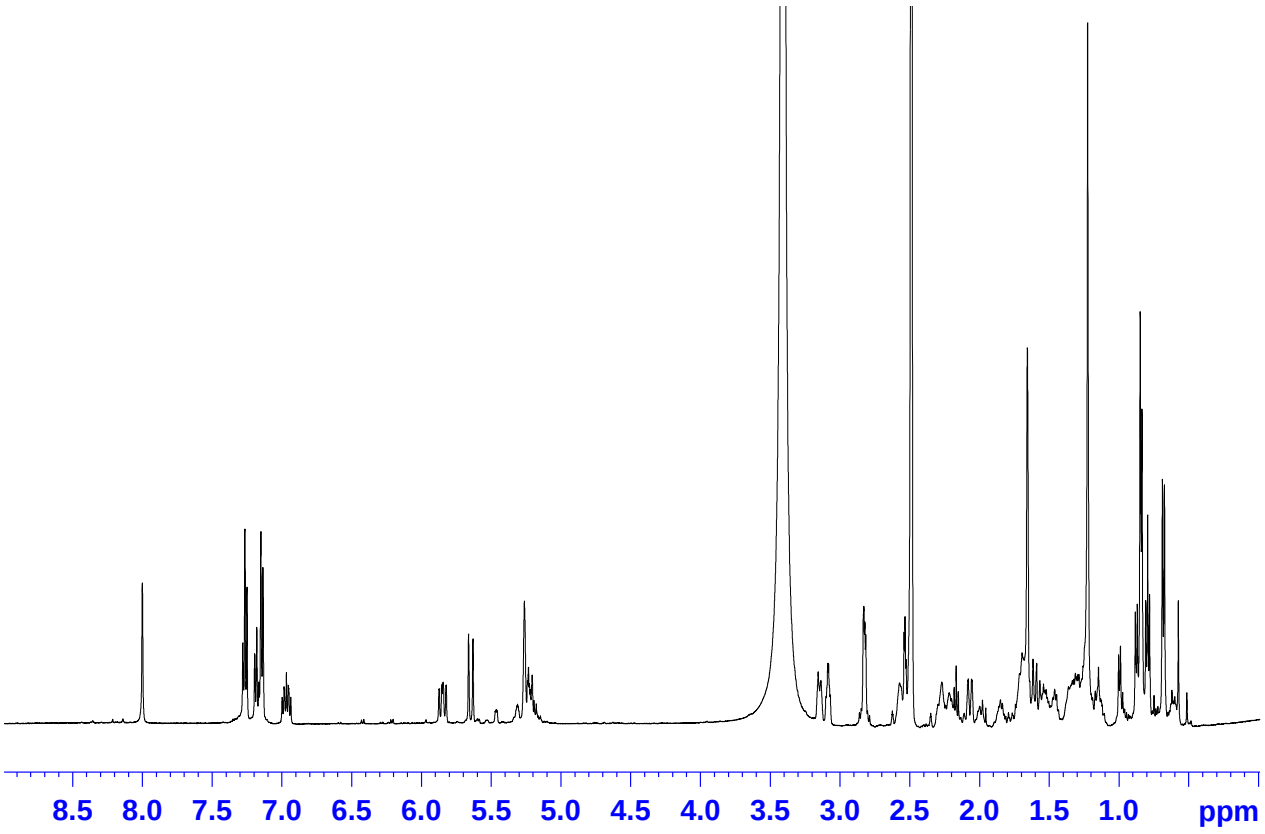

[1] Samson, R.A.; Houbraken, J.; Thrane, U.; Frisvad, J.C.; Andersen, B.. Food and Indoor Fungi. CBS Laboratory Manual Series 2, CBS KNAW Fungal Biodiversity Centre: Utrecht (NL), 2010

S3 DQF-COSY spectrum for Sclerotionigrin A (1) in DMSO-d_6

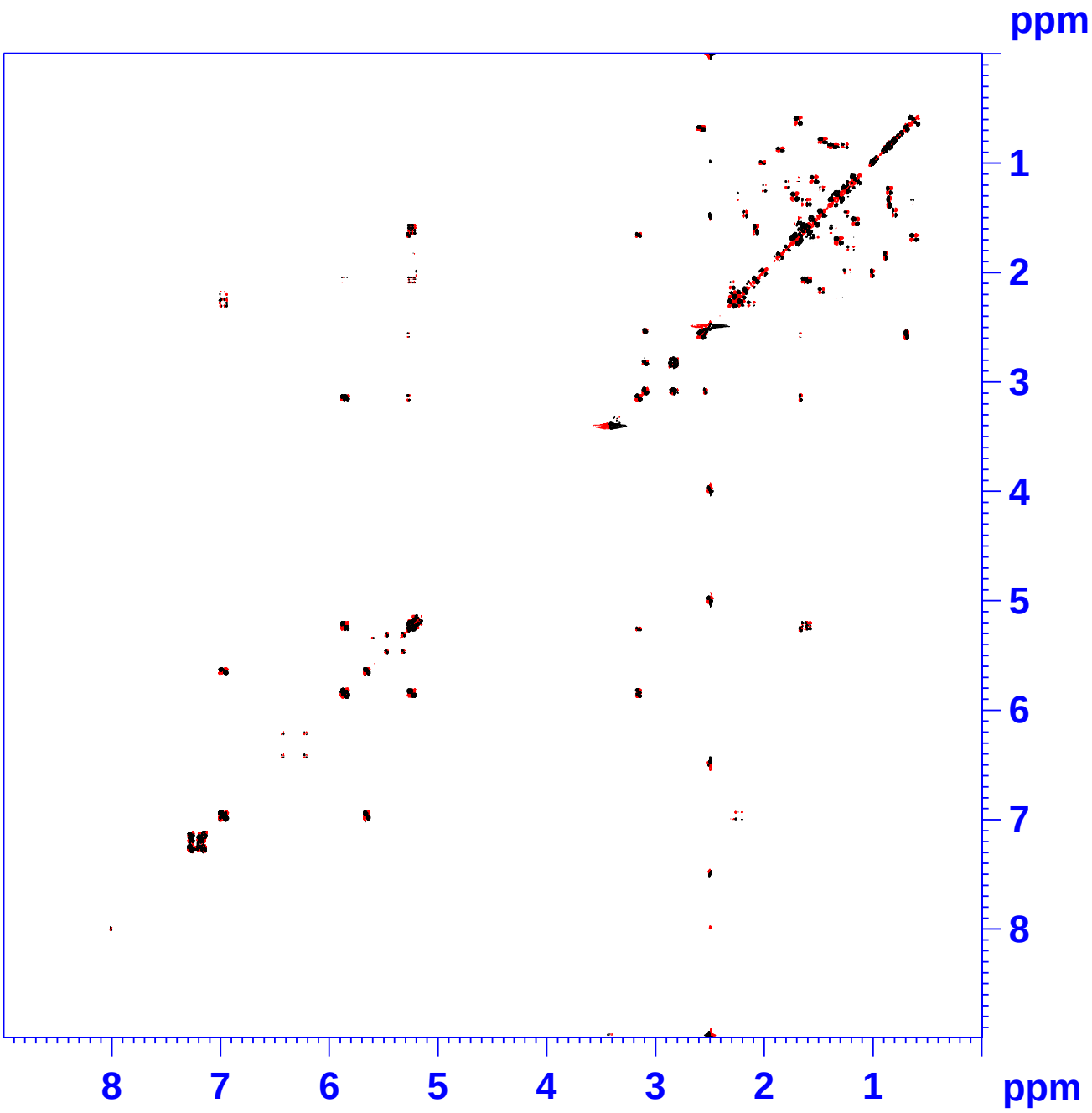

S4 $_{ed}$HSQC spectrum for Sclerotionigrin A (1) in DMSO-d_6

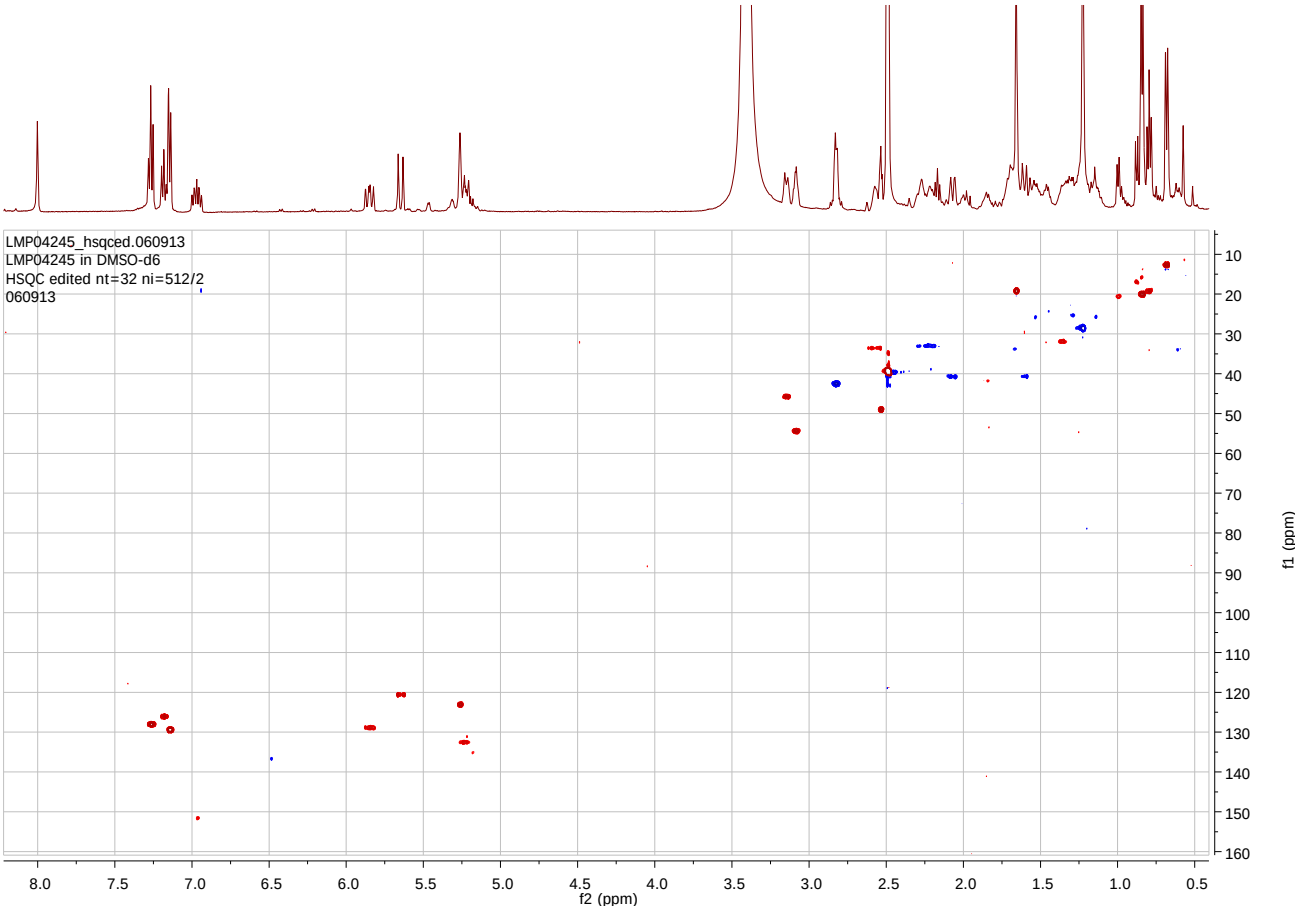

S5 HMBC spectrum for Sclerotionigrin A (1) in DMSO-d_6

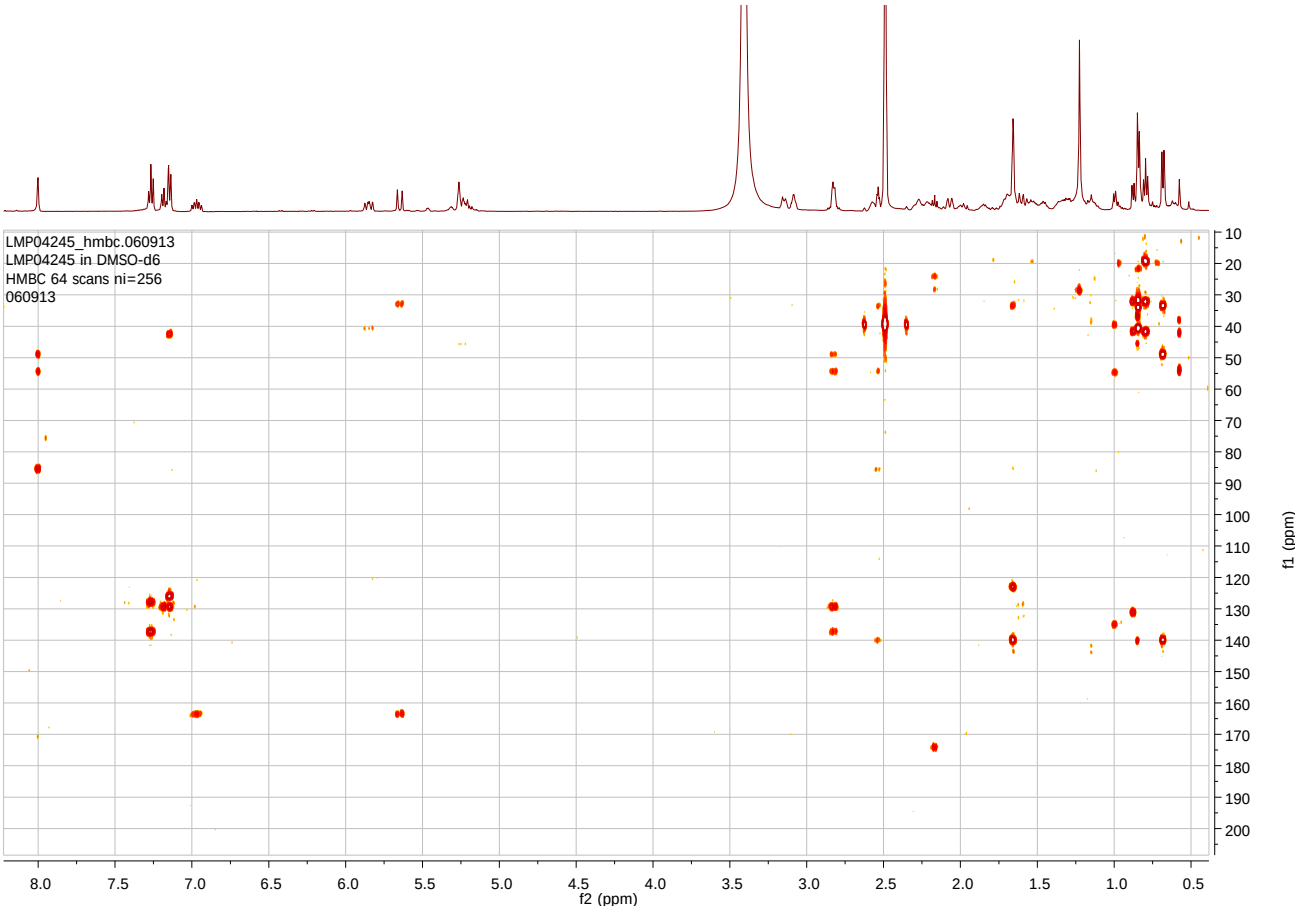

S6 NOESY spectrum for Sclerotionigrin A (1) in DMSO-d_6

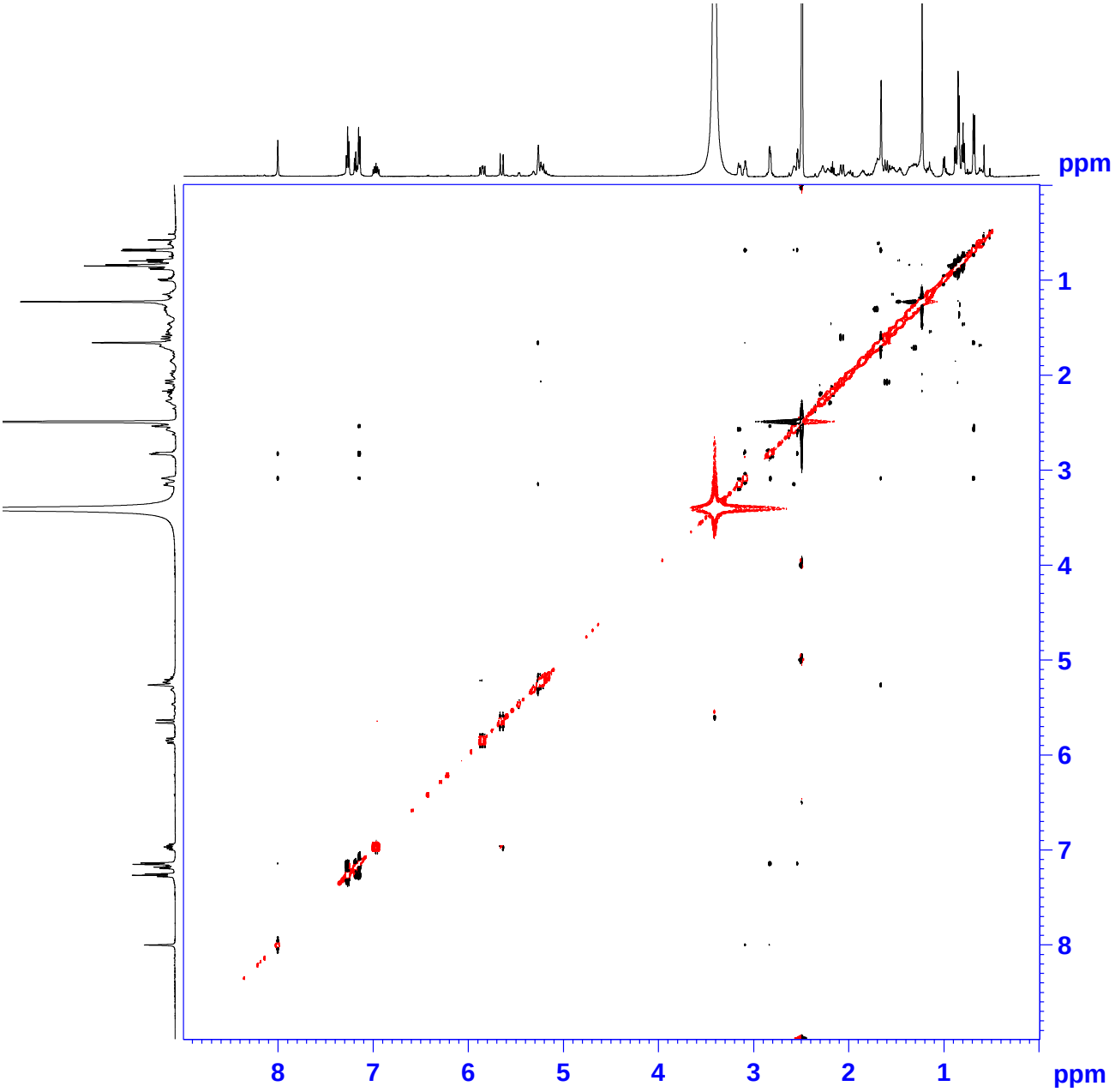

S7 **^{1}H NMR spectrum for Sclerotionigrin B (2) at 500 MHz in DMSO-d_6**

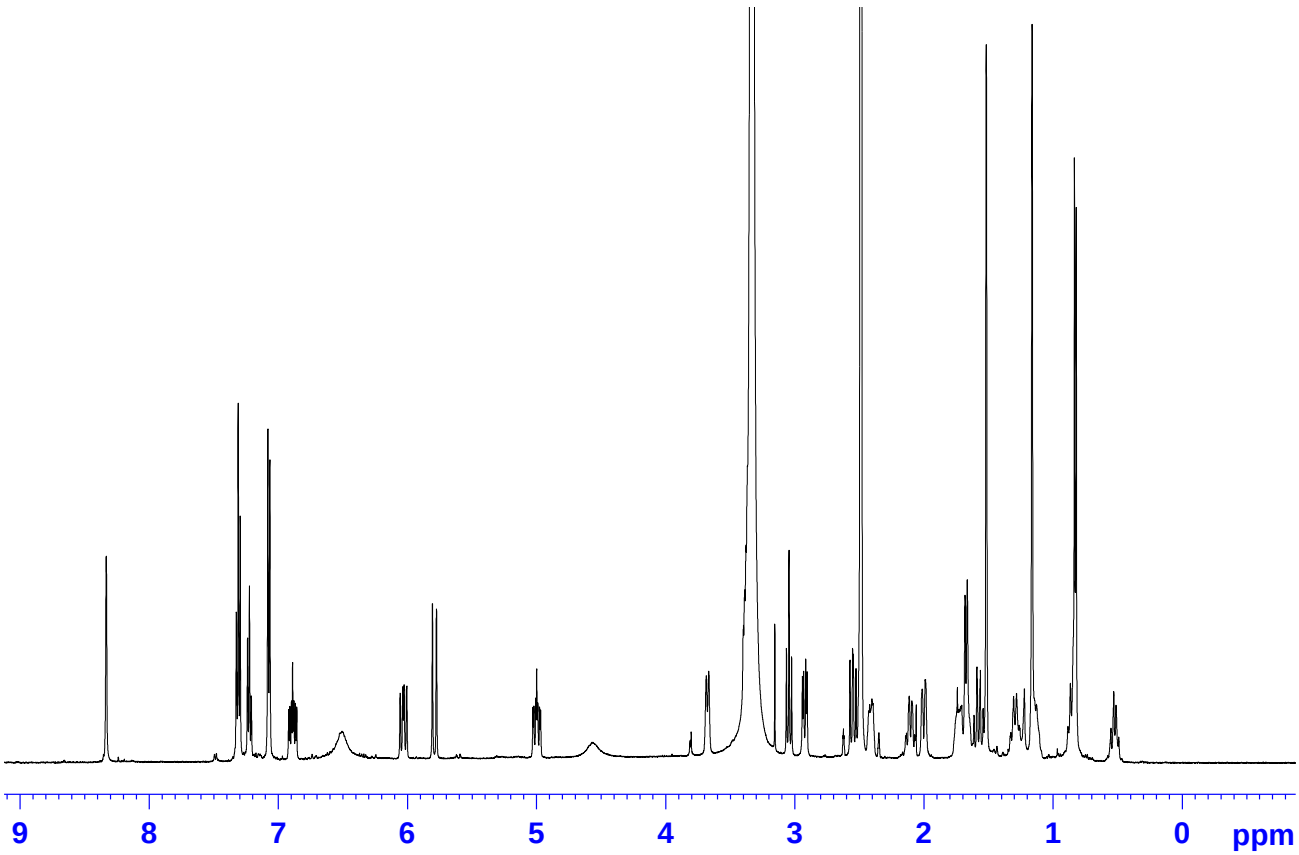

S8 DQF-COSY spectrum for sclerotienigerin B (2) in DMSO-d_6

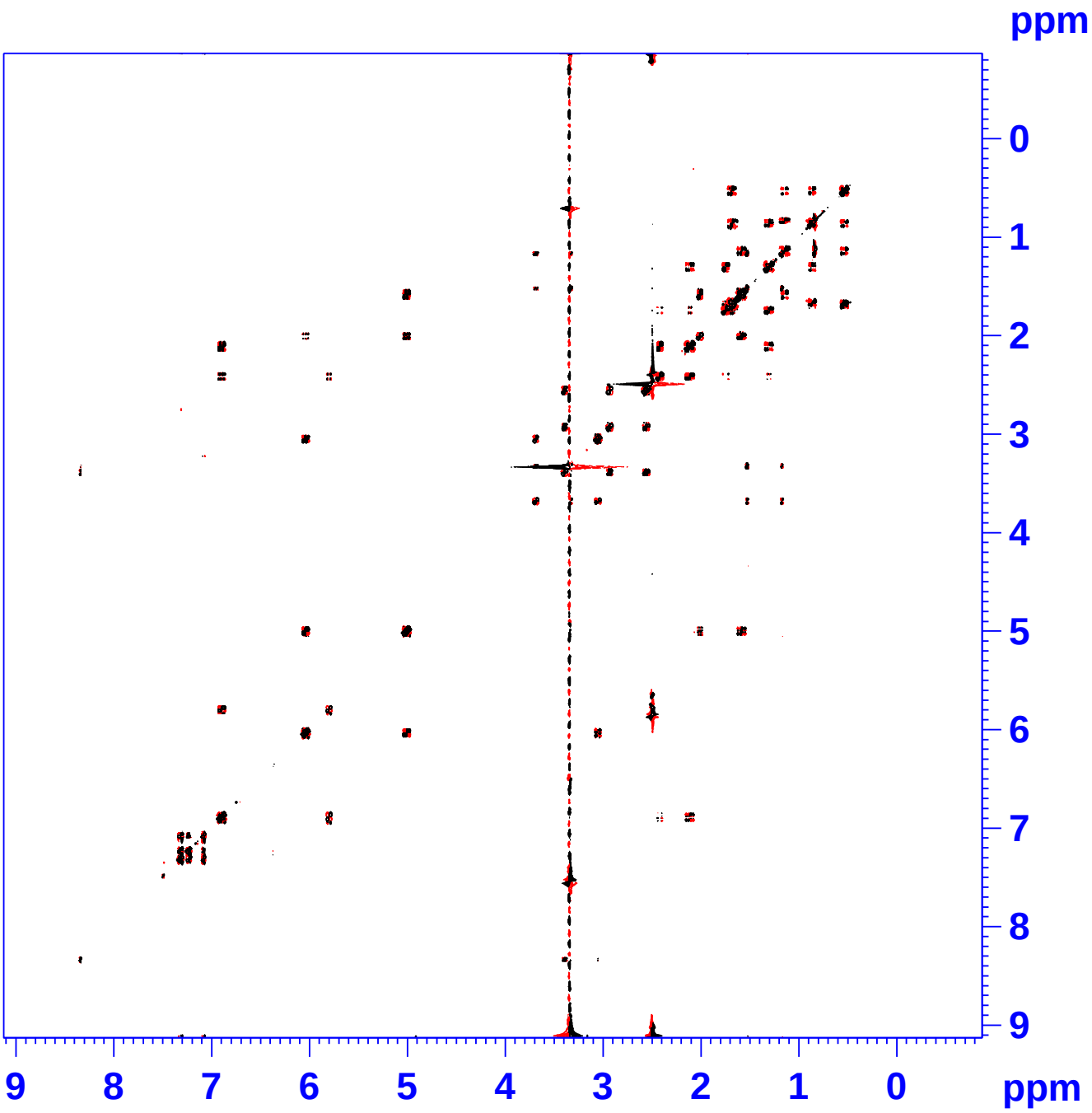

S9 $_{ed}$HSQC spectrum for Sclerotionigrin B (2) in DMSO-d_6

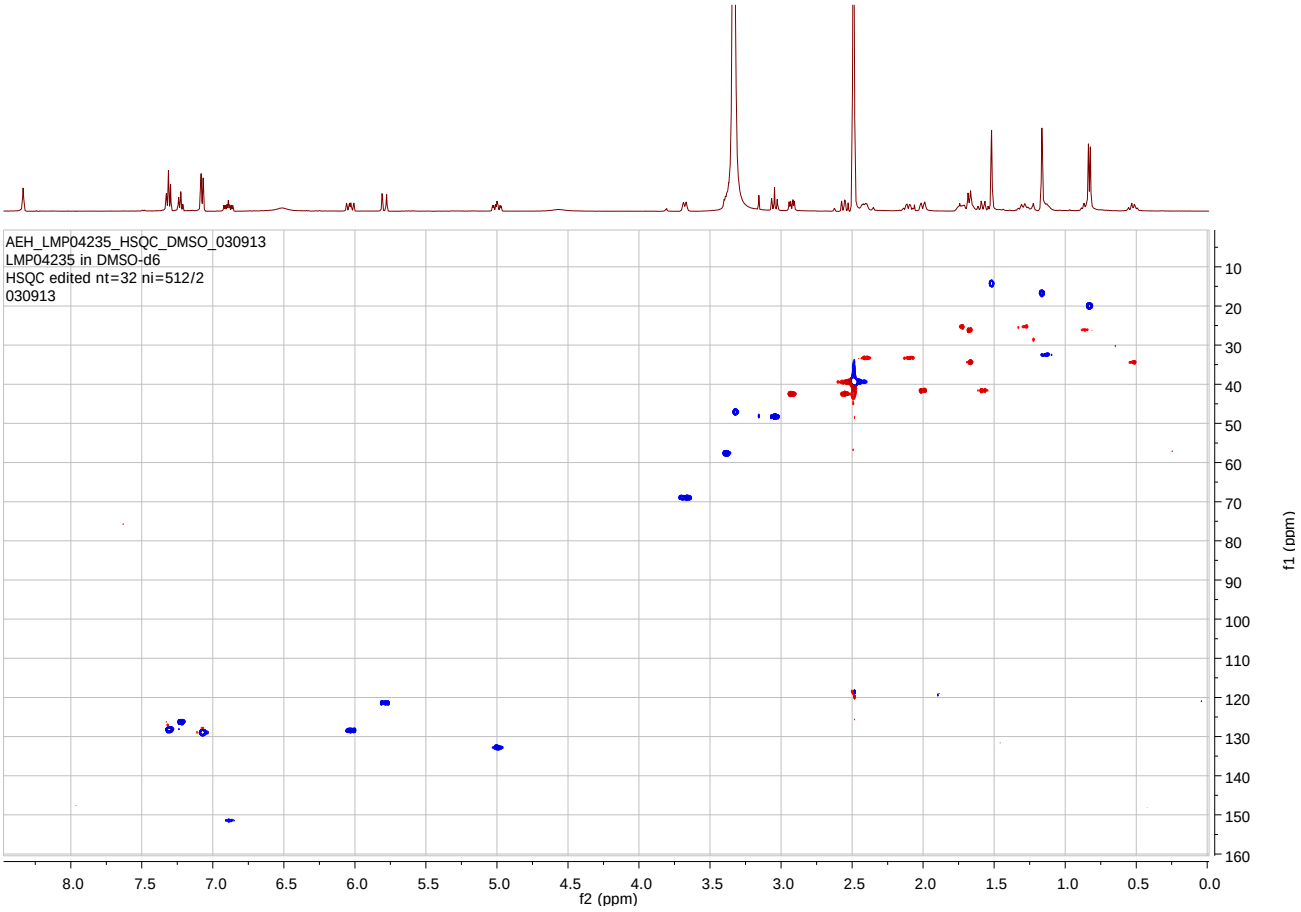

S10 HMBC spectrum for Sclerotionigrin B (2) in DMSO-d_6

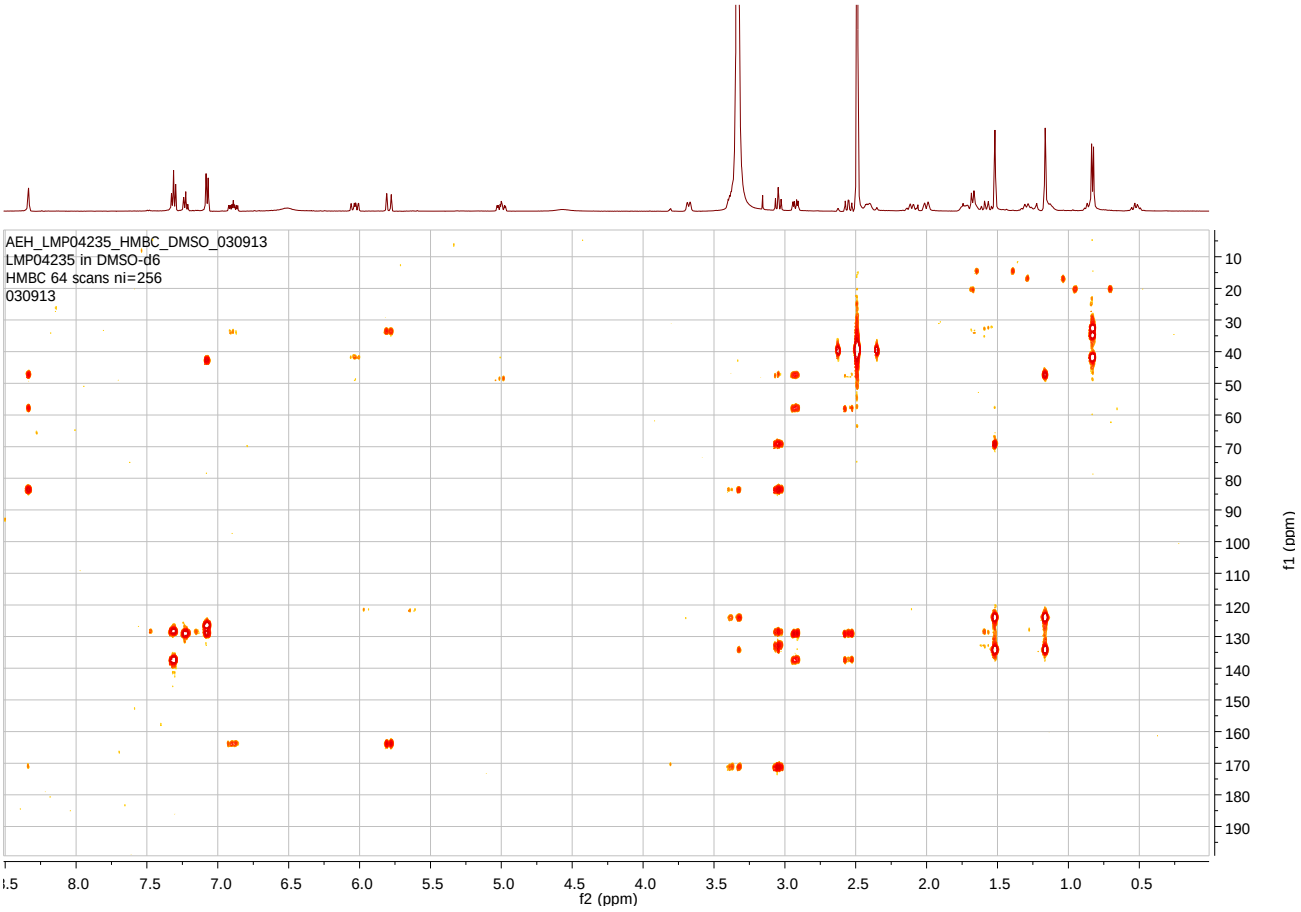

S11 NOESY spectrum for Sclerotionigrin B (2) in DMSO-d_6

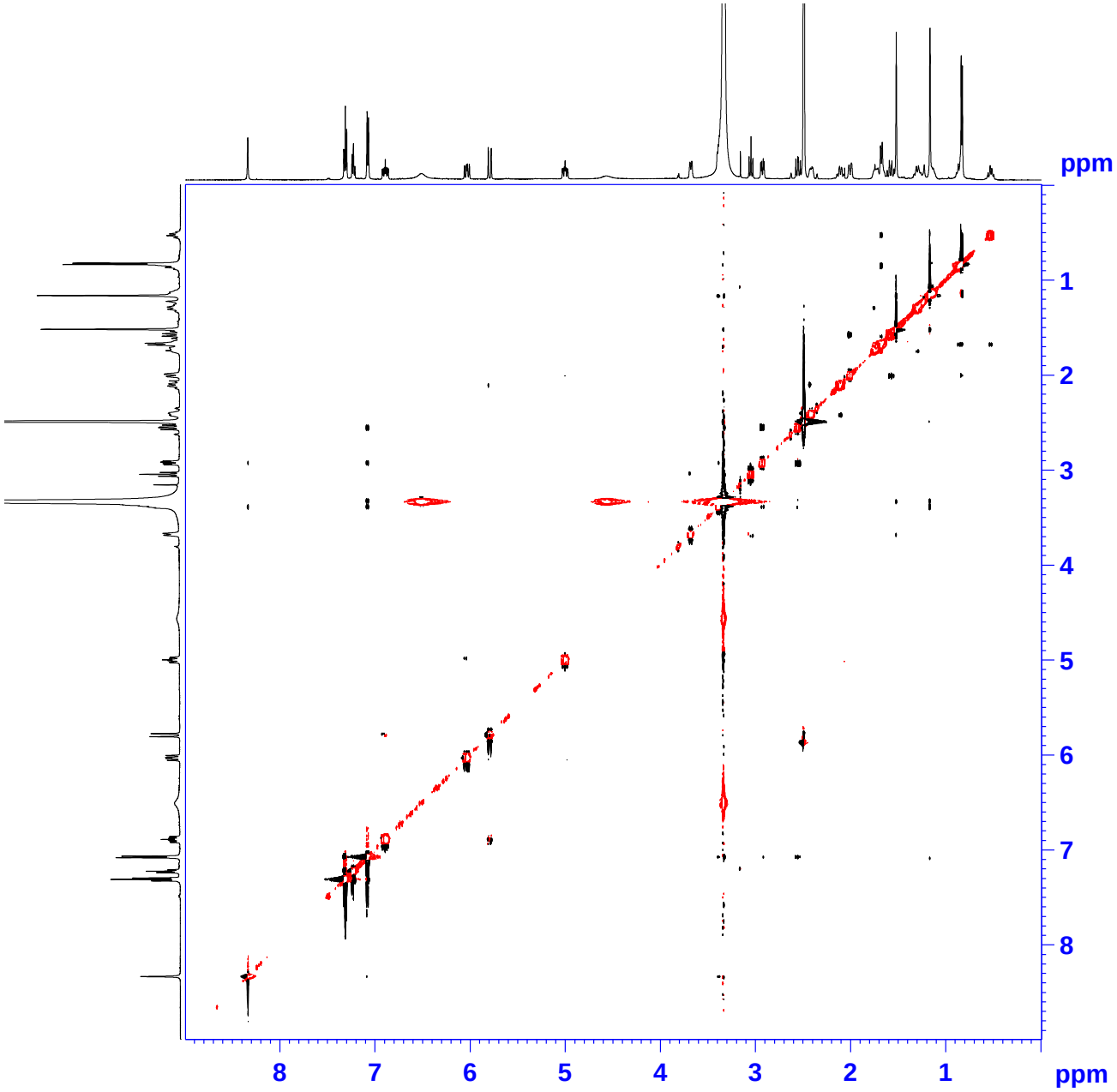

S12 NMR data for proxiphomin (3)

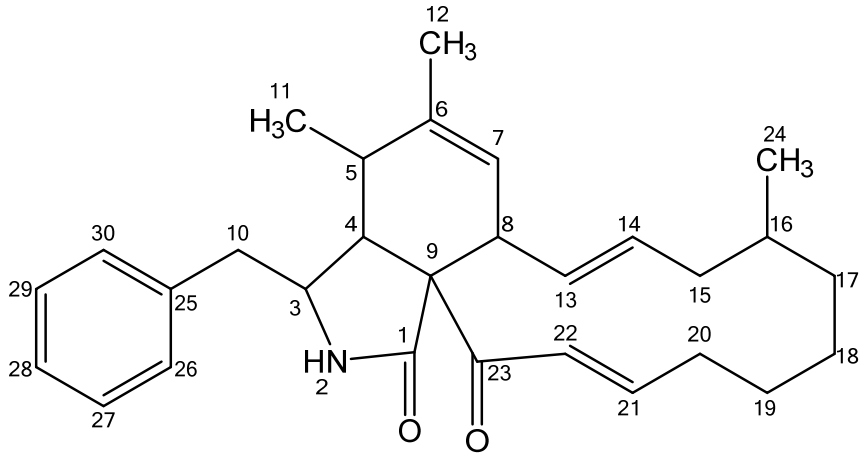

Atom assignment	*^{1}H-chemical shift [ppm]/ J coupling constants [Hz]†*	*^{13}C-chemical shift [ppm]†*	*HMBC correlations*	*NOESY connectivities*
1	-	173.6	-	-
2	7.94 (1H, s)	-	3, 4, 9	3
3	3.25 (1H, m)	53.0	-	2, 4, 10, 10’, 11, 12, 26, 30
4	2.80 (1H, dd, 5.8, 2.6)	47.2	1, 3, 5, 6, 9, 10, 23	3, 5, 10, 10’, 11, 26, 30
5	2.20 (1H, m)	33.7	1	4, 8, 11
6	-	139.1	-	-
7	5.27 (1H, m)	125.8	-	8, 12, 13
8	2.63 (1H, m)	47.0	1	7, 5, 13, 14, 22
9	-	65.7	-	-
10	2.40 (1H, dd, 13.2, 7.3)	43.1	1, 3, 4, 25, 26, 30	3, 4, 10’, 26, 30
10’	2.60 (1H, dd, 13.2, 4.9)	43.1	1, 3, 4, 25, 26, 30	3, 4, 10, 26, 30
11	0.77 (3H, d, 7.2)	12.6	4, 5, 6	3, 4, 5
12	1.66 (3H, s)	19.3	5, 7	3, 7, 13
13	6.18 (1H, ddd, 15.2, 9.8, 1.7)	129.3	15	7, 8, 12, 14, 22
14	5.11 (1H, dddd, 15.2, 14.0, 10.5, 3.1)	131.6	8	8, 13, 15’
15	1.67 (1H, m)	39.7	16	15’
15’	1.99 (1H, m)	39.7	16	14, 15, 16, 17 24
16	1.38 (1H, m)	31.9	-	15’

17	1.23 (2H, m)	28.5	-	15’, 18
18	1.13 (2H, m)	23.1	-	17
19	1.41 (1H, m)	25.2	-	19’
19’	1.56 (1H, m)	25.2	-	19
20	2.02 (1H, m)	31.1	-	20’, 21, 22
20’	2.28 (1H, m)	31.1	-	20
21	6.54 (1H, dddd, 20.6, 15.5, 10.3, 5.3)	145.7	20, 23	20
22	6.86 (1H, d, 15.5)	127.3	20, 23	8, 13, 20
23	-	196.9	-	-
24	0.85 (3H, d, 6.7)	20.8	15, 16	15’
25	-	136.7	-	-
26‡	7.10 (1H, d, 7.5)	129.5	10, 28, 30	3, 4, 10, 10’
27‡	7.25 (1H, dd, 7.4, 1.0)	127.9	25, 29	
28	7.16 (1H, d, 7.5)	126.0	26, 30	
29‡	7.25 (1H, dd, 7.4, 1.0)	127.9	25, 27	
30‡	7.10 (1H, d, 7.5)	129.5	10, 26, 28	3, 4, 10, 10’

† ^{1}H NMR data were obtained at 500 MHz in DMSO-d_6 and ^{13}C data were obtained at 125 MHz in DMSO-d_6.
‡It was not possible to distinguish between 26 and 30 as well as 27 and 29.

S13 ^{1}H NMR spectrum for proxiphomin (3) at 500 MHz in DMSO-d_6

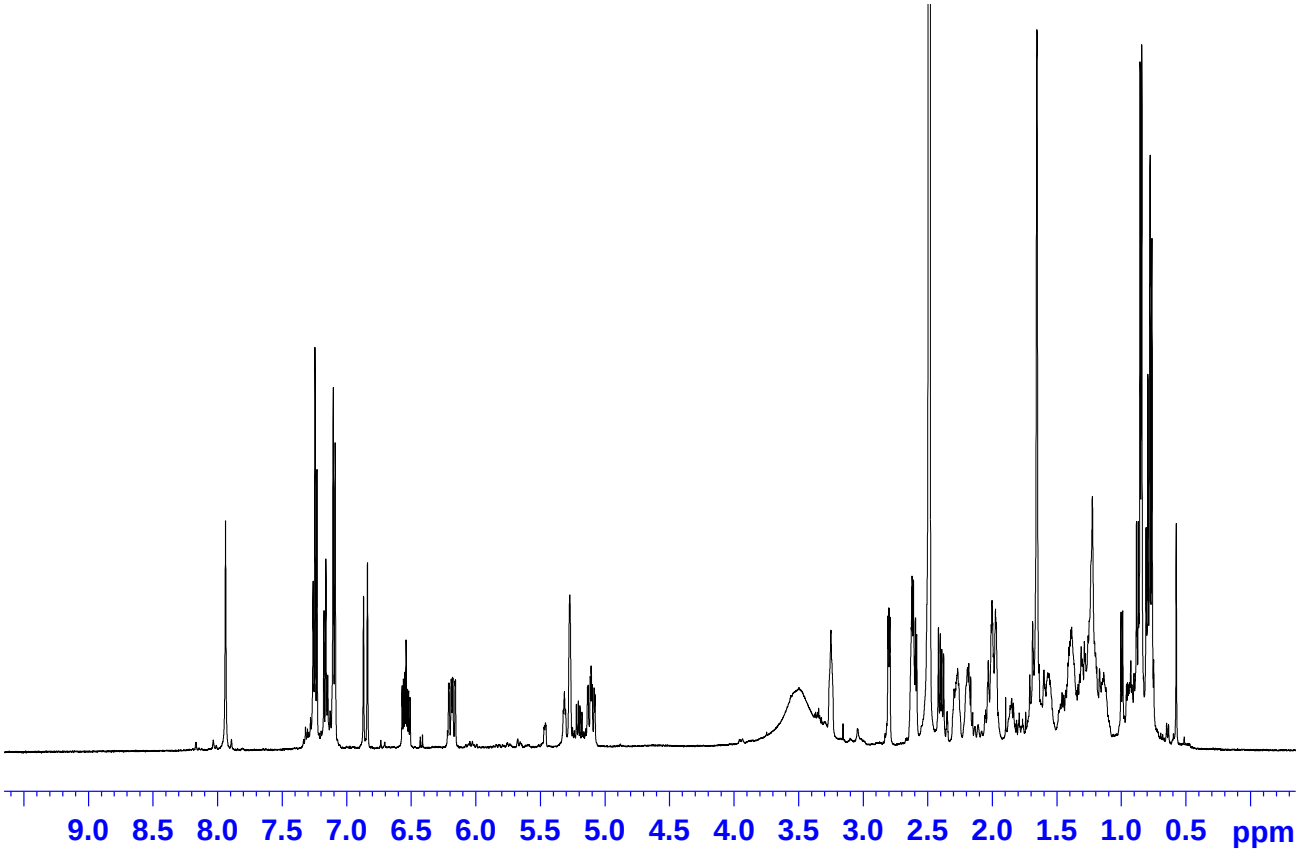

S14 DQF-COSY spectrum for proxiphomin (3) in DMSO-d_6

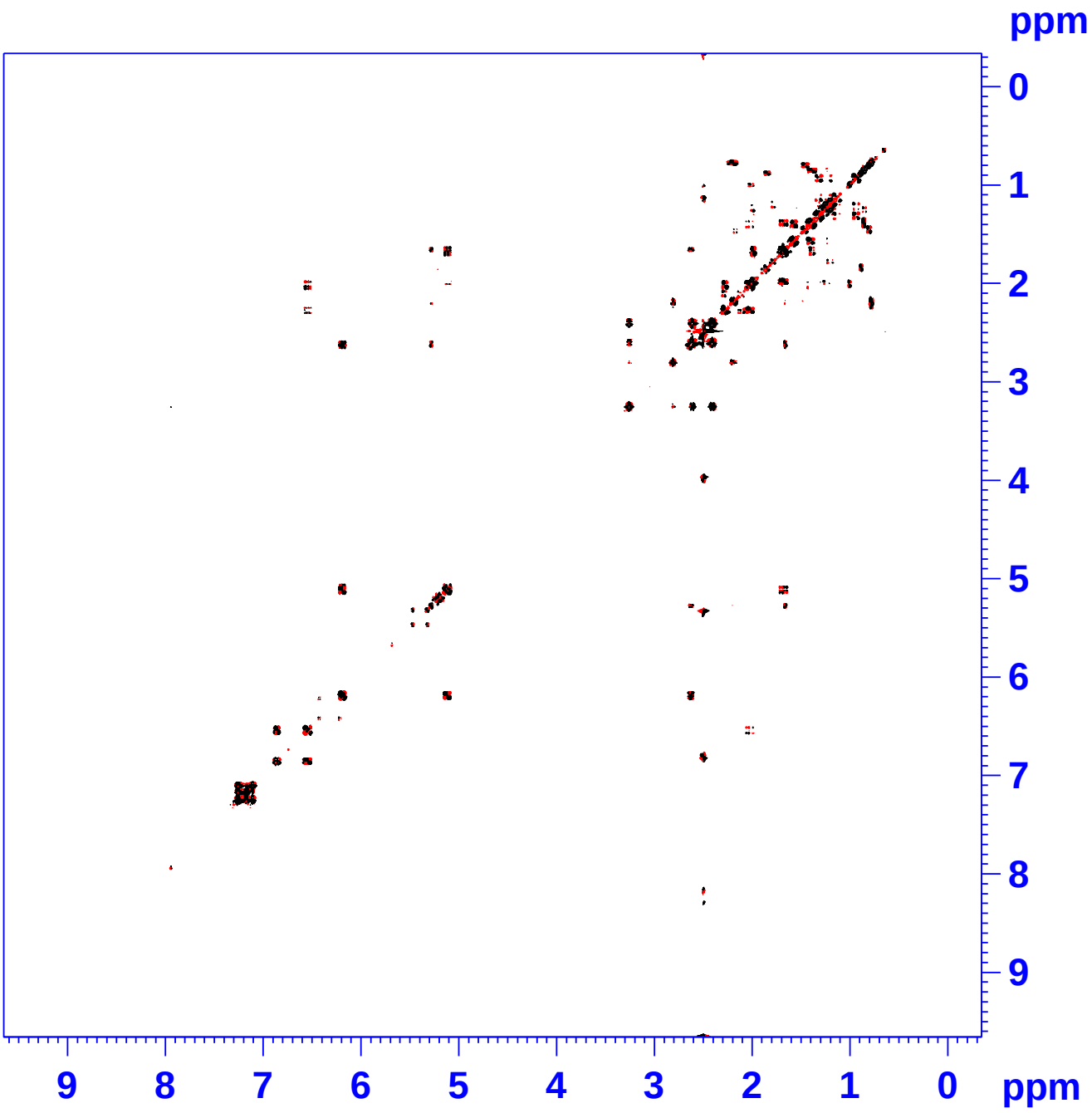

S15 $_{ed}$**HSQC spectrum for proxiphomin (3) in DMSO-d_6**

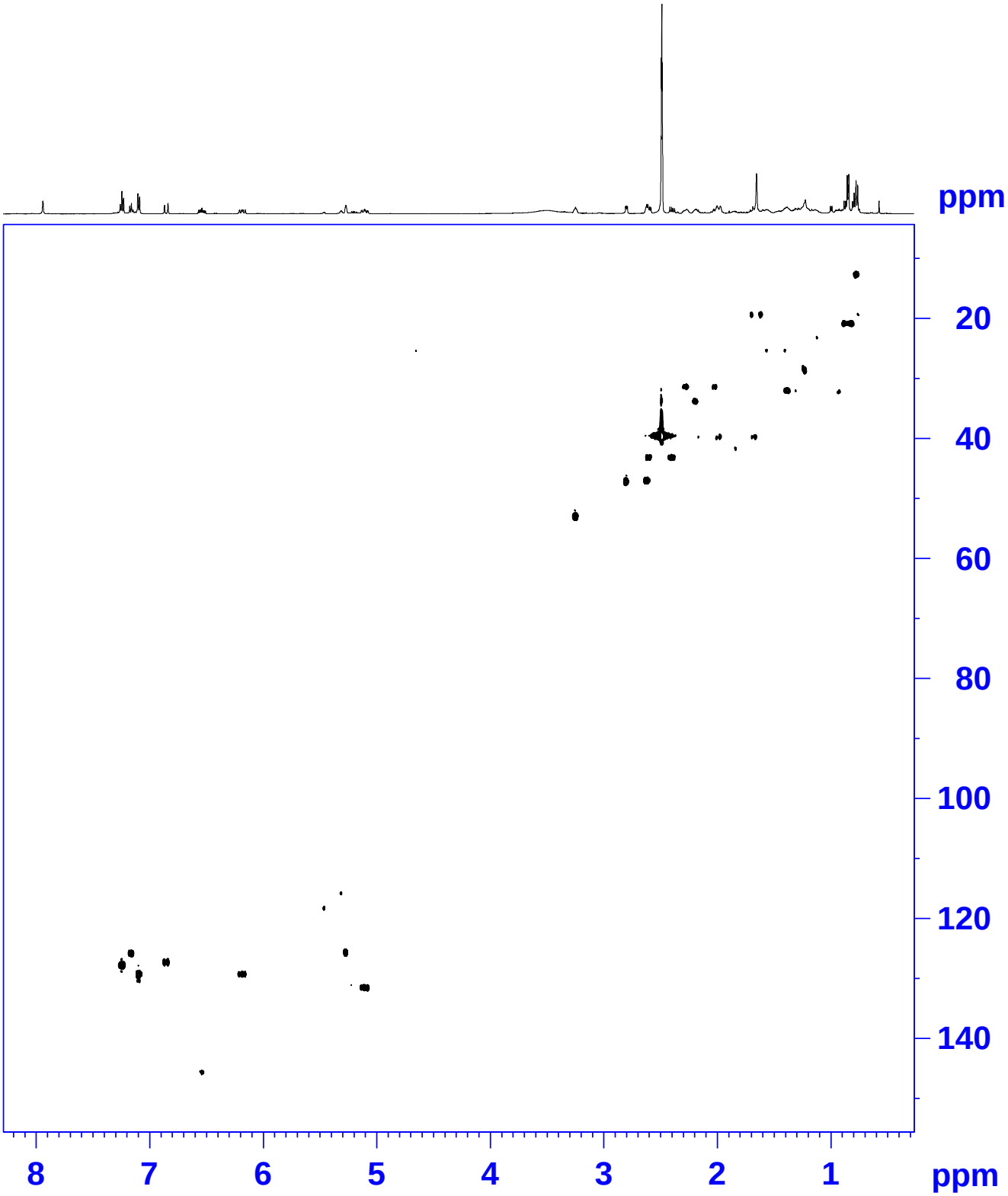

S16 HMBC spectrum for proxiphomin (3) in DMSO-d_6

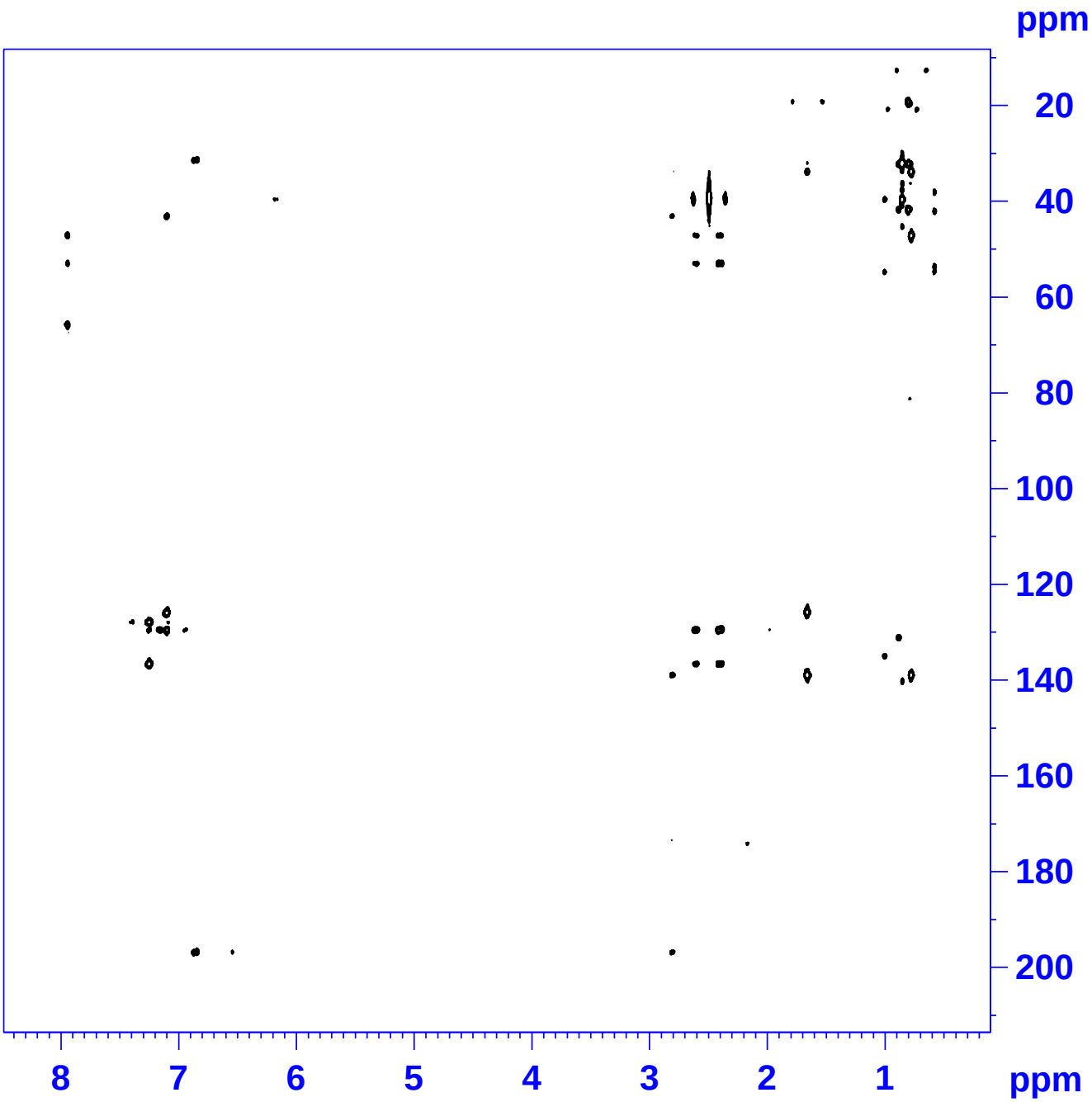

S17 NOESY spectrum for proxiphomin (3) in DMSO-d_6

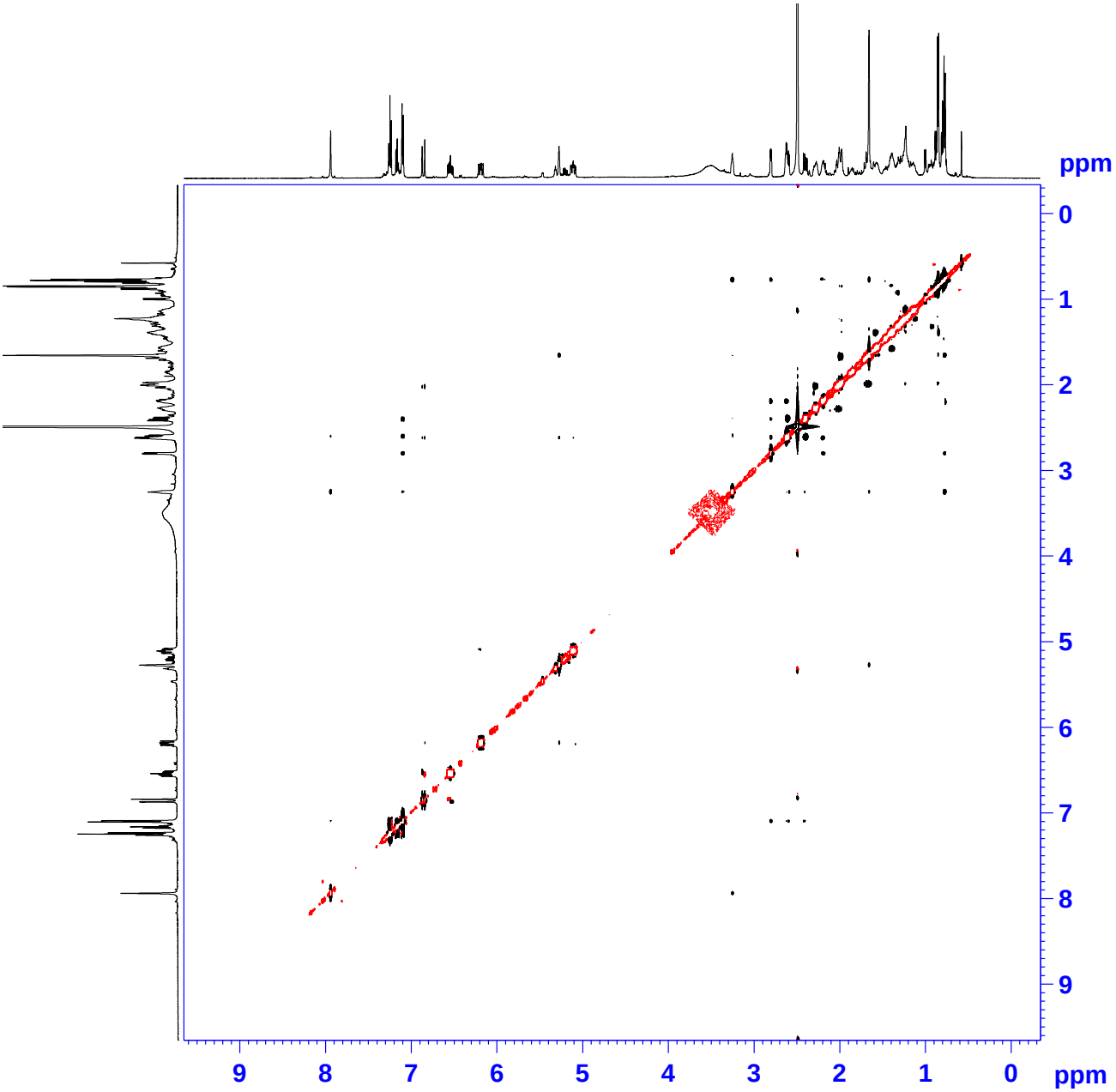

S18 Bioactivity

Whole blood samples were obtained from healthy donors or patients that matched the standard diagnostic criteria for CLL after informed consent in accordance with the Declaration of Helsinki. All studies performed were approved by the ethics committee of the University of Ulm. Peripheral blood B cells were isolated by Ficoll density gradient followed by magnetic cell enrichment using CD19-MACS beads (Miltenyi Biotech, Bergisch Gladbach, Germany). Healthy donor B cells or CLL cells were cultured in conditioned medium of HS-5 cells, which was harvested after 3–4 days of culture and 80% confluency and depleted of HS-5 cells and debris by centrifugation. Cells were seeded in duplicates at a density of 3×10^5 cells/well in opaque-walled 96-well plates. Pure compounds were added in different concentrations and incubated for 24 hours. A final concentration of 0.1% DMSO was used as negative control. Cell viability was assessed using CellTiter-Glo® assay (Promega, Madison, WI, USA) according to manufacturer's protocol. Luminescence signals were recorded using a Mithras LB940 plate reader (Berthold Technologies, Bad Wildbad, Germany). Relative cell viability was calculated as described by Knudsen et al. [2] Mean values ±SEM of four CLL samples and three healthy donor samples are depicted.

Figure S1. Effects of 1-3 on CLL cell viabiltiy. CLL cells were treated for 24 hours with increasing concentrations of 1-3 and cell viability was analyzed by CellTiter-Glo® assay. Relative cell viability is compared to DMSO control (0.1%).

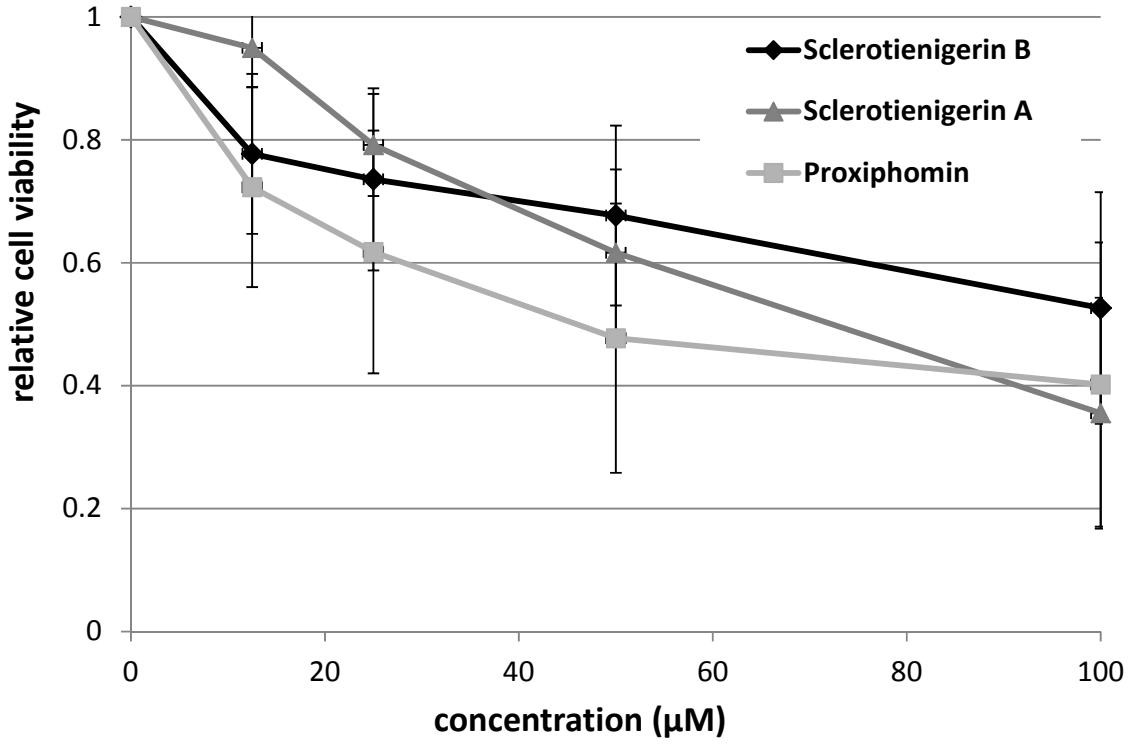

[2] Knudsen, P. B.; Hanna, B.; Ohl, S.; Sellner, L.; Zenz, T.; Stilgenbauer, S.; Larsen, T. O.; Lichter, P.; Seiffert, M. Chaetoglobosin A preferentially induces apoptosis in chronic lymphocytic leukemia cells by targeting the cytoskeleton. *Leukemia* **2013** doi: 10.1038/leu.2013.360. [Epub ahead of print]

Figure S2. Effects of 1-3 on healthy B-cells cell viabiltiy. Healthy B-cells were treated for 24 hours with increasing concentrations of 1-3 and cell viability was analyzed by CellTiter-Glo® assay. Relative cell viability is compared to DMSO control (0.1%).

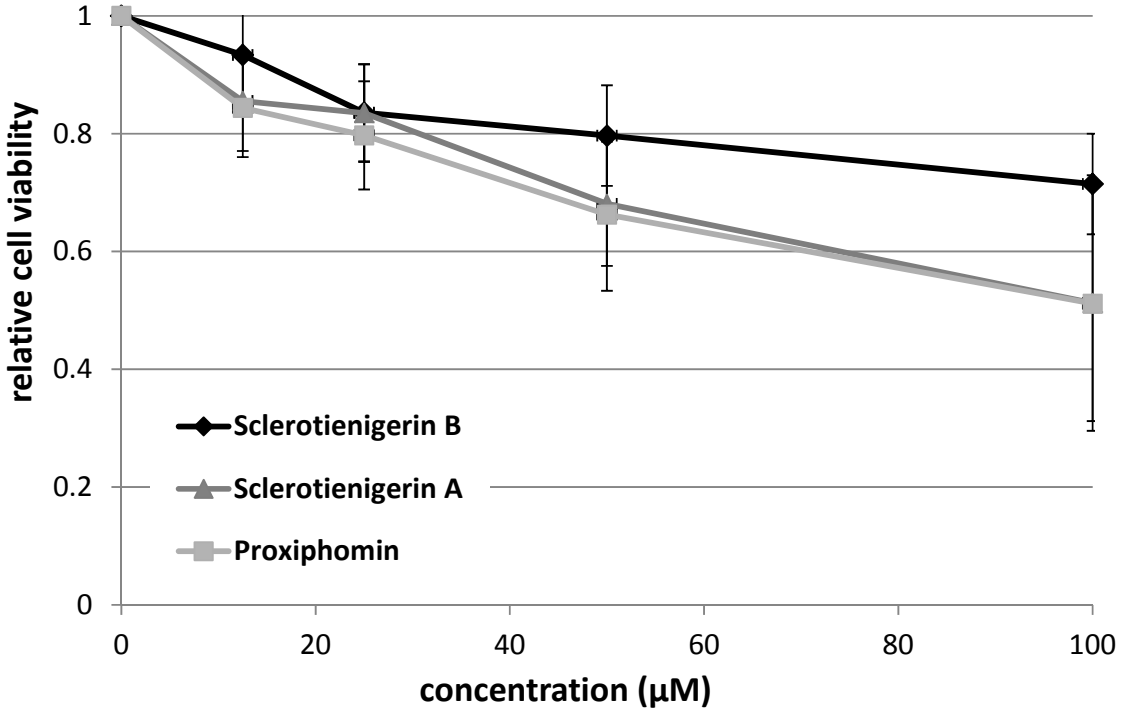

Estimated LC_{50} values

	LC_{50} values	
Compound	CLL	Healthy B-cells
Sclerotionigrin A	72 µM	No effect
Sclerotionigrin B	No effect	No effect
Proxiphomin	48 µM	No effect

Paper 4

Micropeptins from *Microcystis* sp. Collected in Kabul Reservoir, Israel

Bladt, T.T.; Kalifa-Aviv, S.; Larsen, T.O. and Carmeli, S.

Tetrahedron, **2013**, *70*, 936-943

Tanja Thorskov Bladt
Chemical biology of microbial anticancer natural products - appendix

Tetrahedron 70 (2014) 936–943

Contents lists available at ScienceDirect

Tetrahedron

journal homepage: www.elsevier.com/locate/tet

Micropeptins from *Microcystis* sp. collected in Kabul Reservoir, Israel

Tanja Thorskov Bladt [a,b], Sivan Kalifa-Aviv [b], Thomas Ostenfeld Larsen [a], Shmuel Carmeli [b,*]

[a] Department of Systems Biology, Technical University of Denmark, Søltofts Plads, Building 221, DK-2800 Kgs. Lyngby, Denmark
[b] Raymond and Beverly Sackler School of Chemistry and Faculty of Exact Sciences, Tel Aviv University, Ramat-Aviv, Tel-Aviv 69978, Israel

ARTICLE INFO

Article history:
Received 7 October 2013
Received in revised form 17 November 2013
Accepted 2 December 2013
Available online 7 December 2013

Keywords:
Cyanobacteria
Microcystis
Micropeptins
Protease inhibitors
Natural products

ABSTRACT

Three new micropeptins, micropeptin KR1030, KR1002 and KR998 and the known microcyclamide GL546A were isolated from the extract of *Microcystis* sp. bloom material collected in Kabul Reservoir, Israel. The planar structures of the compounds were determined by homonuclear and inverse-heteronuclear 2D-NMR techniques as well as high-resolution mass spectrometry. The absolute configuration of the asymmetric centres of the amino acids was studied using Marfey's method for HPLC. The inhibitory activity of the compounds was determined for the serine proteases: trypsin, chymotrypsin and elastase.

1. Introduction

Cyanobacterial genera that form natural blooms are prolific producers of a large array of toxic and non-toxic metabolites. These genera of cyanobacteria, including the genus *Microcystis*, most frequently produce the toxic microcystins, which are potent protein phosphatase (PP's) inhibitors[1] and mammal hepatotoxins.[2] Ninety different variants of these toxins have been described to date.[3] The non-toxic metabolites that accompany the microcystins, are usually members of five discrete families of protease inhibitors: micropeptins,[4] aerugenosins,[5] microginins,[6] anabaenopeptins[7] and microviridins.[8] Cyanobacterial blooms, toxic and non-toxic, usually contain one or several of these groups of protease inhibitors and in certain cases also other groups of non-toxic metabolites.[9] In most cases the latter non-toxic secondary metabolites are cyclic and linear modified peptides. Modification of proteinogenic amino acids, by cyanobacteria, results in new amino acid mimics, i.e., 3-amino-6-hydroxy-2-piperidone (Ahp), and amino acid derivatives, i.e., hydroxycyclohexenyl alanine (HcAla), dehydroamino butyric acid (Dhb), homotyrosine (Hty), *N*Me-Tyr, *m-Cl* or *Br*-Tyr, *O*Me-Tyr to name only a few incorporated into the micropeptins. The acid residue sequence of the micropeptine family of cyclic peptolides is highly variable, as can be figured from the 139 members of the family.[10] Some of the positions present high tendency and frequency for acid variation while others vary only between two closely related acids. The fifth position from the *C*-termini of these peptolides has attracted most of the attention in this respect, since the nature of the amino acid at this position selects between trypsin and chymotrypsin types of enzyme inhibition.[11] Recently, we have shown that also the second position might alter this selectivity.[12] The side chain of the micropeptins is also highly variable in the length (0–3, most frequently two acid residues) and acid composition and is always terminated by either hydroxy acid (hydroxyphenyllactic acid or glyceric acid derivatives) or a short chain fatty acid (1–8 carbons). The most potent protease inhibitors among the micropeptins are those displaying Phe[13] or Thr[14] at the third position. As part of our continuing interest in the chemical ecology of cyanobacterial water blooms and the search for novel drugs for human diseases,[10] we examined the extracts of a *Microcystis* sp. bloom material collected in September 2009 at Kabul Reservoir, Israel. The extract of this bloom (Sample IL-403) afforded three non-toxic secondary metabolites: micropeptins KR1030 (**1**), KR1002 (**2**) and KR998 (**3**) and the known microcyclamide GL546A.[15] The structure elucidation and the biological activity of the compounds are discussed below.

2. Results and discussion

Micropeptin KR1030 (**1**), a glassy material, presented an ESI MS pseudo-molecular $[M+Na]^+$ ion at *m/z* 1053.5288, corresponding to the molecular formula $C_{53}H_{74}N_8NaO_{13}$ and 21 degrees of unsaturation. Examination of the NMR spectra of **1**, in DMSO-d_6, revealed its peptide nature; i.e., nine carboxyamide

* Corresponding author. Tel.: +972 3 6408550; fax: +972 3 6409293; e-mail address: carmeli@post.tau.ac.il (S. Carmeli).

0040-4020/$ – see front matter © 2013 Elsevier Ltd. All rights reserved.
http://dx.doi.org/10.1016/j.tet.2013.12.009

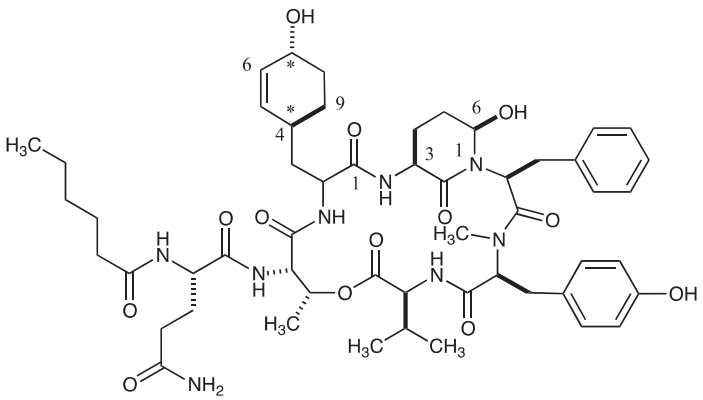

Micropeptin KR1030 (**1**)

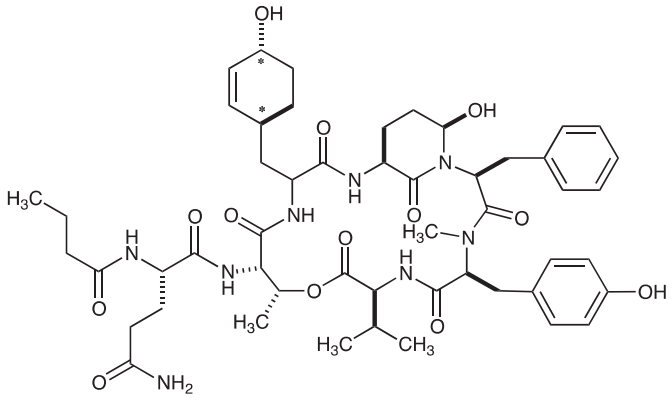

Micropeptin KR1002 (**2**)

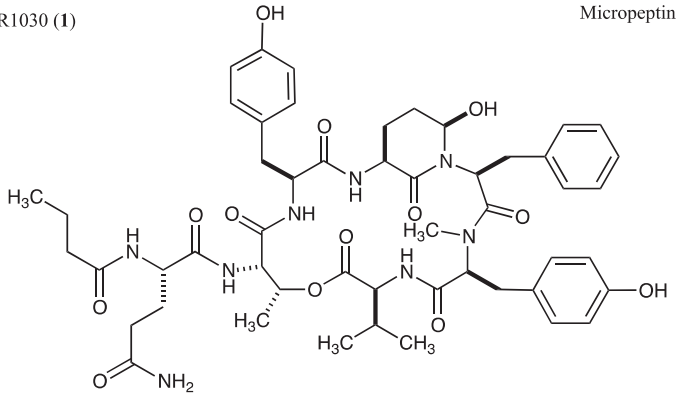

Micropeptin KR998 (**3**)

carbons in the ^{13}C NMR spectrum and five amide doublet protons in the ^{1}H NMR spectrum. Some characteristic signals suggested that it was a micropeptin type compound.[11] Taking into account the *N*Me-aromatic amino acid (*N*MeTyr) and the *N*,*N*-disubstituted-amino acid (*N*,*N*-disubstituted-Phe) of the micropeptins, suggested that this micropeptin was assembled from seven amino acid moieties. In addition, two doublet hydroxyls, resonating at 4.61 and 5.99 ppm were evident in the ^{1}H NMR spectrum. Analyses of the COSY, TOCSY, and HSQC 2D NMR experiments, (Table 1) allowed the assignment of the side chains of three proteogenic amino acids: valine, threonine, glutamine. In addition, these analyses assigned two ABX spin-systems that were in agreement with the aliphatic fragments of two *N*,*N*-disubstituted aromatic amino acids, a *para*-substituted phenol ring and a phenyl ring. Finally, an amino hydroxy piperidone (Ahp) moiety and an extended spin system that didn't fit any proteogenic amino acid were assigned. In the micropeptins, the amide proton of any amino acid residue that occupies the fifth position from the *C*-terminus resonates above δ_H 8.00 ppm.[11] COSY correlation of the amide proton at δ_H 8.40 ppm assigned the methine proton at δ_H 4.33 ppm as H-2 of this amino acid. Using the COSY and TOCSY correlations (see Table 1) the α-methine proton was connected to a methylene, which in turn was connected to a methine that was part of a 4-hydroxycyclohex-2-enyl moiety. This amino acid moiety was thus established as the rare 3-(7-hydroxycyclohex-5-enyl)-alanyl (HcAla) previously identified in four cases in micropeptins.[16–19] Assuming a twisted boat conformation for the cyclohexenyl moiety, the pseudoaxial H-8 (H-8pax) and H-9 (H-9pax) were identified by their shift to higher field. NOE correlation of H-9pax with H-7 and of H-8pax with H-4, as well as, the rest of the NOE's of this spin system shown in Fig. 1, established both as pseudoaxial, and the relative configuration of the hydroxycyclohexenyl moiety as 4*S**,7*R**. Although the NOE pattern of H-2,3a,3b and 4 pointed to a restricted rotation (Fig. 1) it was not possible to assume the relative configuration of positions 2 and 4. The complete structure of the other residues and the assignment of the carboxamide carbons to the amino acid side chains, were achieved by analysis of the HMBC spectrum of **1** (see Table 1). This procedure established the structure of Val, *N*MeTyr, *N*,*N*-disubstituted-Phe, Ahp, HcAla, 3-*O*-substituted-Thr, Gln and hexanoic acid (HA) residues. The sequence of the amino acids of **1**: Val, *N*MeTyr, *N*,*N*-disubstituted-Phe, Ahp, HcAla, Thr, Gln and HA was assigned on the basis of HMBC and ROESY correlations as follows: HMBC correlations between the carboxyamide of *N*MeTyr and Val NH, the carboxyamide of *N*,*N*-disubstituted-Phe and the *N*Me of *N*MeTyr, the carboxyamide of Ahp and H-2 of *N*,*N*-disubstituted-Phe, carboxyamide of HcAla and NH of Ahp, the carboxyamide of Thr and NH of HcAla, the carboxyamide of Gln and the NH of Thr and the carboxyamide of HA and the NH of Gln. The ester-linkage between Thr and Val was established through the HMBC correlation of Thr H-3 and the carboxyl of Val and the NOE between Val H-2 and Thr H-3. Acid hydrolysis of **1** and derivatization with Marfey's reagent,[20] followed by HPLC analysis, demonstrated the L-configuration of Val, *N*Me-tyrosine, phenylalanine, threonine, and glutamic acid residues. Marfey's analysis using 1-fluoro-2,4-dinitrophenyl-5-L-alanine amide (FDAA) as Marfey's reagent[20] fails to distinguish L-threonine from L-*allo*-threonine and thus additional evidence was needed to support their establishment. The observed *J*-value (0–1 Hz) between H-2 and H-3 of the *N*,*O*-disubstituted threonine in **1**, suggested that, as in the case of all known micropeptins, it should be L-threonine and not L-*allo*-

Table 1
NMR data of micropeptin KR1030 (**1**) in DMSO-d_6[a]

Position	δ_C, mult.[b]	δ_H, mult., J (Hz)	LR H-C correlations[c]	NOE correlations[d]
Val-1	172.2 s			
2	55.8 d	4.73 m	Val-1, *N*MeTyr-1	Val-3,4,5
3	31.0 d	2.07 m		Val-4,5,NH, Thr-3
4	19.5 q	0.84 d 6.5	Val-2,3,5	Val-2,3,NH, *N*MeTyr-*N*Me
5	17.3 q	0.71 d 6.9	Val2,3,4	Val-2,3,NH, Ahp-6-OH, *N*MeTyr-*N*Me
NH		7.36 d 9.6	*N*MeTyr-1	Val-4,5, *N*MeTyr-2,*N*Me, Ahp-6-OH
*N*MeTyr-1	169.3 s			
2	61.0 d	4.85 dd 12.0, 2.2	*N*MeTyr-1	Val-NH, *N*MeTyr-3b,5,5′,*N*Me, Phe-2
3	33.0 t	2.70 dd 14.0, 12.0	*N*MeTyr-5,5′	*N*MeTyr-3b,5,5′
		3.08 dd 14.0, 2.2	*N*MeTyr-5,5′	*N*MeTyr-2,3a,5,5′,6,6′
4	127.7 s			
5,5′	130.6 dx2	6.98 dx2 8.2	*N*MeTyr-3,5,5′,7	*N*MeTyr-2,3a,3b,6,6′, *N*Me, Phe-2
6,6′	115.5 dx2	6.74 dx2 8.2	*N*MeTyr-4,5,5′,7	*N*MeTyr-5,5′,7-OH, Phe-6,6′
7	156.4 d			
7-OH		9.33 s	*N*MeTyr-6,6′,7	*N*MeTyr-5,5′,6,6′
*N*Me	30.5 q	2.75 s	*N*MeTyr-2, Phe-2	Val-4,5NH, *N*MeTyr-2,5,5′,6,6′, Ahp-6-OH
Phe-1	170.5 s			
2	50.4 d	4.72 m	Ahp-2	*N*MeTyr-2, Phe-3a,5,5′
3	35.5 t	1.78 dd 14.0, 3.8	Phe-5,5′	*N*MeTyr-6,6′, Phe-2,3b,5,5′
		2.85 dd 14.0, 12.3	Phe-2,5,5′	Phe-3a,5,5′, Ahp-6
4	136.9 s			
5,5′	129.6 dx2	6.82 dx2 7.1	Phe-5′,5,6,7	Phe-2,3a,3b,6,6′, Ahp-4a,6
6,6′	127.9 dx2	7.17 tx2 7.1	Phe-4,6′,6	*N*MeTyr-6,6′, Phe-5,5′
7	126.4 d	7.13 t 7.1	Phe-5	
Ahp-2	169.0 s			
3	48.6 d	3.61 m	Ahp-2	Phe-5,5′, Ahp-4a,NH
4	21.8 t	1.54 m		Ahp-3,4b,5
		2.39 dq 3.0, 12.3		Ahp-4a,5a,6-OH,NH
5	29.4 t	1.66 m		Ahp-4b,6,6-OH
		1.52 m		
6	73.9 d	5.05 dt 1.8, 3.2		Phe-3b,5,5′, Ahp-5a,5b,6-OH
6-OH		5.99 d 3.2		Val-4′,5,NH, Ahp-5a,6, *N*MeTyr-*N*Me
NH		7.08 d 9.1	HcAla-1	Ahp-3,4b, AcAla-2,NH, Thr-3
HcAla-1	170.1 s			
2	49.6 d	4.23 br dd 10.6, 8.8		Ahp-NH, HcAla-3b
3	36.4 t	1.40 br t 10.6		HcAla-3b,4,5,6,NH
		1.69 m		HcAla-2,3a
4	31.7 d	1.92 m		HcAla-3a,5,6,8pax,NH
5	132.2 d	5.37 m	HcAla-7	HcAla-3a,4,6,7
6	132.9 d	5.55 br d 10.3	HcAla-8	HcAla-3a,4,5,7,7-OH
7	65.3 d	3.95 m		HcAla-6,7,7-OH,8peq,9pax
7-OH		4.61 d 5.3	HcAla-6,7,8	HcAla-6,7,8pax
8pax	31.5 t	1.20 m		HcAla-4,7-OH,8peq,9peq
peq		1.79 m		HcAla-7,8pax,9pax
9pax	26.0 t	0.95 td 12.7, 3.0	HcAla-4	HcAla-7,8peq,9peq
peq		1.66 m		HcAla-8pax,9peq
NH		8.40 d 8.8	Thr-1	Ahp-NH, HcAla-3a,4, Thr-2
Thr-1	169.5 s			
2	54.9 d	4.55 d 9.1	Thr-1	HcAla-NH, Thr-3,4
3	71.8 d	5.37 m	Val-1	HcAla-NH, Thr-2,4, Val-3
4	17.6 q	1.17 d 6.6	Thr-2,3	Thr-2,3, Gln-2
NH		7.96 d 9.1	Gln-1	Thr-4, Gln-2
Gln-1	172.8 s			
2	52.2 d	4.38 dt 6.0, 8.0	Gln-1	Thr-4,NH, Gln-3a,3b,NH, HA-4
3	27.9 t	1.69 m	Gln-2,4	Gln-2,3b,NH
		1.84 m		Gln-2,3a,NH
4	31.8 t	2.07 m	Gln-5	
		2.08 m	Gln-5	
5	174.0 s			
5-NH_2 (a)		6.73 s	Gln-4	Gln-4
(b)		7.21 s	Gln-5	
NH		7.98 d 8.0	HA-1	Gln-2,3a
HA-1	172.5 s			
2	35.2 t	2.08 m	HA-1,4	HA-3
3	25.1 t	1.49 m	HA-1,4	HA-2
4	31.5 t	1.20 m	HA-1,3,5	
5	22.0 t	1.23 m	HA-3,4,6	
6	14.0 q	0.84 t 7.0	HA-5	

[a] 500 MHz for ^{1}H, 125 MHz for ^{13}C.
[b] Multiplicity and assignment from HSQC experiment.
[c] Determined from HMBC experiment, $^nJ_{CH}$=8 Hz, recycle time 1 s.
[d] Selected NOE's from a ROESY experiment.

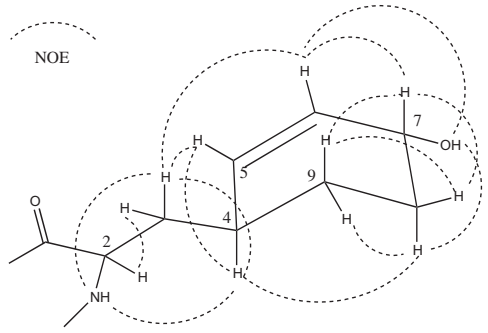

Fig. 1. NOE correlations instrumental for determining the relative configuration of the hydroxycyclohexenyl alanine moiety.

threonine.[11] Jones oxidation[21] of **1**, followed by a similar hydrolysis, derivatization and HPLC analysis, determined the 3*S*-configuration for the Ahp residue (oxidation and subsequent hydrolysis liberated L-glutamic acid from Ahp). An attempt to determine the absolute configuration of C-2 in HcAla by advance Marfey's procedure failed most probably due to its decomposition during hydrolysis. The configuration of C-6 of the Ahp moiety was determined as *R* on the basis of the following evidences: (i) The coupling constants of H-6, 1.8 and 3.2 Hz, with pseudo-equatorial-H-5 and pseudo-axial-H-5, respectively, which pointed to an equatorial orientation of H-6; (ii) The chemical shift of the pseudo-axial-H-4, δ_H 2.39 dq (3.0,12.3), which is down-field shifted by the axial 6-hydroxy-group; (iii) The *trans*-diaxial relationship of H-4pax with H-3 (mutual coupling constant of 12.3 Hz); (iv) The NOE correlation between H-4pax with the 6-OH. Based on these findings the structure of micropeptin KR1030 was established as **1**.

Examination of the NMR spectra of micropeptin KR1002 (**2**) revealed that its ^{1}H and ^{13}C NMR spectra are similar to those of **1**. The molecular formula of **2**, $C_{51}H_{70}N_8O_{13}$, was deduced from the high-resolution ESI-MS measurements of its sodiated molecular ion cluster at *m*/*z* 1025.4958. Comparison of the NMR data of micropeptin KR1030 (**1**) and micropeptin KR1002 (**2**) (see Tables 1 and 2, respectively) revealed that the difference between them is located in the fatty acid moiety at the *N*-termini of these cyclic peptolides. Two methylene carbons (δ_C 31.5 and 25.1) of the aliphatic residue and four proton signal ($\delta_H \sim 1.20$), which appeared in the spectra of **1** were missing from the spectra of **2**, suggesting that the HA residue in **1** is replaced by a butyric acid (BA) residue in **2**. Full assignment of **2** was achieved by interpretation of the COSY, TOCSY, ROESY, HSQC and HMBC 2D NMR correlations (see Table 2), revealing the composition and sequence of acid residues of **2** as, Val, *N*MeTyr, *N*,*N*-disubstituted-Phe, Ahp, HcAla, Thr, Gln and BA. Acid hydrolysis of **2** and derivatization with Marfey's reagent,[20] as described above for **1** followed by HPLC analysis, demonstrated the L-configurations for all of the amino acid residues except of HcAla. The absolute configuration of the Ahp residue was determined in the same way as for **1**. Based on these findings the structure of micropeptin KR1002 was established as **2**.

Micropeptin KR998 (**3**), a glassy material, presented an ESI MS pseudo-molecular $[M+Na]^+$ ion at *m*/*z* 1021.4666, corresponding to the molecular formula $C_{51}H_{66}N_8O_{13}$ and 23 degrees of unsaturation. Comparison with **2** revealed two additional degrees of unsaturation in **3**. The ^{1}H and ^{13}C NMR spectra of **3** were comparable with those of **2**, but revealed some differences as well. In the aromatic region of the ^{1}H NMR spectrum of **3**, two additional mutually-coupled (8.2 Hz) 2H doublet signals at δ_H 6.89 and 6.56 ppm and a singlet proton at δ_H 9.07 ppm were evident. In the aliphatic region two additional benzylic protons (δ_H 3.11 and 2.50) were observed, while the signals corresponding to the HcAla in **2** were missing. In the ^{13}C NMR spectrum of **3** four new aromatic signals (δ_C 128.3 s, 129.8 dx2, 115.2 dx2 and 155.7 s), of a *para*-substituted phenol moiety were observed, while the signals of HcAla observed in **2** were missing (Tables 2 and 3). The data summarized above and the molecular formula of **3** relative to that of **2** suggested that in **3** a tyrosine moiety substitute the HcAla of **2**, while the rest of the structures of these compounds are identical. Full assignment of the tyrosine moiety and the rest of the moieties that compose **3** as well as their sequence was achieved using COSY, TOCSY, ROESY, HSQC and HMBC 2D NMR correlations (see Table 3). Marfey's analysis as described above for **1** established the absolute configuration of all amino acids including C-3 of Ahp as L. The absolute configuration of C-6 of the Ahp residue was determined in the same way as for **1**. Based on these findings the structure of micropeptin KR998 was established as **3**.

2.1. Biological activity

The crude cyanobacterial extract exhibited significant inhibition of the serine protease chymotrypsin at a concentration of 1 mg/ml. Purification of the proteases-inhibiting components of the extract revealed that micropeptins **1**–**3** were responsible for the inhibition of chymotrypsin. This finding was in accordance with the known activity of the micropeptins that contain aromatic or aliphatic amino acid next to the Ahp moiety, which usually are potent chymotrypsin inhibitors.[10] The inhibitory activity of **1**–**3** was determined for serine protease chymotrypsin, elastase and trypsin. Micropeptins **1**–**3** did not inhibit trypsin at a concentration of 45.5 μM. Chymotrypsin was inhibited by micropeptin KR1030 (**1**) with an IC_{50} of 13.9 μM, by micropeptin KR1002 (**2**) with an IC_{50} of 18.8 μM, by micropeptin KR998 (**3**) with an IC_{50} of 5.9 μM. Elastase was inhibited by micropeptin KR1030 (**1**) and micropeptin KR1002 (**2**) with an IC_{50} of 28.0 μM, but not by micropeptin KR998 (**3**) at a concentration of 50 μM. The relative potency of **1**–**3** to chymotrypsin is in accordance with the published data.[11]

3. Conclusions

This study describes the isolation of three new micropeptins together with the known microcyclamide GL546A from the water bloom material of the cyanobacterium *Microcystis* sp. This research adds to the growing library of micropeptins and illuminates the variety of the metabolites produced by these fresh water cyanobacteria. The use of non-proteogenic amino acids allows the expansion of the library of micropeptins that are biosynthesized by cyanobacteria. The purpose for the incorporation of non-proteogenic amino acids into these peptides might be derived from the need to avoid recognition of the amino acids in the peptide by proteolytic enzymes or to produce special epitopes to be recognized by special receptors in the producing organisms. HcAla, which is incorporated in two of the three new micropeptins described here, is most probably derived from L-arogenate, the precursor of phenylalanine and tyrosine. It is presumably biosynthesized by reduction and decarboxylation of L-arogenate (Fig. 2), in analogy with the biosynthesis of the proline mimicking amino acid, Choi, in the aeruginosins.[22] It is of great interest to study the biosynthesis of HcAla, which we intend to do in the near future.

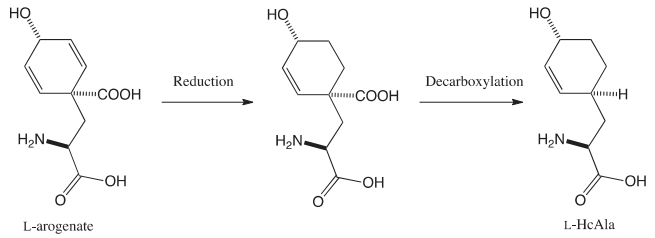

Fig. 2. Possible route from arogenate to HcAla.

Table 2
NMR data of micropeptin KR1002 (**2**) in DMSO-d_6[a]

Position	δ_C, mult.[b]	δ_H, mult., J (Hz)	LR H-C correlations[c]	NOE correlations[d]
Val-1	172.6 s			
2	55.6 d	4.73 dd 9.8, 4.2	Val-5	Val-3,4,NH, *N*MeTyr-2
3	30.9 d	2.07 m		Val-2,4,5
4	19.3 q	0.86 d 6.7	Val-2,3,5	Val-3, *N*MeTyr-*N*Me
5	17.1 q	0.71 d 6.7	Val-2,3,4	Val-3,NH, *N*MeTyr-*N*Me, Ahp-6-OH
NH		7.38 d 9.8	*N*MeTyr-1	Val-2,3, *N*MeTyr-2,*N*Me
*N*MeTyr-1	168.9 s			
2	60.9 d	4.89 dd 11.5, 2.0	*N*MeTyr-1	Val-2, *N*MeTyr-3b,5,5′,*N*Me
3	32.8 t	2.71 dd 13.2, 11.5	*N*MeTyr-5,5′	Val-NH, *N*MeTyr-3b,5,5′,6,6′
		3.09 dd 13.2, 2.0	*N*MeTyr-4,5,5′	*N*MeTyr-2,3a,5,5′
4	127.5 s			
5,5′	130.4 dx2	6.99 dx2 8.2	*N*MeTyr-3,5′,5,7	*N*MeTyr-2,3a,3b, Phe-2
6,6′	115.3 dx2	6.76 dx2 8.2	*N*MeTyr-4,6′,6,7	*N*MeTyr-3a,7-OH, Phe-3a
7	156.2 s			
7-OH		9.33	*N*MeTyr-6′,6,7	*N*MeTyr-6,6′
*N*Me	30.3 q	2.75 s	*N*MeTyr-2	Val-4,5,NH, *N*MeTyr-2,5,5′
Phe-1	170.3 s			
2	50.2 d	4.75 dd 11.9, 3.9	Phe-1	*N*MeTyr-5,5′, Phe-3a,5,5′
3	38.5 t	1.79 m	Phe-5,5′	Phe-2,3b,5,5′, *N*MeTyr-6,6′
		2.85 dd 11.9, 14.0	Phe-5,5′	Phe-3,5,5′, Ahp-6
4	136.7 s			
5,5′	129.4 dx2	6.82 dx2 7.1	Phe-3,5′,6,7	Phe-2,3a,3b, Ahp-4a
6,6′	127.7 dx2	7.17 tx2 7.1	Phe-4,5,6	HcAla-OH
7	126.2 d	7.13 t 7.1	Phe-5	Ahp-3
Ahp-2	169.3 s			
3	48.5 d	3.60 ddd 7.1, 9.1, 12.7		Ahp-4a,NH, Phe-7
4	21.6 t	1.55 m		Ahp-3,4b,6, Phe-6,6′
		2.39 br q 12.7		Ahp-4a,NH,6-OH
5	29.6 t	1.67 m		Ahp-6-OH, HcAla–5
		1.55 m		
6	73.7 d	5.05 br s		Phe-3b, Ahp-4,5,6-OH
6-OH		5.99 d 2.5		Ahp-4b,5,6, Val-5,NH, HcAla-NH
NH		7.08 d 9.1	HcAla-1	Ahp-3,4b, HcAla-2,9,NH
HcAla-1	170.0 s			
2	49.4 d	4.23 br dd 11.4, 7.4		Ahp-NH, HcAla-3b,4
3	36.4 t	1.40 dt 3.7, 11.4		HcAla-3b,4,5,6
		1.71 m		HcAla-2,3a
4	31.6 d	1.92 m		HcAla-2,3a,5,6,8pax,NH
5	132.0 d	5.37 br d 10.2		HcAla-3a,4,6,7
6	132.7 d	5.55 dd 10.2, 1.0	HcAla-4	HcAla-3a,4,5,7,7-OH
7	65.1 d	3.94 br m		HcAla-5,6,7-OH,8peq,9pax
8 peq	31.6 t	1.79 m		HcAla-7,7-OH,8pax,9pax
pax		1.20 m		HcAla-4,8peq,9peq,7-OH
9 peq	25.8 t	1.70 m		HcAla-4,8pax,9pax
pax		0.93 br q 11.3		HcAla-7,8peq,9peq
7-OH		4.61 d 5.4	HcAla-6,7,8	HcAla-6,7,8peq,8pax
NH		8.40 d 8.4		Ahp-NH, HcAla-3a,4, Thr-2,3
Thr-1	169.1 s			
2	54.9 d	4.55 br d 9.1	Thr-1, Gln-1	HcAla-NH, Thr-4
3	71.7 d	5.39 q 6.5	Thr-4	HcAla-NH, Thr-4
4	17.6 q	1.17 d 6.5	Thr-2,3	HcAla-7-OH, Thr-2,3,NH
NH		7.91 d 9.0	Gln-1	HcAla-NH, Thr-4
Gln-1	172.2 s			
2	52.0 d	4.38 m	Gln-1	Thr-NH, Gln-3a,3b,4b
3	27.7 t	1.69 m	Gln-4	Gln-2,3b,NH, BA-3
		1.84 m		Gln-3a,NH
4	31.6 t	2.11 m	Gln-5	Gln-2,NH,5-NH_2
5	173.9 s			
5-NH_2(a)		6.72 s	Gln-4	Gln-4
(b)		7.21 s		
NH		7.99 d 7.5	BA-1	Gln-3a,4
BA-1	172.0 s			
2	37.0 t	2.09 m	BA-1,3,4	Gln-2
3	18.9 t	1.51 m	BA-1,2,4	Gln-3a
4	13.6 q	0.84 t 7.3	BA-2,3	Val-2

[a] 400 MHz for ^{1}H, 100 MHz for ^{13}C.
[b] Multiplicity and assignment from HSQC experiment.
[c] Determined from HMBC experiment, $^nJ_{CH}$=8 Hz, recycle time 1 s.
[d] Selected NOE's from a ROESY experiment.

Table 3
NMR data of micropeptin KR998 (**3**) in DMSO-d_6[a]

Position	δ_C, mult.[b]	δ_H, mult., J (Hz)	LR H-C correlations[c]	NOE correlations[d]
Val-1	172.1 s			
2	55.9 d	4.66 dd 9.5, 4.3	Val-1,3,5	Val-3,4,5,NH, Gln-NH_2
3	31.0 d	2.02 m	Val-2,4,5	Val-2,4,5,NH, Thr-2
4	19.4 q	0.85 d 5.7	Val-2,3,5	Val-2,3,NH, *N*MeTyr-*N*Me
5	17.3 q	0.70 d 6.7	Val-2,3,4	Val-2,3,NH, *N*MeTyr-*N*Me, Ahp-6-OH
NH		7.37 d 9.5	*N*MeTyr-1	Val-2,3,4,5, *N*MeTyr-2,*N*Me, Ahp-6-OH
*N*MeTyr-1	169.0 s			
2	61.0 d	4.89 br d 11.4	*N*MeTyr-1,*N*Me	Val-NH, *N*MeTyr-3b,5,5′
3	33.0 t	2.71 dd 13.4, 11.4	*N*MeTyr-2,5,5′	*N*MeTyr-3b,6,6′
		3.08 br d 13.4	*N*MeTyr-4,5,5′	*N*MeTyr-2,3a,5,5′
4	127.7 s			
5,5′	130.6 dx2	6.99 dx2 8.0	*N*MeTyr-3,5′,5,6,6′,7	*N*MeTyr-2,3b,*N*Me, Phe-2,3a
6,6′	11.5.5 dx2	6.77 dx2 8.0	*N*MeTyr-4,6,6′,7	*N*MeTyr-*N*Me,OH, Phe-3a
7	156.4 s			
*N*Me	30.5 q	2.75 s	*N*MeTyr-2, Phe-1	*N*MePhe-5,5′,7, Val-4,5,NH
Phe-1	170.5 s			
2	50.4 d	4.74 dd 11.3, 3.6	Phe-1	*N*MeTyr-5,5′, Phe-3a,5,5′
3	35.5 t	1.78 m	Phe-5,5′	*N*MeTyr-5,5′,6,6′, Phe-2,3b,5,5′
		2.86 dd 11.7, 13.8		Phe-3a,5,5′, Ahp-6
4	136.9 s			
5,5′	129.6 dx2	6.83 dx2 7.1	Phe-3,5′,5,7	Phe-2,3a,3b, Ahp-3,5a,6
6,6′	127.9 dx2	7.18 tx2 7.1	Phe-4,5,5′,6′,6	Ahp-3
7	126.4 d	7.14 t 7.1	Phe-5,5′	
Ahp-2	169.0 s			
3	49.0 d	3.60 ddd 11.6, 8.2, 6.0	Ahp-2,4	Phe-5,5′, Ahp-4a,NH
4	21.7 t	1.62 m		Ahp-3,4b
		2.40 br q 12.4		Ahp-4a,5b,NH
5	29.4 t	1.68 m		Ahp-6,6-OH
		1.57 m		Ahp-4b
6	73.9 d	5.05 br s		Phe-3b,5,5′, Ahp-5a,5b
6-OH		5.99 d 2.1		Ahp-5b,6, Val-5,NH
NH		7.07 d 10.2		Ahp-3,4b, Tyr-2,NH
Tyr-1	169.7 s			
2	53.6 d	4.35 ddd 3.8, 9.0, 13.0		Ahp-NH, Tyr-3a,3b,5,5′,NH
3	35.1 t	2.50 dd 13.0, 14.7	Tyr-2,4,5	Tyr-2,3b,5,5′
		3.11 dd 3.8, 14.7		Tyr-2,3a,NH
4	128.3 s			
5,5′	129.8 dx2	6.89 dx2 8.2	Tyr-3,5,5′,6,6′,7	Tyr-2,3a,NH
6,6′	115.2 dx2	6.56 dx2 8.2	Tyr-4,6′,6,7	Tyr-5,5′,7-OH
7	155.7 s			
7-OH		9.07 s	Tyr-6,6′	Tyr-6,6′
NH		8.45 d 9.0	Thr-1	Ahp-NH, Tyr-2,3a,5,5′, Thr-2,3
Thr-1	169.0 s			
2	554.4 d	4.45 br d 9.4	Thr-1,4, Gln-1	Tyr-NH, Thr-4,NH, Ahp-NH
3	72.2 d	5.37 q 6.5	Thr-4, Val-1	Ahp-NH, Tyr-NH, Thr-4
4	17.7 q	1.10 d 6.5	Thr-2,3	Thr-2,3,NH
NH		7.69 d d 9.4	Gln-1	Thr-2,3,4, Gln-2,3b
Gln-1	172.3 s			
2	52.2 d	4.30 dt 5.3, 8.3	Gln-3	Thr-NH, Gln-3a,3b,4,NH
3	27.5 t	1.70 m	Gln-2,4,5	Gln-2,NH
		1.80 m	Gln-1,2,4,5	Thr-NH, Gln-2
4	31.7 t	2.05 m	Gln-2,3,5	Gln-2,NH,5-NH_2(a,b)
5	174.3 s			
5-NH_2a		6.81 s	Gln-4,5	Gln-4
b		7.24 s	Gln-5	Gln-4
NH		7.98 d 7.8	BA-1	Gln-2,a3,4
BA-1	172.4 s			
2	37.4 t	2.10 m	BA-1,3,4	
3	18.9 t	1.50 tq 7.3, 7.3	BA-1,2,4	
4	13.8 q	0.85 t 7.2	BA-2,3	

[a] 500 MHz for ^{1}H, 125 MHz for ^{13}C.
[b] Multiplicity and assignment from HSQC experiment.
[c] Determined from HMBC experiment, $^nJ_{CH}$=8 Hz, recycle time 1 s.
[d] Selected NOE's from a ROESY experiment.

4. Experimental section

4.1. General experimental procedures

Mass spectra were recorded on a Waters MaldiSynapt instrument. UV spectra were recorded on an Agilent 8453 spectrophotometer. Optical rotation values were obtained on a Jasco P-1010 polarimeter at the sodium D line (589 nm). NMR spectra were recorded on a Bruker Avance 500 spectrometer at 500.13 MHz for ^{1}H and 125.76 MHz for ^{13}C and a Bruker Avance 400 Spectrometer at 400.13 MHz for ^{1}H, 100.62 MHz for ^{13}C. DEPT, COSY-45, gTOCSY, gROESY, gHSQC, gHMQC and gHMBC spectra were recorded using standard Bruker pulse sequences. HPLC separations were performed on a JASCO HPLC system (model PU-2080 *Plus* pump, model LG-2080-04 Quaternary Gradient unit and model PU-2010 *Plus* Multiwavelength Detector), on a Merck Hitachi HPLC system (model

L-6200A pump and model L-4200 UV–Vis detector), and on a Merck Hitachi HPLC system (model L-7000A intelligent pump and model L-6200 UV–vis detector). An Elisa ELx808 plate reader (BioTek Instruments, Inc.) was used for proteases inhibition assays.

4.2. Cyanobacterial material

Microcystis sp., TAU sample IL-403, was collected in September 2009 at Kabul Reservoir, Israel. Samples of the cyanobacteria are deposited at the culture collection of Tel Aviv University.

4.3. Isolation procedure

The freeze dried cyanobacterial mass (199 g) was extracted with MeOH/water (70:30) and the crude extract (26 g) was separated on a flash RP-C_{18} column with increasing amounts of MeOH in water resulting in 12 fractions. Fraction 5 and 6 were combined (40–50% MeOH in water, 474 mg) and separated on Sephadex LH-20 column with chloroform/MeOH (1:1). The fractions from this column were further separated by preparative HPLC on a Waters Cosmosil 5C_8-MS (250×20 mm, 5 μm) column eluted at a rate of 5 ml/min using DAD detection. Fraction 2 (130 mg) was separated by preparative HPLC with 35:65 ACN/0.1% TFA in water to obtain micropeptin KR1030 (**1**, 3.9 mg). Further isocratic HPLC fractionation of fraction 4 and 5 from the previous HPLC separation with 3:7 ACN/0.1% TFA in water yielded micropeptins KR1002 and KR998 (**2**, 3.7 and **3**, 1.4 mg, respectively).

*4.3.1. Micropeptin KR1030 (**1**).* Glassy material; $[\alpha]_D^{25}$ −19.1 (*c* 0.04, MeOH); UV (MeOH) λ_{max} (Log ε) 202 (4.44), 222 (3.95), 277 (3.18) nm; IR ($CHCl_3$): 3361, 2923, 2853, 1654, 1025, 993, 669 cm^{-1}; HRESIMS *m*/*z* 1053.5288 $[M+Na]^+$ (calculated for $C_{53}H_{74}N_8NaO_{13}$, 1053.5273); Retention times of AA Marfey's derivatives (L-FDAA): L-Thr 33.4 min (D-Thr 36.3 min), L-Glu, 35.2 min (D-Glu 36.2 min), L-Val 44.2 min (D-Val 48.1 min), L-Phe 48.8 min (D-Phe 51.8 min), L-NMe-Tyr 53.3 min.

*4.3.2. Micropeptin KR1002 (**2**).* Glassy material; $[\alpha]_D^{25}$ −14.6 (*c* 0.04, MeOH); UV (MeOH) λ_{max} (Log ε) 202 (3.90), 222 (3.27), 278 (2.73) nm; IR ($CHCl_3$): 3360, 2924, 2853, 1653, 1025, 994, 669 cm^{-1}; HRESIMS *m*/*z* 1025.4958 $[M+Na]^+$ (calculated for $C_{51}H_{70}N_8NaO_{13}$, 1025.4960); Retention times of AA Marfey's derivatives (L-FDAA): L-Thr 33.3 min (D-Thr 36.3 min), L-Glu, 35.8 min (D-Glu 36.7 min), L-Val 44.0 min (D-Val 48.1 min), L-Phe 48.9 min (D-Phe 51.9 min), L-NMe-Tyr 53.6 min.

*4.3.3. Micropeptin KR998 (**3**).* Glassy material; $[\alpha]_D^{25}$ −40.0 (*c* 0.01, MeOH); UV (MeOH) λ_{max} (Log ε) 202 (4.73), 222 (4.30), 278 (3.46) nm; IR ($CHCl_3$): 3360, 2923, 2853, 1654, 1635, 1025, 997, 669 cm^{-1}; HRESIMS *m*/*z* 1021.4666 $[M+Na]^+$ (calculated for $C_{51}H_{66}N_8NaO_{13}$, 1021.4647); Retention time of AA Marfey's derivatives: L-Thr 33.6 min (D-Thr 36.5 min), L-Glu 35.8 min (D-Glu 36.8 min), L-Val 44.5 min (D-Val 48.3 min), L-Phe 48.9 min (D-Phe 51.6 min), L-*N*Me-Tyr 53.4 min, L-Tyr 54.4 min (D-Tyr 57.9 min).

4.4. Determination of the absolute configuration of the amino acids

0.5 mg portions of compounds **1**–**3** were dissolved in 6 N HCl (1 mL). The reaction mixture was then placed in a sealed glass bomb at 110 °C for 16 h. In another experiment, 0.25 mg portions of compounds **1**–**3** were first oxidized with Jones reagent (1 drop) in acetone (1 mL) at 0 °C for 10 min. Following the usual work-up, the residue was dissolved in 6 M HCl (1 mL) and placed in a sealed glass bomb at 104 °C for 18 h. After the removal of HCl, by repeated evaporation in vacuo, the hydrolysate was resuspended in water (40 μL). A solution of (1-fluoro-2,4-dinitrophenyl)-5-L-alanine amide (L-FDAA) (4.2 mM) in acetone (150 mL) and 1 M $NaHCO_3$ (20 mL) was added to each reaction vessel and the reaction mixture was stirred at 40 °C for 2 h. A 2 M HCl solution (10 mL) was added to each reaction vessel and the solution was evaporated in vacuo. The *N*-[(2,4-dinitrophenyl)-5-L-alanine amide]-amino acid derivatives, from hydrolysates, were compared with similarly derivatized standard amino-acids by HPLC analysis: LichroCART RP-18, 5 μm, 4.6×250 mm, flow rate: 1 mL/min, UV detection at 340 nm, linear gradient elution from 0.1% TFA in water (pH 3) to 4:6 0.1% TFA in water/acetonitrile within 60 min. The determination of the absolute configuration of each amino acid was confirmed by spiking the derivatized hydrolysates with the derivatized authentic amino acids.

4.5. Protease inhibition assays

Trypsin, chymotrypsin and elastase were purchased from Sigma Chemical Co. Trypsin (1 mg/mL) and chymotrypsin (10 mg/mL) were dissolved in 0.05 M Tris–HCl/100 mM NaCl/1 mM $CaCl_2$, pH 7.5 buffer solution. Benzoyl-L-arginine-*p*-nitroanilide hydrochloride (BAPNA), the trypsin substrate, was dissolved in a solution of 1:9 DMSO: Tris-buffer (0.85 g/mL). Suc-Gly-Gly-*p*-nitroanilide (SGGPNA), the substrate for chymotrypsin, was dissolved in Tris-buffer (1 mg/mL). Test samples were dissolved in DMSO (1 mg/mL). A 100 μL buffer solution, 10 μL enzyme solution and 10 μL sample solution were added to each microtiter plate well and pre-incubated at 37 °C for 10 min. Then, 10 μL of substrate solution was added and the kinetics of the reaction were measured at 405 nm, 37 °C for 30 min. Elastase (75 mg/mL) was dissolved in 0.2 M Tris–HCl, pH 8 buffer solution. *Z*-Gly-Pro-Arg-4MβNA-acetate salt, the thrombin substrate, was dissolved in Tris buffer (0.5 mg/ml). *N*-Suc-Ala-Ala-Ala-*p*-nitroanilide, the elastase substrate, was dissolved in Tris buffer (1 mg/mL). The test samples were dissolved in DMSO (1 mg/mL). For elastase, 150 μL buffer solution, 10 μL enzyme solution and 10 μL sample solution were added to each microtiter plate well and pre-incubated at 30 °C for 20 min. Then, 30 μL of substrate solution were added and the kinetics of the reaction was measured at 405 nm, 37 °C for 20 min.

Acknowledgements

We thank Noam Tal, The Mass Spectrometry Laboratory of The School of Chemistry, Tel Aviv University, for the ESI mass spectra measurements. T.T.B. acknowledges the funding from Otto Mønsteds Fond. This research was supported in part by the Israel Science Foundation grants 776/06.

Supplementary data

^1H and ^{13}C NMR spectra and HRESIMS of compounds **1**–**3** are available. Supplementary data associated with this article can be found in the online version, at http://dx.doi.org/10.1016/j.tet.2013.12.009. These data include MOL files and InChiKeys of the most important compounds described in this article.

References and notes

1. Yoshizawa, S.; Matsushima, R.; Watenabe, M. F.; Hard, K.; Ichihara, A.; Carmichael, W. W.; Fujiki, H. *J. Cancer Res. Clin. Oncol.* **1990**, *116*, 609–614.
2. Ito, E.; Takai, A.; Kondo, F.; Masui, H.; Imanishi, S.; Harada, K. *Toxicon* **2002**, *40*, 1017–1025.
3. Pearson, L.; Mihali, T.; Moffitt, M.; Kellmann, R.; Neilan, B. *Mar. Drugs* **2010**, *8*, 1650–1680.
4. Sano, T.; Kaya, K. *J. Nat. Prod.* **1996**, *59*, 90–92.
5. Murakami, M.; Okita, Y.; Matsuda, H.; Okino, T.; Yamaguchi, K. *Tetrahedron Lett.* **1994**, *35*, 3129–3132.

6. Okino, T.; Matsuda, H.; Murakami, M.; Yamaguchi, K. *Tetrahedron Lett.* **1993**, *34*, 501–504.
7. Harada, K.; Fujiki, H.; Shimada, T.; Sozuki, M.; Sano, H.; Adachi, K. *Tetrahedron Lett.* **1995**, *36*, 1511–1514.
8. Reshef, V.; Carmeli, S. *Tetrahedron* **2006**, *62*, 7361–7369.
9. Welker, M.; von Dohren, H. *FEMS Microbiol. Rev.* **2006**, *30*, 530–563.
10. Vegman, R.; Carmeli, S. *Tetrahedron* **2013**, *69*, 10108–10115.
11. Linington, R. G.; Edwards, D. J.; Shuman, C. F.; McPhail, K. L.; Matainaho, T.; Gerwick, W. H. *J. Nat. Prod.* **2008**, *71*, 22–27.
12. Gesner-Apter, S.; Carmeli, S. *J. Nat. Prod.* **2009**, *72*, 1429–1436.
13. Gademann, K.; Portmann, C.; Blom, J. F.; Zeder, M.; Juttner, F. *J. Nat. Prod.* **2010**, *73*, 980–984.
14. Grach-Pogrebinsky, O.; Sedmak, B.; Carmeli, S. *Tetrahedron* **2003**, *59*, 8329–8336.
15. Raveh, A.; Moshe, S.; Evron, Z.; Flescher, E.; Carmeli, S. *Tetrahedron* **2010**, *66*, 2705–2712.
16. Harada, K.; Mayumi, T.; Shimada, T.; Suzuki, M.; Kondo, F.; Watanabe, M. F. *Tetrahedron Lett.* **1993**, *34*, 6091–6094.
17. Ishida, K.; Matsuda, H.; Murakami, M. *Tetrahedron* **1998**, *54*, 5545–5556.
18. Itou, Y.; Ishida, K.; Shin, S. J.; Murakami, M. *Tetrahedron* **1999**, *55*, 6871–6882.
19. Adiv, S.; Aharonov-Nadborny, R.; Carmeli, S. *Tetrahedron* **2010**, *66*, 7429–7436.
20. Marfey, P. *Carlsberg Res. Commun.* **1984**, *49*, 591–596.
21. Bowden, K.; Heilbron, I. M.; Jones, E. R. H.; Weedon, B. C. L. *J. Chem. Soc.* **1946**, 39–45.
22. Ishida, K.; Christiansen, G.; Yoshida, W. Y.; Kurmayer, R.; Welker, M.; Valls, N.; Bonjoch, J.; Hertweck, C.; Borner, T.; Hemscheidt, T.; Dittmann, E. *Chem. Biol.* **2007**, *14*, 565–576.

Micropeptins from *Microcystis* sp. collected in Kabul Reservoir, Israel

Tanja Thorskov Bladt [a], Sivan Kalifa-Aviv [b], Thomas Ostenfeld Larsen [a], and Shmuel Carmeli [b]*

[a] *Department of Systems Biology, Technical University of Denmark, Søltofts Plads, Building 221, DK-2800 Kgs. Lyngby, Denmark*
[b] *Raymond and Beverly Sackler School of Chemistry and Faculty of Exact Sciences, Tel Aviv University, Ramat-Aviv Tel- Aviv 69978, Israel*

Supplementary data

* Corresponding author. Tel.: +972-3-6408550; fax: +972-3-6409293; e-mail: carmeli@post.tau.ac.il

Contents

S1. ^{1}H NMR Spectrum of Micropeptin KR1030 (**1**) in DMSO-d_6

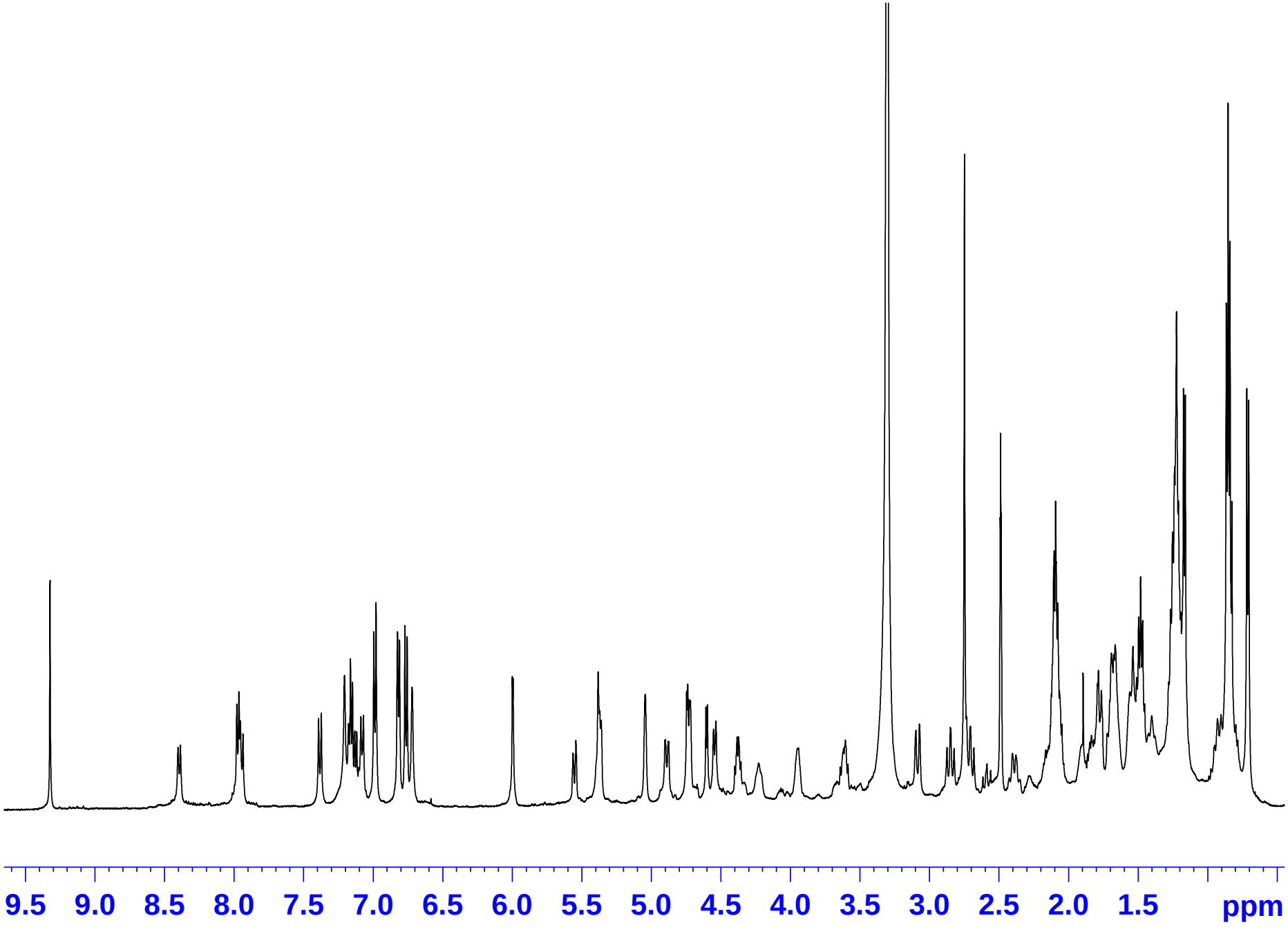

S2. ^{13}C NMR Spectrum of Micropeptin KR1030 (**1**) in DMSO-d_6

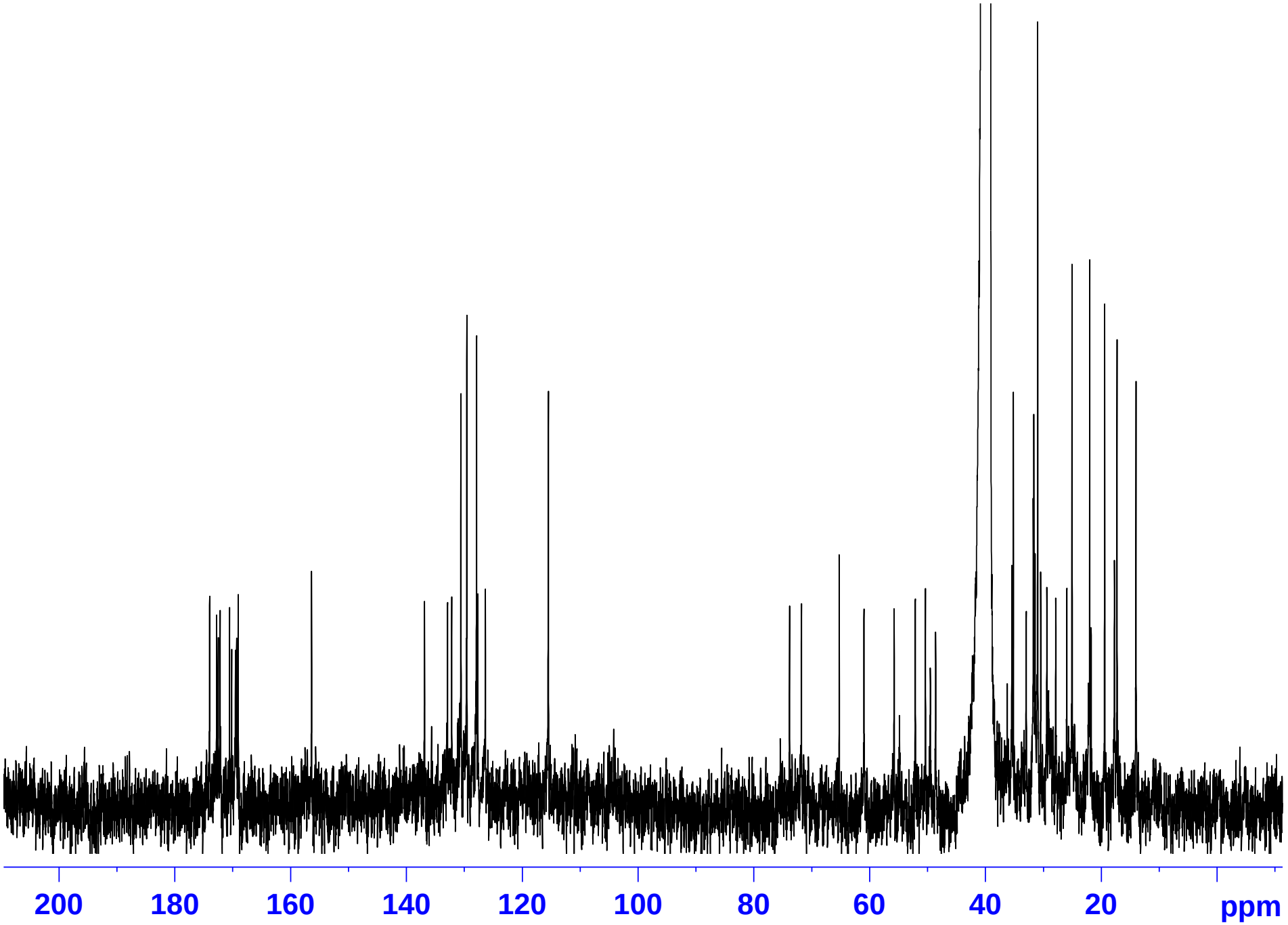

S3. HSQC Spectrum of Micropeptin KR1030 (**1**) in DMSO-d_6

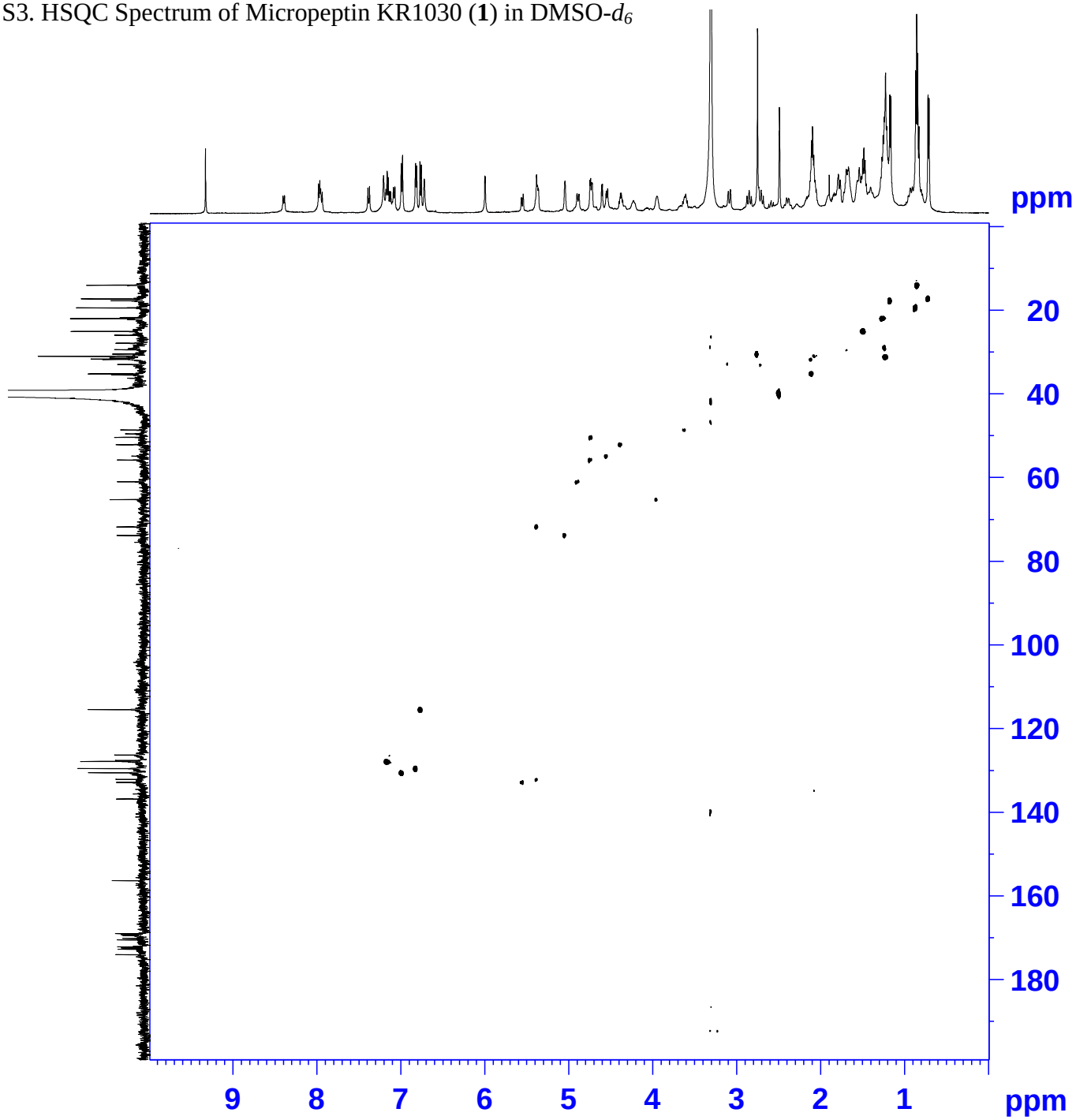

S4. HMBC Spectrum of Micropeptin KR1030 (**1**) in DMSO-d_6

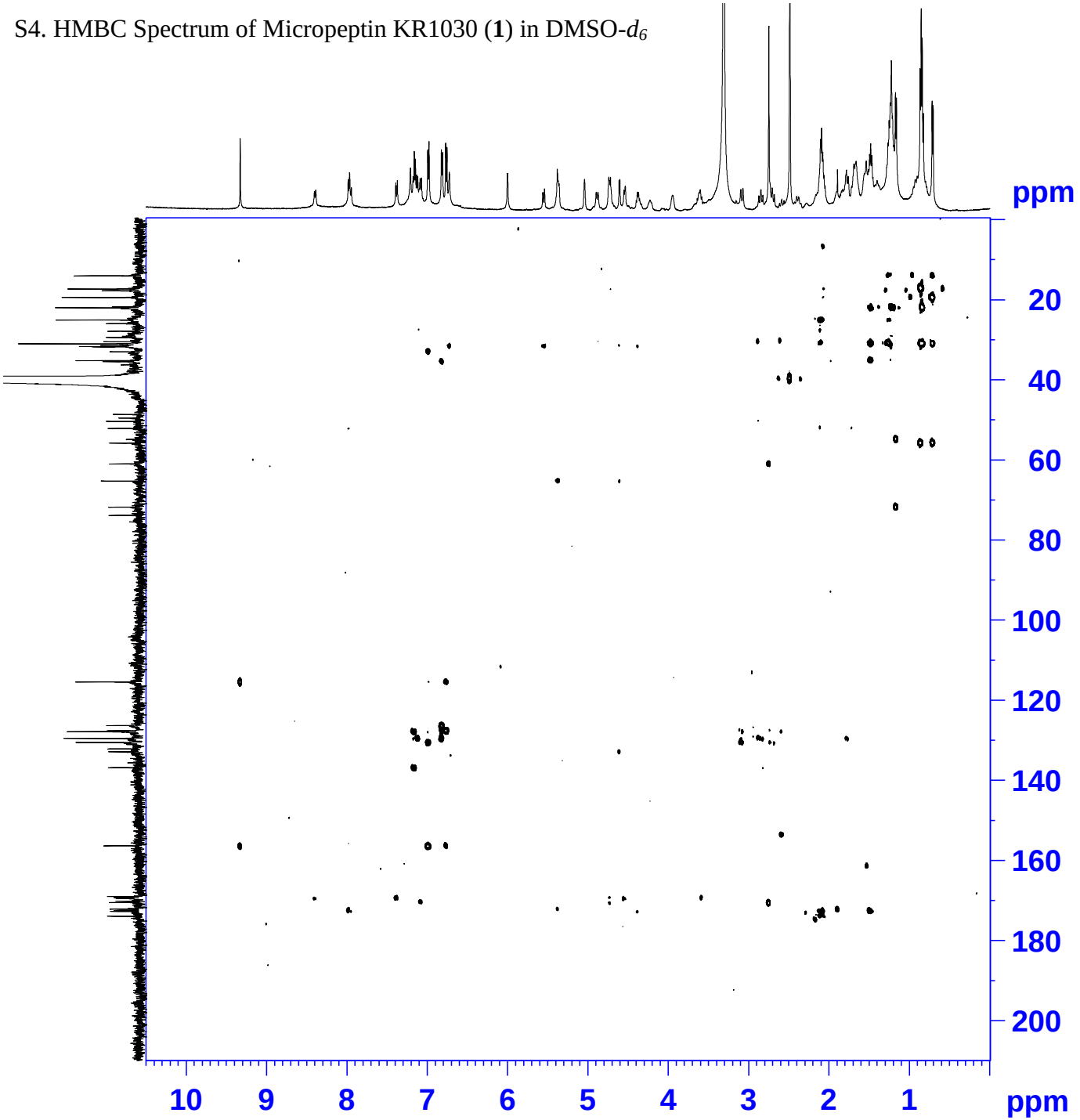

S5. COSY Spectrum of Micropeptin KR1030 (**1**) in DMSO-d_6

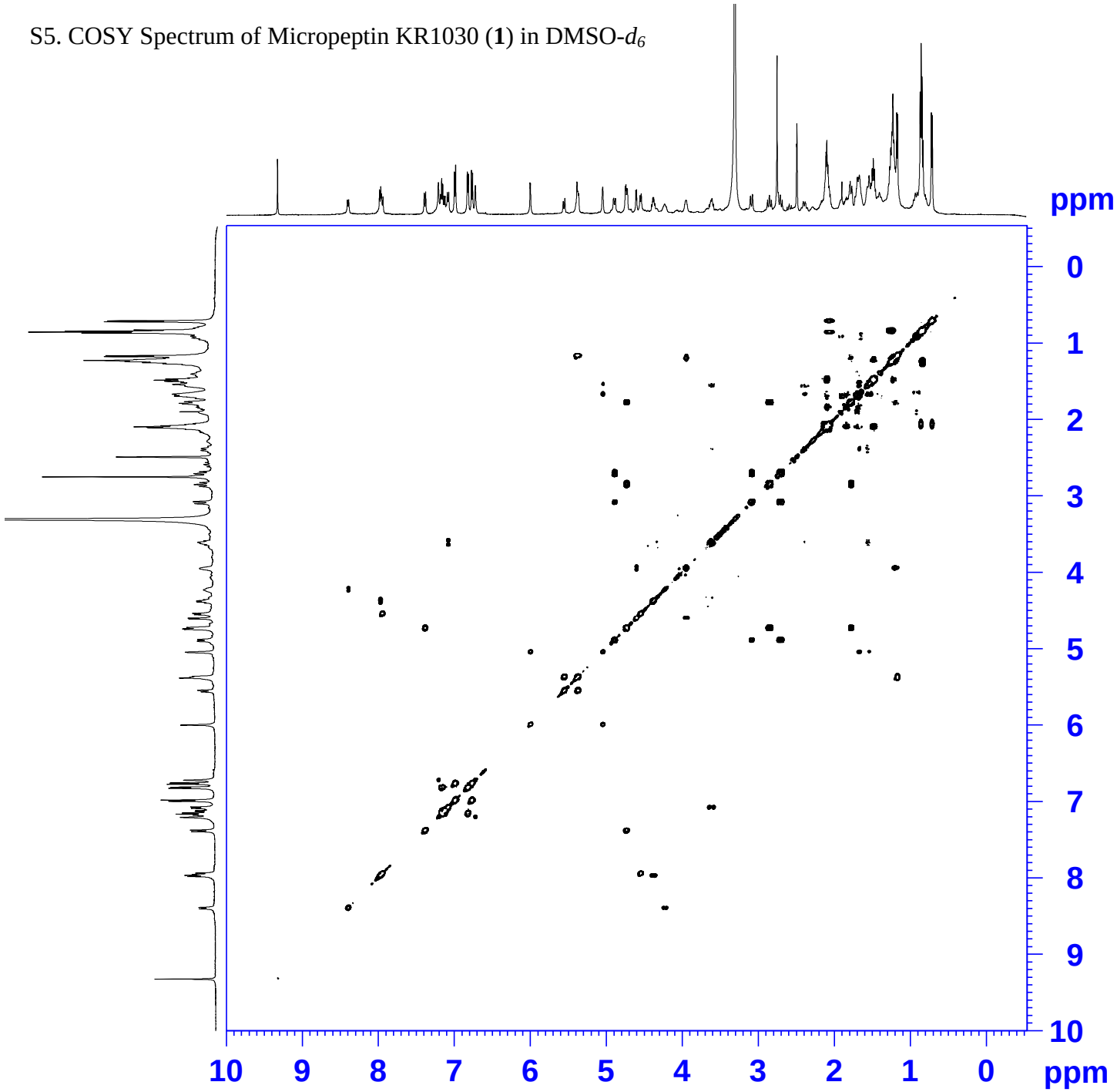

S6. ROESY Spectrum of Micropeptin KR1030 (**1**) in DMSO-d_6

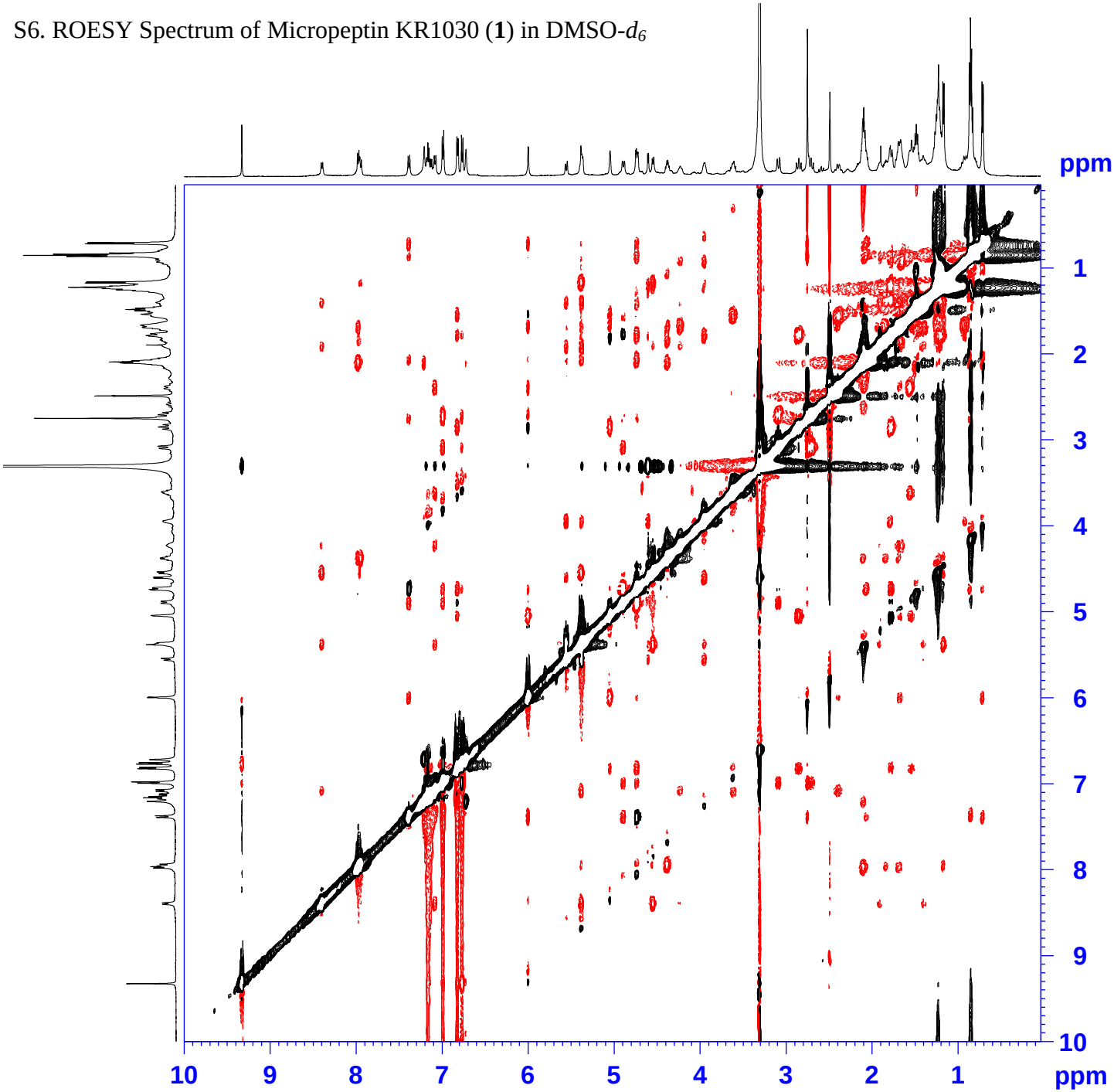

S7. TOCSY of Micropeptin KR1030 (**1**) in DMSO-d_6

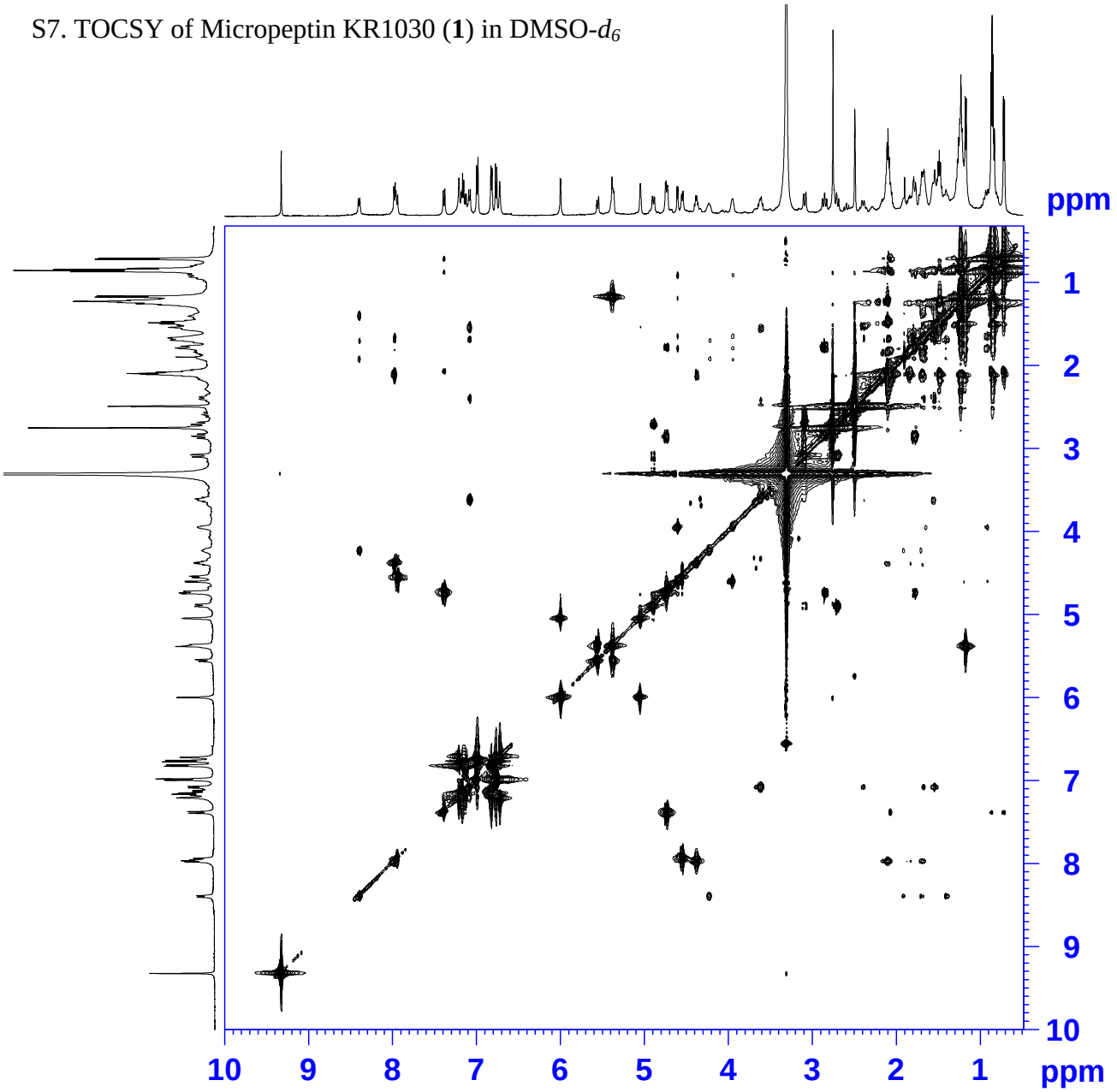

S8. HR ESI MS of Micropeptin KR1030 (**1**)

Elemental Composition Report **Page 1**

Single Mass Analysis
Tolerance = 10.0 PPM / DBE: min = -1.5, max = 50.0
Element prediction: Off
Number of isotope peaks used for i-FIT = 3

Monoisotopic Mass, Even Electron Ions
42 formula(e) evaluated with 3 results within limits (up to 50 closest results for each mass)
Elements Used:
C: 45-55 H: 60-80 N: 6-10 O: 5-15 Na: 1-1

TTBOO557
carmeli570 88 (3.699) Cm (83:93)

1: TOF MS ES+
2.83e+005

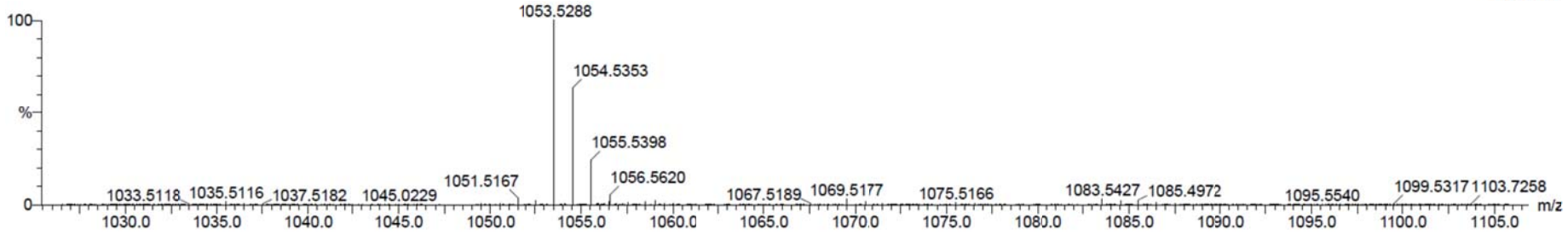

Minimum:				-1.5			
Maximum:		5.0	10.0	50.0			
Mass	Calc. Mass	mDa	PPM	DBE	i-FIT	i-FIT (Norm)	Formula
1053.5288	1053.5273	1.5	1.4	20.5	275.1	0.3	C53 H74 N8 O13 Na
	1053.5233	5.5	5.2	16.5	279.7	4.8	C48 H74 N10 O15 Na
	1053.5385	-9.7	-9.2	20.5	276.4	1.5	C52 H74 N10 O12 Na

S9. ^{1}H NMR Spectrum of Micropeptin KR1002 (**2**) in DMSO-d_6

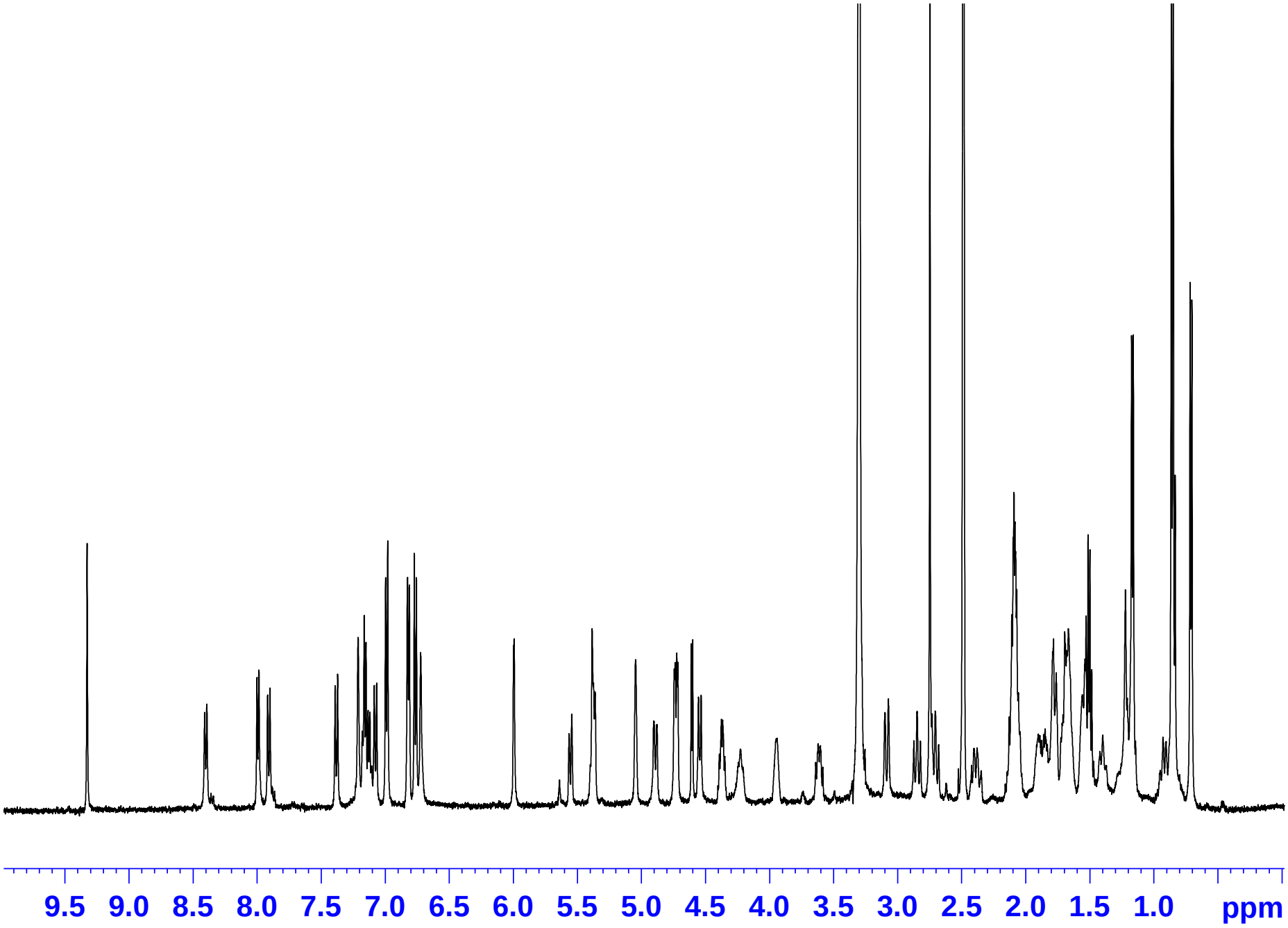

S10. ^{13}C NMR Spectrum of Micropeptin KR1002 (**2**) in DMSO-d_6

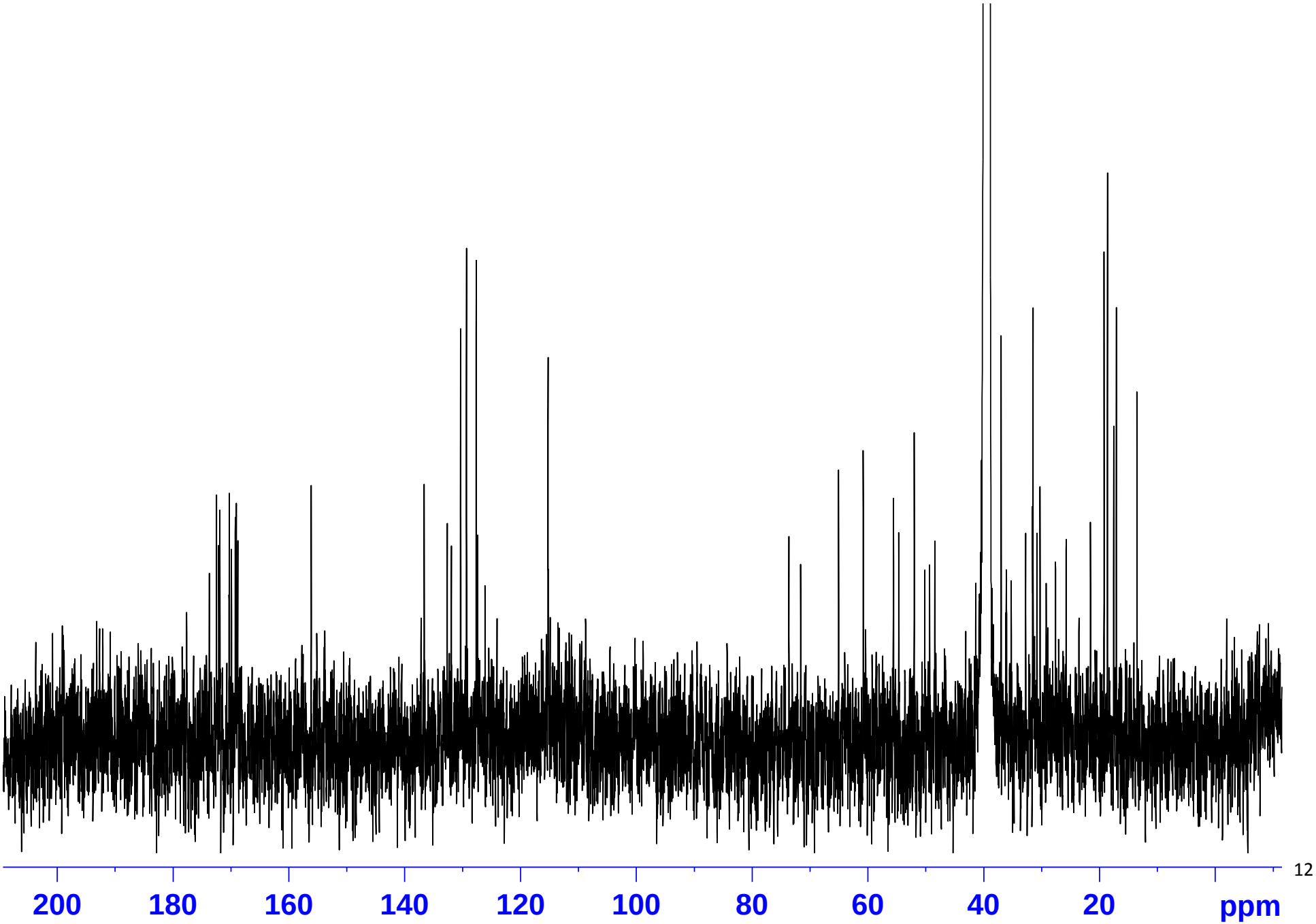

S11. HSQC Spectrum of Micropeptin KR1002 (**2**) in DMSO-d_6

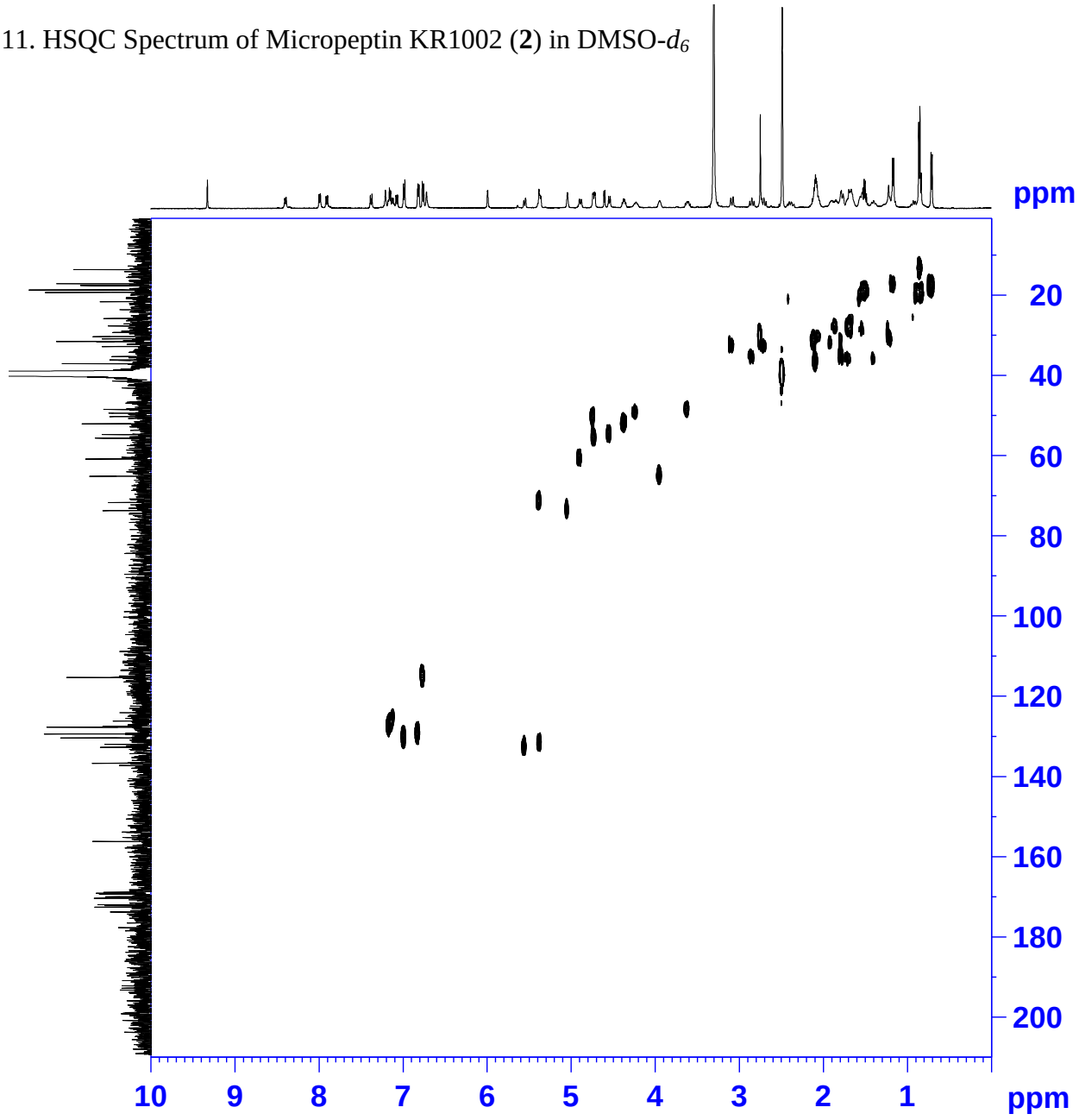

S12. HMBC Spectrum of Micropeptin KR1002 (**2**) in DMSO-d_6

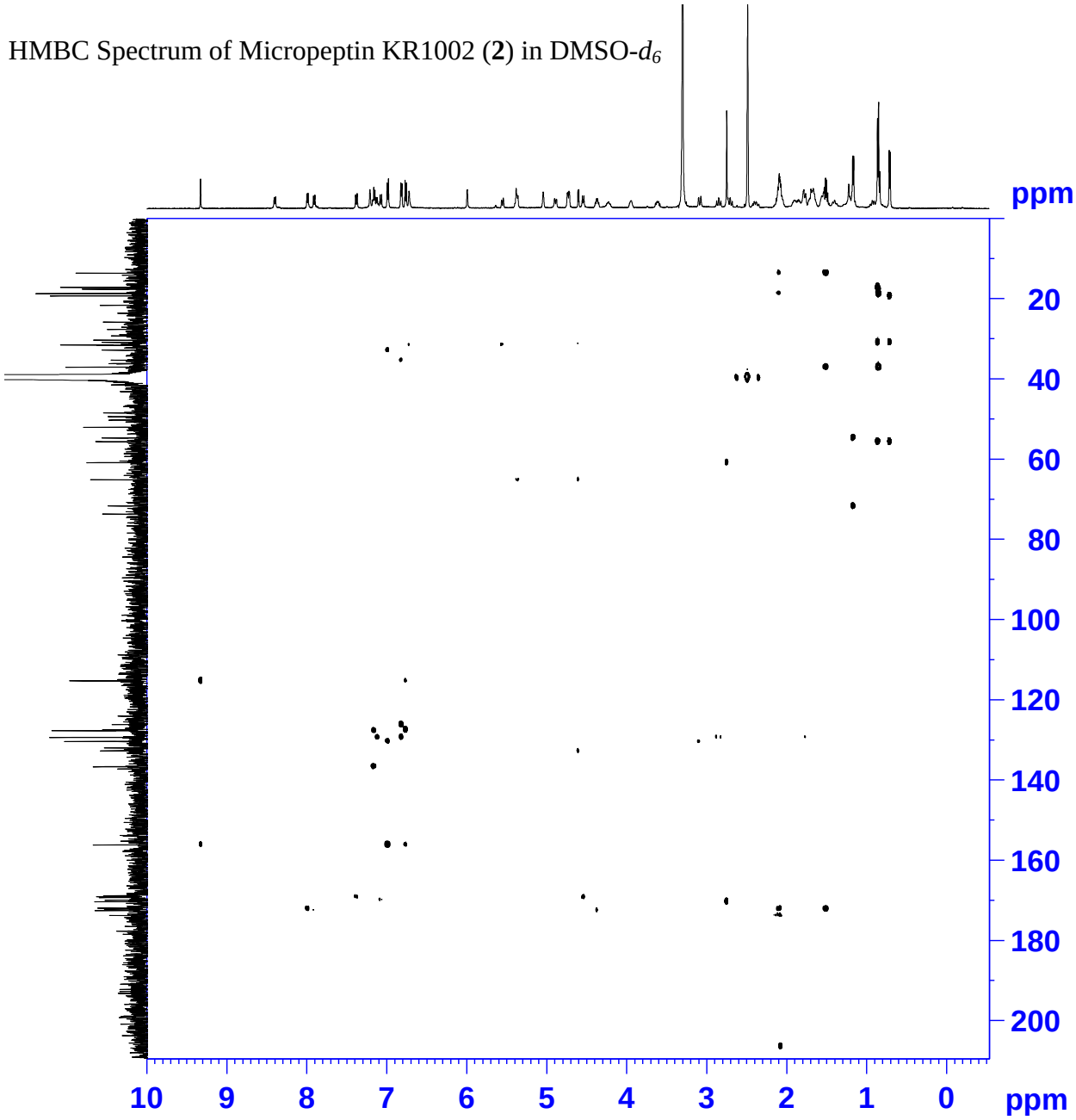

S13. COSY Spectrum of Micropeptin KR1002 (**2**) in DMSO-d_6

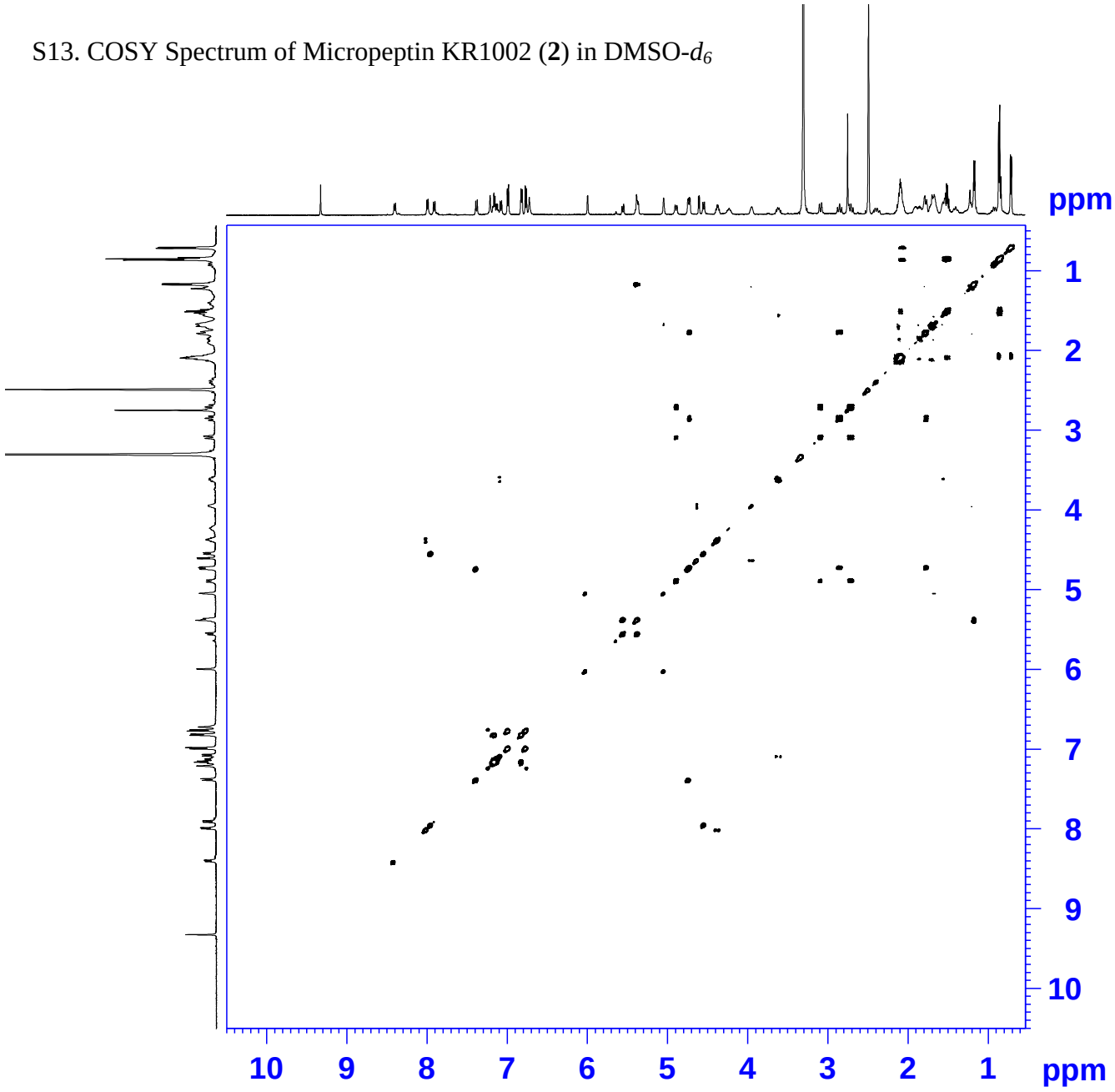

S14. ROESY Spectrum of Micropeptin KR1002 (**2**) in DMSO-d_6

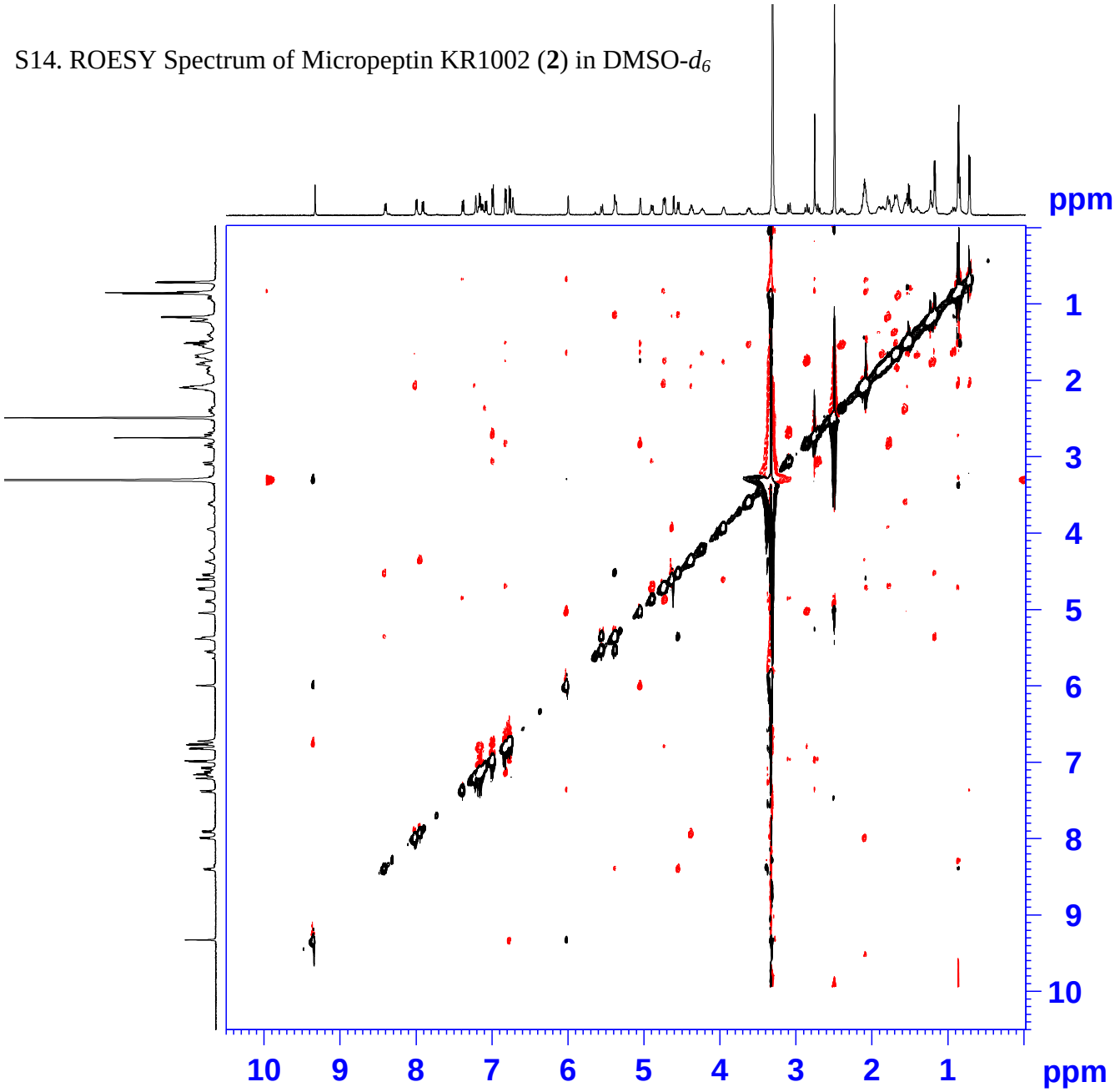

S15. TOCSY of Micropeptin KR1030 (**1**) in DMSO-d_6

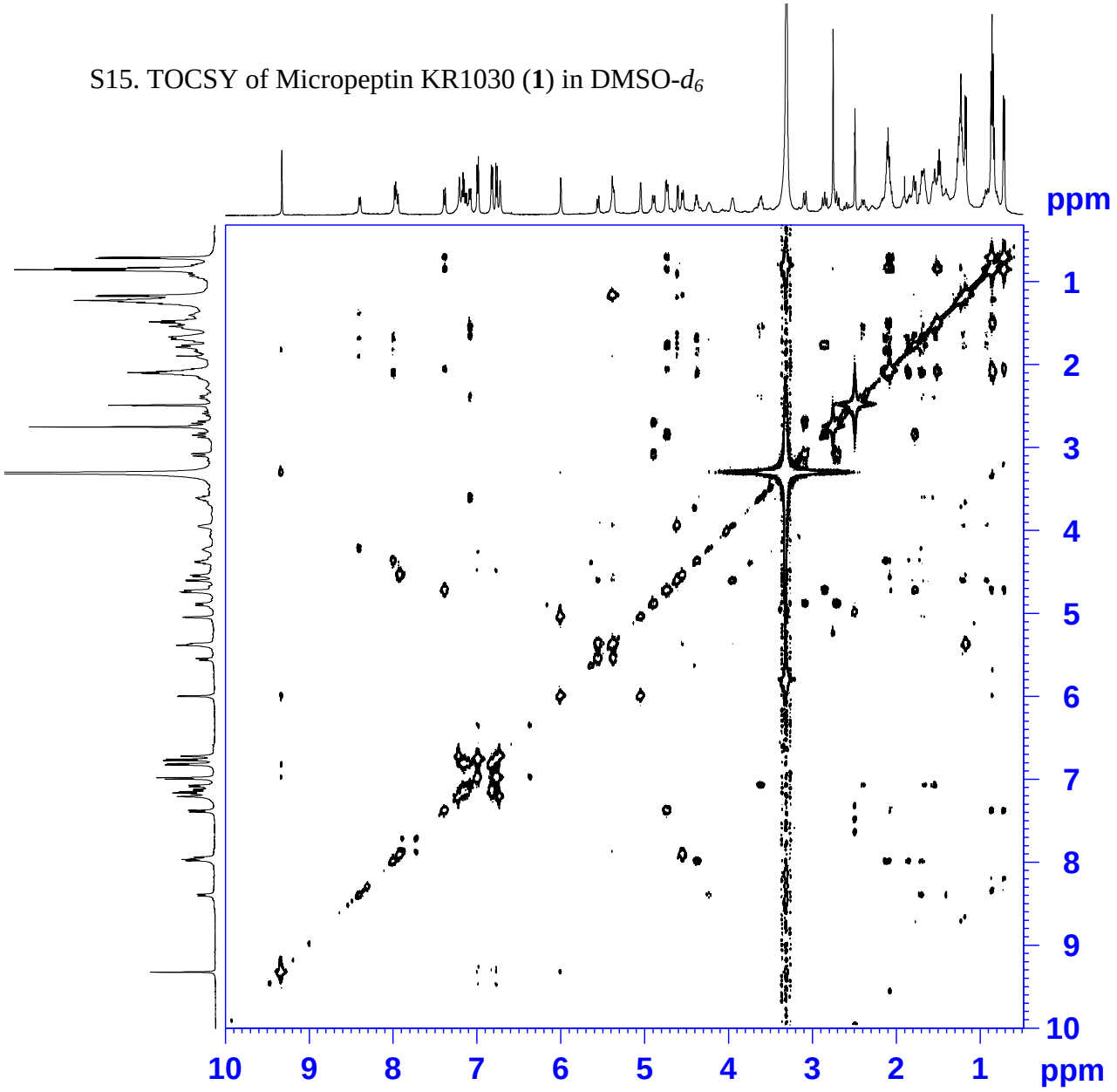

S16. HR ESI MS of Micropeptin KR1002 (**2**)

Elemental Composition Report **Page 1**

Single Mass Analysis
Tolerance = 10.0 PPM / DBE: min = -1.5, max = 50.0
Element prediction: Off
Number of isotope peaks used for i-FIT = 3

Monoisotopic Mass, Even Electron Ions
53 formula(e) evaluated with 3 results within limits (up to 50 closest results for each mass)
Elements Used:
C: 45-55 H: 60-80 N: 6-10 O: 5-15 Na: 1-1
TTBOO564
carmeli572 77 (3.402) Cm (77:78)

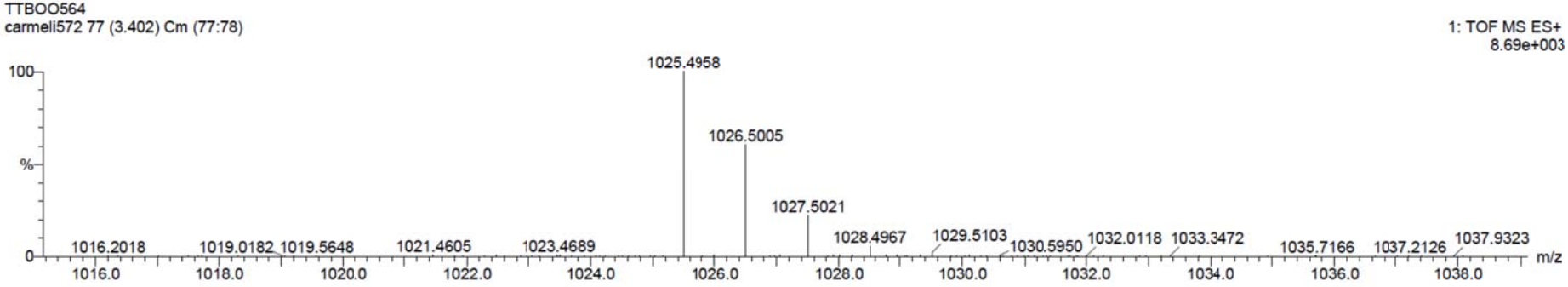

Minimum:				-1.5			
Maximum:		5.0	10.0	50.0			
Mass	Calc. Mass	mDa	PPM	DBE	i-FIT	i-FIT (Norm)	Formula
1025.4958	1025.4960	-0.2	-0.2	20.5	58.1	0.0	C51 H70 N8 O13 Na
	1025.4920	3.8	3.7	16.5	63.4	5.3	C46 H70 N10 O15 Na
	1025.4861	9.7	9.5	25.5	62.6	4.5	C53 H66 N10 O10 Na

S17. ^{1}H NMR Spectrum of Micropeptin KR998 (**3**) in DMSO-d_6

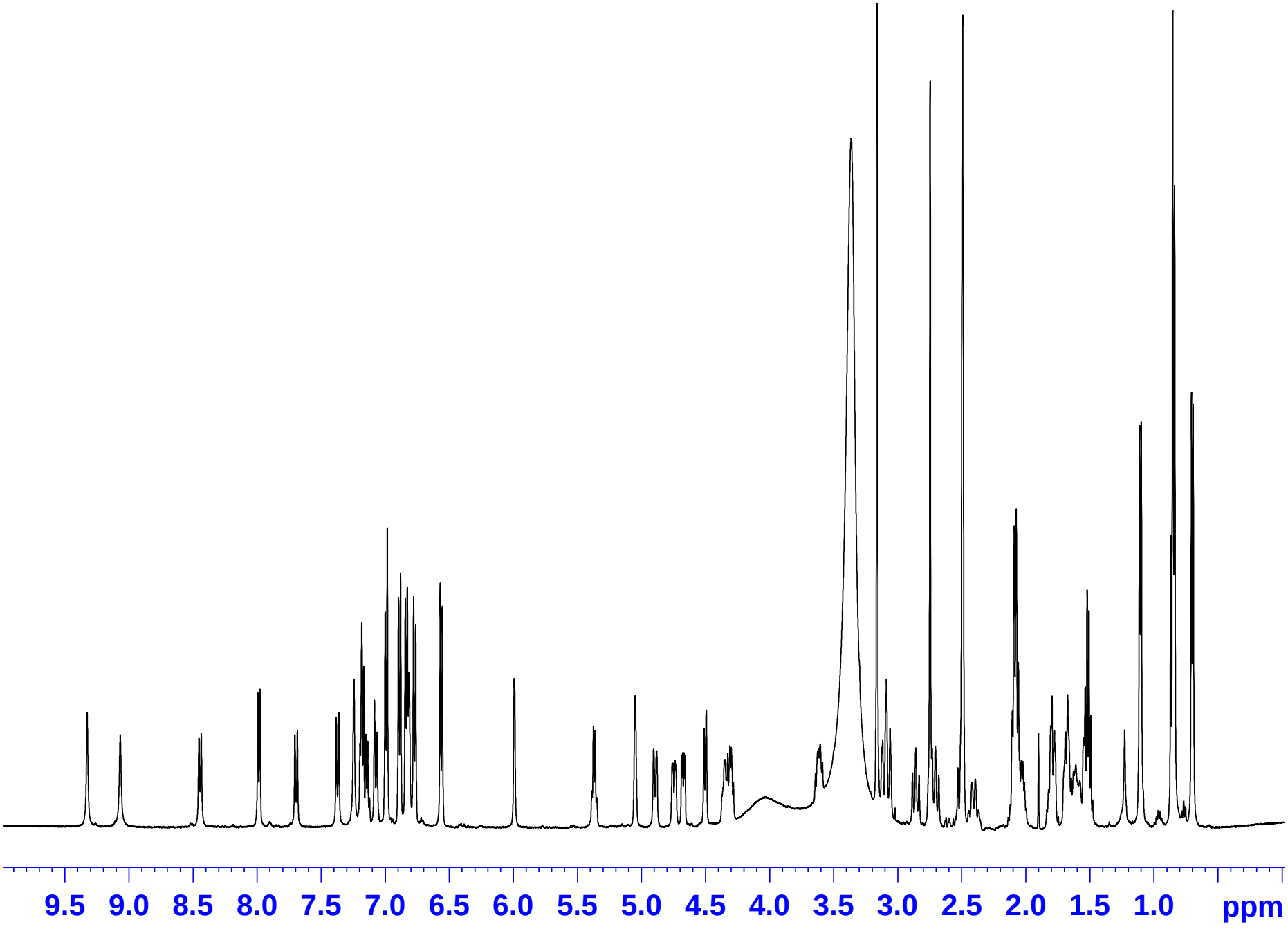

S18. ^{13}C NMR Spectrum of Micropeptin KR998 (**3**) in DMSO-d_6

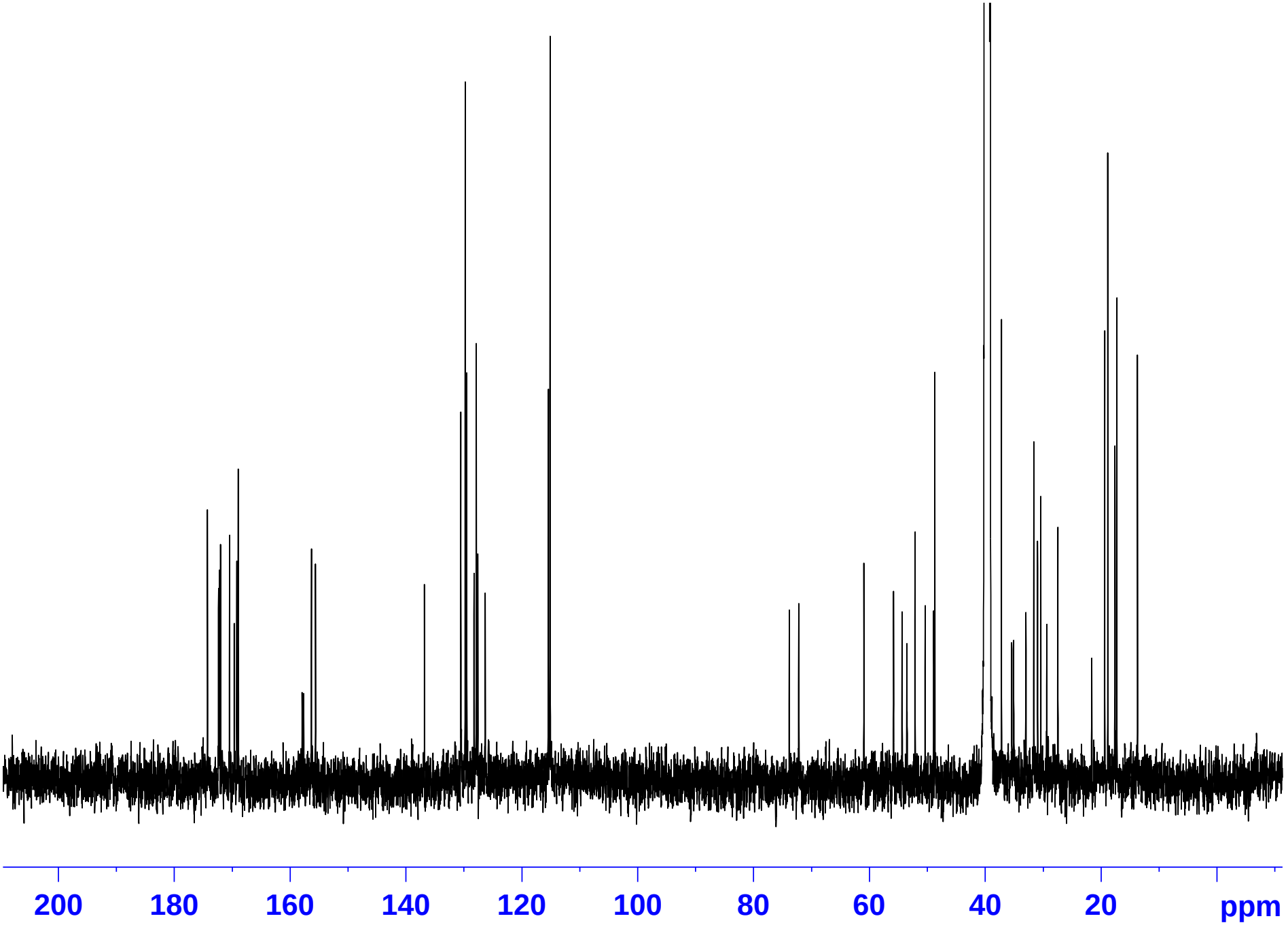

S19. HSQC NMR of Micropeptin KR998 (**3**) in DMSO-d6

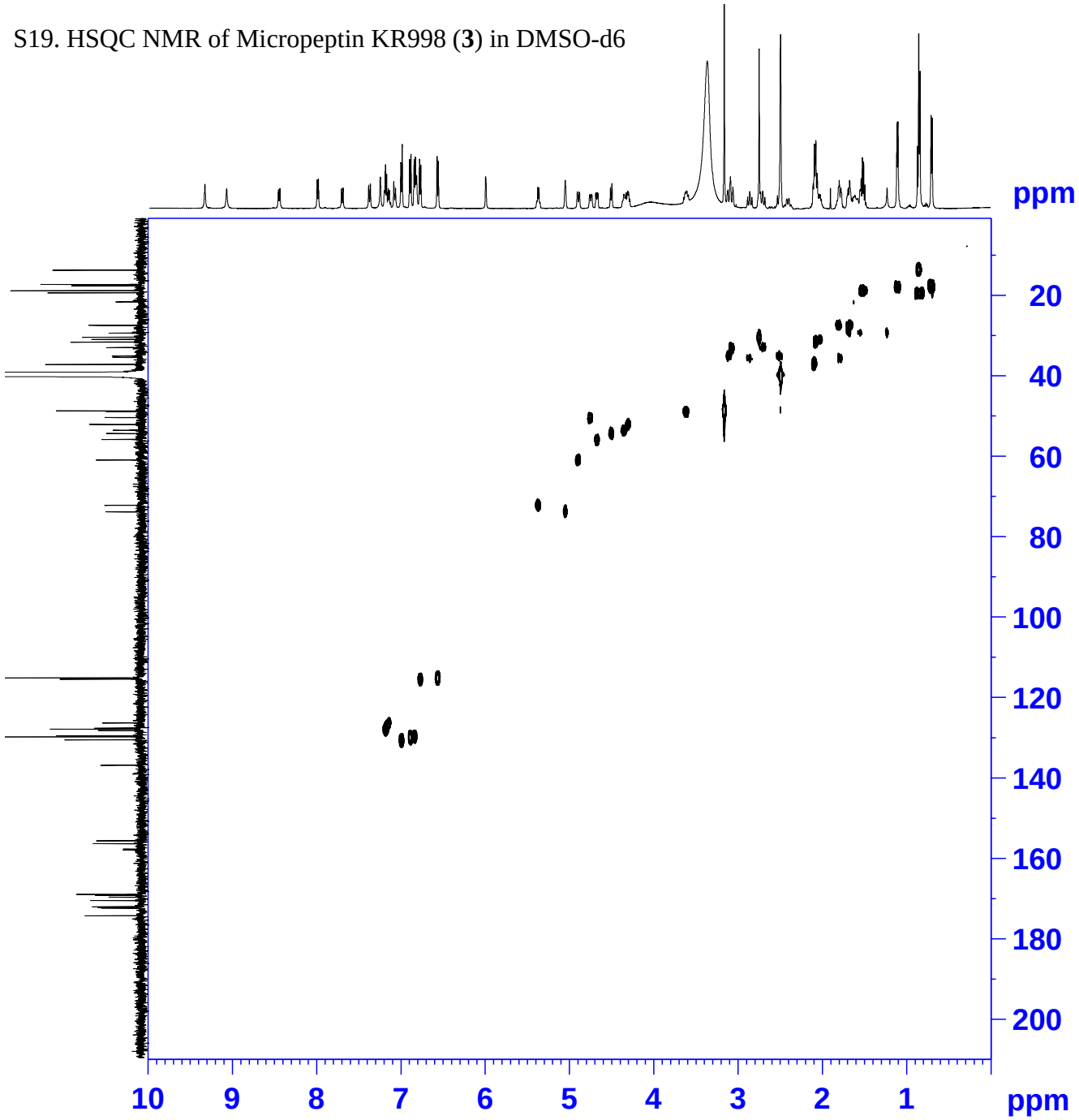

S20. HMBC Spectrum of Micropeptin KR998 (**3**) in DMSO-d_6

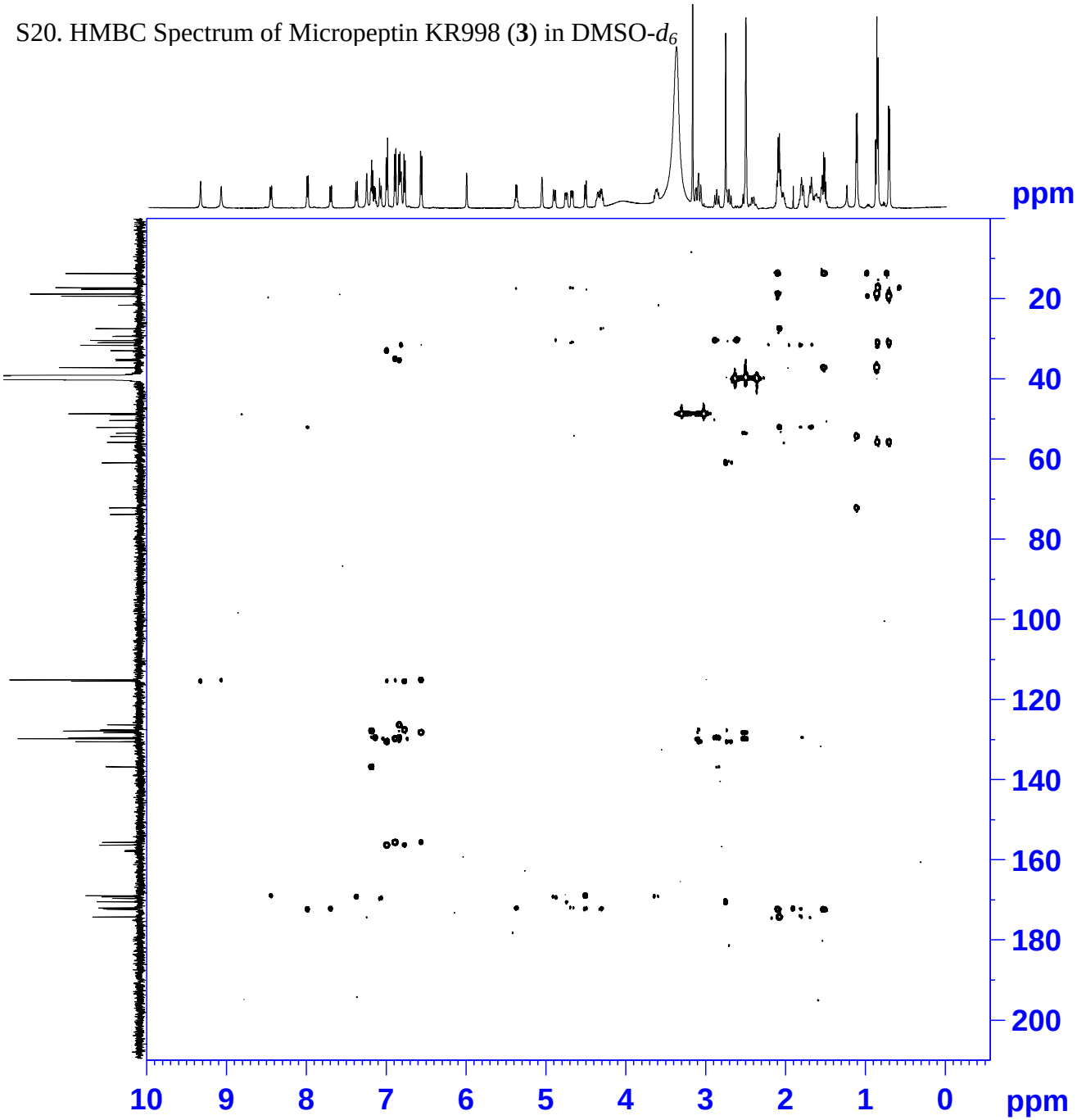

S21. COSY Spectrum of Micropeptin KR998 (**3**) in DMSO-d_6

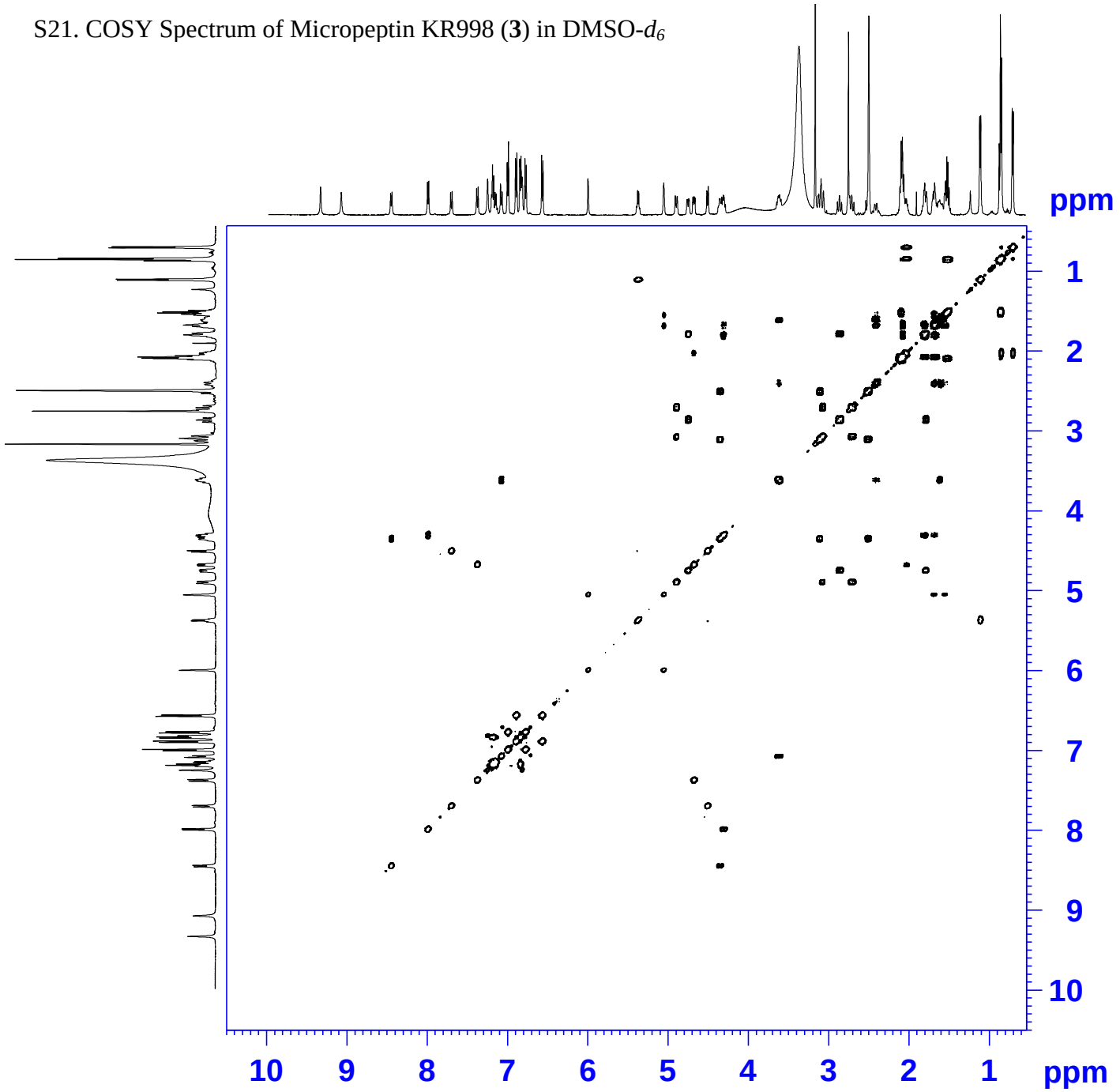

S22. ROESY Spectrum of Micropeptin KR998 (**3**) in DMSO-d_6

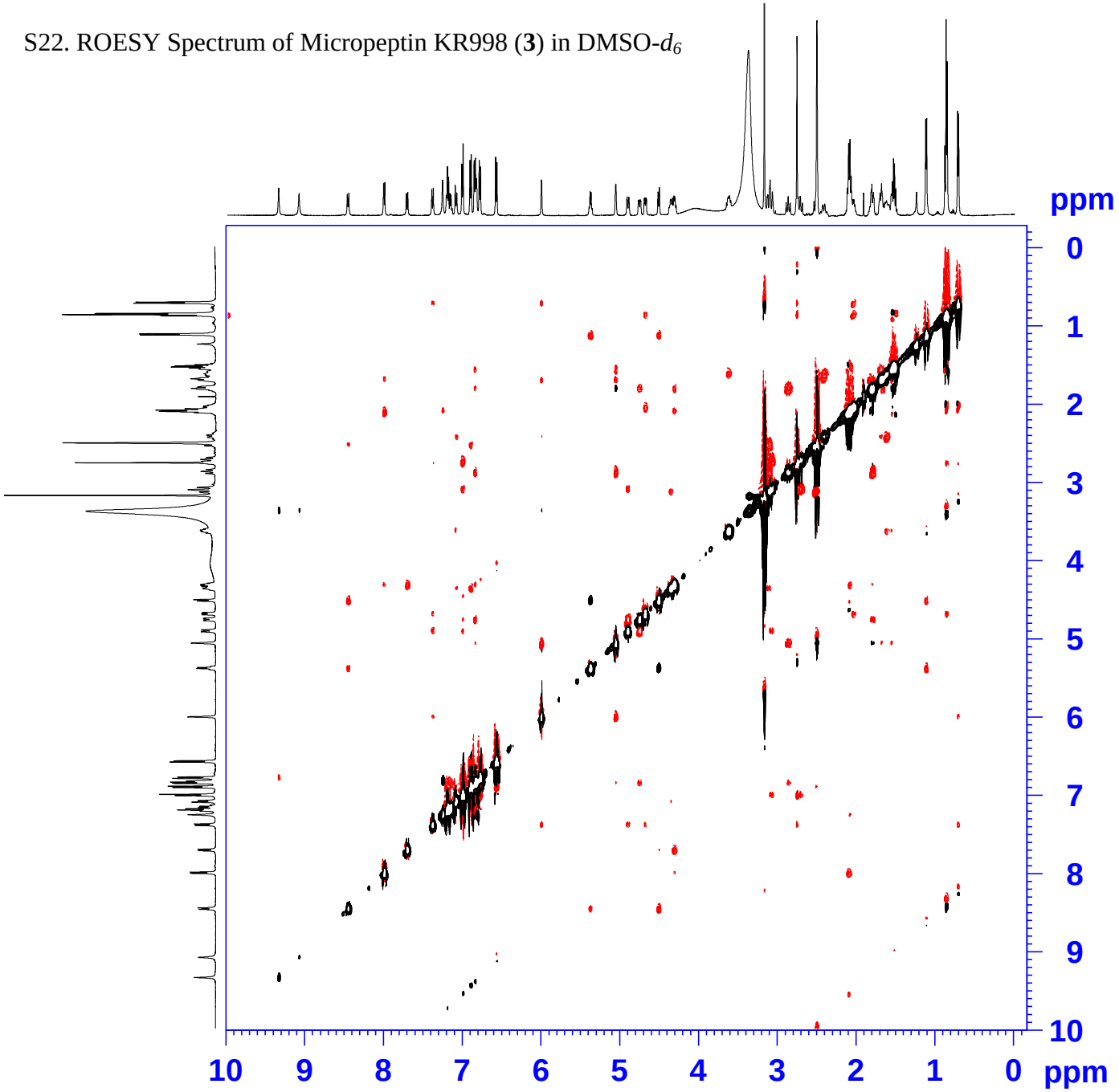

S23. TOCSY of Micropeptin KR1030 (**1**) in DMSO-d_6

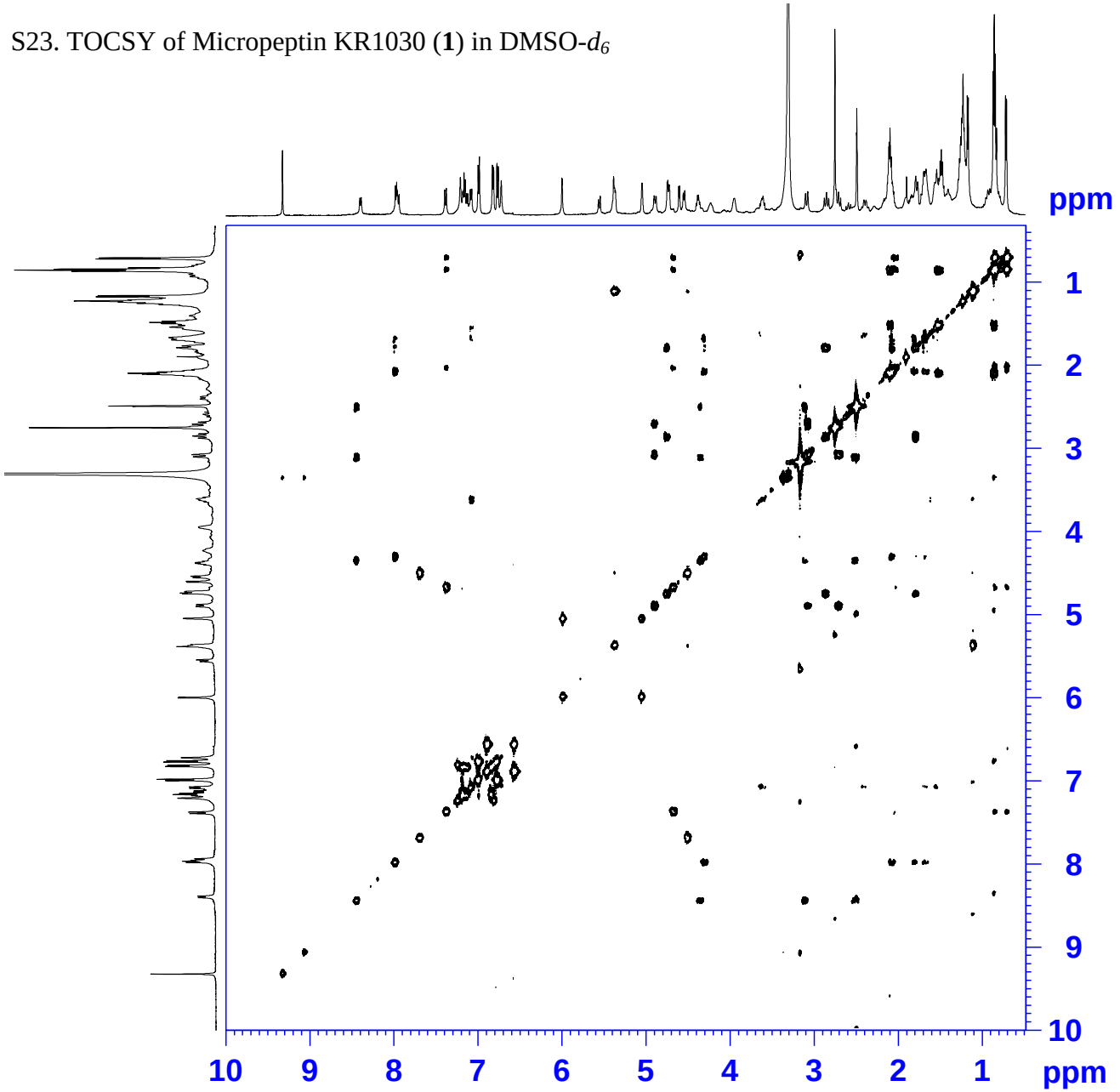

S24. HR ESI MS of Micropeptin KR998 (**3**)

Elemental Composition Report **Page 1**

Single Mass Analysis
Tolerance = 10.0 PPM / DBE: min = -1.5, max = 50.0
Element prediction: Off
Number of isotope peaks used for i-FIT = 3

Monoisotopic Mass, Even Electron Ions
30 formula(e) evaluated with 3 results within limits (up to 50 closest results for each mass)
Elements Used:
C: 45-55 H: 60-70 N: 6-10 O: 5-15 Na: 1-1

TTBOO568
carmeli571 219 (9.627) Cm (216:221)

1: TOF MS ES+
3.48e+003

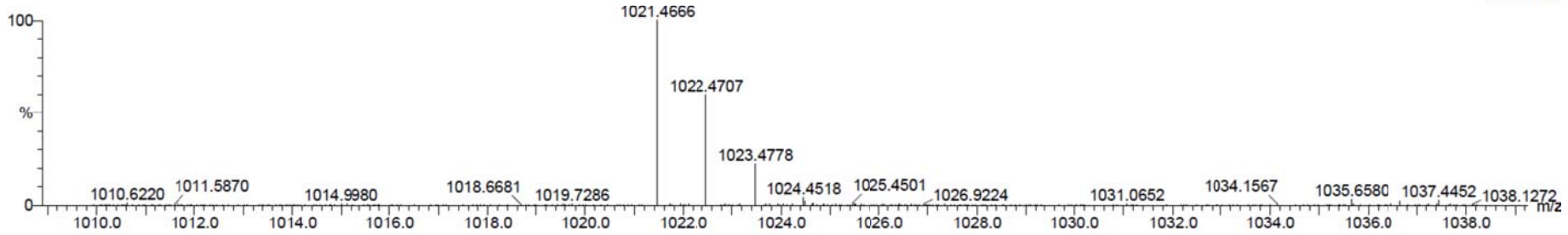

Minimum:				-1.5			
Maximum:		5.0	10.0	50.0			
Mass	Calc. Mass	mDa	PPM	DBE	i-FIT	i-FIT (Norm)	Formula
1021.4666	1021.4647	1.9	1.9	22.5	91.4	0.2	C51 H66 N8 O13 Na
	1021.4607	5.9	5.8	18.5	95.3	4.0	C46 H66 N10 O15 Na
	1021.4759	-9.3	-9.1	22.5	93.2	1.9	C50 H66 N10 O12 Na

Known microcyclamide GL546A

The identity of the known microcyclamide GL546A was found through NMR data that matched the data from the literature [Raveh, A. *et al. Tetrahedron, 66*(14), 2705–2712].

Structure of microcyclamide GL546A (4).

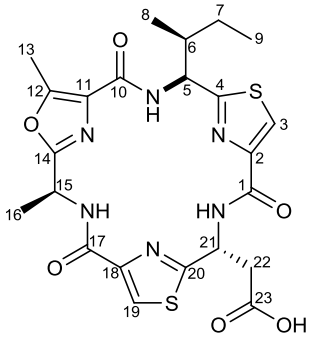

NMR data of microcyclamide GL546A (4) in DMSO-d_6.[a]

Position	δ_C, mult.[b]	δ_H, mult., *J* (Hz)	LR H-C correlations[c]
1	158.9 s		
2	148.1 s		
3	125.2 d	8.37 s	2, 4
4	168.0 s		
5	54.3 d	5.32 dd 7.4, 6.0	4, 6, 9, 10
6	40.2 d	1.97 m	
7a	25.3 t	1.16 m	6
7b		1.58 m	9
8	11.5 q	0.92 t 7.3	6, 7
9	14.5 q	0.79 d 6.8	5, 6, 7
N2(H)		8.39 d 7.4	4, 10
10	159.6 s		
11	127.8 s		
12	153.4 s		
13	11.2 q	2.60 s	11, 12
14	161.3 s		
15	43.9 d	5.19 p 6.3	14, 16
16	19.1 q	1.52 m	14, 15
N(4)H		8.54 d 6.3	14, 17
17	159.2 s		
18	147.6 s		
19	125.7 d	8.40 s	18, 20
20	170.1 s		
21	48.1 d	5.80 dt 8.2, 5.1	20, 23
22	40.5 t	3.07 d 5.1	20, 21, 23
23	171.5 s		
N6(H)		8.77 d 8.2	1

[a]500 MHz for ^{1}H, 125 MHz for ^{13}C. [b]Multiplicity and assignment from HSQC experiment. [c]Determined from HMBC experiment, $^{n}J_{CH}$=8 Hz, recycle time 1s.

Tanja Thorskov Bladt
Chemical biology of microbial anticancer natural products - appendix

DTU Systems Biology's academic profile covers the fields of cellular, molecular and structural biology, bioinformatics, computational biology, industrial biotechnology, biomedicine and health. Systems biology addresses both the overall properties of a biological system and uses scientific approaches to understand specific mechanisms. Therefore, much of the work carried out by our research groups is characterized by the incorporation of several academic disciplines.

Department of Systems Biology
Technical University of Denmark

Building 221
Søltofts plads
DK-2800 Kgs. Lyngby
Tel. +45 4525 2525
Fax +45 4588 4158
www.bio.dtu.dk

ISBN 978-87-91494-77-2